THE UNIVERSITY OF QUEENSLAND

AUSTRALIA

Power system protection problems caused by grid connected PV systems

Subhashish Bhattacharya

B.E (Electrical)

A thesis submitted for the degree of Master of Philosophy at

The University of Queensland in 2014

School of Information Technology and Electrical Engineering

Abstract

Renewable energy sources are clean sources of energy which do not cause emission of greenhouse gases. Wind and solar power are the two most common sources of renewable energy. About two decades back active research work started on improving efficiencies of technologies employed in converting renewable energy sources into electrical energy. With the present concern about climate change and regulations for reduction in carbon-dioxide emissions, development of efficient systems for conversion of solar powers to electricity is considered as a subject of high importance. One of the most common technologies used to convert solar power to electrical power is solar photovoltaic (PV) cells. Proper utilization of solar power can lead to significant reduction of greenhouse gas emissions, but there are several problems associated with large scale generation of power using PV cells. Currently small units rated for individual residences to large megawatt rated PV power generation units are embedded throughout the distribution system. In conventional power distribution network, power is generated centrally and then distributed in a radial network. With distributed generation using PV cells, there are several points of power generation in a system. Conventional methods of protective relaying originally developed for radial distribution do not hold up well in all situations with distributed generators embedded in power system. This is due to the change in fault levels caused by the contribution from distributed generators during faults. Additionally there are several situations of unintentional islanding and problems associated with reconnection of distributed generator with utility. This thesis describes the research work carried out to analyse the protection problems associated with high penetration level of a PV type distributed generator. The main objective of this research work is to investigate the impact of incremental penetration of PV systems on protection issues of low voltage network in suburban distribution systems and to recommend measures to mitigate the protection problems. Photovoltaic generators of small and large sizes have been considered for the purpose of this investigation. Protection problems caused by single phase PV generator installed in individual residences as well as large three-phase PV generators installed in buildings with multiple apartments in a housing complex has been studied. Potential issues in protection system have been identified using a number of different case studies and mitigation measures have been recommended. Finally, future work to extend and further investigate the research has been suggested.

Declaration by Author

This thesis is composed of my original work, and contains no material previously published or written by another person except where due reference has been made in the text. I have clearly stated the contribution by others to jointly-authored works that I have included in my thesis.

I have clearly stated the contribution of others to my thesis as a whole, including statistical assistance, survey design, data analysis, significant technical procedures, professional editorial advice, and any other original research work used or reported in my thesis. The content of my thesis is the result of work I have carried out since the commencement of my research higher degree candidature and does not include a substantial part of work that has been submitted to qualify for the award of any other degree or diploma in any university or other tertiary institution. I have clearly stated which parts of my thesis, if any, have been submitted to qualify for another award.

I acknowledge that an electronic copy of my thesis must be lodged with the University Library and, subject to the General Award Rules of The University of Queensland, immediately made available for research and study in accordance with the Copyright Act 1968 unless a period of embargo has been approved by the Dean of the Graduate School.

I acknowledge that copyright of all material contained in my thesis resides with the copyright holder(s) of that material. Where appropriate I have obtained copyright permission from the copyright holder to reproduce material in this thesis.

Publications during Candidature

(1) Subhashish Bhattacharya, Tapan K. Saha and M. J. Hossain, "Fault current contribution from photovoltaic systems in residential power networks", in the Proceedings of *Australasian Universities Power Engineering Conference 2013 (AUPEC '13),* 29Sep - 3Oct 2013, Hobart, Tasmania, Australia.

(2) Subhashish Bhattacharya, Tapan K. Saha and M. J. Hossain, "Fault current contribution from large photovoltaic systems in building power supply networks", resubmitted for publication in Elsevier Journal on Energy and Buildings after first review (on 15.8.2014).

Publications Included in This Thesis

(1) Subhashish Bhattacharya, Tapan K. Saha, M. J. Hossain, "Fault current contribution from photovoltaic systems in residential power networks", in the Proceedings of *Australasian Universities Power Engineering Conference 2013 (AUPEC '13),* 29Sep - 3Oct 2013, Hobart, Tasmania, Australia.

Incorporated as paragraphs in Chapter 4

Contributor	Statement of contribution
Subhashish Bhattacharya	Simulation and modelling (100%) Result interpretation and discussion (80%) Wrote the paper (85%)
Tapan K Saha	Discussion on Results (10%) Reviewed the paper (10%)
M.J Hossain	Discussion on Results (10%) Reviewed the paper (5%)

(2) Subhashish Bhattacharya, Tapan K. Saha, M. J. Hossain, "Fault current contribution from large photovoltaic systems in building power supply networks", resubmitted for publication in Elsevier Journal on Energy and Buildings after first review (on 15.8.2014).

Incorporated as paragraphs in Chapter 5

Contributor	Statement of contribution
Subhashish Bhattacharya	Simulation and modelling (100%) Result interpretation and discussion (80%) Wrote the paper (85%)
Tapan K. Saha	Discussion on Results (10%) Reviewed the paper (10%)
M. J. Hossain	Discussion on Results (10%) Reviewed the paper (5%)

Contributions by Others to the Thesis

No contributions by others.

Statement of Parts of the Thesis Submitted to Qualify for the Award of Another Degree

None.

Acknowledgements

This work has been accomplished through the generosity and support of my adviser Prof Tapan Saha. First and foremost, I would like to give my sincere gratitude to my adviser for his valuable guidance throughout the duration of this project. I also convey my heartfelt gratitude to my co-adviser Dr Jahangir Hossain for his guidance and advice. It has been a wonderful journey to work under the supervision and encouragement of Prof Tapan Saha and Dr Jahangir Hossain.

I also thank the IT helpdesk department of ITEE for providing valuable assistance in running the PSCAD simulation software for research work and ITEE, UQ for providing me the facilities to conduct research.

Last but not least, I would like to thank my family for their support and encouragement throughout my journey of research and in all my efforts to achieve academic excellence.

Keywords

Photovoltaic (PV) system, inverter, fault current, protection coordination, insulated gate bipolar transistor, islanding, protection relays, under-voltage , grid, utility, network, distributed generator, recloser, fuse, circuit breaker, transformer, overhead line, cables, impedance.

Australian and New Zealand Standard Research Classifications (ANZSRC)

ANZSRC code: 090607, Power and Energy Systems Engineering (excl. Renewable Power), 50 %

ANZSRC code: 090608, Renewable Power and Energy Systems Engineering (excl. Solar Cells) 50%

Fields of Research (FoR) Classification

FoR code: 0906, Electrical and Electronic Engineering, 100%

Contents

List of Figures

List of Tables

List of Abbreviations Used in the Thesis

AC	Alternating Current
AFD	Active Frequency Drift
AS	Australian Standards
AUPEC	Australasian Universities Power Engineering Conference
CCM	Continuous Conduction Mode
CIGRE	International Council of Large Electrical Systems
CTI	Coordination Time Interval
DC	Direct Current
DCM	Discontinuous Conduction Mode
DG	Distributed Generator
ETAP	Electrical Transient Analysis Program
FCL	Fault Current Limiter
HV	High Voltage
IC	Incremental Conductance
IDMT	Inverse Definite Minimum Time
IIDG	Inverter interfaced distributed generator
IGBT	Insulated Gate Bipolar Transistor
IEEE	The Institute of Electrical and Electronics Engineers
kA	Kilo Amperes
kVA	Kilo Volt Amperes

kW	Kilo Watts
LDC	Line Drop Compensation
LV	Low Voltage
MCB	Miniature Circuit Breaker
MCCB	Moulded Case Circuit Breaker
MDB	Main Distribution Board
MM	Minimum Melting
MPPT	Maximum Power Point Tracking
MVA	Mega Volt Ampere
MW	Mega Watts
NDZ	Non Detection Zone
NREL	National Renewable Energy Laboratories
OFP	Optimal Power Flow
OHL	Overhead Line
ONAN	Oil Natural Air Natural
ONAF	Oil Natural Air Forced
OTI	Operations Technology Incorporated
PD	Protective Device
PDS	Power Delivery System
PI	Proportional and Integral
P&O	Perturb and Observe

PLL	Phase Locked Loop
PCC	Point of Common Coupling
PSCAD	Power System Computer Aided Design
PV	Photovoltaic
PWM	Pulse Width Modulation
RCTI	Revised Coordination Time Interval
RMU	Ring Main Unit
RET	Renewable Energy Target
SCE	Southern California Edison
SCSOA	Short Circuit Safe Operating Area
SMP	Slip Mode Frequency Shift
STC	Standard Test Condition
SVR	Static Voltage Regulator
TC	Total Clearing
TCC	Time Current Coordination
TCM	Time Coordination Method
TDS	Time Delay Setting
THD	Total Harmonic Distortion
XLPE	Cross Linked Poly Ethylene

Chapter 1 Introduction

1.1 Introduction

After about two centuries of absolute dependence on fossil fuels and an ever growing demand of energy the world has now started to feel the effect of greenhouse gas emissions. Fossil fuel used for generating electricity and for all modern means of transport includes coal and products obtained through distillation of crude oil. As the demand for electrical power and for transport seems to be ever increasing, the energy hungry world has started to look for alternate fuels. While hydroelectric generation is an alternate to coal and gas and is used worldwide, there is a requirement for substantially high investment as compared to coal based thermal power plant. Also hydroelectric system generation depends heavily on water level and is not as reliable as thermal power. A way to reduce the fossil fuel requirement for generation of energy came with the invention of nuclear fission based reactors. Nuclear fuel is highly efficient for generation of electrical energy and does not generate greenhouse gases. However, very high level of safety is required to ensure that the reactors can be operated safely. The risk associated with failure of controlled nuclear reaction in reactor is very high. The failure of nuclear reactors at Chernobyl in Russia and the recent failure of Fukushima Daiichi reactors (in 2011) in Japan have highlighted the possible problems that can be caused due to nuclear reactor failure.

The other substitutes for fossil fuel are wind power, solar power, and the tidal power. These are renewable resources and unlike fossil fuel they are unlimited sources of energy. Proper utilization of solar power can lead to significant reduction of greenhouse gases but there are several problems associated with large scale generation of power using renewable sources. One of the most widespread ways of utilizing solar energy is solar photovoltaic generation. Photovoltaic generation is a way of converting solar irradiation directly into electrical energy. Large scale use of solar photovoltaic systems can significantly reduce emission of greenhouse gases and help to conserve the environment. Solar photovoltaic systems convert irradiation from sun into direct current which is then converted to alternating current by an inverter. While such systems can be standalone, the current trend in PV generation is use of grid tied inverter systems.

1.2 Background

Use of PV systems for domestic power supply can greatly reduce the generation of greenhouse gases and Government of Australia is trying to encourage use of Solar PV cells. The Renewable Energy Target (RET) scheme has been established to encourage additional generation of electricity

from renewable energy sources. The renewable energy target is designed to ensure that 20% of Australia's electricity comes from renewable sources by 2020 [1]. PV generated electricity will definitely have a big role to play in achieving this target. During the last five years there has been a increasing trend of installing photovoltaic power supply units for residences and commercial complexes, both single phase and three phase units across the globe. This increase has been greatly influenced by the present day drive for reduction of carbon footprint and using more renewable energy to meet the power demand. The technology of PV system has greatly improved over the last decade. A decade back most PV systems generated a few watts, were used in a few isolated applications and were standalone units. Today PV systems are available in range of few kilowatts to thousands of kilowatts. Grid tied inverters have been developed which has made PV systems commercially viable and more practically implementable. Complex power electronic controls have evolved to take care of the technical demand for interfacing the PV inverters with the grid. The efficiency of solar panels has also appreciably improved over the last few years and drive for improving overall efficiency of PV systems and other renewable from the governments across the globe has led to boost of research activity in the field both by government organisations and private sectors. Large electrical component manufacturing companies have considered the PV sector as a major player for business in future and have come up with more reliable products that have helped in the commercialisation of the technology. Mass production of major hardware required for implementation of the PV technology has led to a competitive market and the prices of PV systems are becoming more affordable for people. Many utility companies has schemes that provides incentives to the installer of PV units, thus encouraging people to install PV systems at residences and help them to meet the increasing power demand without making any major impact on environment.

1.3 Motivation

To make an appreciable reduction in the greenhouse gas by the use of PV systems a large number of PV generators have to be embedded in the distributed network. However, large scale installation of PV generators in distribution networks will give rise to potential power system problems. This includes protective device coordination problems, unintentional islanding and power swings. In order to allow successful large scale penetration of PV cells in existing distribution network, substantial work has been done to investigate the nature of these problems and much of research is being done to develop strategies for successful integration of PV generators in existing network. However, the impact of PV units on protection coordination and fault withstand capacity of devices has not been investigated in details for low voltage networks. The fact that the existing network was

designed with a concept of centralized generation and a vertically integrated generation system contributes to much of the protection problems. The distributed generation sources throughout the network increases the probability of unintentional islanding in absence of a central control and monitoring system. However, a control and monitoring system across the network would have to be highly reliable and communication link failures can cause network wide power system stability problem.

1.4 Objective

The main objectives of the thesis are listed below:

- To study the problems caused in protection system of radial network after embedding distributed generation source (which is PV generator in this case).
- To investigate the impact of high PV penetrations on protection systems in distribution networks.
- To recommend modifications and necessary review process of existing protection equipment and protection relay setting.

In order to achieve the objectives mentioned above, a systematic approach has been developed as described in the next section.

1.5 Methodology

In order to carry out the research, a step by step method has been used to achieve the final target of the work.

- Selection of software - For the research work to be carried out it is important that the selected software should have adequate features to allow modeling of PV system and equivalent sources, simulate symmetrical and asymmetrical faults and perform relay coordination. The softwares checked for suitability are ETAP[2] and PSCAD [3]

  ETAP is a power system design, modeling, analysis and planning software developed by Operation Technology Incorporated. This software can be used for short circuit analysis, load flow study, transient study, user-defined dynamic model, protective devices coordination and modeling of Photovoltaic arrays.

  PSCAD is a time domain simulation program developed by Manitoba HVDC research centre. It is mainly dedicated to the study of transients in power systems. PSCAD can be used for power system and power electronic studies. Review of the software features show that relay coordination can be better done in ETAP but PSCAD provides better

platform for performing stage wise simulation of faults and analysis of user defined systems. PSCAD also provides time domain graphical outputs which are very important for the research work. Therefore for the purpose of this research work PSCAD has been exclusively used.

- Development of grid tied inverter model – A PSCAD model of a fully functional single phase, grid tied PV system has been developed. This has helped to analyse the behaviour of PV inverters during faults at the output of inverter.
- Determination of impact on protection systems in residential network due to high penetration of single phase PV- Investigation has been done to understand the impact of the impact of fault current contribution from single phase PV system on the capacity of protection components in residential networks. Case study has been done using selected simulation software and test network to support the theoretical assumptions made regarding possible outcomes.
- Determination of impact on protection systems in building power supply networks due to high penetration of large three-phase PV- Investigation has been done to understand the impact of the impact of fault current contribution from large three - phase PV system on the relay coordination in a three phase building power supply networks. Case study has been done using selected simulation software to analyse the protection coordination problems.
- Conclusion of research outcomes – The outcome of the research works has been analysed and concluded in order to provide a clear understanding of the protection issues identified. Recommendations has been made to address issue of proper sizing of fault withstand and fault clearing capacity of switchgear as well as the issue of reviewing existing protection settings to restore reliable protection coordination .
- Recommendation for future works – At the end of the research work, fields of future investigation has been identified and described. This is to enable future research works to use the outcomes of this work and further refine and build upon this work.

1.6 Overview of thesis

An overview of the thesis is presented in this section. The thesis is made up of six chapters and four appendices. A summary of content of each chapter is provided below. The appendices contain the simulation models and outputs for various investigations done as a part of the research work.

- Chapter 1 – This chapter describes the current trend of harnessing renewable energy and highlights the role of PV systems in this context. Description of motivation, objective and the methodology of research has been provided in this chapter.
- Chapter 2 – As the research work is based on the impact of integrating PV systems in network on protection systems, this chapter provides a detailed description of grid tied PV systems. Simulations carried out to investigate the behaviour of grid tied PV system during fault have been provided in this chapter.
- Chapter 3 – This chapter captures the research works done in the past to investigate the protection and fault related problems in distributed generation system with special reference to inverter tied distributed generators. The results and observation of the published research work has been discussed in details and a comprehensive understanding of the known problems has been presented.
- Chapter 4 – Chapter 4 presents an investigative study to understand the impact of high penetration of single phase PV systems in residential power system network. A test network has been used for simulation of case study and the findings have been analysed. Outcome of the investigation has been presented in this chapter. The investigation presented in this chapter has been presented as a conference paper in the proceedings of AUPEC 2013 and has been referenced in this chapter.
- Chapter 5 – This chapter presents an investigation carried out to study the impact of high penetration of large three phase PV systems in network for power supply to buildings. Case studies have been performed on test network and simulation results have been analysed in details to understand the impact of fault current contribution on protection coordination. The investigation presented in this chapter has been submitted (resubmitted after first review on 15.8.2014) for publication in Elsevier journal for Energy and Buildings and has been referenced in this chapter.
- Chapter 6 –This chapter concludes the outcomes of the research work and future work that can potentially use the finding of this research and build upon it has been discussed.

Chapter 2 Grid Tied PV Systems

As the primary objective of this research is studying impact of fault current from grid tied PV system in network, this chapter provides details of functionality of a grid tied inverter. A grid tied inverter is made up of PV panel, a DC-DC boost converter and a single or three phase inverter .The PV panel converts solar irradiance to DC power .The DC power is then fed to a boost converter .The boost converter steps up the input voltage, providing lift to the DC link voltage of the inverter and the process also realises the maximum power point tracking (MPPT) for the PV array output. The output inverter comprises of power transistors or IGBTs. This is the DC to AC conversion device. The inverter ensures that the output current is in phase with the utility voltage thus achieving power delivery at unity power factor. A simple block diagram representing a grid tied PV system is shown in Figure 2.1.

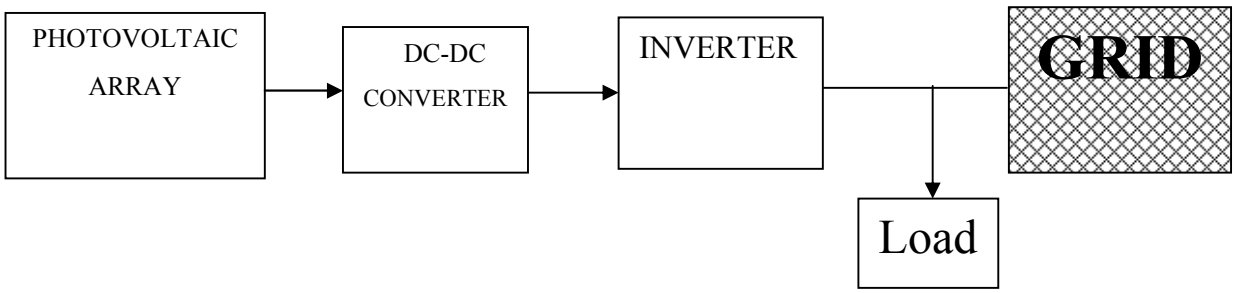

Figure 2.1 Block diagram –Grid tied PV system

2.1 PV Panel

A PV panel is built using number of PV cells connected in series parallel strings and packed into mechanically protected modules. A solar photovoltaic cell is the basic unit that converts solar irradiation to electrical energy. The amount of power generated depends on factors like temperature and irradiance level. In order to study the characteristics of solar cells and the impact the PV systems complete with inverter an equivalent electrical model is required. This section discusses the method to determine parameters required for modeling PV system. The equivalent model of a solar cell is based on the basic working theory of solar cells in which solar cell is considered as a diode in which light energy in form of photon with appropriate energy level, falls and generates electron hole pairs. The electron and holes are separated by electric field established at the junction of the diode and are then driven around an external circuit by junction potential. There are losses associated with shunt and series resistance of the cell as well as some of the current back across the p-n junction [4]. The Figure 2.2 represents the equivalent model of a PV cell.

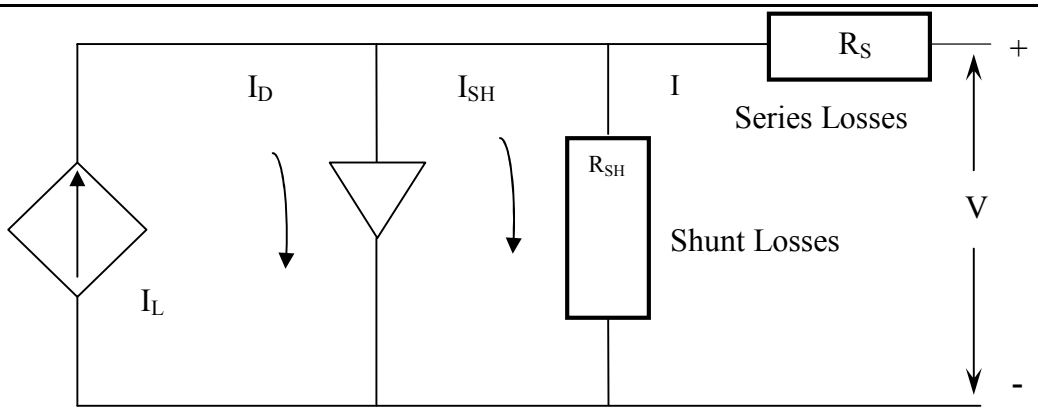

Figure 2.2 Model of PV cell

The current produced by a solar cell is proportional to its surface area and incidence of irradiance and the voltage is proportional to potential drop across p-n junction. From the equivalent circuit it is evident that the current produced by the solar cell is equal to that produced by the current source, minus that which flow the diode, minus that which flows through the shunt resistor.

$$I = I_L - I_D - I_{SH} \quad (2.1)$$

I = Output current in amperes

I_L = Photo generated output

I_D = Diode current (amperes)

I_{SH} = Shunt current (amperes)

The current through these elements is governed by the voltage across them:

$$V_j = V + IR_S \quad (2.2)$$

Where

V_j = Voltage across both diode and resistor R_{SH} (Volts)

V = Voltage across the output terminals (Volts)

I = output current (ampere)

R_S = Series resistance (Ohms)

By the Shockley diode equation, the current diverted through the diode.

$$I_D = I_0 e^{\left[\frac{qVj}{mkT} - 1\right]} \quad (2.3)$$

I_O = Reserve saturation current (amperes)

m = diode ideality factor (for an ideal diode)

q = elementary charge

k = Boltzmann's constant

At 25^OC, $\frac{kT}{q}$ =0.0259 Volts

$$I_{SH} = V_j / R_{SH} \quad (2.4)$$

Where R_{SH} = Shunt Resistance (Ω)

Substituting these into the first equation produces the characteristic equation of a solar cell, which relates solar cell parameters to the output current and voltage:

$$I = I_L - I_0 e^{\left(\frac{qV_j}{mkT}-1\right)} - \frac{(V+IR_S)}{R_{SH}} \quad (2.5)$$

It is however, difficult to use this formula to model PV panel as manufactures data sheet for PV cells does not provide data like R_S and R_{SH} and parameters provided relates to module voltage and current rather than to single cell. Therefore there is a requirement to derive the parameters of the above equation in terms of data provided by the manufacturer's data sheet. Typical manufacturer's data for PV cells is as given in Table 2.1(Data based on datasheet for Sunpower E19/238 Solar Panel [5]). Data sheets for other makes of PV panels contain similar details.

Table 2.1 Data Sheet extract for PV Panel [5]

Measured at STC ,Irradiance - 1000 W /m^2($G_{a,0}$),25 ^{o} C (T^C_0)			
Parameter	Symbol	Value	Unit
Nominal Power	$P^M_{max,0}$	238	Watts
Efficiency	η	19.1	%
Rated Voltage (module)	$V^M_{mpp,0}$	40.5	Volts
Rated Current (module)	$I^M_{mpp,0}$	5.88	Amps
Open circuit Voltage	$V^M_{oc,0}$	48.5	Volts
Short Circuit Current	$I^M_{sc,0}$	6.25	Amps
Maximum System Voltage		1000	Volts
Temperature Coefficients			
Power	K_P	(-) 0.38	%/^{0}k
Voltage	K_V	(-) 132.5	mV/^{0}k
Currents	K_I	3.5	mA/^{0}k
Nominal Operating Cell Temperature	NOCT	45	^{0}C
Measured at NOCT, Irradiance - 800 W /m^2($G_{a,\ ref}$) , 20 ^{o} C ($T_{a,\ ref}$)			
Nominal Power	$P_{max,\ ref}$	177	Watts
Rated Voltage (module)	$V^M_{mpp,\ ref}$	37.3	Volts
Rated Current (module)	$I^M_{mpp,\ ref}$	4.73	Amps
Open circuit Voltage	$V^M_{oc,\ ref}$	45.4	Volts
Short Circuit Current	$I^M_{sc,\ ref}$	5.06	Amps

Number of Cells in Series	N_{SM}	72
Number of parallel Branches	N_{PM}	1

In order to convert the single diode based equation (2.5) to a form where data sheet values can be used in order to model the system Lorenzo's model shall be used. Lorenzo (1994) model [6] can be applied to standard manufacturing data.

Based on equation (2.5), the PV module current I^M under arbitrary conditions can be described as

$$I^M = I_{SC}^M \left[1 - e^{\left\{ \frac{V^M - V^{OC} + R_S^M I^M}{N_S^M V_t^C} \right\}} \right] \quad (2.6)$$

The parallel resistance R_{SH} is quite large and therefore is neglected in the equation (2.6).

The expression of the PV module's current I^M is an implicit function, being dependent on -

The short circuit current of the module $I_{SC}^M = N_{PM}\, I_{SC}^C$ (2.7)

The open circuit Voltage of the module $V_{OC}^M = N_{SM} V_{OC}^C$ (2.8)

The equivalent series resistance of module $R_S^M = \frac{N_{SM}}{N_{PM}}\, R_S^C$ (2.9)

The thermal voltage in the semiconductor of a single solar cell $V_t^C = \frac{mkT_0^C}{q}$ (2.10)

Where $I^C{}_{SC}$, $V^C{}_{OC}$, , $R^C{}_S$ are the cell short circuit current, cell open circuit voltage and cell series resistance.

Based on the information on manufacturer's data sheet the cell data is computed

$$P_{max,0}^C = \frac{P_{max,0}^M}{N_{SM}\, N_{PM}} \quad (2.11)$$

$$\boldsymbol{V_{OC,0}^C = \frac{V_{OC,0}^M}{N_{SM}}} \quad (2.12)$$

$$\boldsymbol{I_{SC,0}^C = \frac{I_{SC,0}^M}{N_{PM}}} \quad (2.13)$$

$$V_{t,0}^C = \frac{mkT_0^C}{\mathrm{q}} \qquad \text{(Temperature should be expressed in Degree Kelvin)} \quad (2.14)$$

$$v_{OC,0} = \frac{\mathrm{V_{OC,0}^C}}{V_{t,0}^C} \quad (2.15)$$

The fill factor is then computed. Fill factor is the ratio of the maximum power that can be delivered to load and the product of $I^C{}_{SC}$ and $V^C{}_{OC}$. The fill factor diminishes as the cell temperature is increased.

Fill factor $FF = \frac{v_{OC,0} - ln(v_{OC,0} + 0.72)}{v_{OC,0} + 1}$ (2.16)

$$FF_0 = \frac{P_{max,0}^C}{V_{OC,0}^C\, I_{SC,0}^C} \quad (2.17)$$

$$r_s = 1 - \frac{FF}{FF_0} \tag{2.18}$$

$$\boldsymbol{R_S^C = r_s \left(\frac{V_{OC,0}^C}{I_{SC,0}^C}\right)} \tag{2.19}$$

The next step is to determine cell parameters for operating conditions V^M, T_a, G_a

The working temperature of cells T^C depends exclusively on irradiation G_a and ambient temperature T_a

$$T^C = T_a + G_a \frac{[NOCT - T_{a,ref}]}{G_{a,ref}} \tag{2.20}$$

The current of a solar cell is affected by ambient temperature T_a and solar irradiation G_a

$$\boldsymbol{I_{SC}^M = \left(\frac{G_a}{G_{a,0}}\right)\left[I_{SC,0}^M + K_V\left(T^C - T_0^C\right)\right]} \tag{2.21}$$

The open circuit voltage of cells depends exclusively on temperature.

$$\boldsymbol{V_{OC}^M = V_{OC,0}^M + K_V\left(T^C - T_0^C\right)} \tag{2.22}$$

$$\boldsymbol{V_t^M = N_{SM} \frac{mkT^C}{q}} \qquad (\textit{Temperature should be expressed in Degree Kelvin}) \tag{2.23}$$

$$\boldsymbol{R_S^M = \left(\frac{N_{SM}}{N_{SM}}\right) R_S^C} \tag{2.24}$$

The required parameters for solving the module current voltage equation (2.6) are now available. The equation has been modelled in PSCAD to obtain the Current – Voltage and Power – Current characteristic of solar panel. Details of the model have been shown in Figure A.1 of Appendix A.

I-V plot of E19/238 (Sunpower) solar panel [5] PV at varying irradiance and module temperature are shown in Figure 2.3.

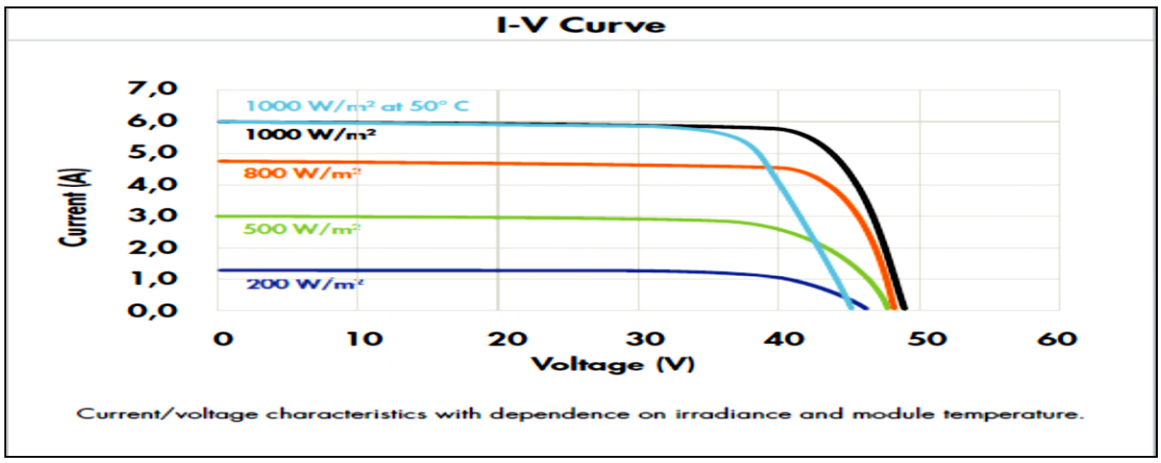

Figure 2.3 I-V Curve for varying temperature and irradiance

The model of solar panel has been developed in PSCAD using the datasheet parameters for E19/238 Sunpower solar panel and the simulation result is shown in Figure 2.4.

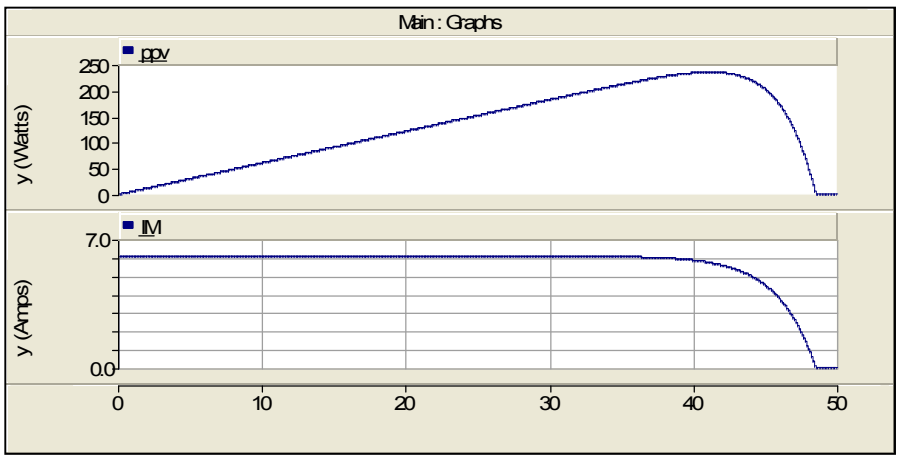

Figure 2.4 Simulation output –P-I and I-V curves of solar panel

The curve has been generated by running the simulation for STC condition and the curve is very close to the manufacturer's curve which implies that the PV panel has been modeled to adequate accuracy for fulfilling the requirement of research.

2.2 Maximum Power Point Tracking and DC-DC Converter

The PV cells operate under varied environmental conditions and require control at its output terminal to extract maximum power from the system. This is done by a process called maximum power point tracking (MPPT). There are several process of Maximum power point tracking .Each technique has its own advantage and disadvantages. Some commonly used techniques are Incremental conductance method (IC), Hill top, Perturb and Observe etc. Hohm and Ropp [7] performed a comparative study of various MPPT techniques using experimental method. The output of PV module changes with direction of sun, irradiance level and temperature. There is a single maximum power point in I-V characteristics of a PV module under a particular operating condition. It is desired that PV module operates close to the maximum power point which occurs at the knee point of I-V characteristics. For the purpose of research a DC– DC boost converter has been connected at the output of the PV panel. The MPPT controller determines the duty cycle of the boost converter to achieve the required extraction of power at maximum power point. *Perturb and Observe* (P&O) method has been be used in research for carrying out the MPPT. The flowchart for P&O algorithm is shown in Figure 2.5.

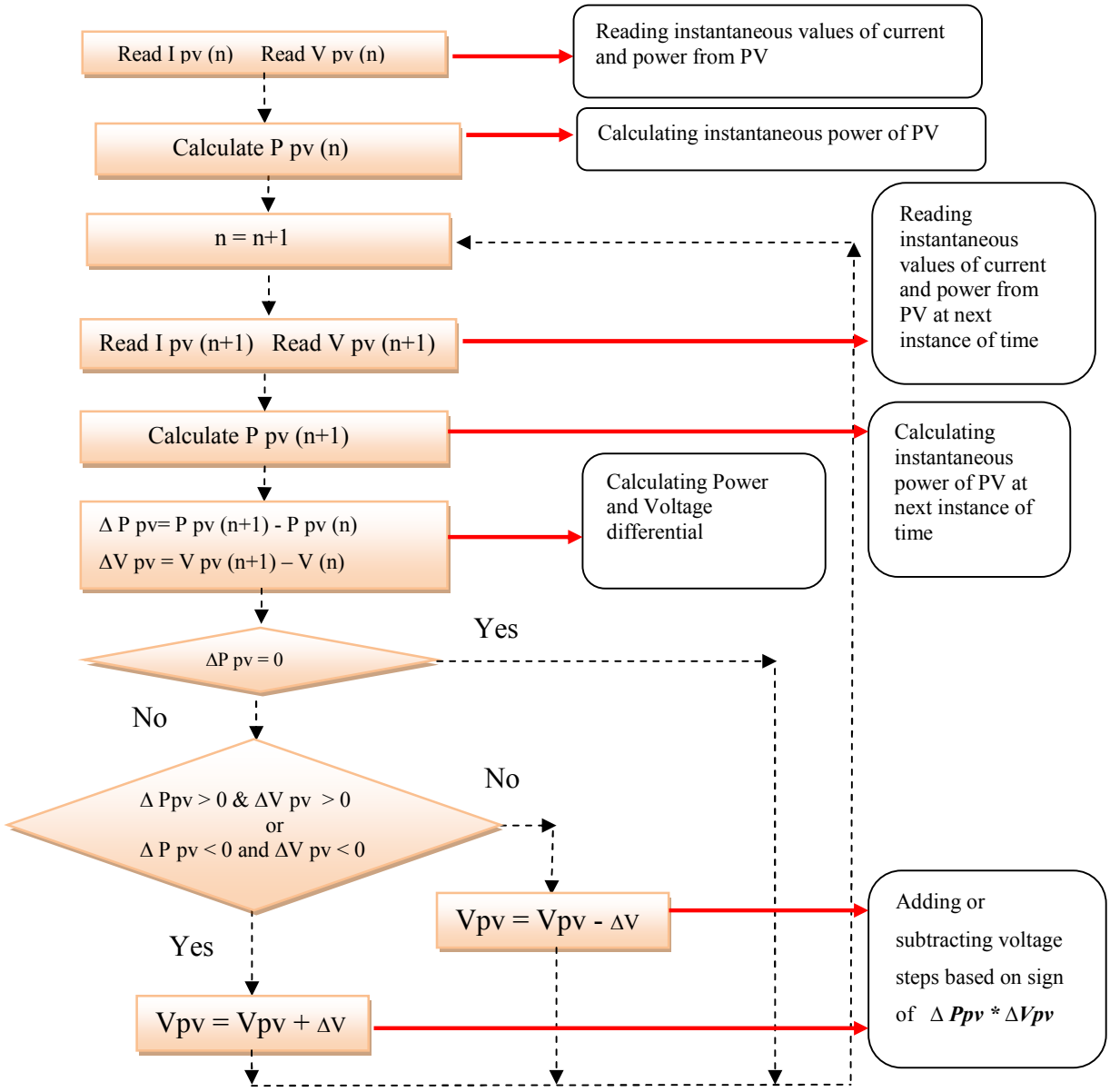

Figure 2.5 Flow-chart for P&O MPPT Algorithm

PSCAD model for P&O MPPT algorithm has been developed and details of model have been provided in Figure A.2 of Appendix A. The result of simulation is shown in Figure 2.6. It can be seen that at maximum power point is detected based on the algorithm

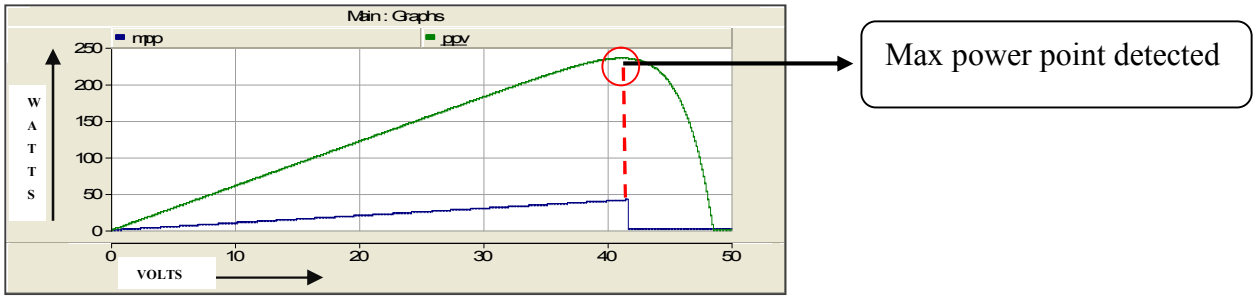

Figure 2.6 Maximum power point detected by MPPT model developed in PSCAD

The value of MPP detected is same as the data sheet value of E19/238 solar panel. As described above the output of MPPT controller is used to set reference for setting the duty cycle of the DC-DC converter. This is done by comparing the MPPT output with metered voltage output at PV output and the error is then fed to proportional-integral (PI) controller to generate the necessary reference for duty cycle of DC-DC converter. A converter has been modelled in PSCAD with current source and output of the simulation is as shown in Figure 2.7. Input voltage has been stepped up by the DC-DC boost converter.

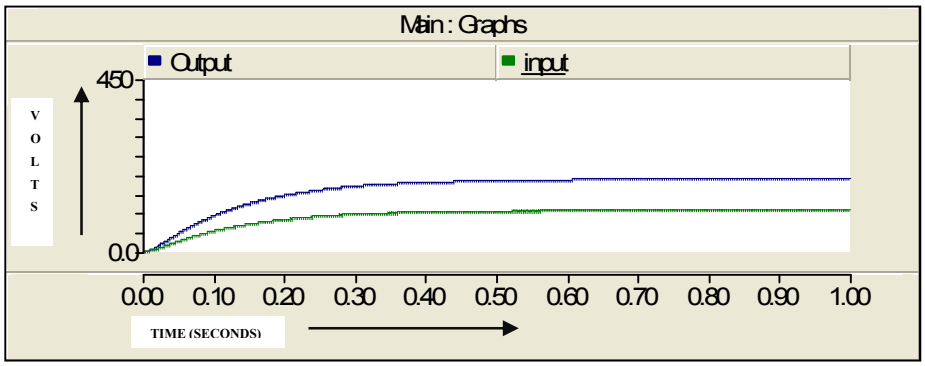

Figure 2.7 Input and output voltage waveform of boost converter

Complete design procedure for DC-DC boost converter has been detailed below. The PSCAD model details have been provided in Figure A.3 of Appendix A. Figure 2.8 is the circuit arrangement of a DC-DC boost converter. L and C out are the boost converter inductance and capacitance. The capacitor C holds the voltage for the boost converter.

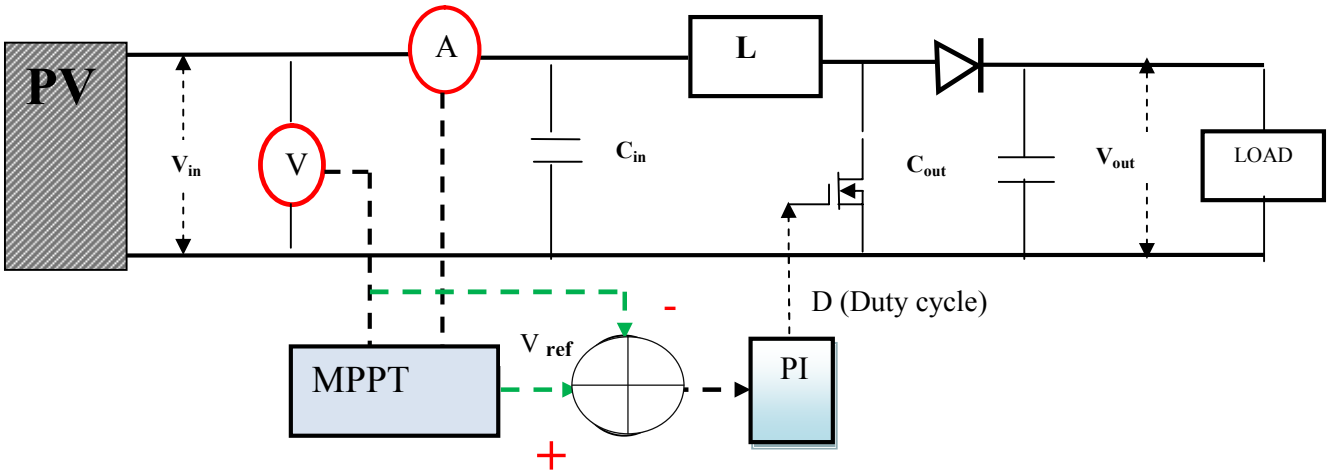

Figure 2.8 Block Diagram for Boost Converter

The output voltage of converter is related to the duty cycle by equation (2.25) given below

A DC-DC converter can operate either in continuous conduction mode (CCM) or discontinuous conduction mode (DCM). In continuous conduction mode, the output voltage of converter can be calculated using equation 2.25[8].

$$V_{out} = \frac{V_{in}}{(1-D)} \tag{2.25}$$

In equation (2.25), V_{in} is the input voltage V_{pv}, V_{out} is the output voltage V_{dc} and D is the duty cycle of the converter.

For designing boost converter values of inductance L and capacitance C has been calculated.

The parameter L shall be as per equation (2.26)

$$L \geq [(1-D)^2 D]\min \times \frac{R_{min}}{2f_{IGBT}} \tag{2.26}$$

f_{IGBT} is the switching frequency of IGBT (6kHz has been assumed for the purpose of design)

For the purpose of this research, total power rating for PV panel considered is 2856 watts. The voltage at MPP for each panel is 40.5 Volts and Current rating of each panel at MPP is 5.88 Amps. The power rating of each panel is 238 Watts. The arrangement of the PV panels is shown is the Figure 2.9.

Considering output voltage of DC-DC converter to be 400V,

$$R_{min} = \frac{400^2}{2856} = 56\Omega$$

At STC the voltage at maximum power point is $40.5 \times 4 = 162V$

At an ambient temperature of 50°C at irradiance of 1000 Watts /m^2, voltage at maximum power point = ($34.2 \times 4 = 137V$ a.c. approximately)

The duty cycle will therefore vary between the requirements at STC and at 50°C and the boundary limits shall be as shown below:

$$1 - \left(\frac{162}{400}\right) < D < 1 - \left(\frac{137}{400}\right)$$

$$0.59 < D < 0.65$$

$$[(1-D)^2 D]min = [(1-0.65)^2 \times 0.65] = 0.0796$$

$$L \geq 0.0796 \times \left(\frac{56}{2 \times 6000}\right) \geq 371\mu H(0.0003H)$$

The parameter C_{out} for continuous conduction shall be as per equation (2.27)

$$C_{out} \geq \frac{D_{max} V_{out}}{2 f_{IGBT} R_{min} V_r} \quad (2.27)$$

$\frac{V_r}{V_{out}}$ is the ripple ratio target and for this case it is considered 0.01%

$C_{out} \geq \frac{0.65 \times 10^4}{(2 \times 6000 \times 56)}$ =9670 µF

The converter has been designed with L= 0.0003 H and C_{out} = 10000 µF

The converter response is steady but further improvement is possible in the model to achieve more accurate results.

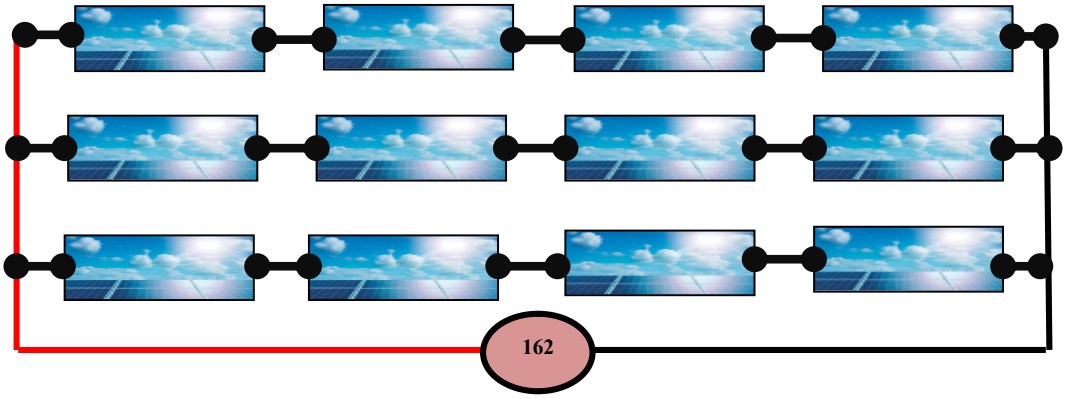

Figure 2.9 Arrangement of E19/238 Sunpower Panels – Total capacity- 2856 Watts

2.3 Inverter

A six pulse single phase inverter model has been developed in PSCAD. Its Sinusoidal PWM firing control circuit has been also developed and the model worked successfully. The idea behind developing this model is to make a functional single phase inverter in PSCAD and then integrate it with overall system controls of grid tied system to study its characteristics during fault.

Figure 2.10 shows the inverter pulse width modulated (PWM) output voltage waveform for single phase inverter generated by PSCAD model during a simulation run at switching frequency of 6000 Hz.

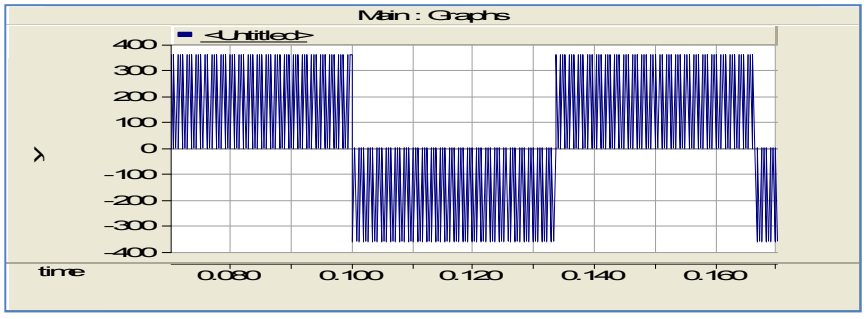

Figure 2.10 Simulation output -Single phase PV inverter output voltage

2.4 Control strategy of grid tied inverter

For the purpose of control, grid is considered as a voltage source with infinite capacity controlling the output current of the inverter PWM algorithm of the grid connected inverter is based on a double closed loop current control as shown in Figure 2.11.

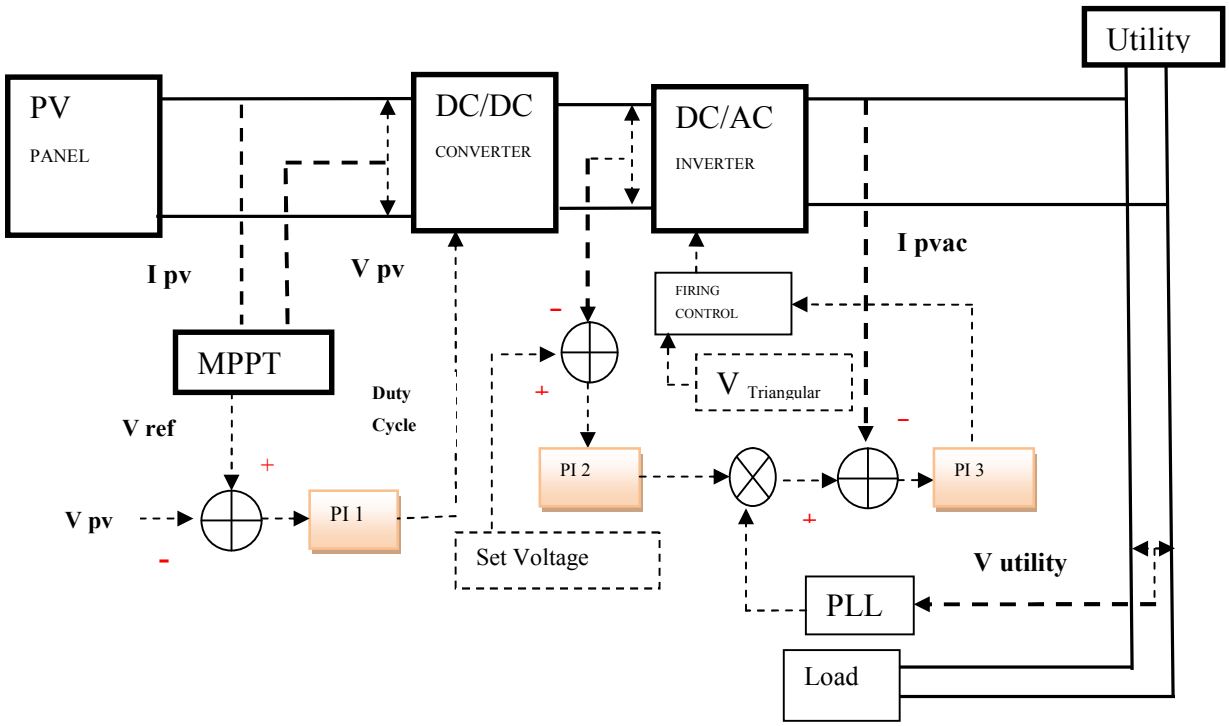

Figure 2.11 Block diagram-grid tied PV system controls

The voltage loop is the outer loop and current loop is the inner loop. The outer loop functions to stabilize the DC voltage of the photovoltaic array. The aim of inner loop is to track the given current signal. PLL (Phase Locked Loop) is used to achieve the output current of the inverter such that it is in sinusoidal and in phase with utility voltage .The reference current produced by the voltage loop is multiplied by Sin θ which is captured from PLL. This produces an AC reference .The AC reference is the compared with the load current in grid to generate reference for PWM inverter switching. To reduce steady state error and increase system stability PI type controller is used in current loop. To reduce disadvantageous perturbation of grid voltage, feed forward compensation is added to the system. This method does not change system characteristics but improves stability. A PSCAD model for a single phase grid tied inverter has been developed with all its control aspects as described in this section. PSCAD model for the PV system has been shown in Figure A.5 of Appendix A.

2.5 PSCAD model and simulation outputs

Simulation results for PV system with inverter have been obtained. Both normal operation and operation in faulted condition has been simulated to investigate the behaviour of voltage and current parameters of the inverter.

2.5.1 Behaviour of inverter during normal operation

Load voltage with inverter in standalone mode and grid tied mode are shown in Figure 2.12.This represents normal operation (i.e. operation with no fault at inverter output).The outputs indicate that a steady load voltage of approximately 230Va.c. rms is available at load terminals.

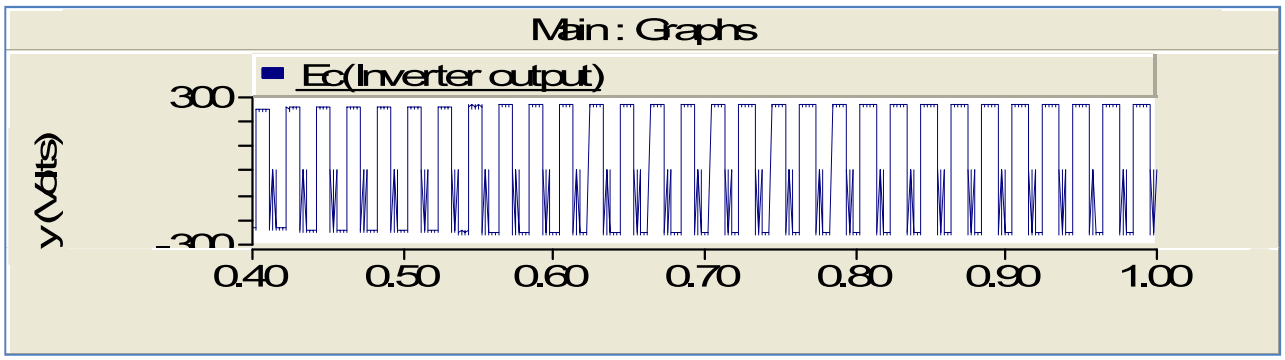

Figure 2.12 Load voltage – Inverter stand alone operation

A single phase load of 2 kVA has been considered for modeling and load has been modeled as a resistance of 26.4Ω. This selection represents a 2 kVA load at unity power factor. At an inverter output voltage of 230V a.c., the load current shall be 8.7A when connected to inverter output. Based on the 2856 Watts of PV power the output inverter is rated for 2.5 kVA. The rated current of the inverter at 230V a.c. shall be 10.8 amps. In the Figure 2.13, simulation output for rms voltage and load current is shown during normal inverter operation. The simulation output closely matches the calculated current flow and the inverter output voltage considered.

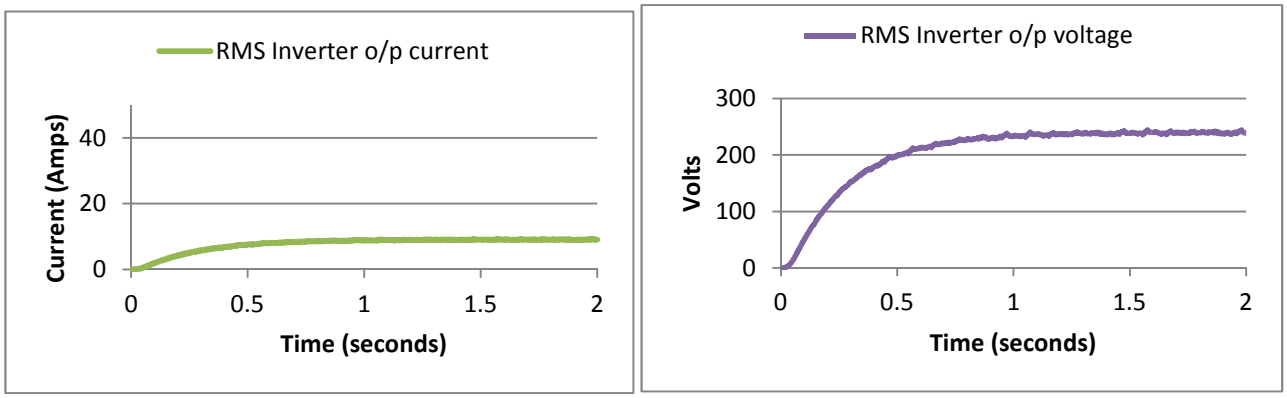

Figure 2.13 Load voltage and load current – Inverter stand alone operation

Simulation output of inverter output voltage during grid tied operation is shown in Figure 2.14.

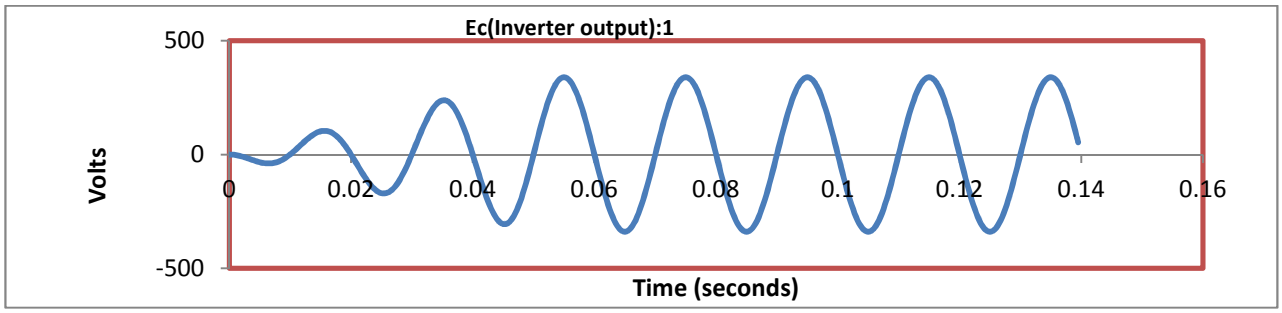

Figure 2.14 Load voltage – Inverter Grid tied operation

2.5.2 Behaviour of grid tied inverter during fault

Following the development of the complete model of grid tied inverter the behaviour of the inverter during fault has been investigated. It is a well accepted fact that the inverter behaves very differently during faulted conditions as compared to synchronous generator. While the synchronous generators can contribute 6 to 8 time of rated current during fault, inverters are current limiting sources which generally provides no more than 2 to 2.5 times the rated current. Previous studies done to establish this has been discussed in great details in chapter 3. The purpose of the study is to establish the accuracy of the model in terms of fault current contribution which is the major subject of this research.

For the purpose of the investigation fault current has been simulated at the inverter output at 1 second for 0.4 seconds and the fault current and output voltage profile has been observed. Figure 2.15 shows the results voltage and current profile obtained.

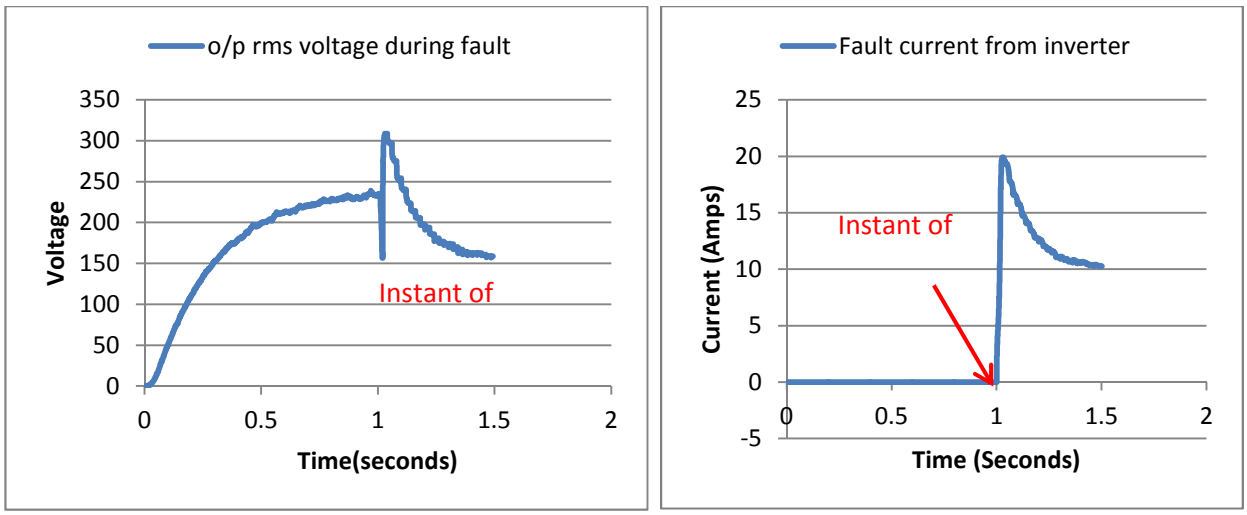

Figure 2.15 Voltage and current profile during fault

It is observed that the voltage spikes from 230 V to around 300 V during the first instant of fault and then gradually ramps down to around 150 V in 25 cycles. The fault current rises to around 20 amps and then gradually reduces to around 10 amps in 25 cycles. The peak current however, sustains for around 5cycles only. The inverter being rated at 10.8 amps full load capacity is expected to deliver 2 times of rated current (i.e. 21.6 amps) during fault. The simulation output is in good agreement with the estimated value of fault current.

When tied to grid the additional fault current contribution from inverter will increase the fault level at the point of fault. Due to relatively smaller contribution of fault current as compared to fault contribution from grid, the inverter contribution may not always impact the protection coordination of an existing system. However, such assumption does not hold well with cumulative contribution of fault current from multiple grid connected PV system in network. This issue has been elaborated in chapters 4 and chapter 5 using different case studies. The fault contribution from PV inverter may not be in phase with fault contribution from the grid during the first few cycles and time varying contribution has is possible. This aspect has been discussed in chapter 3 using studies done in the past. A simulation output is shown in Figure 2.16 for a fault in grid tied configuration. For a single line to ground fault initiated at 1 second, the time varying component of the contribution from PV inverter has been further illustrated in Figure 2.16.

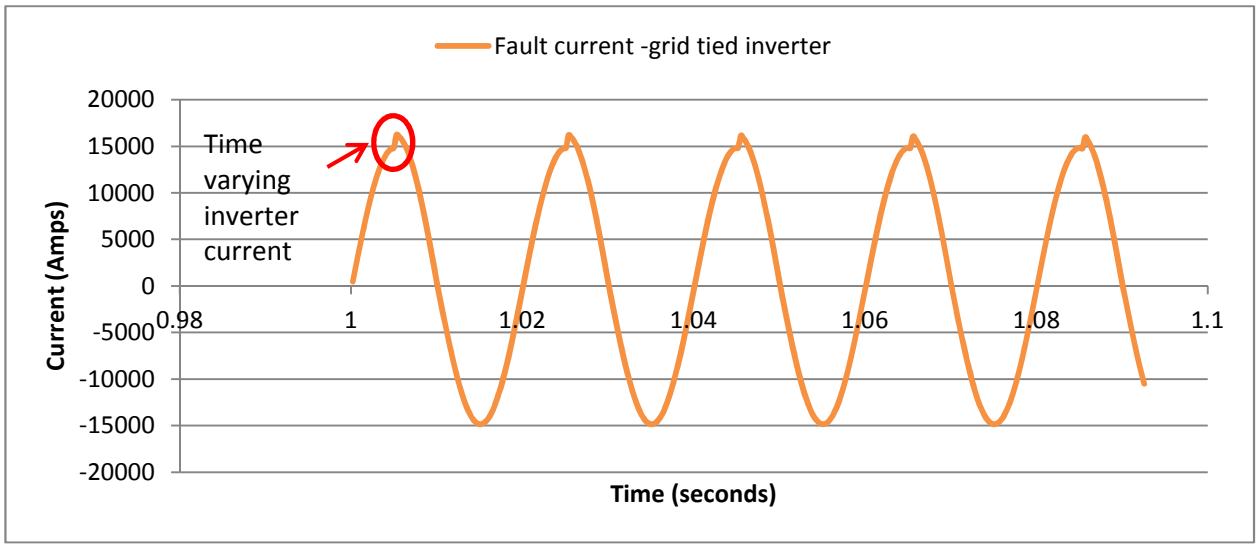

Figure 2.16 Fault current profile during fault

The impact of fault contribution from PV inverter on network protection has been studied in details in this research work.

2.6 Summary

This chapter presents the fundamentals components of PV systems. The functionality of each component of a grid tied PV system and the associated control mechanism has been discussed in details. Various design issues for the individual components of PV system has been provided. A detailed description of PSCAD models of individual components of the PV system as well as the complete system built to investigate the features of grid tied inverter has been presented. Inverter operation in both grid tied mode and stand alone mode has been discussed. Description of simulations carried out with special reference to fault contribution from inverter has been provided. The contribution from inverter during a network fault and its impact on network protection is the main subject of interest in this research and has been discussed in the subsequent chapters. With increase in PV penetration in network this issue are of significant interest. Such wide scale integration of local generators in network is referred as distributed generation or embedded generation. Research work has been done in the past to investigate this issue for integration of various types of distributed generators in general as well as specifically for PV type distributed generators. In the next chapter the research done in the past on the subject has been discussed and comprehensive description of works done in the past has been provided.

Chapter 3 Protection Problems in Distributed Generation

In this chapter a review of literature of the work done in the past to identify the problems caused by distributed generation is discussed. First section of this chapter discusses the problems associated with distributed generators of all types in general. The second part of this chapter discusses problems specific to PV system (i.e. for inverter interfaced DG) where the magnitude of fault current contribution is relatively much lesser in magnitude as compared to conventional synchronous generator.

3.1 General protection issues in distributed generation

This section describes the various issues associated with system protection in distributed generation.

3.1.1 Protection coordination issues

There are several new situations introduced when there is a possibility of bidirectional power flow .These situations were not considered when designing the protection systems of present distribution networks which are based on radial power flow. These issues were studied by Brahma and Girgis [9] and are discussed in this section.

In the Figure 3.1, if we consider that no distributed generator (DG1) is connected, for a coordinated system, fuse F1 and fuse F2 are selected so that for any fault on feeder1, F1 operates before F2. This is possible if total clearing (TC) characteristic of F1 is below the minimum melting (MM) characteristics of F2 by a safe margin for any feeder fault.

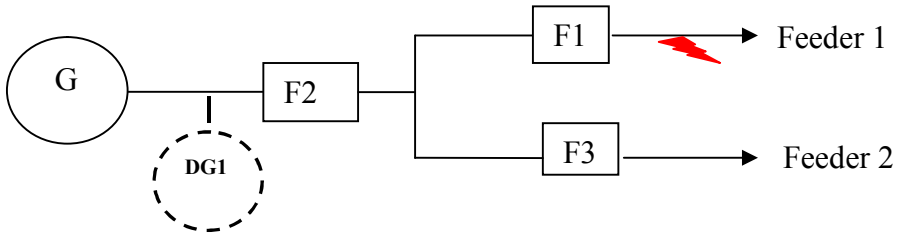

Figure 3.1 DG1 connected upstream of fault location

For the same network, if a distributed generator DG1 is added as shown in Figure 3.1 and consider a fault in feeder1, the maximum and minimum fault current will increase from the source side due to the upstream DG unit. In this case fuse coordination is not likely to be affected if fuses can still coordinate with the changed level of fault currents. This is because fuses will see only downstream faults. For the same network, if a distributed generator DG2 is connected in the downstream of feeder 1, for a fault as shown in Figure 3.2, fuse F2 has to operate before fuse F1 to maintain system reliability. This is not achievable as both F1 and F2 will see same magnitude of fault current in either case (i.e. for both downstream and upstream faults). This illustrates a case of fuse-fuse coordination problem with distributed generator in network.

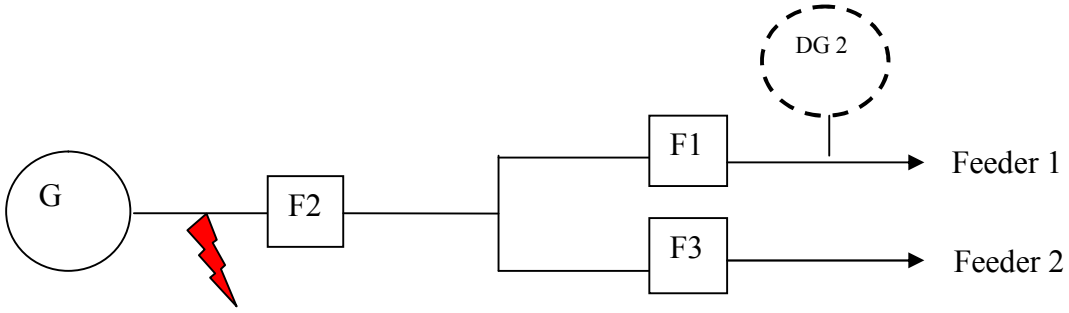

Figure 3.2 DG1 connected downstream of fault

In the network discussed above a distributed generator DG3 is added as shown in Figure 3.3 and two different cases of faults are considered and the impact of DG size on protection coordination.

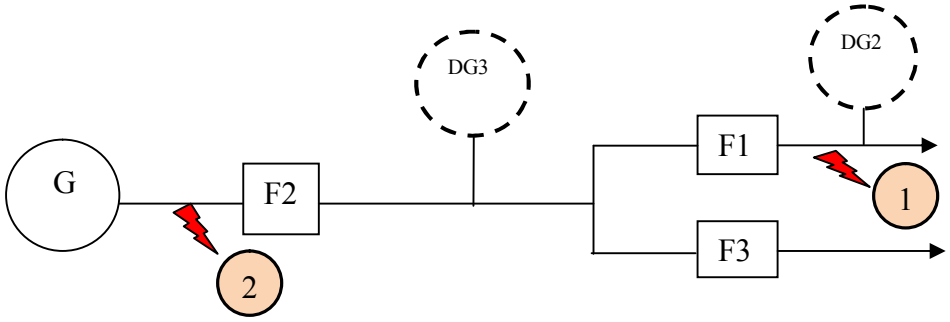

Figure 3.3 Impact of DG size on fuse coordination

If fault occurs at location 1, current passing though fuse F2 (I_{F2}) is less than the current flowing through fuse F1 (I_{F1}), while if fault is at location 2, I_{F2} is greater than I_{F1}.The difference in magnitude of I_{F1} and I_{F2} depends on the size of generator DG3. When $I_{F1}>I_{F2}$ the coordination always holds well. When $I_{F2} > I_{F1}$ the difference between the magnitude of I_{F1} and I_{F2} decides the level up to which the coordination will hold well. If the difference in magnitude between I_{F1} and I_{F2} is not above a minimum value, the coordination will not hold well. As the difference in the magnitude of I_{F2} and I_{F1} depends on the size of DG3, when the size of DG3 exceeds a size which is

adequate to provide enough fault current to ensure minimum difference in magnitude between I_{F1} and $I_{F2,}$ the protection coordination will not be disturbed.

Distributed generator also has the potential of disturbing the protection coordination between fuse and recloser. This issue has been discussed in details in several papers [9], [10], [11] and [12]. The recloser fuse coordination problem caused by distributed generators has been described below.

In the network shown in Figure 3.4, it is initially assumed that the DG is not connected.

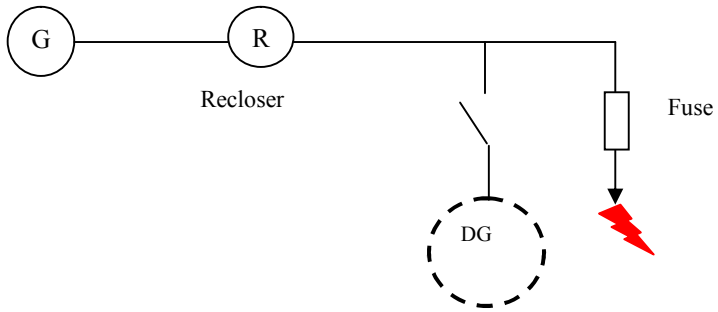

Figure 3.4 Fuse – recloser coordination –Impact of DG placed between recloser and fuse

The recloser on the main line has to coordinate with this fuse for all faults taking place on the feeder. For all faults on load feeder current in the fuse and recloser will be the same. The two devices should coordinate for all values of fault current on the load feeder. Coordination curve is shown in Figure3.5.

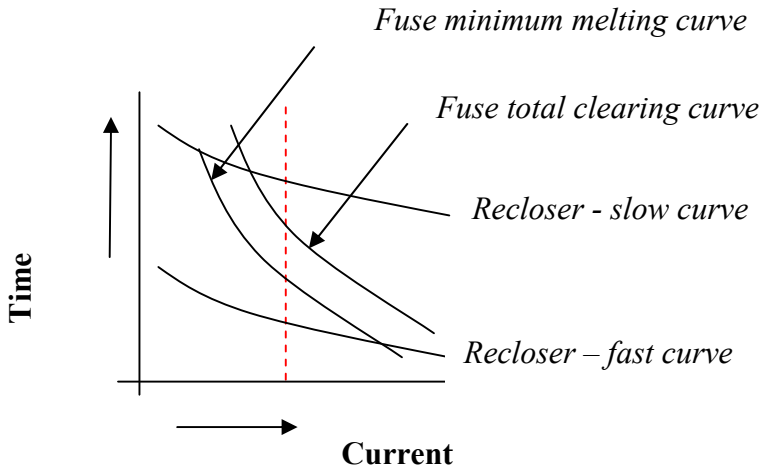

Figure 3.5 Fuse – recloser coordination

The protection principle is to ensure that the fuse should only operate for a permanent fault in load feeder. For temporary faults recloser should disconnect the circuit with fast operation and give the fault a chance to clear. If the fault is permanent then only the fuse will open. Recloser slow mode is a backup to the fuse. Relative location of recloser and fuse has also a role to determine the criteria of coordination.

Now if the DG is considered then the fault current seen by the recloser and fuse shall not be same. If the fault current through the fuse is I_F and the fault current seen by the recloser is I_R then the coordination holds good only if fault currents lie within allowed margin. If the disparity between I_F and I_R is more than the margin, fuse will operate before the recloser operates. This disparity will depend upon the size of DG and distance of the DG from the feeder. Thus if DG injects more fault-current, chances of coordination being lost are more.

Other problem with recloser closing operation after fast mode opening is that the recloser normally energizes a dead system if there were no DGs but in this case it connect back to live system. If this closing operation is done without synchronization it can lead to severe damage of DG. Girgis and Brahma [9] also studied problems faced in relay coordination with distributed generation and problems are similar to fuse coordination.

Chaitusaney and Yokoyama [10] studied the problem of DG and reduced reliability of supply due to fuse blowing and false tripping (Sympathetic tripping).

The problem of fuse blowing is illustrated in Figure 3.6. In a conventional protection temporary fault occurring at lateral feeder should be discriminated by fast operating recloser .However, with DG installed this may not occur (as discussed in fuse recloser coordination problem) and fuse may clear fault thus reducing reliability.

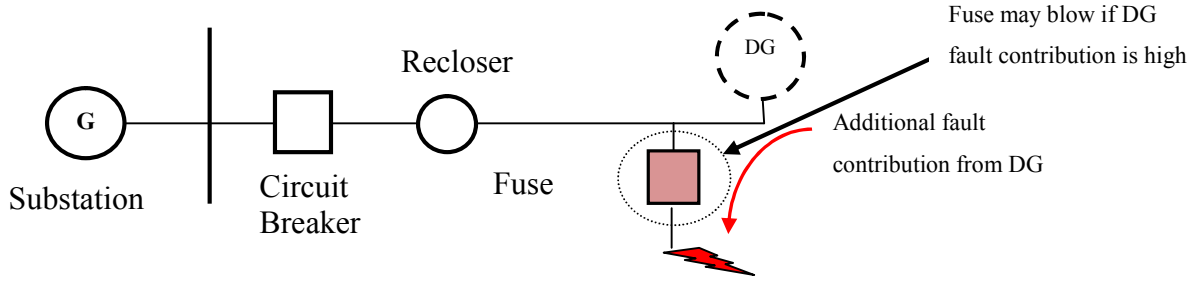

Figure 3.6 Fuse blowing due to fuse – recloser miscoordination

The problem of false tripping is illustrated using the Figure 3.7. When a fault occurs in feeder 2, the circuit breaker in feeder 2 should trip, however, the circuit breaker in feeder 1 may operate as DG will try to feed fault and cause unreasonable interruption of electricity. False tripping on healthy feeder may be somewhat solved by using directional over-current relay for the circuit breakers.

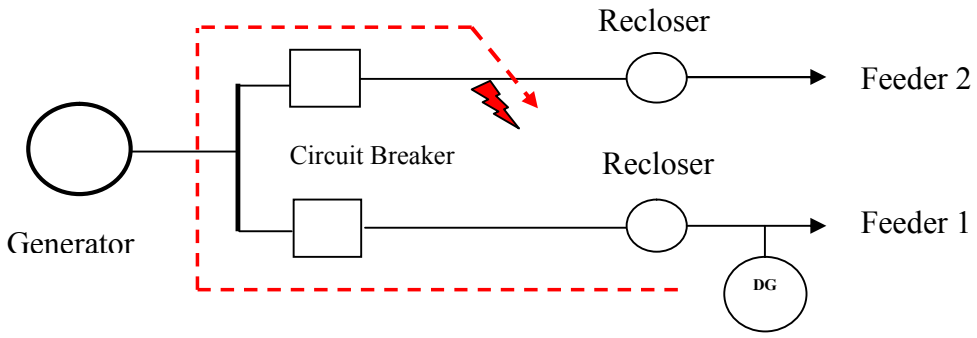

Figure 3.7 False tripping of circuit breaker (sympathetic tripping)

Chaitusaney and Yokoyama [10] also discussed a method of DG sizing to resolve false fuse blowing and achieving better fuse recloser coordination in systems with DG. As the recloser fuse coordination holds good up to a particular size of DG it is important to calculate the optimum DG size that can be integrated in a system without disturbing the coordination.

Figure 3.8 shows contribution of fault current from substation and DG during a fault.

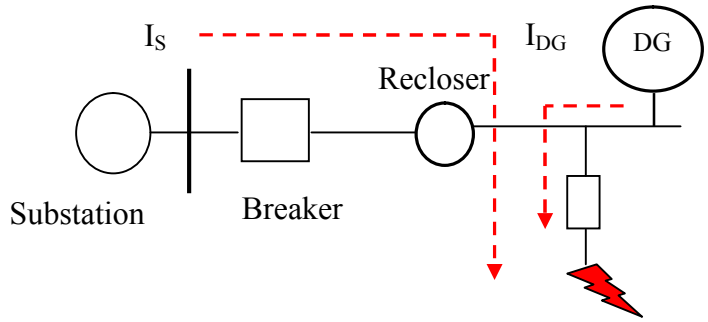

Figure 3.8 False-recloser coordination and DG sizing

If fault current from DG = I_{DG}, fault current from Substation = I_S

The DG size should be selected so that,

$$I_S + I_{DG} < I_{Fuse\ margin} \tag{3.1}$$

$I_{Fuse\ margin}$ is the maximum fault current that can be allowed to flow through fuse without disturbing the coordination. If current more than $I_{Fuse\ margin}$ flows through the fuse, coordination will be lost.

Recloser operating time can be represented by the equation below

$$t = \frac{A}{\left[\left(\frac{I_S}{I_P}\right)^P - 1\right]} + B \tag{3.2}$$

Where A, B and P are curve constants and I_P is the set value of current for tripping

The fuse operating time can be represented by the equation below

$$\log(t) = a.\log(I) + b \tag{3.3}$$

Where 'I' is the current flowing through the fuse and 'a' and 'b' are curve constants

When $I_s + I_{DG} = I$ flows through fuse, $I_{DG} = 10^{\frac{[\log(t)-b]}{a}} - I_s$ (3.4)

For the condition $I_S + I_{DG} < I_{Fuse\ margin}$ to hold good, fuse tripping time shall not exceed recloser tripping time and therefore to calculate maximum size for DG, fuse tripping size shall be considered equal to maximum tripping time of recloser.

Substituting the value of time 't' in equation (3.4) by recloser tripping time from equation (3.2), we can find maximum value of I_{DG} which will keep the coordination undisturbed.

Size of DG can therefore be stated in terms of short circuit MVA as

Short circuit $MVA = \sqrt{3} \times V_{DG} \times I_{DG}$ (3.5)

V_{DG} is the line to line voltage of the distributed generator.

Using value of I_{DG} from equation (3.4) and using equation (3.5) and if V_{DG} is the DG voltage, maximum capacity of DG can be calculated as:

$$S_{DG} = \sqrt{3} \times V_{DG} \times \left(10^{\frac{[\log(t)-b]}{a}} - I_s\right) \tag{3.6}$$

The subject of fuse recloser coordination has also been discussed by Chaitusaney and Yokogama together with the cost function for optimization [11]. The paper has discussed the case studies of using optimally DG sized (to avoid fuse recloser coordination) in network using conventional Optimal Power Flow (OFP) of distribution system in order to evaluate cost issues. The cost function in the study is combination of electricity cost both from utility and DG and the outage cost from energy not supplied. For calculating the outage cost the electricity cost from the utility substation and DG are assumed to be equal. Also average cost per MW-hr has been used instead of varying cost. Outage cost has been considered in two portions. The first portion is due to failure of system equipment and second portion is due to capacity limit of DG which is either due to DG capacity or protection coordination constraints.

The cost function can be written as –

$$\text{Energy Cost} = \text{Electricity Cost}_{\text{Substation}} + \text{Electricity Cost}_{\text{DG}} + \text{Outage Cost}_{\text{Equipment Failure}} + \text{Outage Cost}_{\text{DG limit}} \quad (3.7)$$

$$\text{Energy cost} = (\text{CS} \times \text{QS}) + (\text{CDG} \times \text{QDG}) + (\text{C0} \times \text{Q01}) + (\text{C0} \times \text{Q02}) \quad (3.8)$$

CS- Electricity cost of utility substation ($/MW-hr)

QS- Dispatched energy from utility substation (MW)

CDG- Electricity cost of utility substation ($/MW-hr)

QDG- Dispatched energy from utility substation (MW)

C0-Cost of Electricity Outage ($/MW-hr)

Q01-Energy not supplied due to equipment failure (MW)

Q02-Energy not supplied due to DG limit (MW)

The constraints for traditional OPF are set of power flow equations, real and reactive power limits and voltage angle limits. In addition to these constraints, the constraint of protection coordination needs to be simultaneously included in the calculation.

Chaitusaney and Yokogama further studied the issue of system reliability [12] based on fuse recloser coordination problem. In general load point indices has been used to evaluate the reliability of distribution systems. For the i^{th} system component, three systems have used to evaluate the system reliability $\boldsymbol{\lambda_i}$ (average failure rate f/yr), $\mathbf{r_i}$ (average outage time in hours) and $\mathbf{U_i}$ (average annual outage time in hours/yr). In this analysis $\boldsymbol{\lambda_i}$ is assumed to be resulted from electricity faults regarding thermal limits, planned outage etc.

The average failure rate can be written as below

$$\lambda_i = \lambda_{p,i} + \lambda_{t,i} \quad (3.9)$$

Where $\lambda_{p,i}$ and $\lambda_{t,i}$ are the permanent and temporary average failure rates .

Both of them give different average outage time r_{pi} and r_{ti} for permanent and temporary faults.

The average annual outage time of faults can be calculated by the following equations –

$$U_{pi} = \lambda_{p,i} \times r_{p,i} \quad (3.10)$$

$$U_{ti} = \lambda_{t,i} \times r_{p,i} \quad (3.11)$$

Therefore the total annual outage time can be written as –

$$U_i = U_{p,i} + U_{t,i} \quad (3.12)$$

The above analysis holds well, with proper recloser fuse coordination. However, if due to distributed generation, recloser - fuse coordination is disturbed temporary faults may be cleared by fuse instead of recloser. This causes the average interruption time for temporary faults to change to repair time of the fuse $\mathbf{r}_{f,i}$ .The protection system of each DG system is different. Some DG sources disconnect immediately in an abnormal condition whereas some DG feeds for several cycles after fault. Due to such uncertainty the of the DG systems, the fault current from the DG sources will affect recloser –fuse miscoordination in a probabilistic manner. Therefore, if the probability of miscoordination 'p' is given, the average annual outage time for temporary faults can be formulated as follows:

$$U_{t,i} = \lambda_{t,i} \times \left[(1-p) \times r_{t,i} + p \times r_{f,i}\right] \quad (3.13)$$

Duration of $\mathbf{r}_{t,i}$ is very negligible and equation 3.13 can be written as

$$U_{t,i} = \lambda_{t,i} \times p \times r_{f,i} \quad (3.14)$$

As $\mathbf{r}_{f,i}$ is definitely longer than conventional temporary fault clearing duration, the load experiences longer interruption which will be considered as a permanent fault.

3.1.2 Impact of fault current limiters in distributed generators

To minimize the impact of DG in power delivery systems (PDS) an alternate approach was studied by El Khattam and Sidhu [13]. The concept is to introduce fault current limiters (FCL) to limit the impact of DGs during fault.

The current practice is to disconnect DGs during fault to restore original relay coordination. This however, causes loss of DG power due to temporary faults and synchronization problems for reconnecting those DGs into PDS. By using FCL in series with DGs to limit fault current helps in

suppressing the DG impact on original relay setting during faults. If this approach is used disconnection of DG during faults is not required.

In this approach most optimal relay setting are obtained by minimizing the total primary operating time in the original PDS without DG in two phase process. In the two phases proposed optimization model, phase I model is formulated as nonlinear programming and phase II model is formulated using linear programming. When DG is introduced in the system the original coordination of PDS will be disturbed. Based on the optimum relay settings and engineer's experience, the FCL impedance, type and minimum value, required to restore the original PDS relay coordination are provided with revised coordination time interval (RCTI) between relays. The relay setting optimization method is described in the section below.

The total time objective function J for N primary relay near end fault is minimized, subject to various constraints. These constraints are relay setting constraints and back-up relay constraints.

Minimize $J = \sum_{i=1}^{n} t_i$ (3.15)

The coordination constraints are

- Relay setting constraints
- Relay operating time
- Back up relay coordination time interval

Two sets of constraints are introduced for each optimization model's phase.

An algorithm is used to obtain most optimal relay setting. In this method, Phase I of optimization model is done to obtain I_P (relay pick-up setting) and TDS (time delay setting) and Phase II of optimization model is computed to obtain TDS and CTI (Coordination time interval). In phase I, I_P is fixed. In phase II, TDS is fixed and it is checked whether or not CTI constraints are satisfied. If CTI constraints are satisfied then most optimum relay setting is obtained. If CTI constraints are not satisfied then using engineer's experience either RCTI (Revised coordination time interval) or new I_P is set for the optimization model and phase II optimization process is repeated. The iterative process continues till the optimal relay setting is obtained.

As introducing DG in the PDS will disturb relay setting, introducing FCL is required for restoring original relay settings. The process for determining the FCL parameters is described below.

In this process FCL type and minimum impedance is determined. The impedance value of FCL, Z_FCL is a function of individual DG capacity (SDG), number of DGs (NDG), candidate DG location (CDGL) and fault location (fl) in the PDS.

$$z_{FCL_i} = f(SDG, NDG, CDGL, fl) \forall \mathrm{i} \in \mathrm{NDG}, \mathrm{NDG} \in \mathrm{CDGL} \quad (3.16)$$

If NDG, and CDGL are known then it is possible to calculate relay operating time and identify backup primary relay pairs that have CTI less than preset RCTI, while maintaining the relay settings unaltered. The RCTI value is chosen on the basis of engineer's experience and feasible cost of commercially available Z_FCL. The process of selecting Z_FCL is iterative starting from zero value and a low value based on commercially available Z_FCL. The value is increase until the lowest CTI_ $_{j,i}$ in the PDS is greater or equal to RCTI. Each time Z_FCL value changes, the PDS has to be modified taking into consideration the new value of Z_FCL during fault calculation. After obtaining the minimum value of Z_FCL, the most economical value is chosen.

3.1.3 Fault contribution of distributed generators

As discussed earlier, fault current contribution from the distributed generator disturbs the existing relay coordination system designed for radial distribution systems. While the fault current will always be increased by adding generation, the consequences on the fault clearing elements can be in two opposite directions. If a fault occurs upstream of fault clearing device (i.e. towards substation), the clearing device will see the current flowing upstream to contribute to the fault. If a fault occurs downstream of the fault detection and clearing device , the fault seen by the clearing device will be reduced and may even be shadowed by the contribution of local generation and thus remain undetected.

Turcotte and Katiraei [14] discussed the issues of DG interconnection in terms of total fault current contribution and changes in short circuit capacity requirements of circuit breakers or under load disconnecting switch only. The circuit breaker must carry fault current until opening of protective device. The minimum opening time of circuit breaker is 3, 5 or 8 cycles. Consequently a DG source capable of tripping within 50 ms will have no effective contribution to short circuit capacity of system. The investigation highlights the distinction between rotating machines and inverter based power sources with respect of their fault contribution. For the purpose of investigation a PSCAD model of a typical distribution grid was developed for an inverter based photovoltaic plant and the same work was done with a synchronous generator model representing a small hydro plant. The current measurement was done at fault location, at generation plant and at bus breaker. The

distributed generation capacity was considered as 7.5 MW (both photovoltaic and Hydro electric) and plants were considered located at a distance of 25km from substation. The fault was studied for two different scenarios i.e. fault at substation and fault at end of line.

The study concluded that the photovoltaic generation inverters are capable of stopping delivery of power within first cycle or few cycles subsequent to fault. The fast disconnection is achieved using instantaneous protection features (over-current and under-voltage protection). As a result the short circuit contribution of inverter based DG units are insignificant. Even if the inverter protection function would be dysfunctional, the inverters will feed fault current in the range of 1.1 to 1.5 times their nominal current which is significantly less that fault current contribution from rotating machines which is the range of 4 to 10 times the nominal current. The study also concluded that while medium voltage rotating machines are more prone to feed fault, their impact on feeder breaker fault duty is minimum or non- existent when they are located at the end of the line.

3.1.4 Methods to improve time-current coordination in distributed generation

Evolutionary Programming

So and Li [15] studied the application of evolutionary programming technique for time coordination methods. For any radial system without DGs the protection relays are coordinated using time coordinated using time coordination method. When multiple DGs are connected to the radial distribution system the scenario however, changes. The fault level at different point changes depending on how many DGs are operating at a particular time. In such a situation it is not possible to apply conventional coordination method to obtain effective protection. A time coordination method (TCM) method is therefore designed to coordinate the protection system by simulating all faults at various locations and all system operating condition. It can find out all possible coordination pairs of relays that are necessary to be coordinated in various system conditions. The purpose is to search for an optimal protection setting to minimize the system disturbance time as well as time of interruption of customer supply.

The modified evolutionary programming technique that is tailor made for TCM is developed. It is a stochastic parallel search method for multi- variables. It employs a multi-point search methodology to find out optimum relay settings in a fixed number of generations with maximum satisfaction of coordination constraints .Relay settings will be in each generation and the newly generated relay settings will be passed to constraint checking and goodness of settings will be passed to constraint checking and the goodness of settings will be calculated for subsequent process.

In this process several set of relay settings are required to be generated randomly. Each set of relay settings will be checked against all system constraints and configuration. The effectiveness of relay settings is calculated using equation –

$$\text{Objective} = \propto \times \sum Ri + \beta \times \sum CMj + \gamma \times \sum CV^{\delta}{}_{K} \quad (3.17)$$

R_i, CM_j ,CV_k are the relay operation time at that particular system configuration i, the coordination margin difference between the coordination pair of relays j and the constraint violations of coordination pairs for relay k. α, β ,γ and δ are coefficients governing the amount of contribution to overall objective value. The supply reliability is calculated when each set of relay settings has passed the coordination checking process The TCM (Time coordination method) will stop after a fixed number of generations . The number of generations required to carry out optimum relay settings depends on pattern and number of initial relay settings.

The study was carried out in a Ring – Mains distribution system with distributed generators. The Time coordination method is applied to coordinate the relay settings with various combinations distributed generations. Investigation was carried out with different combinations of distributed generators in service and also without distributed generator in service. The investigation revealed that for one particular case with one distributed generator in service zero supply failure rate and zero interruption frequency can be achieved. The study concluded that future trend of development should be focused on automatic real time protection relays for systems with distributed generation.

Adaptive protection Schemes for Distribution Systems with High Penetration

In a distributed generation the effect of high DG penetration on coordination depends upon the size, type and placement of DG. Brahma and Girgis [16] suggested adaptive protection scheme as a solution to the problem in coordination. From the study of coordination problems it is clear and evident that o take care of coordination in a distributed generation system the protection devices has to be sensitive to direction. Fuses and reclosers are not direction sensitive features. It is economically impossible to replace all the reclosers with direction sensitive devices. Therefore a detailed analysis is required to identify exactly the problems of fuse-fuse and fuse-recloser coordination due to high penetration of DG. Once the problems are identified, solutions need to be found which are practically acceptable and independent of size number and placement of DG in distribution system. To avoid miscoordination without making changes to existing system is to disconnect all DGs instantaneously in case of fault. But this would mean disconnecting the DG even for temporary faults. In case of a fuse – recloser coordination studies have concluded that

coordination in presence of DG can be achieved with microprocessor based recloser. This recloser has to be made directional towards the downstream side of feeder. But in this case also all DG downstream of recloser has to be disconnected before first reclose takes place to avoid connection without synchronization. Throwing off all DG each time a temporary fault occurs is an unreliable and therefore adaptive scheme has been proposed.

In this scheme the whole system is divided into zones as shown in Figure 3.9

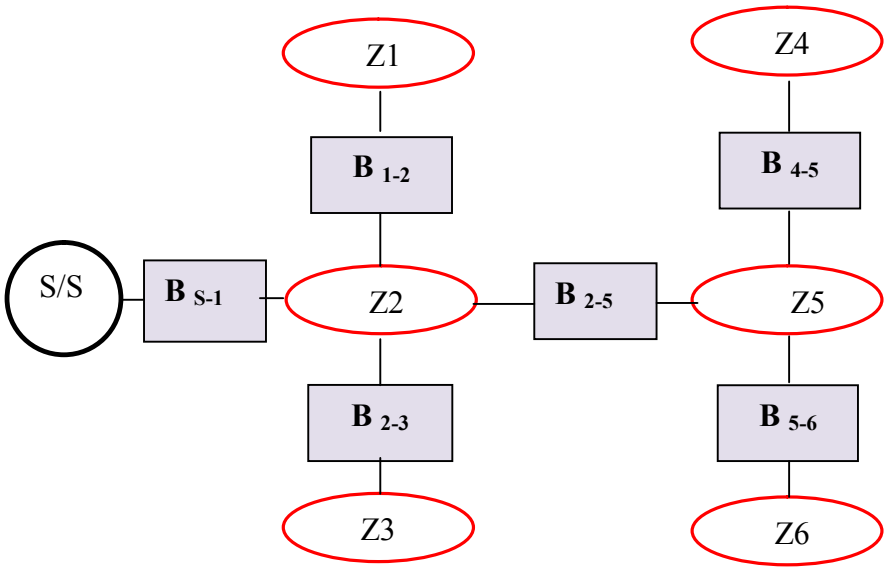

Figure 3.9 Distribution system divided into breaker separated zones

A zone will be formed such that it has a reasonable balance of load and DG, DG capacity being a little more than the load. One DG in the zone (the biggest in the zone) should have load frequency control. The zones needs to be separated by breakers that are communication capable and capable of repeatedly opening and closing on receiving signal from main relay located in substation. The relay would sense a fault, identify the type of fault, the faulted section and isolate the faulted zone by tripping the breaker. This scheme requires following continuous measurements are recommended for this scheme.

- Synchronized current vectors for all three phases from every DG in system and from main source.
- A signal indicating current direction in every zone- forming breakers.

This method requires a load flow study and a complete short –circuit analysis for all types of fault involving different types of fault at each bus .The load and short circuit analysis need to be updated

after every significant change in load, DG or the system configuration. Change in load or DG would require to running of the load flow and short circuit analysis and change in system configuration would require the bus admittance and impedance matrices as well.

For sensing the fault current phasors from the main source and all DGs are continuously monitored. When the system is normal the sum of three phasors will be equal to the total load of the system. In case of fault in any part of the system, this sum would exceed the total load substantially. Once a fault in the system is sensed, the total fault current in the each phase can be determined using the following simple equation

$$[I_{fabc}] = \sum_{i=1}^{n} [I_{fabc}] \tag{3.18}$$

Where [I $_{fabc}$] is the total fault current (phasors) in three phases, [I $_{fabc}$] $_{source\ i}$ is the fault current contribution in three phases from '*source i'* and 'n' is the total number of sources in the system.

In order to identify the faulted section of network is generally done by fuses. In this case coordination between fuses is lost and the faulted section needs to be determined before the fuse is damaged. A method is required to identify faulted section in order for the relay to give tripping signals to appropriate breakers for isolating the faulted zone. Fault contribution from each source is available on line. Total fault current is the sum of fault current from all sources. For fault point every source can be represented by a voltage source behind a Thevenin's impedance. If the fault point shifts from one bus to an adjoining bus, for a given type of fault, Thevenin's impedance to a given source can either increase or decrease. Thus as shown in Figure 3.10, if fault point shifts over a section (i-j) bus from one bus i to another bus j for a given type of fault, Thevenin's impedance to a given source can either continuously increase (IF_{MIN} to IF_{MAX}) or continuously decrease from ($IF_{MAX'}$ to $IF_{MIN'}$).

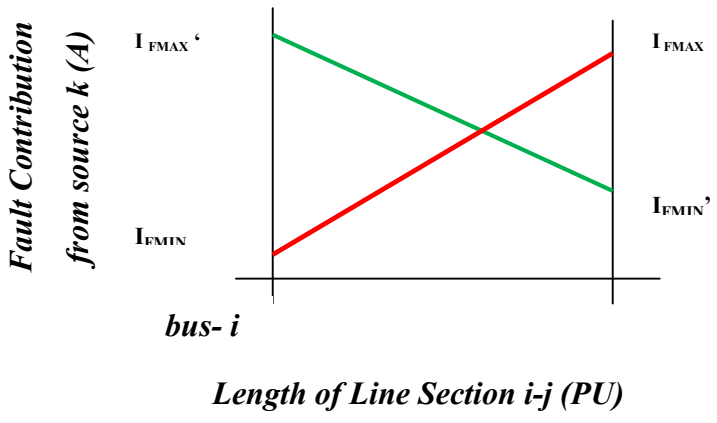

Figure 3.10 Fault from source (k) to line section between bus i &j

Thus fault contribution from source k for a given type of fault occurring at any point between bus i and j will always lie between contributions from source 'k' to same type of fault on bus i and bus j. This means for a given type of fault on same section, fault contribution from each source must lie between contributions from that source for same type of fault on buses connected to this section. Fault current contribution from each source for every type of fault for all buses is already known from the short circuit analysis. Using this network property and short circuit analysis the faulted section can be identified as a section for which measured fault contribution from each source is between the calculated fault-contributions at the two buses connected to this section from that source for a given type of fault.

Once faulted section is identified, the relay would send a trip signal to isolate the faulted zone and the DG in the faulted zone. The process needs to be completed before any fuse in the system is damaged.

Once the faulted zone and DG connected to it is isolated the next step is restoration in case of temporary faults. As the isolated zone is dead, one of the zone breakers can be closed without synchronization problems. If fault persists the breaker would open immediately, if fault is cleared other breakers will close one by one. A check synchronization function will be required while closing the other breakers. Finally the DG breakers will be closed to restore system to normal condition. In case of a permanent fault, the fault would have to be cleared by maintenance personnel before incorporating that zone back to system.

This scheme will not work well for systems with low DG penetration, however, in systems will low penetration the coordination will not be lost.

3.1.5 Voltage Issues in Distributed Generation System

Impact of distributed resources on power systems was summarized by IEEE working group on distributed generation integration and voltage issues in distributed generation has been discussed in details [17].

It is well known that that the load current through power and distribution transformer and line impedances causes voltage drops which reduces voltage magnitude at loads. Voltage magnitudes at specific location shall be maintained within specified ranges. This is managed by proper conductor sizing, transformer tap settings, fixed capacitor bank, automatic load tap changers, switched capacitors and step type voltage regulator. Connection of distributed generator can significantly

change the voltage profile and interact with static voltage regulator (SVR) or capacitor control operations.

Standard [18] specifies that DG should not actively regulate distribution voltage. This prevents automatic or manual adjustment of DG reactive power in response of voltage changes. Even if DG does not actively control system voltage it can cause system voltage to change depending on DR type. The incremental flow of real power interacting with feeder resistance will tend to make the voltage at DG location rise. Injection of reactive power by DG will cause rise in voltage while consumption of reactive power will cause reduction of voltage. If regulation by DG is permitted by local utility, DG reactive power can be varied to achieve the desired voltage. The effectiveness of regulation depends on short circuit ratio of DG and the system. If the ratio is small, influence on voltage change will be small. DG can cause voltage rise when connected in small residential areas connected to a distribution transformer by reducing voltage drop through transformer and secondary conductors.

DG impact on capacitor switching depends on DG type, location and capacitor switching control. Voltage controlled capacitor should not be impacted by DG if DG operates in voltage control mode. If current control is used, DG can impact capacitor switching since it can offset line current. The reactive power flow control will not be impacted when operating DG at unity power factor. However, if DG is downstream of the reactive power control is operating at unity power factor mode and the capacitor control senses reactive power flow towards the downstream load that exceeds the threshold , it will switch in the capacitor . This is a correct action from reactive power demand requirement but it may aggravate a high feeder end voltage caused by reverse power flow from the DG. The DG impact when it operates on at a constant power factor rather than unity power factor can aggravate the voltage more. As a result some adjustment of reactive power generation may be needed.

DGs also have impact on operation of voltage regulators. Step type voltage regulators controls have line drop compensation (LDC) feature. This estimates the line drop and performs voltage corrections based on line current, line R and X parameters and load side voltage. It is generally assumed that current flow downstream of regulator is roughly proportional to the current at the regulator location with the constant of proportionality steadily decreasing with increasing downstream distance from the regulator. With DG in network reverse power flow back to the substation is possible .During reverse power flow LDC must have adequate control algorithm to

properly perform voltage correction. There are various types of SVR control and impact of DG is different in each type.

Absence of ground source can lead to overvoltage condition. Figure 3.11 shows contribution from DG using Wye-delta transformer.

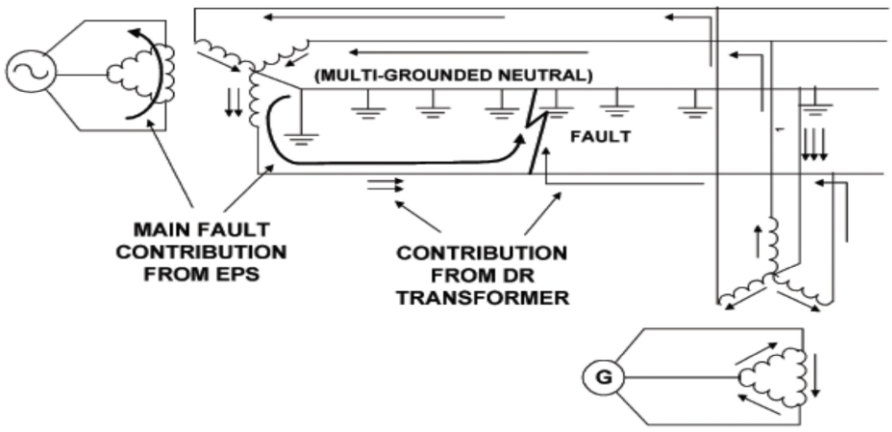

Figure 3.11 Ground fault contribution from DG using Wye-Delta Transformers

It is often thought that the best connection for DG is grounded Wye –Delta (Wye on the utility side). However, this connection is not acceptable without proper study because ground fault contribution from transformer can upset the ground fault coordination of recloser and circuit breaker on utility sides. However, if no ground source is provided by the DG, overvoltage can occur if feeder becomes islanded during ground fault. Such overvoltage can be of the order of 1.5 to 2 times the rated voltage. Although the island cannot persist long, overvoltage can be damaging to utility equipment and customer equipment. Too strong of a grounding source can desensitize feeder ground current relaying and may expose the grounding equipment to excess duty due to utility faults, load unbalance and open line conditions.

3.1.6 Problems in automatic reclosing

There are different problems encountered in conventional recloser operation with a network with DG connected in line [17]. Recloser used for fuse saving interrupt fault current very quickly. While they are rated for 3 cycle interruption, in some cases the interruption is as fast as 1.5 cycles. This makes it difficult for DG protective device to detect fault before the utility system operates. Thus if voltage seen by DG does not promptly deviate from the normal after the recloser opens, there is a chance that DG be still be connected and fault arc will not clear due to prolonged in-feed from DG. This has also been discussed by Rojewski, et al., [19]. Another aspect to consider is when the DG connected in downstream side of recloser does not disconnect during fault before the recloser closes, the reclosing will occur in an energised system. This will cause unsynchronised closing resulting in

severe switching surges and torque transients on motors and mechanical loads. This issue has been further discussed in section 3.2.2 of this chapter.

3.2 Protection issues in distributed generation specifically for PV systems

With all the PV installation and benefits that environment will derive from use of PV systems, there comes a requirement to address the changes to the established science of power delivery and protection to successfully integrate photovoltaic source in the existing power network. Conventional science of power system protection is based on the assumption that power flow is from the generation station to load at residences. However, with installation of grid tied PV generators in residences, power is now generated in small units distributed across the network. This calls for reviewing the systems protection setup of existing network. The increase in fault current contribution as penetration of PV system in network increases with time is likely to need a revisit of the fault interruption capacity of devices as well as need for revisiting the protection coordination.. Though the present codes for grid tied PV inverters prevents any possible islanded operation of PV system, failure of hardware logics could lead to unintentional energisation of isolated power lines and lead to safety issues. With research work progressing for performance reliability and improvement of PV systems, there has been substantial research done to address and understand the protection issues arising out of the increase in PV penetration in power distribution network.

3.2.1 Impact of PV inverters on system fault levels

PV inverters are inverter interfaced distributed generators (IIDG) and the fault current contribution varies considerably due to fast response of inverter controller. In a conventional distribution system, substation is the only source of power, and since substations are generally away from generating units, the fault current transients usually do not have the initial high sub-transient component. Therefore the fault current is usually approximated by its steady state value and the feeder can be represented using a steady state model where the substation can be represented by a Thevenin's equivalent and the lines can be represented by series impedances. The corresponding circuits can be analyzed using nodal equations.

$$[Y_f] \times V_f = I_{inj} \tag{3.19}$$

Where Y_f is the node admittance matrix, V_f is the voltage at each node and I_{inj} is the current injected at each node. If there are conventional synchronous generators on feeder then the above feeder model can be extended easily by simple Thevenin's equivalent model of generators. However, for

IIDG the same technique cannot be applied. This issue has been discussed by Baran and Markaby [20] and the new approach required in order to incorporate IIDG into fault analysis is described in the subsequent paragraphs.

Figure 3.12 below shows the main components of an IIDG.

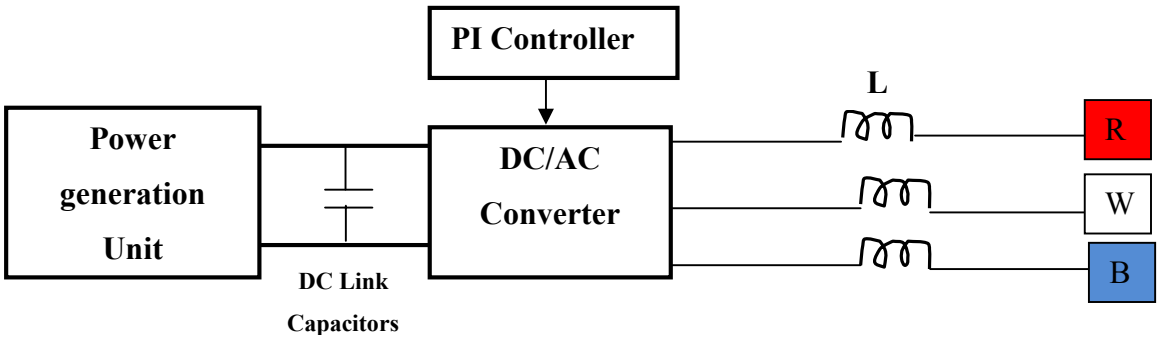

Figure 3.12 Block diagram –Inverter interfaced DG

During a transient the IIDG response mainly depends mainly on the inverter controller. There are two main control schemes for inverter controller.

- Voltage based scheme – Converter helps inverter to synthesize a three phase balanced ac voltage at the inverter terminals. To regulate the real and reactive power output of DG the controller adjusts the amplitude and phase of the synthesized inverter voltage with respect to terminal voltage.
- Current control scheme – This scheme uses two loops, the inner loop controls the power output of DG and outer loop regulates the power output. The outer power controller acts like a supervisory controller and determines (I ref) for the fast inner current controller.

To illustrate the response of an IIDG to a fault a simulation was carried out on a prototype feeder shown in Figure 3.13. An IIDG has been connected to upstream of recloser and current through RC has been studied during a fault in the downstream of recloser.

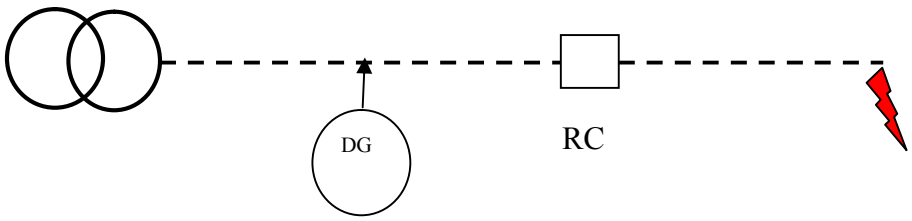

Figure 3.13 Network with IIDG connected upstream of recloser

The simulation showed that under the voltage control scheme the initial current overshoot is higher and then the controller brings the current to steady state within a few cycles. In the current control scheme the current increases to steady state rather slowly and decreases back to steady state rather

slowly. The slow corrective action is due to the slow response of the outer corrective loop. However, the current is much controlled under this scheme. The fault current contribution is generally within the maximum rating of the converter which is 2 times the normal rating. The fault contribution of an IIDG will be high especially during the transient period if IIDG is under voltage control scheme and therefore IIDG with voltage control scheme has been further investigated.

Fault analysis including IIDG showed that fast response time of IIDGs make it necessary to consider their fault contribution during the sub-transient as well as transient period.

The impact of fault contribution in the presence of PV grid connected systems was studied in details by Phuttapatimok, Sangswang,Seapan,Chenvidhya and Kiritikara [21]. Historically the effects of PV generation on fault current was not considered major because there were few installations of PV system ,they were small in size and they make limited fault current contribution due to inverter based interface with grid. However, with increase in PV penetration this can no longer be ignored. When a fault occurs at a particular bus which is fed both from grid and from PV system, the grid side breaker opens to clear the fault. The PV system will then identify islanding using islanding detection mechanism after loss of mains power and the anti-islanding protection system will operate to open within 2 seconds (as per IEEE 1547[18]) to isolate the PV system. Therefore for this duration of time (i.e. 2 seconds) PV system can potentially feed power to the point of fault. In the study a hardware setup has been used made to determine duration for which an inverter can supply power after detection of islanding and behaviour of current and voltage after disconnection from main power supply. The parameter recorded from experimental setup has been used as a basis for developing a PV model. A power system comprising 51 buses and 11 branches rated at 22 kV has been considered as a test network to study the effects of faults with high PV penetration. PV generators been embedded in various buses with power rating of 100 % of the total load .The PV generators has been modelled both as a current source and as a voltage source. A three phase fault has been simulated for 3 cycles. The results generated with PV source modelled as voltage source indicated that the overall fault current increase by 7% at 100% PV penetration while the results generated with PV system modelled as current source indicated that at 100% and 150% penetration there was an increase in fault current of 0.5% and 0.7% respectively. The study concluded that circuit breaker interrupting capacity and bus fault withstand capacity that has been designed for a network without PV penetration should be reviewed when the PV penetration of the network increases.

A similar study has been carried out by Phuttapatimok and Sangswang [22]. An experimental setup with a 6 kW grid tied inverter has been used to determine the inverter disconnection time after islanding. The experiment inferred that in case of an inverter loading of 33% the disconnection time for inverter is 376.9 milliseconds as compared to a 95 millisecond disconnection time when the inverter is loaded 100%. The PV system has been modeled as a constant current and constant power source and the network described in paragraph above has been considered as test network. 100% PV penetration in network has been considered and a three phase fault was simulated for 3 cycles Result indicated that when modeled as a constant current source, the increase in fault current due to PV penetration is 0.59% while when modelled as constant power source the increase in fault current was 12.5%. It has been highlighted in the study that results for increase in fault current varied depending on the type of PV model used for simulation.

An investigation to study the maximum PV connectivity in a Utility distribution feeder has been carried out by Varma, Berge, Axente, Sharma and Walsh [23]. The study evaluates the effect of introducing a PV system in a network on steady state voltage, voltage variation (due to cloud effect), short circuit current, temporary overvoltage and harmonic distortion. The study system (test network) has been taken from London Hydro Distribution network and comprises a 27.6 kV feeder supplied from a transformer station and two sub-feeders (sub-feeder #1- 913 m long and sub-feeder #2 -12 km long). The study establishes the possible integration of PV generator from the range of 500 kW to 20 MW in the network without violating the technical recommendations of London Hydro on feeder voltage, feeder voltage variation, short circuit current rating, temporary over voltage, reverse power flow and harmonic generation. The PV system has been modelled as a voltage source behind equivalent reactance. The reactance is sized to achieve a short circuit current of 2.05 p.u. The transmission lines have been modelled as pi-section model. To validate the model two types of studies has been performed. The system ha been first modeled in PSS/E software with initial generation of PV system 500 kW and load flow analysis has been performed. The same model has been then modelled in PSCAD and short circuit current and temporary overvoltage study has been done. The steady state voltage rise along sub feeder 1 and sub feeder 2 has been studied with varying PV generation (from 500 kW to 20 MW) connected to a bus in sub feeder 1. A similar study has been done with varying PV generation connected to a bus in sub feeder 2. It both cases voltage rise was observed at the common bus for sub-feeder # 1 and sub-feeder # 2. The voltage variation due to sudden fall in PV generation caused by passing cloud over PV array has been simulated by sudden drop in output by 60% for a 20 MW PV generator connected to a bus on sub feeder# 1. The simulation result indicated no appreciable voltage fluctuation due to cloud effect. A short circuit study considering PV generation up to 20 MW (connected to a bus at sub-feeder #1)

has been completed. Faults at different points in the system have been considered and increment of fault current with PV in the network has been compared with the situation of no PV generation in

Temporary overvoltage study has been conducted to check the overvoltage in healthy phase caused by single phase to ground faults in the network. The TOV limit of 125% stipulated by London Hydro was not violated even at a generation level of 20 MW. The study also included impact of inverter based generation on harmonic levels and THD (total harmonic distortion) in feeder voltage. It was observed that large bus capacitors in the network interacted with the various inductances and resulted in impedance resonance. The network impedance has been plotted as a function of frequency at maximum and minimum short circuit condition and with one and two capacitors connected to the network. For no capacitor connected to the network no resonance occurs. For maximum short circuit level resonance occurs at 6^{th} harmonic with one capacitor and around 4^{th} harmonic with two capacitors. For minimum short circuit level the resonance occurs at 4^{th} harmonic for one bus and 3^{rd} harmonic for two bus capacitors. It has been pointed out that the system strength varies over the day, month and season and may be resonant at 5^{th} harmonic frequency for one capacitor and 3^{rd} harmonic frequency for two capacitors. If there is presence of 3^{rd} or 5^{th} harmonic injection from PV inverter, the system is susceptible to harmonic amplification. The voltage THD level with varying PV power generation (connected at various point in network) was recorded. It has been noted that THD increases linearly with the generator size. This study also discussed the possible tuning of multiple inverters to cause harmonic cancellation and the effect of X/R ratio of the system on bus voltage. It has been shown that for a lower value of X/R at the transformer station produces lower THD levels along the feeder.

The magnitude and duration for which a PV system contributes to fault during a short circuit is an area of major interest and a lot of studies have been done. A collaborative research between the National Renewable Energy Laboratory (NREL) and Southern California Edison (SCE) was done to do a laboratory short circuit testing of single phase inverters [24]. Present industry standard is to use a “rule of thumb” of two (2) times rated current for the magnitude of current contribution from inverter based PV generator. Short circuit tests on 20 single phase (240Volts) inverters ranging from 1.5kW to 7kW has been carried out to see if this value (i.e. the rule of thumb) of fault current contribution is accurate for current inverter technology. 14 inverter units (from six different manufacturers) have been tested at SCE and 6 inverter units have been tested in NREL. It is known that fault contribution from inverters does not behave in the same way as the synchronous or induction machines. Power electronic inverters have a fast decaying fault current envelope because

the devices lack predominantly inductive characteristics that are associated with rotating machines. The test setup at NREL comprised -

- 5kW constant voltage (240V) source as grid simulator with maximum fault current of 300 Amps (used as grid simulator)
- DC power source rating 16-17 kW, 0-20A, 0 - 600 V d.c.(used as PV simulator)
- AC Load bank 3 kW (Load)

The test setup at SCE comprised -

- 55kW constant voltage (240V) source as grid simulator with maximum fault current of 300 Amps.(used as grid simulator)
- DC power source rating 45 kW, 100 - 1000 V d.c.(used as PV simulator)
- AC Load bank 10 kW (Load)

To perform the test, a short circuit has been placed between phase and ground until the inverter tripped off. The grid simulator allowed controllable contribution of fault current for personal safety. Test results at NREL indicated that for most inverter, maximum short circuit current magnitude was as high as 4 to 5 p.u. but the duration of peak current contribution was less than a cycle. After the peak cycle the contribution continued at lower steady state value for about 3 cycles. In a couple of cases the peak value persisted for about 3 cycles. Test results at SCE reiterate the fact that duration of fault contribution was very short but the contribution varied for different inverters. In one particular test, the peak contribution from inverter during fault recorded was 326% of rated value and the duration of contribution was 228ms.

The results obtained from the tests indicate that the current rule of thumb of using 2 to 3 times rated current of inverter as the short circuit contribution may be inaccurate and extensive testing is required to determine the true simulation models for PV sources for use in power system studies.

In a similar study carried out by J.E Muljadi, et al., [25] as collaboration between NREL and SCE, a dynamic model for PV system in PSCAD /EMTDC simulation software has been developed and response of the model for single phase to ground fault and three phase fault has been observed. The paper mentions about two different types of inverter protection; one is fast disconnection (i.e. in less than a cycle) and other with continued operation up to 10 cycles. In most cases inverter fault contribution varies for duration of 4 cycles to 10 cycles. When the grid voltage is low, the output current that can be supplied to grid is limited by the current carrying capacity of the (insulated gate bipolar transistor) IGBT in the inverter. The control and protection parameter of the PV model used

for simulation has been tuned to represent the power inverter tested. The results of the observation have been validated with experimental setup and the simulation results closely follow the measured values of the experimental setup. Due to the variation in the control and protection schemes of PV inverters, the responses of all PV systems during fault are not similar. Therefore accuracy of the PV model has major impact on obtaining reliable results during power system studies. Customising a generic PV model to meet the specific control and protection features of the PV inverter considered for study is very important.

The requirement of reliable model for PV behaviour during fault has been further discussed in another study [26].This study has mentions that one of the reasons hampering the integration of PV is the difficulty in representing PV inverter characteristics for short circuit studies. Inverter behaviour during fault is based on the control strategy of the inverter and protection engineer has to use full time domain representation which is time consuming. This study describes a load flow based technique for analysing distributed network with inverter interfaced generation. The inverter model implements grid synchronisation, a filter inverter current control loop, power control (performed in synchronous reference frame by deriving output current references based on output voltage using instantaneous power theory) and current limiting function . As the power electronic switches in the inverter bridge exhibit low thermal inertia, it needs to be protected from overheating by actively limiting the filter inductor current. There are several different strategies proposed for achieving this function. However, as grid codes are likely to require grid support services for generator connected to grid, the strategy proposed is to limit instantaneous magnitude of inductor current by switching to a predefined inductor fault current reference once the inductor current reference has exceeded a threshold. An analysis for fault response of a single inverter has been included in this study to conclude that during normal operation the inverter can be represented by a P&Q source behind a coupling reactance and during voltage sags (faults are characterised by temporary decrease in voltage magnitude on one or more phases) when current threshold is exceeded, the grid connected inverter can be represented as a constant positive sequence current source in parallel with the filter capacitor. An analysis fault response of multiple inverters has also been included where it is proposed that the grid connected inverter can be represented as constrained PQ nodes. In this concept, during normal operation inverters can be considered as PQ nodes but once their inductor current is above threshold limit they switch to current source node. In order to determine the number of current limiting inverter in network during fault an algorithm has been proposed. For analysing the fault response of a single inverter, the analytical results obtained using MATLAB simulation software has been compared with the experimental results and the

results closely matched. For analysing the fault response of multiple inverters, the response of three grid connected inverters in CIGRE European Low Voltage Distribution Network Benchmark has been simulated using PSCAD. The algorithm based response has been compared with the simulation output and good alignment between the two in identifying current limiting inverters has been observed. This study has also stressed on the importance of well tested fault models for inverters which has been discussed in the study conducted by NREL and SCE [25].

A new control strategy to mitigate the impact of inverter based DG has been proposed in a separate study [27]. Methods of minimising the DG impact which includes limiting maximum penetration level, use of directional relaying, use of fault limiters and adaptive control has already been discussed in this chapter. The new strategy [27] is based on control strategy for inverter based DG. In this paper impacts of inverter based systems on fuse recloser coordination has been investigated and the effects of reactive power injection has been analysed and a control strategy based on limiting inverter current output based on terminal voltage has been proposed. The concept is based on allowing the inverter to have ride through during small duration voltage disturbances by limiting the output current according to severity instead of disconnecting the inverter. The inverter based DG nearest to fault will significantly decrease the fault current contribution while the DG located at distant end which will have no effect on protection system will continue to deliver power.

In order to implement current control as a function of terminal voltage the DG reference current can be determined by the following equation.

$$\begin{cases} I_{ref} = \left(\frac{P_{desired}}{V_{PCC}}\right) \quad for\ \mathrm{V_{PCC}} \geq 0.88\text{p.u.} \\ I_{ref} = k \times V_{PCC} \times I_{max}\ for\ \mathrm{V_{PCC}} < 0.88\text{p.u.} \end{cases} \tag{3.20}$$

I_{ref} is the inverter reference current and I_{max} is the maximum current that occurs at V_{PCC}=0.88 p.u.
V_{PCC} is the rms voltage at DG connection nodes.
'n' and 'k' are constants.
'n' determines the sensitivity of the control scheme for voltage output and once n is selected the value of 'k' can be determine using the equation below

$$k = \frac{P_{desired}}{\{0.88^{n+1} \times I_{max}\}} \tag{3.21}$$

Simulations were performed using MATLAB/SIMULINK (simulation software) on a 13 node test feeder system. Performance of the proposed scheme for a low impedance fault condition, high

impedance fault condition and other disturbances has been evaluated .The simulation results has shown that the scheme successfully mitigated the coordination problems.

A detailed study has been carried out on the Quanta Technology for technical issues regarding connection of PV systems to Ontario electrical grid in Canada with special focus on short circuit current impact [28]. Six different PV manufactures models were obtained and tested to obtain the short circuit responses. Based on the short circuit response of the inverters PV inverters were grouped into two categories as listed below:

- Category 1 (model 1) - The inverters in this category have fast disconnection feature, i.e. the inverter current is interrupted in less than a cycle when the terminal voltage falls below 50% of rated voltage.
- Category 2 (Generic model) - The inverters in this category have a continued operation up to 10 cycles after fault has occurred (i.e. even after the terminal voltage falls below 50%).

A benchmark (test) 115 kV transmission system model was developed in consultation with Hydro-One (Transmission distribution company) which represents an actual portion of distribution network. PSCAD has been used for performing the simulations. Single and multiple PV systems with sizes equal or smaller than 500kW has been connected to the test network at different points. The total capacity of PV system connected for simulation purpose is 16MW.For obtaining the simulation outputs during fault, unbalanced and three phase faults has been applied at various points in network with different combination of PV systems connected in the network. An assessment of the impact of PV inverters on close-latch capacity of the circuit breaker has also been done. In addition to the observations made regarding fault current magnitude in other studies described in this chapter, the following points have been mentioned:

- PV inverter current and system contribution to the fault have their maximum values at first half cycle but during different time instances.
- The frequency of PV inverter current during a three phase fault at PV inverter terminal may be different than the pre fault grid frequency.
- Arithmetic addition of inverter fault current to utility fault current represents the worst case situation. In reality this should be the vector addition which would result in lower value.
- From the view point of circuit breaker close latch rating for existing circuit breakers connected to network, PV inverter contribution is not a limiting factor. The PV inverter current contribution during the peak of first cycle of fault (on which circuit breaker close-latch rating is calculated) is about 20% of aggregated PV inverter rated current.

A study has been carried out to address the aspect of time varying fault current from PV system and the difficulty in estimating the time taken by the over current relay to respond during fault [29]. In this study current injection from PV system during fault has been considered as a function of terminal voltage and the power rating of the PV system, the absolute maximum current injection value being limited to two times the rated current when the terminal voltage drops below 0.5 p.u. In addition to the magnitude of fault current, the study has included the voltage based trip time recommendation as per IEEE Standard 929 [30]. The standard recommends disconnection time based on terminal voltage. The concept of time varying fault contribution has been illustrated by considering a number of PV system connected along the length of a radial feeder and a fault has been considered at the end of the feeder. As the voltage will be lowest at the point nearest to the fault, the PV system nearest to the fault will see lower terminal voltage, inject fault current (2 times rated current) and get disconnected within 6 cycles. The PV panels located away from the point of fault will either ride through the fault or have a higher disconnection time. Once the PV panels nearest to fault trips, the feeder voltage will drop and cause disconnection of the PV panels further away from the fault along the feeder at an lower time than the protection scheme of PV has initially estimated (i.e. when PV system nearest to the fault were connected). Due to disconnection of PV at various times a time varying fault current profile is generated. For fault analysis with time varying fault profile an algorithm has been proposed. A PSCAD simulation has been performed on a 22 kV test network and fault magnitudes at various nodes in the network has been observed. The simulation results closely aligned with the values obtained by proposed algorithm. Also as it is difficult to estimate the relay trip time with varying fault current, the study provides equations for estimating trip times of both electromagnetic and microprocessor based relays and an algorithm for determining the tripping time. In this study the fact that the varying profile of fault current in PV embedded feeder has an impact on protection system, has been emphasised.

A detailed study has been undertaken to illustrate the effects of PV system in network on the operating time of protective devices [31]. A 22 kV residential distribution feeder with high penetration of PV system has been used as test network in the study. The variation in fault current seen by a protective device (PD) caused by presence of DG (PV system in this case) is explained using the Figure 3.14. R_f in Figure 3.14 represents fault resistance.

Figure 3.14 Effect of DG on fault current seen by PD

When the PV is located upstream of PD it will increase the fault current seen by the PD but when located downstream of PD it will reduce the fault current seen by the PD. This is because in this case the current injection from PV system will cause the voltage on the fault resistance to be higher, and this in turn will result in reduction in fault current coming from source side seen by the PD. The change in fault current will cause change in amount of time of relay operation. One of the potential problems identified in this concept is the possible protection under-reach if the downstream PV system can source enough fault current during fault such that the pickup current seen by the over-current relay will fall below relays pick-up value. In order to evaluate effect of PV systems on PDs operating time, different faults at different locations of the test network has been simulated with variations in fault resistance and PV power output. The test result concludes that the PV systems can make PD operation faster or slower depending on the location of the PV system. Possible issues of miscoordination between two PDs when the PV is located between two PDs have also been highlighted in his study. An investigation to study the impact of the PV penetration on the voltage profile of feeder has been done. As PV systems are sensitive to cloud effect, the intermittent power output can affect the feeder voltage operation of voltage regulation devices. In general PV power injection will increase the feeder voltage level; however, this is much dependent on feeder topology and location of PV system in the feeder. In order to study the voltage issues, various cases were simulated in the test network with different combination of PV penetration and loads. It has been observed that the when the PV generation exceeds load, the feeder voltage rises. During the study it has been observed that there is no severe voltage fluctuations caused by PV systems, due to intermittent output from the PV system due to cloud effects unacceptable voltage flicker may be created.

3.2.2 Islanded operation of grid connected PV systems and associated problems

Islanding is a potentially dangerous mode of operation of a grid connected PV inverter. Islanding is defined as continued operation of grid connected inverter when the utility grid has been switched off so that no electric energy is delivered by utility to the load. Islanding is a dangerous situation because of the following reasons –

- Safety of person – If utility is switched off line workers may assume that the line is de energized and not take safety measures which may in turn lead to accidents.
- Safety of equipments – Voltage amplitude and frequency of supply is controlled within acceptable limits by various methods but when operating in islanding mode there is no control over these parameters which may lead to severe equipment damage.

Therefore various methods are employed to make sure that islanded operation does not take place.

These methods can be divided in four categories –

- Passive Inverter resident method
- Active method -Inverter resident method.
- Active method - not resident in inverter.
- Communication based methods where which involves transmission of data between inverter and grid.

Anti -Islanding algorithms for PV systems using Passive method has been discussed by De Mango, et al., [32]. The passive method for islanding detection employs a monitoring Phase locked loop for estimation of voltage amplitude and frequency. Methods includes over/under- voltage, over –under frequency, voltage harmonic monitoring and phase monitoring.

The grid is subject to disturbances and islanding protection has to be immune to these disturbances.

During normal operation the active and reactive power component of load is supplied by PV system and grid. After grid disconnects the available voltage depends on ratio of Power supplied by PV system and power demand of load. The reactive power is tied to frequency and amplitude of voltage. When the reactive and active power component supplied by grid is low, it is probable that it will fall in Non detection Zone (NDZ) of over/under voltage and over /under frequency (the range in which islanding detection scheme fails to detect islanding).This makes standard under/over voltage and frequency protective devices alone inadequate for the purpose.

In the voltage harmonic monitoring method the total harmonic distortion at point of common coupling is measured to detect islanding. However, if the grid harmonic distortion is not high or low enough such that the total harmonic distortion changes when islanding occurs, it can be difficult to detect islanding .In the paper harmonic monitoring method has been studied taking into account grid impedance influence and dc-link ripple .

The paper also discusses the phase monitoring method. This method consists of detection of sudden jump in phase displacement between terminal voltage and current of inverter. With a fast PLL the jump between the inverter phase and voltage will be negligible. Therefore a modified method has been proposed.

Under normal operation when inverter is producing zero reactive power there is no phase displacement between PV system output terminals. The reference current for inverter control is synchronized with fundamental voltage at PCC. The variation of voltage frequency consequent to islanding causes a drift in the voltage vector and a corresponding change in phase.

The detected angle is stored and compared with the value measured after a whole multiple of period of fundamental.

$$\Delta\theta = \theta_t - \theta_{t-1} \tag{3.22}$$

The output phase is a ramp with a certain slope. A frequency change causes alteration of phase and can be detected.

It is possible to calculate phase of load using equation

$$\theta = \tan^{-1}[R(\omega C - \frac{1}{\omega L})] \tag{3.23}$$

Pulsation ω corresponds to normal frequency of grid. If islanding occurs with load resonating at grid frequency the phase does not vary, but if load is resonating at a difference frequency the load changes. Therefore it is possible to set θs such that when $|\theta| \geq \theta s$ islanding is detected. As this method is dependent on reactive power, the NDZ of this method is same as under and over frequency method. Unlike passive anti-islanding methods, active anti-islanding method schemes make perturbation into the PV inverter output by injecting an active signal. Active anti islanding method consisting of a frequency variation method as AFD (active frequency drift) method and a start phase variation method SMS (slip mode frequency shift) method has been discussed by Yu, Jung, Hwang and Yu [33] . The study presents a combined active anti-islanding method consisting

of AFD and SMS method. Active anti-islanding methods are classified into three parts with respect to what the variation parameters is ; they are magnitude (I_m), frequency (f) and start phase (θ) of inverter output current as shown is equation (3.24).

$$I_m = I_m \sin(2\pi f t + \theta) \quad (3.24)$$

On one hand, the magnitude variation of inverter output current can cause a change of output voltage magnitude after islanding occurs, which causes voltage based detection of islanding. On the other hand both frequency (f) and start phase (θ) variation makes the islanding frequency of inverter output voltage drift away from trip window of frequency relay if an islanding has occurred. The active frequency drift method makes the inverter output current drift up or down with chopping fraction, a parameter defined in equation (3.25). This is illustrated in Figure 3.15.

$$\text{Chopping fraction } C_f = \frac{\text{Tz}}{\text{Tutility}/2} \quad (3.25)$$

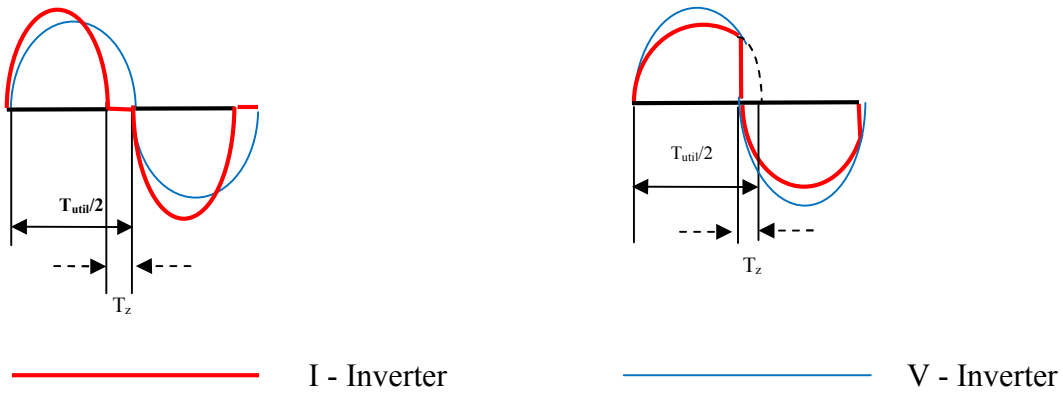

Figure 3.15 Inverter output waveform using AFD method

In slip mode frequency shift method, start phase of output current is made a function of output voltage frequency as shown in equation (3.26). This is illustrated in Figure 3.16.

$$\theta = f(\text{freq } v) \quad (3.26)$$

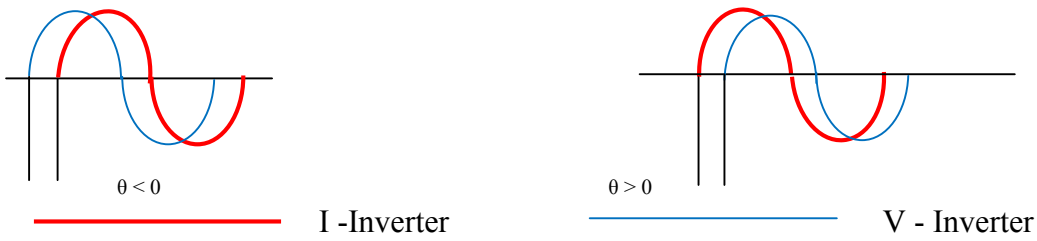

Figure 3.16 Inverter output waveform using slip mode frequency shift method

Frequency and current start phase control are implemented by digitally controlled phase locked loop. In a combined active anti islanding method the detection time is faster due to large phase error

during transient time and less non detection zone. A computational algorithm has been included in the study for combined islanding detection.

Passive and active anti islanding measures can however, adversely impact system dynamic behaviour. With growing DG penetration attention will have t be paid between the need to eliminate island and impacts of measures used to detect and eliminate islands on system performance when no islanding occurs. This has been discussed by Walling and Miller [34].

IEEE 1547 [18] and IEEE 929 [30] mandates control and protection measures to minimize probability of inadvertent islanding. When the DG capacity is small compared to the system measures of islanding does not have significant influence on power system performance. However, in systems with large DG penetration, measures to prevent inadvertent islanding can aggravate local disturbances.

The requirement of detecting and eliminating islanded operation of DG and minimizing DG impact on system performance are conflicting objectives with present day protection systems.

Generally a fault will be cleared by opening of feeder circuit breaker, recloser or fuse. Ideally fault should be detected by the DG and system tripped before islanding can occur. However, this may not happen due to the following reasons –

- The fault is a single phase to ground fault and DG interconnection does not provide a primary ground current source.
- The DG is single phase connected to un-faulted phase.
- The fault is self extinguishing once the high current utility source is open and the fault current falls to a low value when fed by DG.

In this case the DG will continue to operate in islanded mode if the aggregate real and reactive power for all DGs supporting the load is close to the load demand; else the islanded operation is terminated by the operation of over/under frequency and over/under voltage relays.

In order to avoid out of phase reclosing very quick islanding detection is required. In many cases reclosers are instantaneously closed without an intentional delay .Delay due to mechanical operating time is about 150- 200 ms from opening to reclosing. In order to prevent out of phase reclosing the DG must detect islanding within that small period of time. Out of phase reclosing causes large mechanical torques and with a typical damping, the switching transients can exceed 2

p.u. can occur. It is important that the DG islanding protection is coordinated with the circuit reclosing practice.

DGs are provided with under-voltage and under -frequency protections. Faults can cause under voltage and under voltage can cause unnecessary DG tripping. For example a fault in adjacent feeder can result in voltage at the DG below under voltage set point. This will lead to under voltage tripping of DG even if tripping of DG was not required to clear the fault. In a well designed system loss of one DG will not disturb the system but sensitive under-voltage setting can lead to large scale tripping of DG. If DG penetration in system is small then the DG tripping is inconsequential. However, if DG penetration is extensive, simultaneous under voltage trip of DG in an area can lead to voltage collapse in a local area.

When generation is inadequate with respect to load demand, under frequency transient is resulted. To trip generation systems during under frequency is contrary to system benefit. Turbine – generator sets are tripped for protection of generation machinery itself. In distributed generation system the tripping due to under frequency is to prevent Islanded operation. In rare case of interconnected power system suffering severe under frequency event, system wide DG tripping will further aggravate the situation.

The active anti islanding functions seeks to destabilize an unintended island. If large interconnected systems are considered individually as islands, active anti islanding can destabilize the entire connection if DG penetration is high.

There can be several negative consequence of an unintended island supported by DG. However, the measures used to detect and eliminate islands can also have significant impact on dynamic performance of power system. As DG interconnection standard evolve the dynamic performance impact needs to be addressed.

3.3 Summary

In this chapter provides a comprehensive discussion on the presently understood problems in the protection of power networks with distributed generators. The first part of the chapter introduces the concepts of general problems caused by the DGs in network and the second part of the chapter discusses specifically the problems associated with inverter interfaced DGs. PV system is an inverter interfaced DG and therefore second part of the chapter is of main interest in this research work. The discussion lays emphasis on the fact that the PV systems (inverter interfaced DGs) can cause network protection issues when the penetration is high. This is in spite of the fact that the

contribution from PV system is generally low due to the current limiting nature of the output side inverters of the systems. Works done on other issues associated with high penetration of PV system like voltage stability has also been discussed. Several methodologies studied in the past for overcoming the protection problems caused in existing network with increased DG penetration has been presented in details. In subsequent chapters 4 and 5, analysis of case studies carried out has further highlighted some of the problems discussed in this chapter and will provide a more detailed understanding of the problems when specifically investigated in low voltage networks for suburban power distribution.

Chapter 4 Impact of fault contribution from single phase PV

The issues due to increase of fault current level due to contribution from distributed generator and inverter interfaced distributed generator has been specifically discussed in the previous chapter. In this chapter an investigation carried out using a case study for analysing the impact of additional fault current from PV systems on interrupting capacity of the protection device has been described. This study has been presented as a conference paper in AUPEC 2013 held at Hobart [35]. Generally solar PV systems are considered to make very minimum contribution to network in terms of fault current. It is therefore expected to make minimum impact on the fault rating of components in power network and protective device coordination. The industry rule of thumb for fault current contribution from PV systems considered for studies and modeling is twice the [24] the inverter rated current. This can however, vary between 1.2 -2.5 times the inverter rated current depending on different types and manufacturers of inverters for PV systems. In this case study it has been illustrated that the low fault current contribution from PV system does not necessarily mean that proper evaluations of fault withstand capacity and relay coordination is not required when PV systems are added to network. Study carried out in the past indicate that there is an increase in the order of 7% in fault current magnitude [21] that can be caused due to PV systems introduced in network. The magnitude of fault current contribution depends on the size and number of PV system installed in a particular network. Therefore the level of penetration of PV system in a particular size of network determines the importance of evaluation of impact of PV system on network fault and fault withstand capacity of the network devices. For a grid tied PV system inverter there is anti-islanding protection provided. As per IEEE standard 1547 [18], all grid connected inverter system shall successfully detect islanding and stop energizing within a given limit of time. In a grid tied system during a fault in the network, the grid side fault clearing device opens to clear the fault. The PV system then detects islanding and thereafter trips on detection of islanded condition within specified time (within 2 seconds) [18],[36].However, as the anti-islanding protection operates within 2 seconds from the instant of fault, the PV system can potentially contribute short circuit current to the point of fault for this duration. Therefore PV systems installed upstream of a fault clearing device may necessitate replacement of existing fault clearing device with a fault clearing device of higher breaking capacity as the contribution from PV system will increase the network fault level. A typical suburban power distribution network has been used as a test network for performing the analysis Subsequent sections of this chapter discusses the network, network modeling and the case study in details.

4.1 Network description

Three phase power at 33000 Volts is fed via overhead transmission line from main substation to suburban area substation. The suburban area substation comprises a 33/11 kV, 15/20 MVA (oil cooling/forced air cooling-ONAN/ONAF) transformer. The 11 kV power is then fed to the suburban distribution network via three -phase, three- wire overhead line (OHL) installed on poles. The pole top overhead line is terminated at the kiosk substation units via high voltage cable and surge diverters. Kiosk units are suitably located in the vicinity of residential clusters to allow ease distribution of power to residential customers. Each kiosk comprises 11 kV ring main unit (RMU) (with 2 off ring switch and one off transformer feeder), 11/0.4 kV, 630 kVA ground-mount transformer and a low voltage (400 Volts) distribution board. The low voltage (LV) distribution board is fitted with low voltage outgoing switch fuse units. The switch fuse feeders are typical cable feeders. Low voltage cables are terminated at the terminals of switch fuse units at one end and the other end is terminated at the low voltage overhead lines on the pole top. Low voltage overhead lines installed on poles feed low voltage power using a three-phase four-wire configuration to individual residential block. Power is tapped at pole tops to feed to individual residential distribution boxes at customer premises. This can either be three phase or single phase depending on the load size at customer premises. However, for the purpose of this study only single phase load distribution at customer premise is considered. The connection from pole top to individual residence is done using insulated aerial conductor which is terminated at the customer main switch board. To allow connection both from grid and solar PV system, the customer main switch board has provision to allow two incoming switches. Each switch is complete with over-current protection device. The over-current protection device is designed to isolate the power from grid in case of a downstream fault. Figure 4.1 shows a block diagram of the network described above.

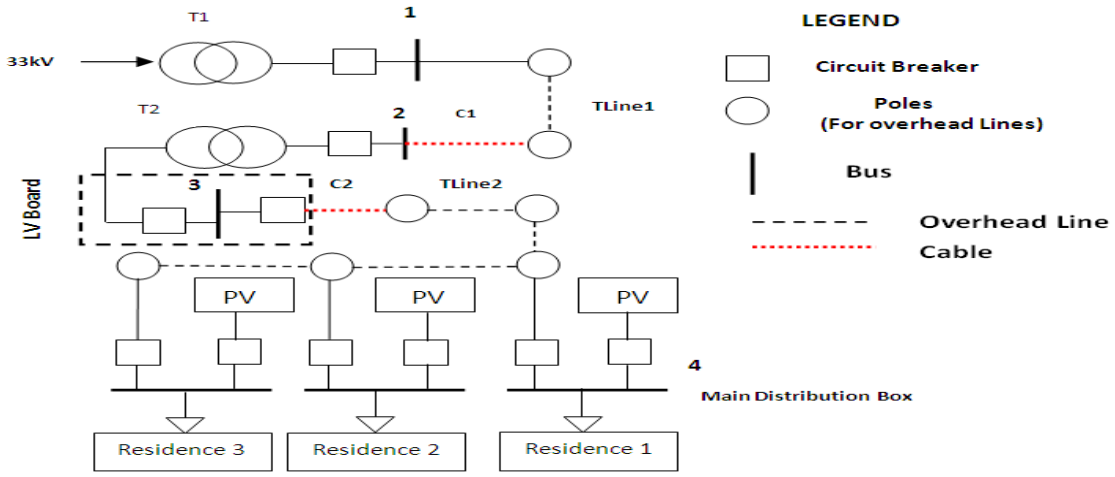

Figure 4.1 Suburban power distribution network block diagram

4.2 Network Parameters

In order to carry out the case study it is essential to establish the sizes and ratings of network components of the network shown in Figure 4.1. Following the selection of component sizes, the electrical parameters of the network components has been determined. The parameters of components has been subsequently used to model the power system in PSCAD and for carrying out analytical calculation for determining the short circuit current levels at various points in the network.

The following steps have been sequentially performed in order to obtain data required for short circuit calculation and development of power system model in PSCAD.

- Equipment and conductor sizing
- Calculation of overhead line Inductance and capacitance
- Calculation for impedance of components

4.2.1 Equipment and conductor sizing

The calculation provided in this section validates the adequacy of the selected size of network components and establishes the suitability of the network for carrying out a power system case study.

As a basic assumption the transformer in the main suburban substation is assumed to be a 15/20 MVA transformer with a transformation ratio of 33/11 kV capable of feeding power to the entire suburb.

The cable connecting the 11 kV switchboard in the suburban substation to the 11 kV overhead line has not been shown in figure and has not been included in the calculations. Due to the relatively short length of the cable it will not have much effect on the overall results of calculations.

The 11 kV OHL (Tline1) from the suburban substation to the pole located near 11 kV kiosk substation is rated for carrying capacity of 409 Amps. This feeds power to the 630 kVA transformer kiosk (through the ring main unit and the transformer feeder).

Transformer primary full load current is 33amps {calculated as: $\frac{630}{(1.732\times11)} = 33$}

The overhead line sizing is therefore adequate to feed power to the kiosk unit without appreciable voltage drop.

The 11 kV cable (C1) that connects the overhead line to the RMU in the kiosk using a set of three single core 35 mm2 cross linked polyethylene (XLPE) insulated cable .The cable is rated for carrying 140 amps (assuming that the cable is installed in conduit and buried underground). As the full load primary current of transformer is 33 amps, so the cable size is adequate for carrying current.

Transformer (T2) full load secondary current is 909 amps {calculated as:$\frac{630\times1000}{1.732\times400} = 909$}

The outgoing cable switching units in the low voltage board are rated at 400 amps each.

240 mm^2, XLPE insulated (aluminium conductor) LV cable (C2) has been considered for connecting the cable switching units in the kiosk unit to the LV OHL(Tline2) The cable has a current carrying capacity of 320 amps (assuming that the cable is installed in conduit and buried underground).

Based on the cable capacity it shall be possible to feed approximately 220 kVA {calculated as: $1.732 \times 400 \times 320$} in the low voltage network using each cable feeder.

The overhead line (Tline2) that powers the residential clusters is rated for carrying capacity of 562 amps This is adequate for carrying 320 amps of power without appreciable voltage drop.

The adequacy of network component for transferring power as described in section 4.1 is thus established and the network is therefore suitable for carrying out power system analysis.

4.2.2 Overhead Line Inductance and capacitance calculation

In order to determine the impedance of the OHL it is necessary to determine the inductance and capacitance of overhead lines. As this depends on the geometry of arrangement of conductors the impedance values cannot be directly obtained from manufacturer's datasheet and therefore has to be calculated Based on the conductor parameters and conductor arrangement the geometric mean radius (GMR) and geometric mean diameter (GMD) has been calculated which subsequently allows calculation of inductance of OHL The inductance and capacitance of the overhead lines has been calculated in the subsequent sections. The conductor type for TLine1 is Iodine, AAAC/1120 and the conductor type for TLine2 is Neon, AAAC, 1120. The conductor data has been obtained from manufacture's data sheet [37].

TLine1

For the overhead line TLine1, the conductor parameters are as follows –

- Number of strands – 7
- Wire diameter -4.5 mm
- Nominal overall diameter -14.3 mm
- Cross sectional area – 124 mm^2

The arrangement of conductor on pole is as shown in Figure 4.2.

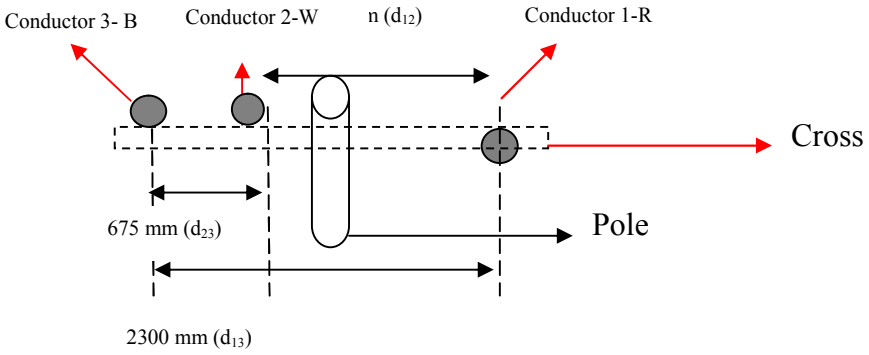

Figure 4.2 Arrangement of conductor -TLine 1

$$GMR = e^{-0.25}r' \tag{4.1}$$

$$r' = F_C\sqrt{\left(\frac{qn}{\pi}\right)} \tag{4.2}$$

F_c- Lay factor (1.06 for 7 strand conductor)

qn – Nominal cross sectional area of conductor in mm^2

GMR = 0.005184 m using equation (4.1) and (4.2)

$$GMD = \sqrt[3]{(d_{12} \times d_{23} \times d_{13})} \tag{4.3}$$

GMD = 1.36 m

$$X_L = 0.0628 \times I_e \left(\frac{GMD}{GMR}\right) \tag{4.4}$$

X_L= 0.349 ohms/km

Equation (4.1), (4.2), (4.3) and (4.4) are based on Australian Standard AS 3851[38].

Capacitive reactance for overhead line (with unsymmetrical spacing) can be calculated as below [39].

Capacitance of overhead line $$C = \frac{2\pi\epsilon_0}{\ln\left\{\frac{\sqrt[3]{(d_{12}\times d_{23}\times d_{13})}}{r}\right\}} \quad (4.5)$$

ϵ_0 – 8.854 x 10 $^{-12}$ F/m – Permittivity of free air

r – Radius of conductor (7.15 mm based on overall diameter of conductor)

Using equation 4.5, C = 10.6 x 10 $^{-12}$ F/m

C = 10.6 x 10 $^{-9}$ F/km

C = 0.0106 x 10 $^{-6}$ µf /km

Capacitive reactance $X_C = \frac{1}{(2\times\pi\times 50\times 10.6\times 10^{-12})}$ = 300 MΩ–m

TLine2

For the overhead line TLine 2, the conductor parameters are as follows –

- Number of strands – 19
- Wire diameter -3.75 mm
- Nominal overall diameter -18.8 mm
- Cross sectional area –210 mm2

The arrangement of conductor on pole is as shown in Figure 4.3

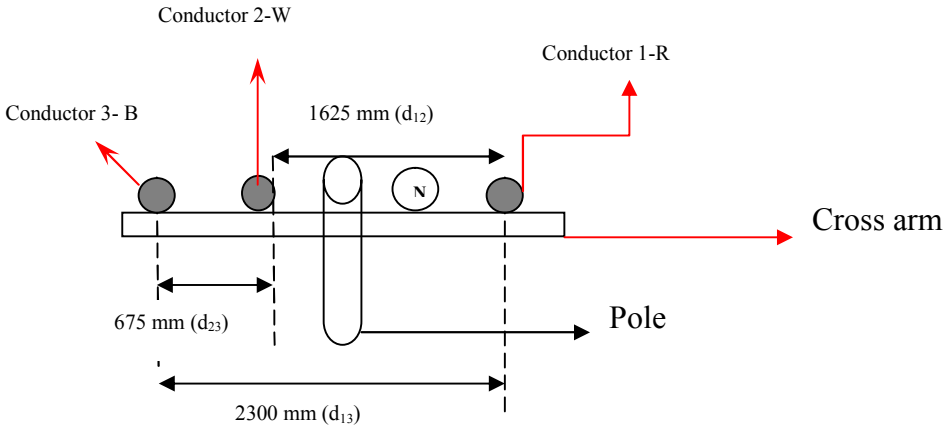

Figure 4.3 Arrangement of conductor -TLine 2

F_c- Lay factor (1.12 for 19 strand conductor)

qn – Nominal cross sectional area of conductor in 210 mm^2

GMR = 0.0071 m Using equation (4.1) and (4.2)

GMD =1.36 m Using equation (4.3)

Inductive reactance X_L =0.330 ohms/kilometre using equation (4.4)

Capacitive reactance for overhead line (with unsymmetrical spacing) can be calculated as below-

Capacitance of overhead line C is calculated using equation (4.5)

r – Radius of conductor (9.4 mm based on overall diameter of conductor)

C =11.19 x 10^{-12} F/m

C = 0.01119 x 10^{-6} μf /km

Capacitive reactance $X_C = \frac{1}{(2\times\pi\times50\times11.19\times10^{-12})}$ = 284 MΩ–m

Overhead line inductive and capacitive reactance has been thus calculated in this section and the network impedances can now be determined.

4.2.3 Impedance calculation

In order to carry out analytical calculations for determining short circuit calculation at different points in the network it is necessary to determine the impedances of the network components.

Source Impedance

The impedance upstream of 33/11 kV transformer is neglected for the purpose of this calculation Based on the MVA ratings and percentage impedance of the 33/11 kV transformer the 3 phase short circuit current at the 11 kV busbar of the suburban substation SS1 can be calculated as follows:

$$I''_{KQ} = \frac{15}{(1.732 \times 11 \times 0.086)} = 9.15kA$$

This value shall be used as the source short circuit level for rest of the calculation

The X/R ratio of the transformer is calculated using the formula shown below [38]:

X/R ratio of transformer = $30 \log_{10} MVA_{rating} - 20$ (4.6)

For a 15MVA transformer, X/R = 15 using equation (4.6)

Positive sequence source impedance $z_Q = \frac{cU_n}{\left(\sqrt{3}\times I''_{KQ}\right)}$ (4.7)

Z_Q= 0.75 Ω (using equation 4.7)

Where c = 1.09 for 11 kV system, U_n is the rated system Voltage and I''$_{KQ}$ is the short circuit current.

Based on an X/R ratio of 15,

Positive sequence Z_{Q1}= (0.050+ j 0.75) Ω

Zero sequence impedance is assumed to be 0.8 times positive sequence impedance

Zero sequence impedance = Z_{Q0} = (0.04 + j 0.6) Ω

Impedance of Overhead Lines

The overhead line resistance values have been obtained from manufacture's datasheets [37].

The resistance of overhead line TLine1 at 20^{o}C =0.239 Ω/km

The inductive reactance of the overhead line at 50 Hz =0.349 Ω/km

Line length = 1 km

Total line resistance = 0.239 Ω

Total line inductive reactance = 0.349 Ω

Therefore the positive sequence impedance of the conductor TLine1

Z $TL1_1$= 0.239 + j 0.349 Ω

Zero sequence impedance of overhead line can be approximated using the following equation.

$$ZTL1_0 = R_C + (1.571 \times 10^{-7} \times 2\pi f) + j\left\{2 \times 10^{-7} \times 2\pi f \log\frac{de}{GMR}\right\} \Omega/\text{m} \quad (4.8)$$

Where R c is the conductor resistance in Ω/m and de is the earth return of equivalent depth

$$de = \frac{1650}{\sqrt{\frac{\rho}{2\pi f}}} \quad (4.9)$$

For f = 50 Hz and ρ= 100 Ω-m value of de= 930 m

$$ZTL1_0 = 0.239 \times 10^{-3}(4.935 \times 10^{-5}) + j\left(628 \times 10^{-7} \times \log\frac{930}{0.005184}\right) \Omega/m$$

$ZTL1_0$= (0.2883+j 0.753) Ω /km

For a length of 1 km the zero sequence impedance of overhead line TLine1 is (0.2883+ j 0.753) Ω

The resistance of overhead line TLine2 at 20^{o}C =0.142 Ω/km

The inductive reactance of the overhead line at 50 Hz =0.330 Ω/km

Total line resistance for 1km line length = 0.142 Ω

Total line inductive reactance for 1km line length = 0.330Ω

Therefore the positive sequence impedance of the conductor TLine2

$ZTL2_1$= 0.142 + j 0.330 Ω

Zero sequence impedance of overhead line can be approximated using equation (4.8)

$$ZTL2_0 = 0.142 \times 10^{-3}(4.935 \times 10^{-5}) + j\left(628 \times 10^{-7} \times \log\frac{930}{0.0071}\right)\Omega/m$$

$ZTL2_0$= (0.191 +j 0.739) Ω /km

For a length of 1 km the zero sequence impedance of overhead line TLine2 is (0.191 +j 0.739) Ω

Impedance of cables

Impedances of cables have been obtained from manufacturer's data sheets [40] and power distribution company's underground cable data [41].

Impedance values of cable C1 connecting the 11 kV overhead line to the Ring main unit in the Kiosk Substation are given below:

Positive Sequence impedance = 0.524+ j 0.147 Ω /km

Zero Sequence impedance = 1.05+ j 0.08 Ω /km

The total positive sequence impedance of the cable C1 for a cable length of 30 m is $0.03(0.524 + j0.147)$ =0.0157 +j 0.0044 Ω

The total Zero sequence impedance of the cable C1for a cable length of 30 m is $0.03(1.05 + j0.08)$ = 0.031+j 0.0024 Ω

Impedance values of cable C2 connecting the 400V switchboard in the Kiosk Substation to the overhead line.

Positive Sequence impedance = 0.126+j0.062 Ω /km

Zero Sequence impedance = 0.050+j0.062 Ω /km

Total positive sequence impedance of the cable (cable length of 30 m)

$C2 = 0.03 \times (0.126 + j0.062)$ = (0.0037 + j 0.0018) Ω

Total Zero sequence impedance of the cable (cable length of 30 m)

$C2 = 0.03 \times (0.050 + j0.062)$= (0.0015 +j 0.0018) Ω

Impedance of Transformer

Transformer % impedance for 630 kVA transformer is considered as 4%

Transformer Impedance $ZT = \left(\frac{U_Z}{100}\right) \times \left(\frac{UrT^2}{SrT}\right)$ (4.10)

ZT = (4/100) *{4002/ (630*1000)} = 0.010 Ω

Uz – Impedance Voltage, UrT- Rated Voltage and SrT- Rated kVA

Considering X/R ratio of transformer = 10, ZT = (0.001 + j 0.010) Ω, (for a 3 limb delta star transformer zero sequence impedance can be considered as 100% of positive sequence impedance).

Using the impedances obtained the short circuit current at distribution board will be calculated.

4.3 Short Circuit Calculation

The 3 phase short circuit current at end of TLine2 and single line to ground fault current at customer's main distribution board is calculated in this section.

Impedances as shown in Figure 4.4 used for calculating fault currents at point FA and FB. The short circuit current has been calculated in accordance with Australian Standard AS 3851[38].

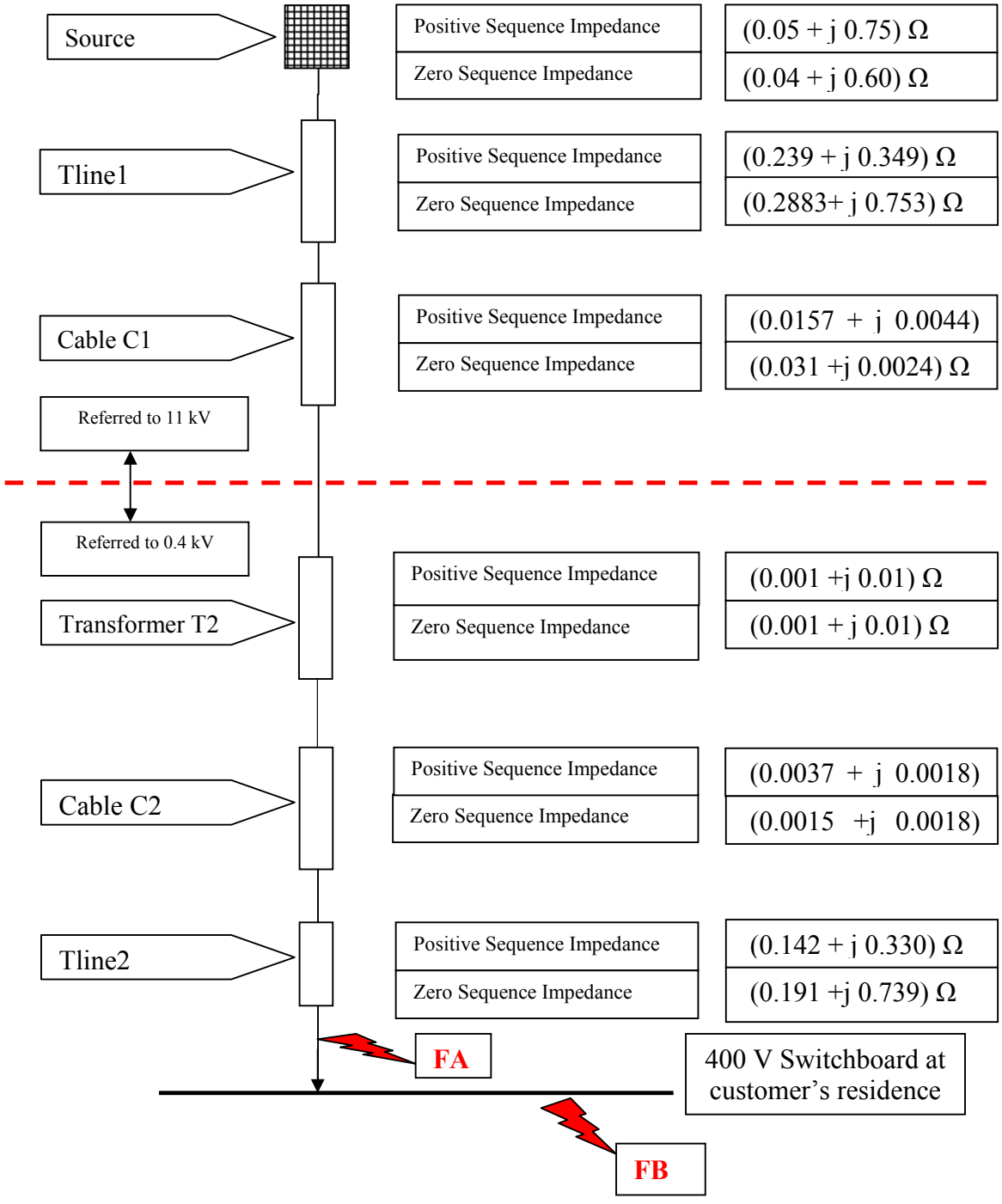

Figure 4.4 Network Impedance diagram

3 Phase fault FA at end of 1 km length of overhead line Tline 2, $I''_{K1} = \frac{\mathrm{Un}}{\sqrt{3}\times \mathrm{Z}_1}$ (4.11)

Single line to ground fault (FB) current at customer's main distribution board

$$I''_{K0} = \frac{\sqrt{3}\times \mathrm{Un}}{(2\times \mathrm{Z}_1 + \mathrm{Z}_0)} \quad (4.12)$$

Z_1 is the positive sequence impedance as seen from the point of fault

Z_0 is the zero sequence impedance as seen from the point of fault

Total positive sequence impedance upstream of transformer T2

- referred to 11 kV = (0.3047 + j 1.1034) Ω
- referred to 400 V = $\left(\frac{400}{11000}\right)^2 \times (0.3047 + \text{ j } 1.1034)$=0.0004 +j 0.00146 Ω

Total positive sequence impedance downstream of transformer T2

- referred to 400 V = (0.1467 + j 0.3418) Ω

Total positive sequence (referred to 400 Volts) as seen from the point of fault

Z 1 = (0.1471 + j 0.3432) Ω

Zero sequence impedance upstream of the transformer T2 has no impact on the fault at 400 volt side of transformer. This is because in a Dyn11 transformer the primary side is delta and zero sequence current cannot flow in the delta side of transformer.

Therefore the total zero sequence impedance as seen from the point of fault Z0 = 0.1935 + j 0.7508

Using the calculated values of positive and zero sequence impedance, the fault current for

Three phase fault at point FA = 618 Amps

Single line to ground fault at point FB = 484 Amps

4.4 PSCAD model of network and validation of model

The power distribution system defined in section 4.1 has been modeled in PSCAD and simulation output at end of each impedance component of the model has been compared with analytical value of fault level to validate the accuracy of model. The model has been split into 5 parts to check response of the model during fault simulations. The Figure 4.5 shows the five parts of the power system which has been analysed for faults. Three phase fault has been simulated at source and end of each part and in part 5, single line to ground fault has also been simulated. This value has been used as the source short circuit level for simulations done for faults at customer distribution board. The simulation outputs have been included in Appendix B. The PSCAD model of the power system

of the test network has been provided in Figure 4.6.The runtime settings for PSCAD were set to 0.5s duration of run, 50µs solution step time and 250µs channel plot step.

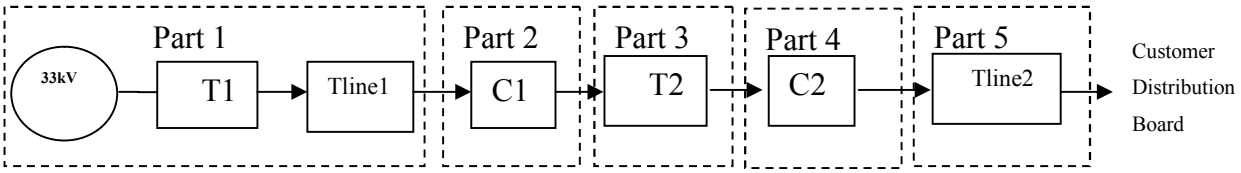

Figure 4.5 Network splits for analysis

Table 4.1 lists the difference between analytical (calculated) and simulated value of fault current. Values listed in the table shows that simulated results are very close to the analytical results which prove the accuracy of the developed network model. The simulation outputs are provided in Appendix B.

Table 4.1 Analytical and simulated value of fault current

Fault at end of part	Type of fault	Fault Current kA-simulation	Fault Current kA-analytical	Difference (%)
1	3 phase	5.9	6.1	3
2	3 phase	5.8	6.0	3.33
3	3 phase	19.9	20.0	0.5
4	3 phase	16.1	16.25	0.92
5	1phase-E	0.490	0.484	1.23

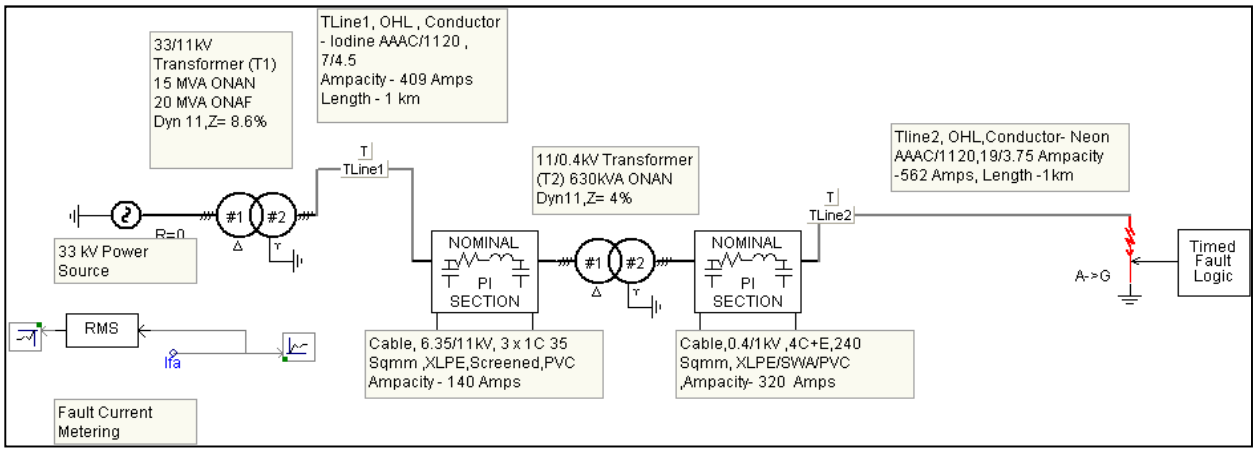

Figure 4.6 PSCAD model of power network

4.5 Power distribution at residences

The 400 volt distribution to customer distribution board is shown in the Figure 4.7 and is described in details in this section.

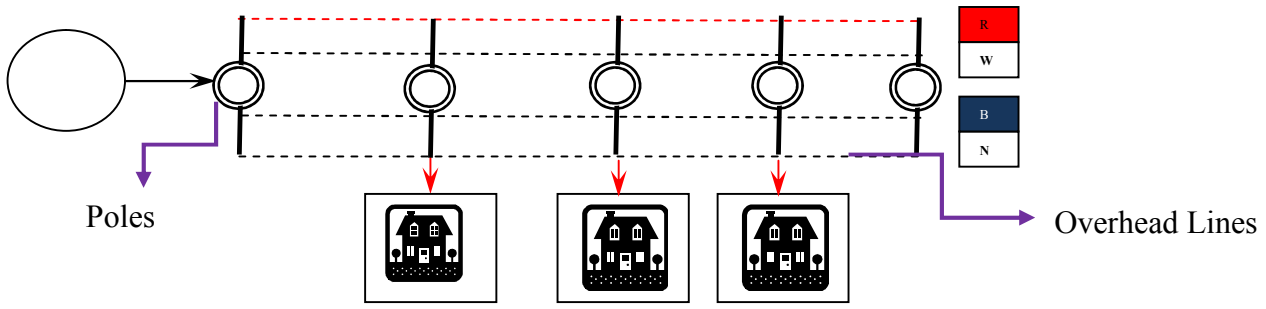

Figure 4.7 400 V distribution from OHL

As discussed in section 4.1, the 11000/400 Volts transformer (Transformer T2) installed in the kiosk has a rated capacity of 630 kVA transformer. The transformer provides supply to the 400 volts power distribution board installed in the Kiosk. There are two 400 amps outgoing circuit feeder from the distribution board which feed the 400 volt overhead circuits through buried cables. The complete system is sized to cater for 220 kVA per 400 volts circuit. Therefore load of the two circuits together does not exceed the transformer rating at any time. A 220 kVA balanced 3 phase circuit can feed 73 kVA (i.e. 220/3 per phase. Considering average domestic consumption of 5 kVA per residence, each phase can feed 18 residences. For the purpose of this research work a load of 14 residences per phase has been considered.

To investigate the effect of adding a PV system as a power source for domestic power distribution board of residential units, a PV unit has been assumed to be installed each of the 14 residences supplied by the red phase of 400 Volts overhead line. It is assumed at this point that inclusion of PV system in domestic networks will lead to increase in fault current available during a prospective short circuit in a customer main distribution board. This will be validated by simulation of faults and result analysis in the subsequent sections.

4.6 Analysis of fault current contribution

4.6.1 Analysis of fault current with PV considering single residence

Figure 4.8 shows a typical power distribution arrangement at customer's main distribution board. During a fault in the customer distribution board, fault current when:

- PV is not connected is I_A
- PV is connected is $I_A + I_B$

I_A is the fault current contribution from utility and I_B is the fault current contribution from PV.

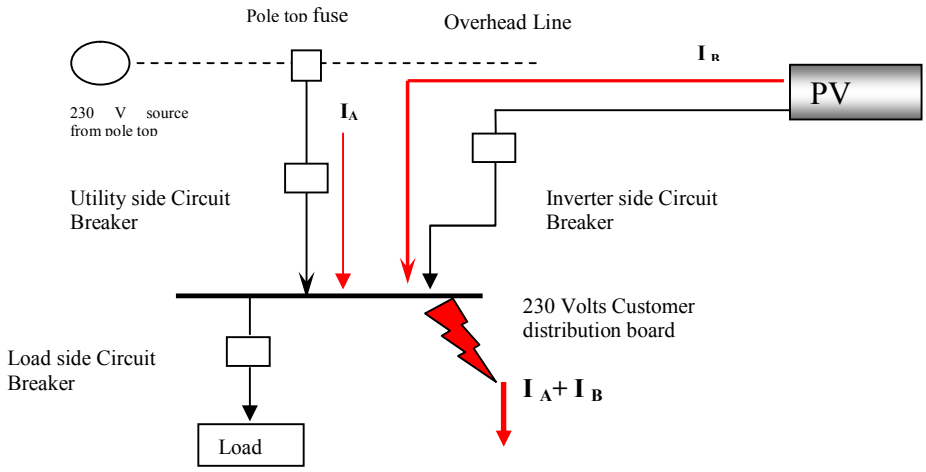

Figure 4.8 Fault current contribution from PV-Single residence

It can be observed that the utility side circuit breaker will have to successfully interrupt fault current contribution from utility and the PV side circuit breaker has to interrupt the fault contribution from PV. Circuit breakers are sized to interrupt the fault contribution from individual sources and therefore no upgrade or evaluation utility side circuit breaker is required. The other factor to consider is the effect of contribution of additional fault current from PV system on the fault withstands capacity of the busbar arrangement of the main distribution board.

For a bus bar system it is important that-

- The busbar assembly should be capable of withstanding the mechanical forces exerted on the conductor during the fault.
- The busbar conductor material should be able to withstand the temperature rise caused by the increase in magnitude of current during the fault.

In many cases the single phase mains distribution board do not have a busbar assembly and the switching devices are connected using wire looping (based on the arrangement inside main distribution board). In all cases it is however, important that one or both of the criteria should be satisfied.

The maximum size of PV system connected to residential main distribution board considered in this research work is 2.5 kW. The current handling capacity power electronic switching component in the PV inverter limits the fault current contribution at the output of the inverter. Generally this value is no more than 1.5 to 2 times the inverter full load current rating as discussed in chapter 3 and also shown using simulation result in chapter 2. So for a 2.5 kW inverter the fault current value is in the order of 16.5 to 20 amps. The switchboard busbar withstand capacity is of the order of 15000 amps

to 20000 amps for 0.2 to 0.5 seconds depending on specification of installation. Therefore additional fault current contribution of the order of 16-20 amps from PV generator has limited effect on the fault withstands capacity of the busbar.

4.6.2 Analysis of fault current with PV considering multiple residences

Figure 4.9 shows a typical power distribution arrangement at customer's main distribution board with PV system connected to multiple residences.

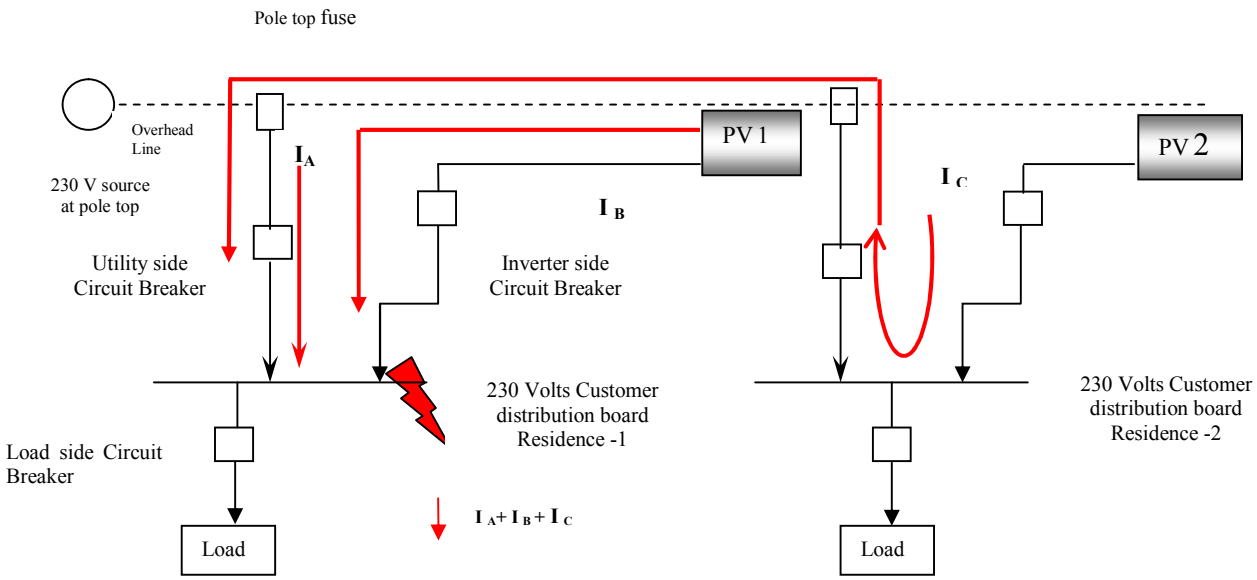

Figure 4.9 Fault contribution from PV-Multiple residences

During a fault in the customer distribution board, fault current if:

- PV is not connected is I_A
- PV is connected – $I_A + I_B + I_C$

Where I_A is the fault current contribution from utility, I_B is the fault current contribution from PV1 and PV 2 is I_C.

As discussed in section 4.6.1, utility side circuit breaker is selected to interrupt the utility side contribution of fault current, and the PV side circuit breaker has to interrupt the fault contribution from PV 1.

Unlike the case where analysis is based on PV connection in single residence, with PV units installed in multiple residences, the utility side circuit breaker will now have to interrupt the summation of fault current contribution from utility side and fault current contribution from the PV units of other residences connected to the same phase of overhead line to successfully clear the fault.

The fact to note here is that the fault current contribution from PV system connected to main distribution board of other residences will collectively contribute to the fault occurring in the distribution board of a particular residence. This fault current will have to be cleared by the main short circuit clearing device installed in the distribution board where the fault has occurred. While fault current contribution from a single PV unit may be not significant compared to the utility fault contribution, with multiple PV units the scenario will not be the same.

It will therefore be important to ensure the following:

- The utility side fault interruption device has the required fault breaking capacity.
- The fault withstand capacity of the busbar is adequate.

Though for a 2.5 kW inverter the fault current value is in the order of 20 amps, 14 units together can cumulatively add up to 0.3 kA. Addition of more residences with PV or introduction of higher size PV systems can significantly increase the fault current, which may necessitate requirement for checking size of short circuit protection device and fault withstand capacity of the busbar.

4.7 PSCAD model for PV connection at customer distribution board

The customer end power distribution data used in the PSCAD model developed for research is based on Figure 4.10 and the data in Table 4.2.

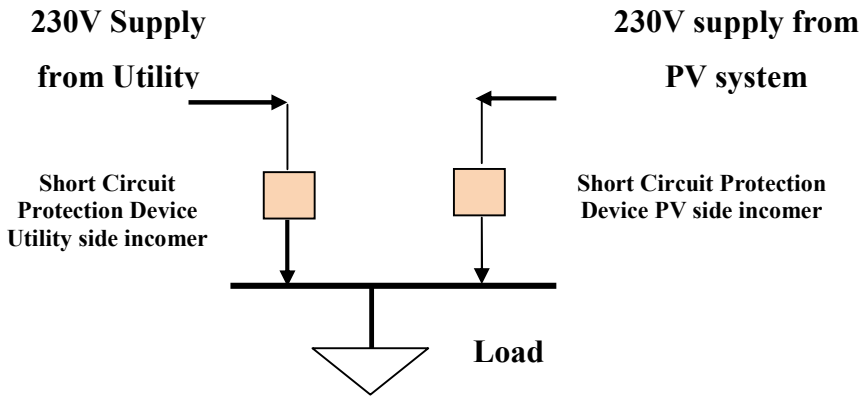

Figure 4.10 Customer end 230 V power distribution

In the simulation the PV source has been modelled as a voltage source that can contribute about 50% the power requirement for the 5 kVA load. PV systems has been modeled as both constant current and constant voltage source in the studies done in the past [21].During a fault in the main distribution board the fault current contribution from the PV system is limited to a value of 1.5 times of inverter full load current. Though the current from PV during fault varies from 1.5 to 2 times of the rated inverter, 1.5 times has been considered to see the minimum impact. Full load

current for a 2.5 kW inverter (considering unity power factor) = 10.9 Amps. The maximum possible fault contribution from inverter during fault is $1.5 \times 10.9 = 16$ Amps (approximately).The load of 5 kVA is represented by a 10.5 ohms resistance which will absorb 5 kVA at unity power factor. Table 4.2 provides details of equipment for power distribution at residences.

Table 4.2 Specification for power distribution at residences

Description	Specification
Load per customer	5000 kVA
Main distribution Board	230 Volts, 50 Hz ,Single Phase
PV Panel	• Configuration- 72 cells per panel, 12 panels (3 parallel sets, each set made up of 4 panels connected in serial) • Total Voltage -162 Volts • Power – 238 Watts /panel, Total Power = 2.85 kW
PV Inverter	2.5 kW, 230 Volts Single Phase output

Simulations for different scenarios have been carried out to in a step wise manner to obtain current readings. The current readings obtained for various scenarios have been listed in Table 4.3.The simulation outputs are provided in Appendix C.

Table 4.3 Simulation results

Scenario	Source	Connected to MDB	Normal/ fault at MDB	Contribution (amps)
1	PV1	No	Normal	0
1	Utility	Yes		22
2	PV1	Yes	Normal	11
2	Utility	Yes		11
3	PV1	No	Fault	0
3	Utility	Yes		480
4	PV1	Yes	Fault	16.5
4	Utility	No		0
5	PV1	Yes	Fault	16
5	Utility	Yes		478
6	PV1	Yes	Fault	16
6	Utility	Yes		478
6	PV2	Yes		16

Scenario 2 results indicates that both utility and PV contributes 11amps of current indicating 50-50 load sharing between the sources. When only utility is connected, during a fault, current contribution from utility is 480 amps, but when PV1 is connected as well the fault current at the point of fault increases by 16 amps which is the PV1 contribution. With PV2 connected in the next residence, the fault current increases to 510 amps due to contribution from both PV1 and PV2.

In the simulations carried out, effort has been made to illustrate the fact that though individual PV system might not contribute enough fault current to be able make appreciable affect the fault interruption capacity of circuit breakers, multiple PV units connected to the network will make cumulative contribution to be the point of fault and thus impact the ability of short circuit protection device to clear the fault.

An important factor in the analysis is the duration of contribution from PV system to the fault. This has a significant impact on the fault withstand capacity of the short circuit protection device as well as the downstream busbar network.

The protection device at the customer main switchboard in the case studied in the previous section a 25 Amps Curve C miniature circuit breaker (MCB) with a fault breaking capacity of 6 kA. The protection device that control power flow from PV system to customer main switchboard is a 16 Amps Curve C miniature circuit breaker with a fault breaking capacity of 6 kA. The miniature circuit breakers are sized on the basis of the load. The load per residence is 5 kVA. The utility side circuit breaker will allow 5 kVA to flow to load. The PV side circuit breaker will allow 2.5 kVA (approximately) based on the PV panel size considered in this case.

A curve C, MCB [42] has a trip characteristic which trips the breaker at 5 to 10 times of rated current of the device almost instantaneously. At a current less than this but above 110% of rated current the device follows IDMT characteristics.

Therefore the magnitude of instantaneous tripping current for MCB on the utility side is 125 amps to 250 amps and on the PV side it is 80 Amps to 160 Amps.

The fault current contribution for single line to ground fault from utility is 484 amps and from PV side is 16.5 amps (approximately). Total contribution from PV connected to 14 residences will be 231 amps. So the total fault current seen at the point of fault is = 715 amps (484 + 231).

Fault seen by the short circuit current interrupting device on utility side is {484 + (n-1) * 16.5} amps, where ‘n’ is the number of residences. So the fault current seen by the utility side short circuit

protection = (484 +214.5) = 699 amps. This magnitude of current is 28 times the rated value of the circuit breaker and the breaker will trip in about 0.01 seconds as shown in Figure 4.11 and Figure 4.14. The magnitude of fault current fed by individual PV system is about 105% of the rated current rating of the circuit breaker. This indicates that the breaker will not trip during short circuit as shown in Figure 4.12.

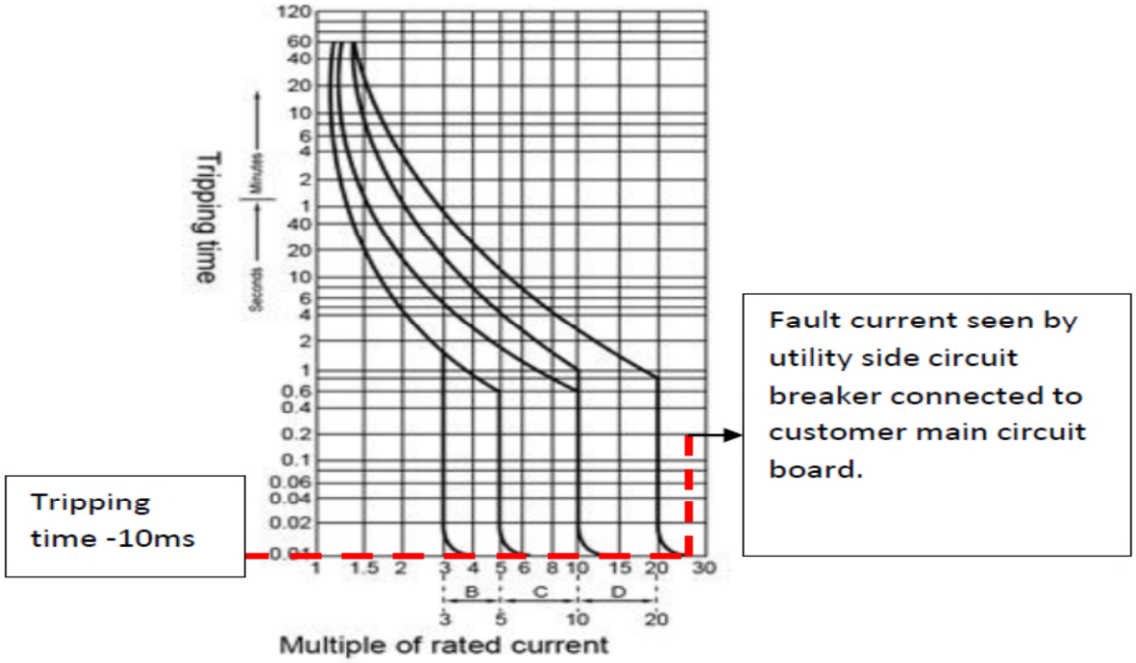

Figure 4.11 MCB Trip curve –Trip point for utility side MCB

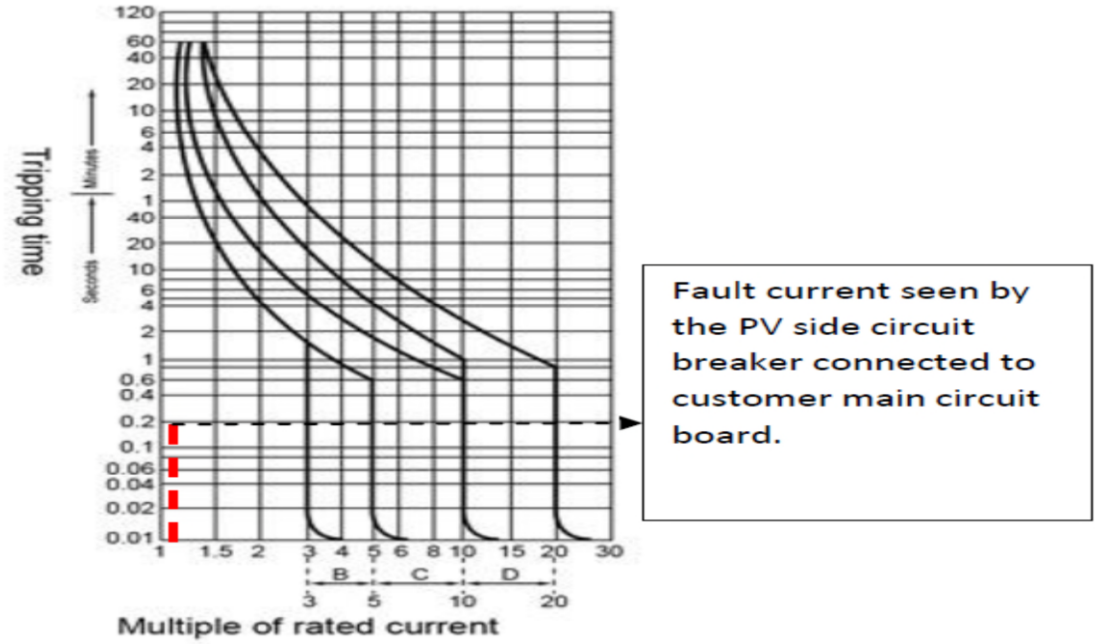

Figure 4.12 MCB Trip curve –Trip point for PV side MCB

However, for a PV system the circuit breaker on the outgoing line is not the only device for isolating current feed to fault. As discussed in chapter 2, PV systems are IIDGs. A single phase inverter converts DC power to AC using controlled firing (using PWM techniques) of four IGBTs (Insulated Gate Bipolar Transistor). In event of a short circuit at the load side IGBT collector current will rise. Once it rises to a particular level the collector to emitter voltage will spike. Depending on device characteristic the collector current can be kept at or below a certain level, however, the IGBT will still be subjected to high current and voltage and this situation should be removed immediately. The time allowed between the start of short circuit until the current is cut off is limited by the short circuit withstand capacity of the IGBT [43]. The short circuit withstand time of IGBT can be controlled by the V_{GG+} (voltage across gate and emitter of IGBT during conduction). Smaller the value of V_{GG+}, higher is the short circuit endurance time. IGBT collector current is a function of the gate emitter voltage V_{GE} and temperature. The transfer characteristics of an IGBT (I_C Collector current versus V_{GE}) indicate the maximum possible collector current at a particular $V_{GE.}$ This is generally 1.5 to 1.8 times the nominal current which is much less than the short circuit current which is of the order of 6 to 7 times the nominal value [44]. The short circuit safe operating area (SCSOA) of IGBT, a curve with ratio of short circuit collector current to normal collector current on one axis and V_{CE} on the other, defines the limit of safe control of IGBT. Figure 4.13 shows a typical SCSOA curve of IGBT (Typical manufacturers curve).

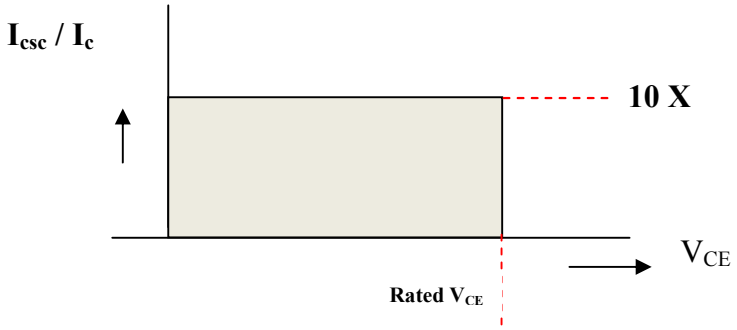

Figure 4.13 Short circuit safe operating area of IGBT

The boundary conditions associated with the curve are as follows:

- The short circuit has to be detected and turned off within max of 10 µS.
- The time between two short circuits has to be at least 1 second
- The IGBT must not be subjected to more than 1000 short circuits during the total operating time.
- The short circuit endurance time for a typical IGBT used in an inverter for similar application is in the order of 10 µS.

The fault contribution with current values limited to 1.2 to 1.5 times the full load current (rated collector current) can keep feeding the fault for longer time as it will be well within the safe short circuit operation zone of IGBT. The maximum time for which the fault feed can happen at about 1.5 times the normal full load current is limited by the temperature rise in the IGBT which will eventually lead to the destruction of IGBT. Investigation carried out in the area of fault contribution from PV systems connected to grid indicated that there had been post fault contribution from PV in the range of 4 to 10 cycles [28].

This time of 4 -10 cycles is equal to 80 milliseconds to 200 milliseconds for a 50 Hz supply system which is much more than the fault clearance time of main utility side circuit breaker on a customer distribution board .This therefore implies that the fault current contribution from PV systems on a particular phase will cumulatively add and increase the fault current seen by the protection device resulting in requirement of higher fault current interrupting capacity of the utility side circuit breaker. The utility side circuit breaker will basically clear a fault current of magnitude equal to the summation of fault current contribution from the utility and fault current contribution from PV systems (refer Figure 4.14). Therefore increase in number of residences connected to a particular utility distribution phase or increase in size of PV systems connected to residences on a particular phase will result in higher fault contribution from the PV systems and limit needs to be established on maximum PV penetration so as to eliminate possibilities of fire and accidents in customer power distribution boards due to unsuccessful attempt by short circuit clearance device to clear fault.

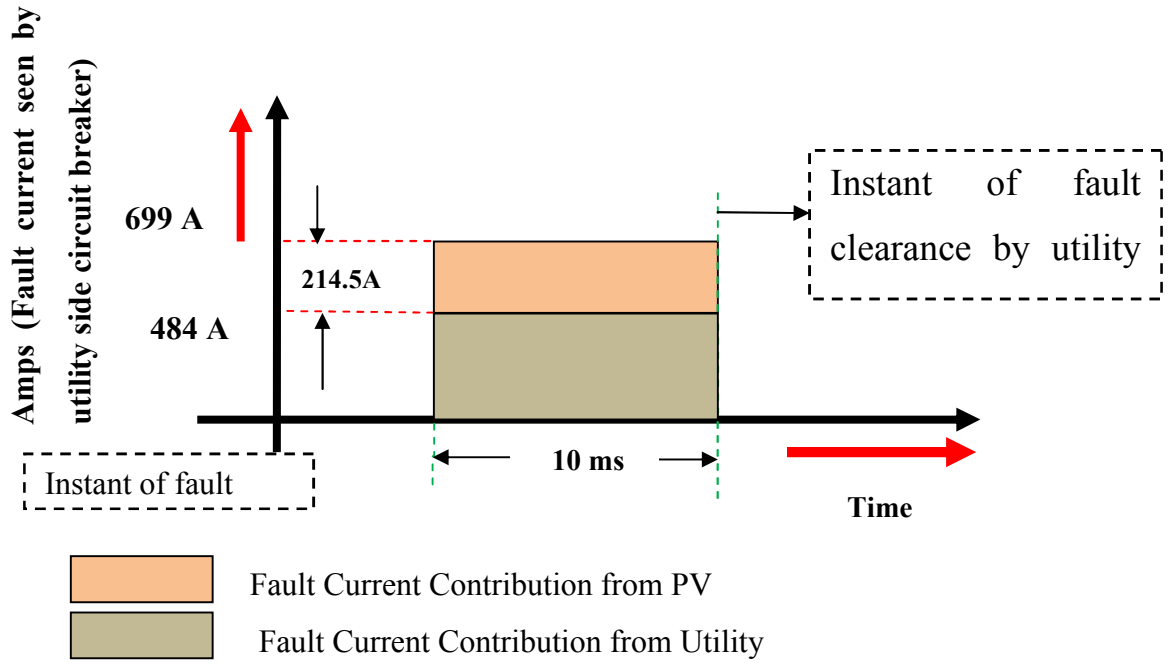

Figure 4.14 Fault Contribution from PV and Utility (seen by utility side CB)

The other aspect to consider in terms of disconnection of PV inverter is disconnection by grid protection device of inverter.

The requirement as per Australian Standard [36] is that the grid protection device shall operate if supply from grid is disrupted or when grid goes outside set limits and ensure prevention of islanded operation. The grid connection device shall incorporate passive anti-islanding protection in terms of under and over voltage and under and over frequency within 2 seconds.

During the fault the system will experience under-voltage and with a set band of 200V to 230V for minimum voltage (as stated in Australian Standard AS4777.3), it is very likely that the anti-islanding protection will sense the fault but the utility breaker will trip well before operation of anti-islanding protection and isolate fault. The tripping of utility side breaker will inhibit any current flow from utility as well as from PV systems of neighbouring units. However, fault feed to main distribution board from the PV connected to the board will continue until the PV inverter over current protection isolates the system. If this fails to operate then subsequently grid anti-islanding protection will isolate the PV system. Figure 4.15 illustrates the time sequence for isolation discussed in this paragraph.

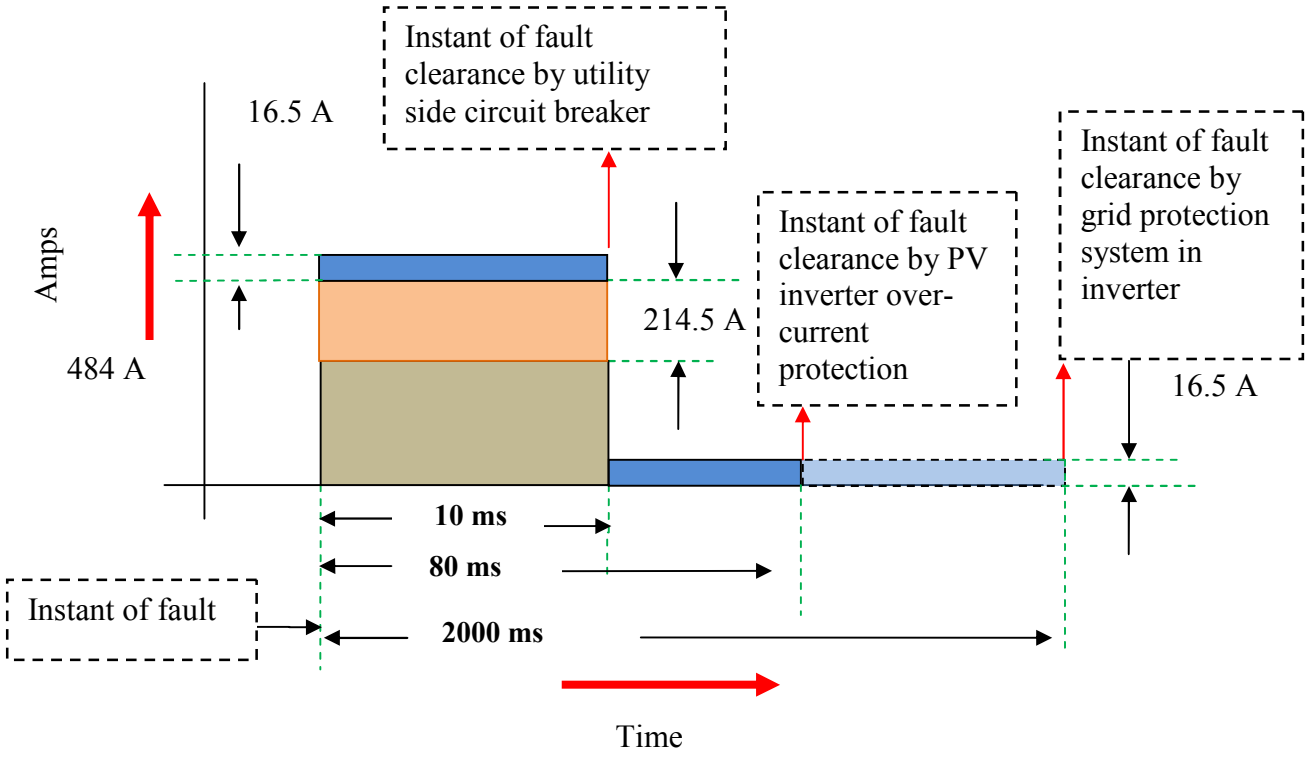

Figure 4.15 Fault Contribution from PV and Utility (seen by point of fault by DB)

4.8 Conclusion

The investigation concludes that even though the fault current contribution from individual PV systems installed on residences is not high, collective contribution from multiple PV systems connected across the network can make significant increase in fault current. With increased level of PV penetration, networks needs to establish the level of penetration beyond which there can be significant problems in fault current interruption by existing fault clearing devices. Attempt by the protective device to clear fault higher than the capacity of the device can result in significant safety issues and lead to fire incidents. In the next chapter a study done to investigate the impact of high penetration of large three phase PV systems on protection coordination in the power distribution network has of large multi- apartment buildings has been presented.

Chapter 5 Impact of fault contribution from large three phase PV systems on protection coordination

The protection coordination problems caused due to the increase in fault current level caused by contribution from distributed generators has been discussed in chapter 3. In chapter 4 a case study to illustrate the potential capacity limitation of circuit breakers and power busbars in distribution boards due to increase in fault current caused by high PV penetration in a network has been presented. In this chapter, multiple case studies conducted for analysing the impact of additional fault current produced from large three phase PV systems on protection coordination in low voltage residential network has been presented. This work has been submitted (resubmitted after first review) for publication as a journal paper in Elsevier Energy and Buildings Journal [45]. As discussed in the previous chapters, the fault current contribution from PV systems considered for studies and modeling is twice [24] the inverter rated current. This can however, vary slightly depending on different types and manufacturers of inverters for PV systems. The fault current contribution time generally varies from 4 cycles to 10 cycles [25]. The low fault current contribution from PV system does not necessarily mean that evaluations of existing relay coordination is not required when PV systems are added to network. The magnitude of fault current contribution depends on the size and number of PV system installed in a particular network and therefore the level of penetration of PV system in a particular size of network determines the impact of PV system on protection coordination.

All grid tied PV system inverters are provided with anti-islanding protection in addition to PV systems internal fault current limiting system. As per IEEE standard 1547 [18], all grid connected inverter system shall successfully detect islanding and stop energizing within a given time frame. During a fault in the network, the grid side fault clearing device opens to clear the fault. The PV system then detects islanding and thereafter trips on detection of islanded condition within specified time (within 2 seconds) [18, 36].

The existing work mainly analyses protection problems in network caused by fault contribution from synchronous generators, which can feed substantial fault current and cause protection issues like fuse recloser coordination problems [11] and out of phase closing of recloser during fault. Such issues are more relevant for high voltage power distribution networks as recloser is typically used in high voltage networks only. Some literatures have analysed fault current contributions from PV systems but studies described therein are related mainly to high voltage power networks [23]. A

detailed investigation of protection and voltage regulation issues caused due to high penetration of PV systems in low voltage has been discussed in some literature [27][31]. However, these papers focus on the protection issues in high voltage side of network caused by high PV penetration in the low voltage side of network. Not much literature is available on protection coordination issues in low voltage network due of high penetration of PV system in low voltage. Presently a number of large three phase PV systems are connected to low voltage networks, in particular to large buildings with multiple apartments in a housing complex or in commercial and industrial premises, which can cause protection problems in low voltage network.

In this chapter several case studies to analyse protection coordination issues due to increased PV penetration in low voltage network has been described in details and also the preferred method of adjustment of time current coordination settings in order to avoid repeated adjustment of protective setting (each time when a new PV system is added to the distribution network) has been provided.

A typical power distribution network has been used as a test network for performing the analysis. In the subsequent sections of this chapter, network modeling and the case studies has been described in details.

5.1 Network description

11 kV power is supplied via overhead line (OHL) from main substation to pole mounted 11/0.4 kV Transformer (T1). The transformer is protected by drop out fuse on the high voltage side and the secondary side is connected to a ground mounted low voltage distribution board using single core XLPE insulated cable. The low voltage distribution board comprises one off 630 amps incoming air circuit breaker (ACB) and four off 160 amps outgoing feeder moulded case circuit breakers (MCCBs). The outgoing MCCBs are connected to building MDB using XLPE insulated cables. To allow connection from grid and PV system, the building MDB has two incoming switches. The utility side incomer is provided with over-current protection devices. Integral over current and anti–islanding protection device has been considered for the PV inverter module. The block diagram in Figure 5.1 represents the network model.

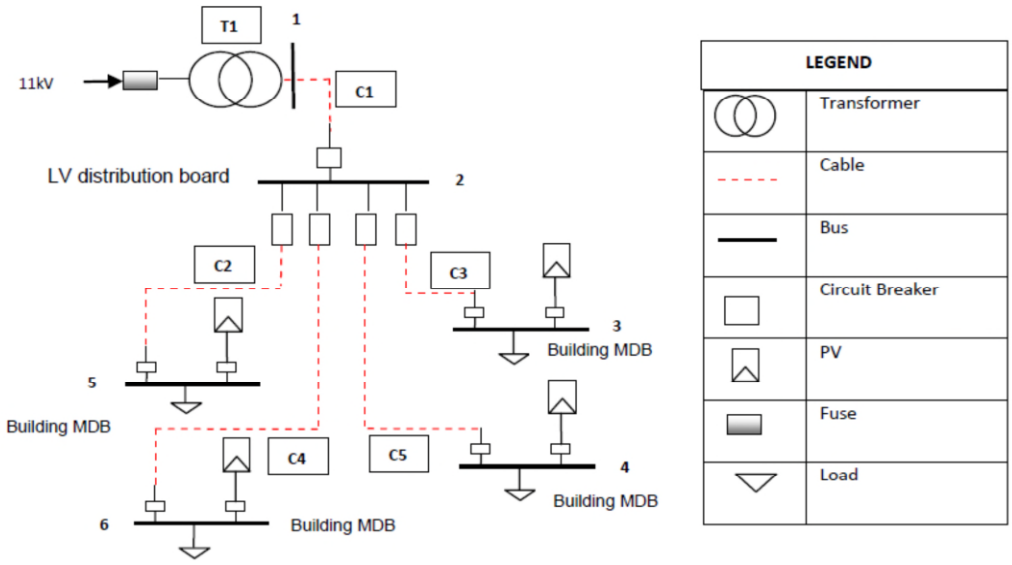

Figure 5.1 Network Model

5.2 Network Parameters

In order to carry out the case study it is required to establish the sizes and ratings of network components of the network shown in Figure 5.1. Following the selection of component sizes, the electrical parameters of the network components has been determined. The parameters of components has been subsequently used to model the power system in PSCAD and for carrying out analytical calculation for determining the short circuit current levels at various points in the network.

The following steps have been sequentially performed in order to obtain data required for short circuit calculation and development of power system model in PSCAD.

- Determination of equipment and conductor size
- Calculation of impedance for different components

5.2.1 Equipment and conductor sizing

The pole mounted Transformer T1 is a 315 kVA transformer with a transformation ratio of 11/0.4 kV. Transformer primary and secondary currents have been calculated below.

$$\text{Full Load Primary Amps} = \frac{315}{1.732 \times 11} = 17 \text{ amps}$$

$$\text{Full Load Secondary Amps} = \frac{315 \times 1000}{1.732 \times 400} = 455 \text{ amps}$$

The low voltage board is rated based on the secondary current of the transformer.

The cable (C1) from the transformer to the low voltage distribution board is a set (3 Phase + neutral) of single core 300 mm^2 XLPE insulated copper conductor cable. The cable has a current carrying capacity of 469 amps (assuming that the cable is installed in conduit and buried underground).

LV cable (C2, C3, C4 and C5) are $25mm^2$, XLPE insulated (copper conductor). Cable switching units in LV switchboard are connected to the building MDBs using these cables. Each cable has a current carrying capacity of 125 amps (assuming that the cable is installed in conduit and buried underground).Based on the cable capacity it shall be possible to feed approximately 86 kVA {calculated as: $1.732 \times 400 \times 125 = 86$} of power to individual building.

5.2.2 Impedance calculation

In order to carry out analytical calculations for determining short circuit calculation at different points in the network it is necessary to determine the impedances of the network components.

Source Impedance

15 MVA, 33/11 kV transformer with a percentage impedance of 8.6% (same as the source substation considered in chapter 4) has been assumed to be the source substation for 11 kV power supply. Three phase short circuit current at the 11 kV side of transformer can be calculated as follows:

$$I''_{KQ} = \frac{15}{(1.732 \times 11 \times 0.086)} = 9.15kA$$

This value shall be used as the source short circuit level for rest of the calculation

Source X/R ratio = 10 (assumed)

Positive sequence source impedance = Z_{Q1}= 0.75 Ω using equation (4.7)

Based on X/R ratio of 10, positive sequence source impedance Z_{Q1}= (0.075+ j 0.75) Ω

Impedance of cables

All cable impedances have been obtained from on Australian Standard AS3008.1.1 [46]

Positive Sequence impedance of cable C1 = 0.0812+ j 0.0961 Ω /km and cable length is 500m.

Therefore the total positive sequence impedance of the cable $C1 = 0.5 \times (0.0812 + \text{j}\, 0.0961)$ = (0.0406+j 0.04805) Ω

Positive Sequence impedance of cable C2, C3, C4 and C5 = (0.884+j0.0853) Ω /km and cable length is 20 meters each.

Therefore the total positive sequence impedance of the cable $= 0.02 \times (0.884 + j0.0853)$
= (0.01768+ j 0.001706) Ω

Impedance of Transformer

For 315 kVA transformer with percentage impedance of 4%, using equation (4.10),
Transformer Impedance Z_T = 0.02031746 Ω
Considering X/R ratio of transformer = 10
Z_T = (0.002021663 + j0.020216629) Ω
Using the impedance values calculated the short circuit current at customer distribution board has been calculated. The short circuit current has been calculated in accordance with Australian Standard AS 3851[38].

5.3 Short Circuit Calculation

Impedance diagram for calculation of single line to ground fault at customer distribution board is shown in Figure 5.2.

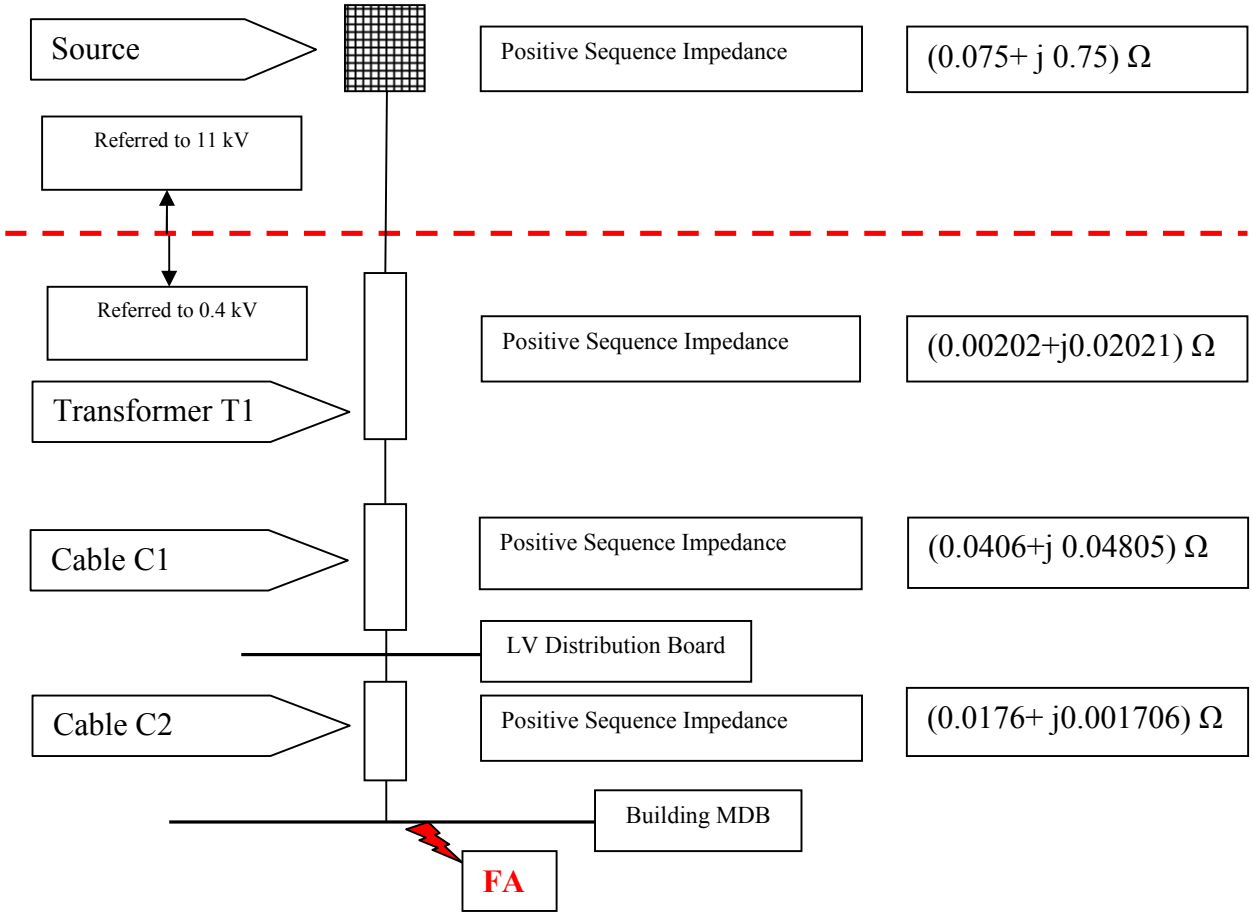

Figure 5.2 Network impedance diagram

Source positive sequence impedance

- referred to 11 kV = (0.075+ j 0.75) Ω
- referred to 400 V = $\left(\frac{400}{11000}\right)^2 \times (0.075 + \text{ j } 0.75)$ = (0.00009 + j0.0009) Ω

Total positive sequence impedance seen from the point of fault = (0.06040+ j 0.07096) Ω
Using equation (4.11), three phase fault at point FA = 2478 Amps.

5.4 PSCAD model of network and validation of model

The power system defined in section 5.1 has been modeled in PSCAD software environment. The power system model has been first validated to check its accuracy without introducing the PV systems. Fault current magnitude calculated analytically in accordance with AS 3851[38] has been compared with simulation output for faults at different points in the network. Figure 5.3 shows the points (A, B, C, D) in the power system at which fault has been placed and analytic values have been compared with simulation output. The high voltage side protection has not been included in model as this has no significance of the high voltage protection device in this study done. For ease of modeling, without effecting overall accuracy, only two out of four buildings have been modeled and cumulative effect has been considered for the other two buildings.

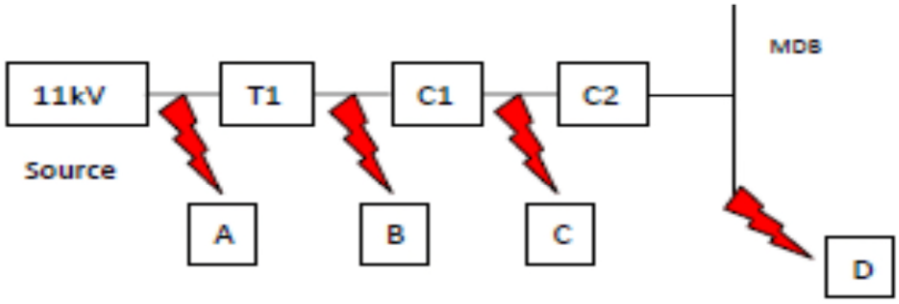

Figure 5.3 Analytical and simulation output compared at A, B, C and D

Table 5.1 lists the difference between analytical (calculated) and simulated value of fault current. Fault was simulated for duration of 0.2 seconds. The runtime settings for PSCAD were set to 0.5s duration of run, 50µs solution step time and 250µs channel plot step.

Values listed in the table shows that simulated results are very close to the analytical results which prove the accuracy of the developed network model.

Table 5.1 Analytical and simulated value of fault current

Fault at Point	Type of fault	Fault Current kA-simulation	Fault Current kA-analytical	Difference (%)
A	3 phase	9.14	9.15	0.1
B	3 phase	10.7	10.8	0.9
C	3 phase	2.80	2.84	1.4
D	3 phase	2.44	2.47	1.2

The PSCAD model of the test network described in section 5.1 is shown in Figure 5.4 with PV systems. The complete model system with protection and controls has been provided in Appendix D.

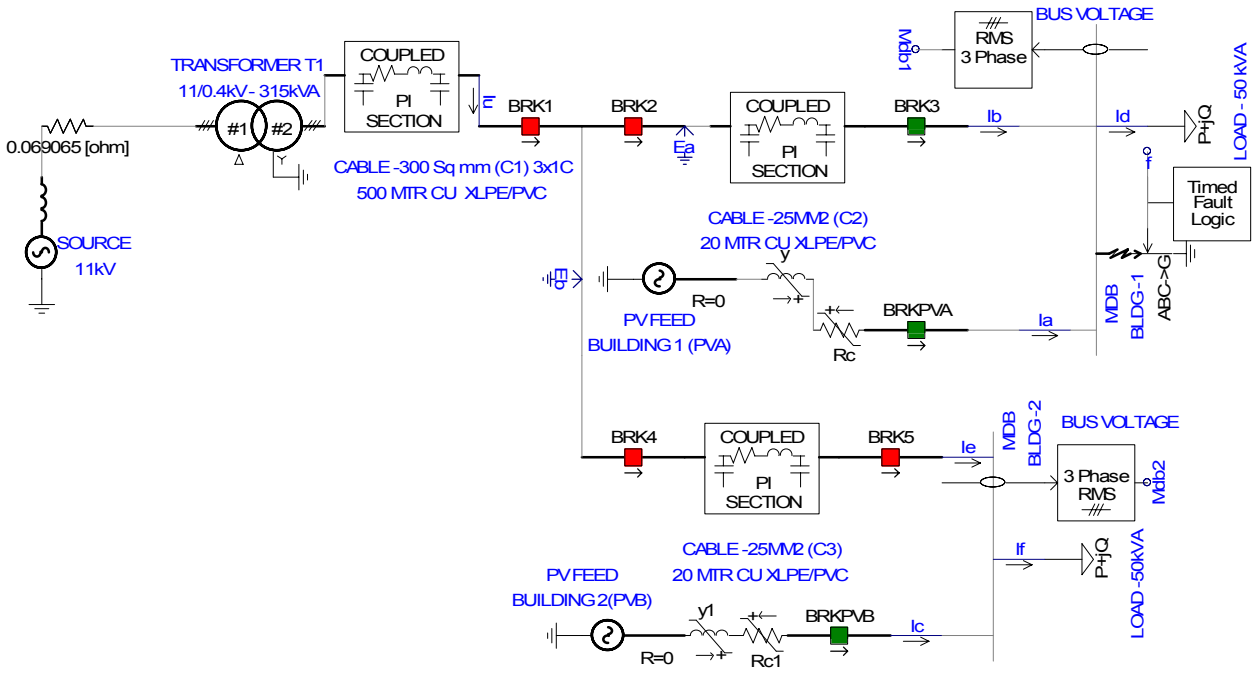

Figure 5.4 PSCAD Model of Network

As described in Section 5.1, transformer T1 provides power to the low voltage distribution board. The low voltage distribution board powers the MDB of each building using a 160 amps feeder. Each feeder (MCCB with connected cable) is sized to cater for 86 kVA per outgoing circuit. This study investigates the effect of adding a 50 kVA roof top mounted PV system to each building. Table 5.2 lists the values used for modeling the PV system connected to MDB of individual buildings.

Table 5.2 Specification for power distribution at buildings

Description	Specification
Load per building MDB	50 kVA (Each building has 10 apartment ,each with a load demand of 5 kVA)
MDB	400Volts, 50 Hz , Three Phase
Individual PV panel rating	238 Watts /panel, V mpp = 40.5V, I mpp= 5.88A
PV Panel connection and installation	Configuration- 210 panel Number of panels connected in series - 11 panels Number of panels connected in parallel - 20 panels Total voltage - 445 Volts, Total current – 115 Amps Installation type – Building Roof Top Total Power – 50 kW
PV Inverter	50 kVA ,400 Volts Three Phase output

Figure 5.5 shows the power distribution arrangement at the building MDB and the load sharing between PV and utility. PV system is modeled as a constant voltage source which can contribute about 67% of the power requirement for the building (i.e. 33.5 kVA) load and the rest 33% (i.e. 16.5 kVA) is contributed by the utility power supply. Figure 5.6 shows simulation outputs for the contribution from PV and utility to load during normal operation (i.e. when there is no fault).

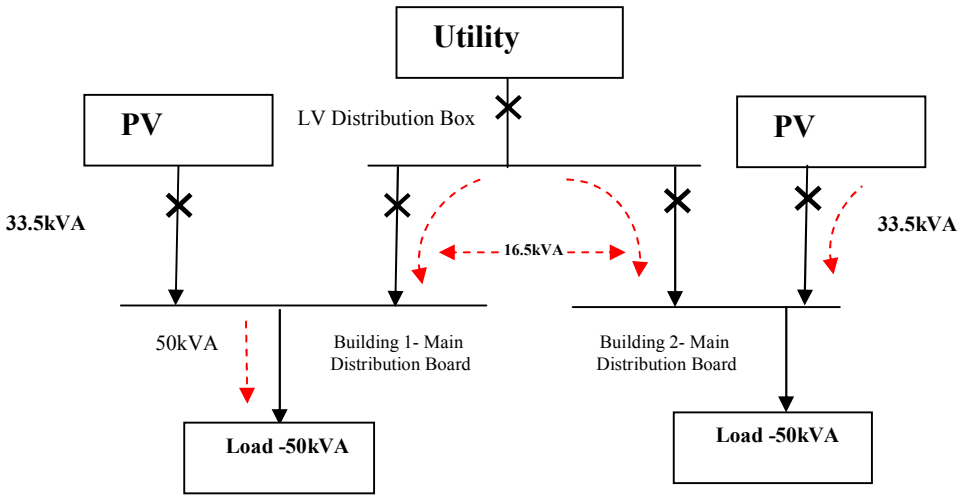

Figure 5.5 Power flow at building main distribution board

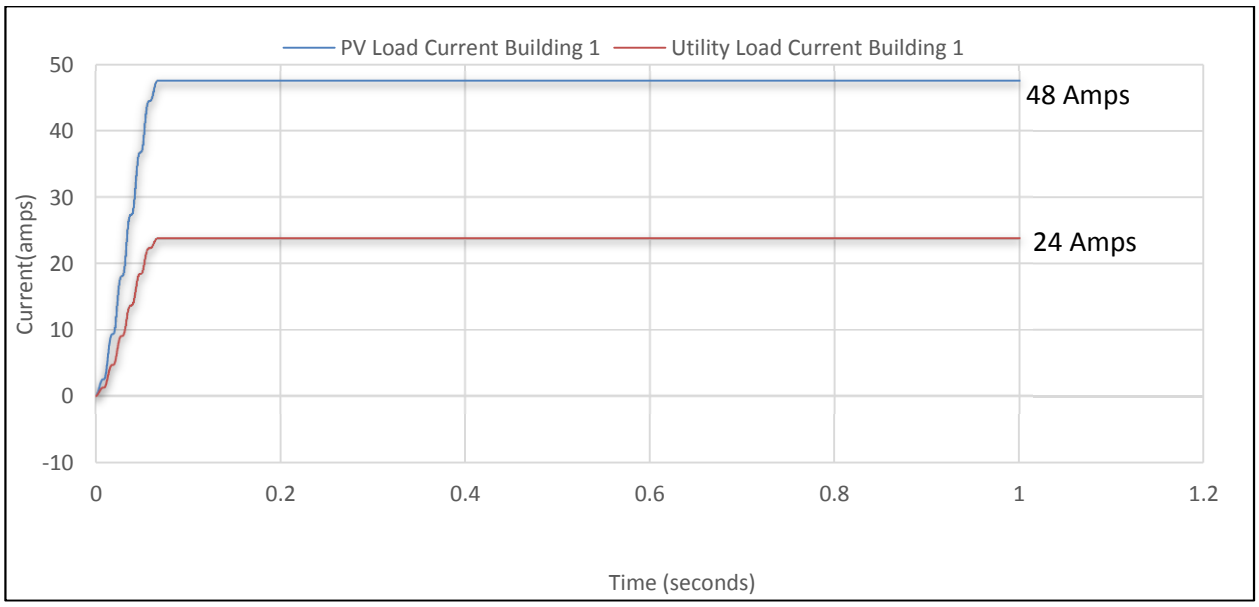

Figure 5.6 Load sharing between PV and utility during normal operation

During a fault in the system, the PV system contribution is limited to a value of 2 times of inverter full load current. Full load current for a 50 kVA inverter interfaced system is 72 Amps. The maximum possible fault contribution from inverter during fault is 144 amps (2 times 72 amps approximately).The control of contribution of current from the PV system during normal operation and fault is adjusted in the model by changing the source impedance of the constant voltage source used to represent the PV system [23].

5.5 Protection setting of network

Over current protection devices controls the tripping of circuit breakers BRK1, BRK2, BRK3, BRK4 and BRK5. When PV system is not connected, TCC ensures proper discrimination between upstream and downstream protection devices during fault and overload protection to devices during normal operation, thus ensuring reliability. The relay settings of the circuit breakers are shown the Table 5.3.

Table 5.3 Protection settings

Circuit Breaker	IEC-225-3 Curve	Current Setting	TSM	Definite Time setting
BRK1	Normal Inverse	460	0.5	3400 (Delay 0s)
BRK2	Normal Inverse	125	0.2	2750 (Delay 0s)
BRK3	Normal Inverse	125	0.1	2500 (Delay 0s)
BRK4	Normal Inverse	125	0.2	2750 (Delay 0s)
BRK5	Normal Inverse	125	0.1	2500 (Delay 0s)

The integral output switching and protection unit of PV system is represented by BRKPVA for the system connected to main distribution board of building 1 and BRKPVB for the one connected to main distribution board of building 2. During a fault at the output of the inverter, the PV system shall trip using one of the two protective functions listed below.

- Inverter over-current –Trip on over current within 4 cycles to 10 cycles [28]
- Anti islanding protection –Trips on loss of mains that within 2 seconds [18] of loss of utility power source.

Figure 5.7 shows the time current coordination requirement for the distribution system described in section 5.1.

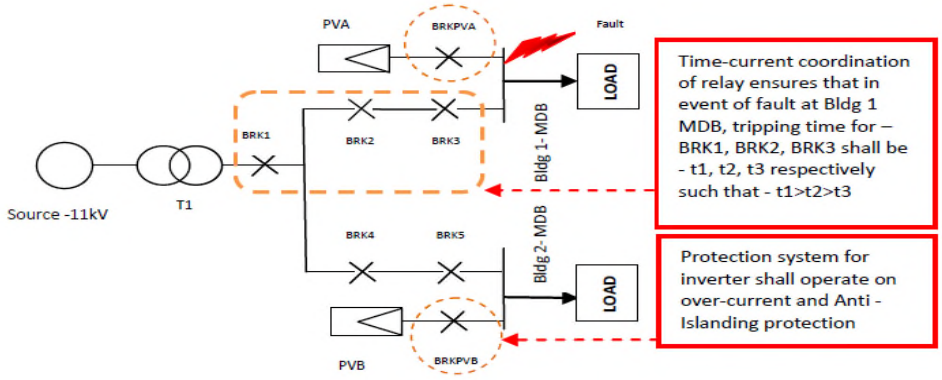

Figure 5.7 Time current coordination requirement of the network

5.6 Case studies

Four cases have been analysed during a fault in the Building1 MDB which have been described in the section below:

Case 1-Fault at the MDB of Building1 when only utility power source is connected to building MDB *(PV system is not connected).*

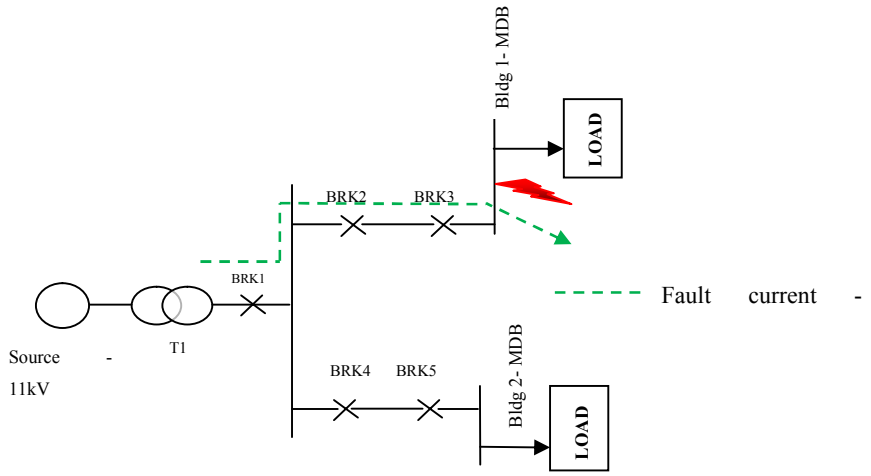

Figure 5.8 Fault current path–PV not connected

Figure 5.8 represents the flow path for fault current during a three phase fault in the MDB of building 1 when PV system is not connected to the building MDBs. The simulation output for the fault is shown in Figure 5.9.

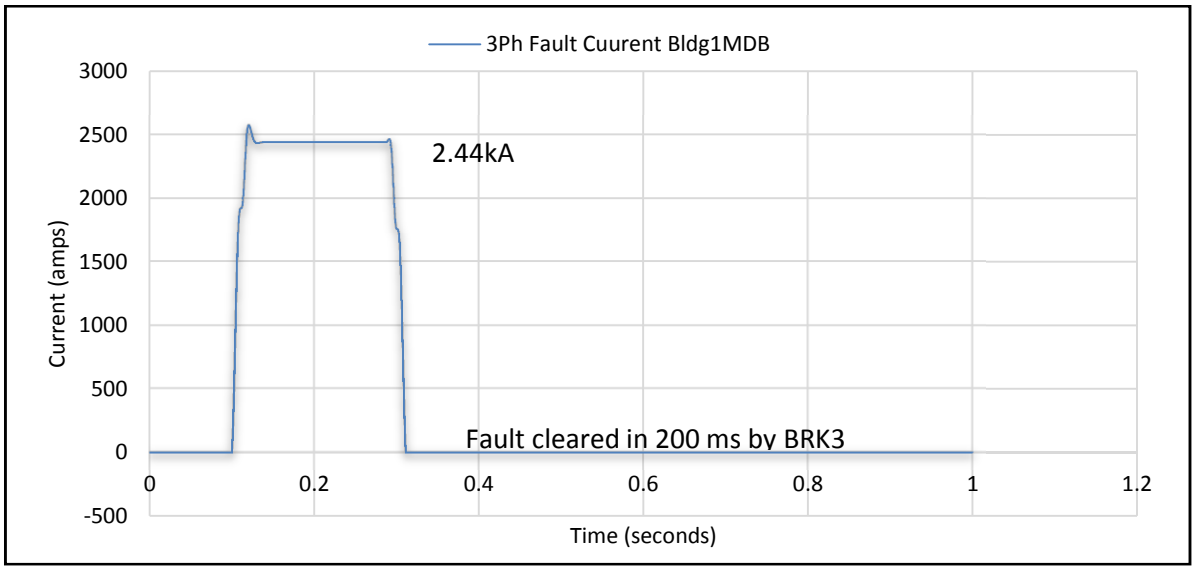

Figure 5.9 RMS value of fault current for case 1

A three- phase to earth fault is simulated at 0.1 seconds for duration of 0.3 seconds. The fault was cleared by BRK3 in approximately 0.2 seconds. This time equals the time indicted in TCC based on Table 5.2 shown in Figure 5.10. In this case the contribution to the fault current is made only by the utility power supply. In this situation the protection system is properly coordinated.

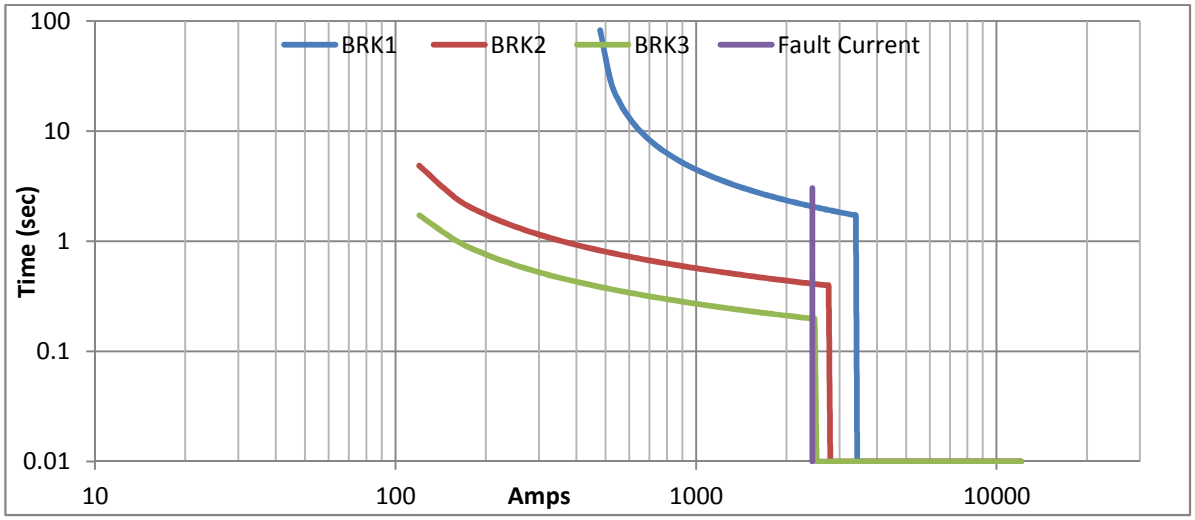

Figure 5.10 TCC – Well coordinated system (PV is not connected)

Case 2-Fault at the MDB of building1 when utility power source is available and PV system (PVA) is connected to MDB of Building1only.

Figure 5.11 represents the flow path for fault current during a three phase fault in the MDB of building 1 when PV system is connected to the MDB of building 1.

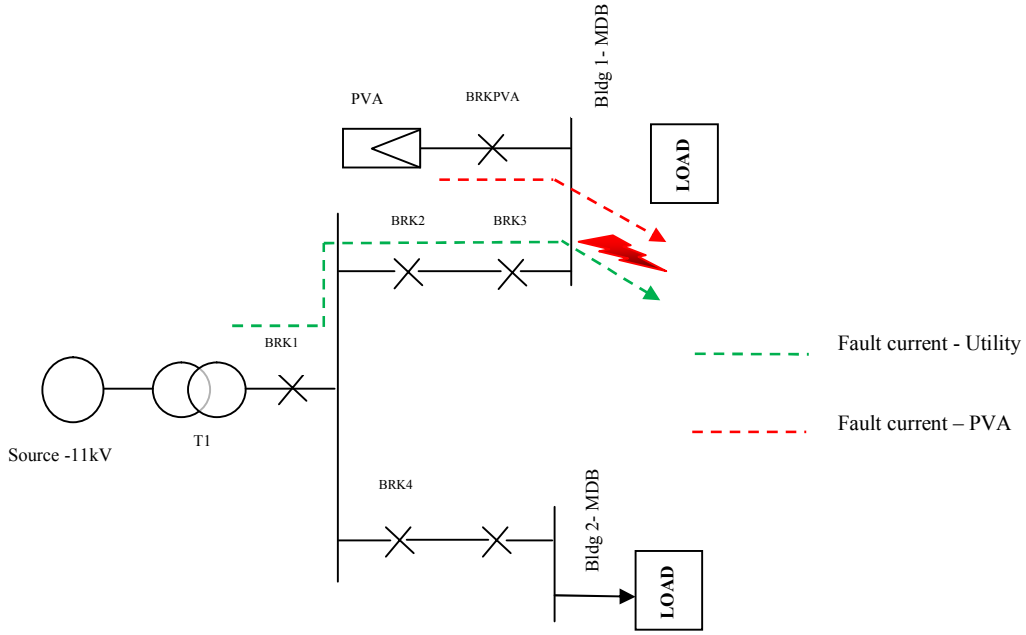

Figure 5.11 TCC – Fault current path – PV connected to building1 MDB

The simulation output for the fault is shown in Figure 5.12.

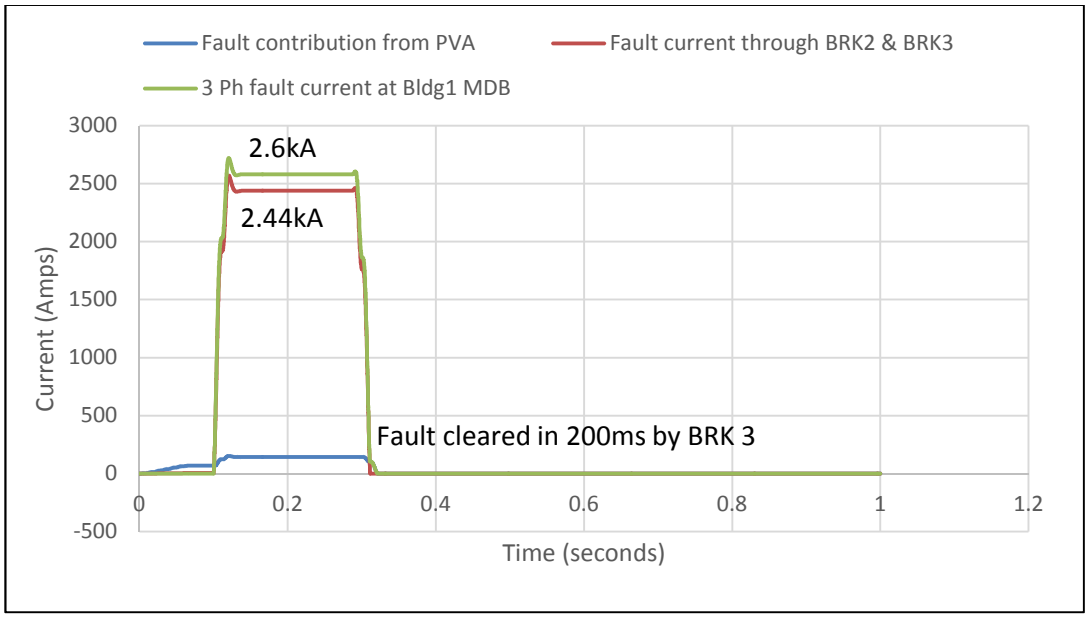

Figure 5.12 RMS value of fault current for case 2

A three-phase to earth fault simulated at 0.1 seconds for duration of 0.3 seconds at of building1 MDB is cleared by BRK3 in 0.2 seconds.

In this case additional fault current of 144 amps (approximately) by PVA. Though this increased the value of total current at the point of fault from 2.44kA to 2.6kA, the fault current flowing through circuit breaker BRK2 and BRK3 is still the same (i.e. 2.44kA) as case 1. The additional fault current contribution from PVA therefore does not disturb the protection coordination of the network.

Case 3 -Fault at the MDB of building1 when utility power source is available and PV systems PVA is connected to MDB of Building1and PVB is connected to MDB of Building2

Figure 5.13 represents the flow path for fault current during a three phase fault in the MDB of building 1 when PV system is connected to the MDB of building 1

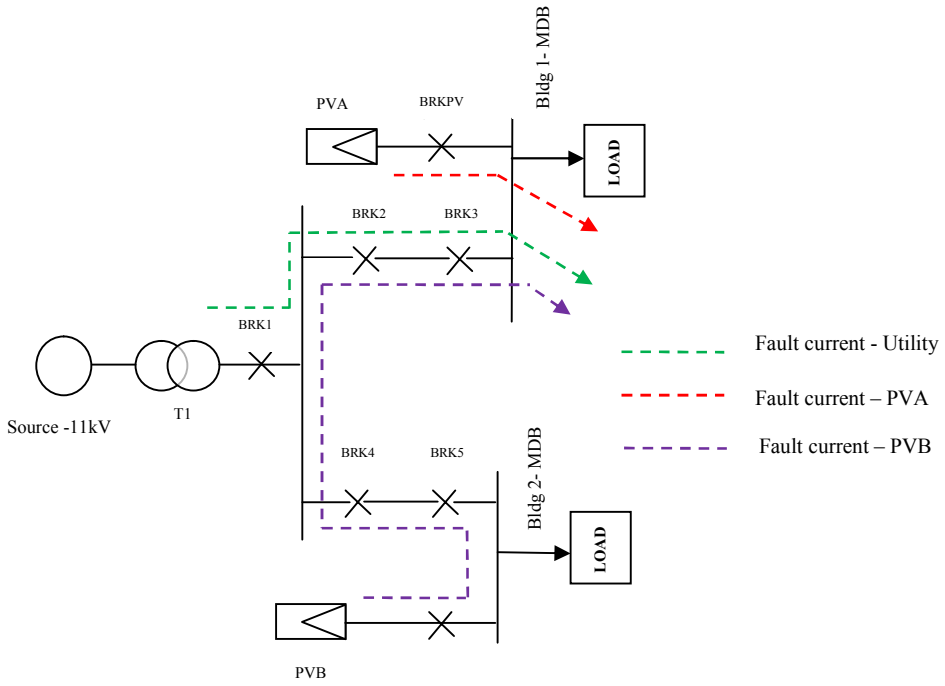

Figure 5.13 Fault current path– PV connected to buildings1 &2 MDBs

The simulation output for the fault is shown in Figure5.14. In this case, there will be an additional fault current contribution of 144 amps (approximately) from PVA and 115 amps from PVB .The value of total current at the point of fault will increase from 2.6kA (in case 2) to 2.7kA. The fault current flowing through circuit breaker BRK2 and BRK3 in this case will increase from 2.44kA to 2.55kA due to contribution from PVB.

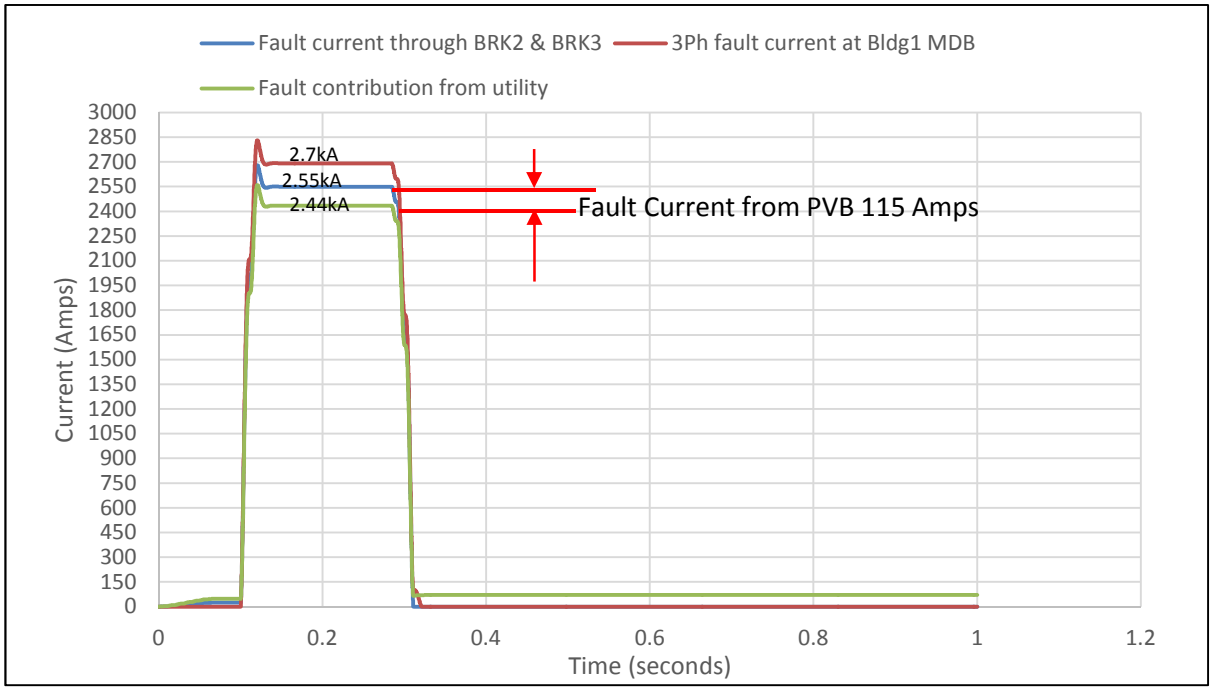

Figure 5.14 RMS value of fault current for case 3

A three-phase to earth fault is simulated at 0.1 seconds for a duration of 0.3 seconds at building 1 MDB is cleared by BRK3 in instantaneously as shown in Figure 5.15 (2550 amps > instantaneous trip threshold of BRK3). No impact on relay coordination is observed in this case.

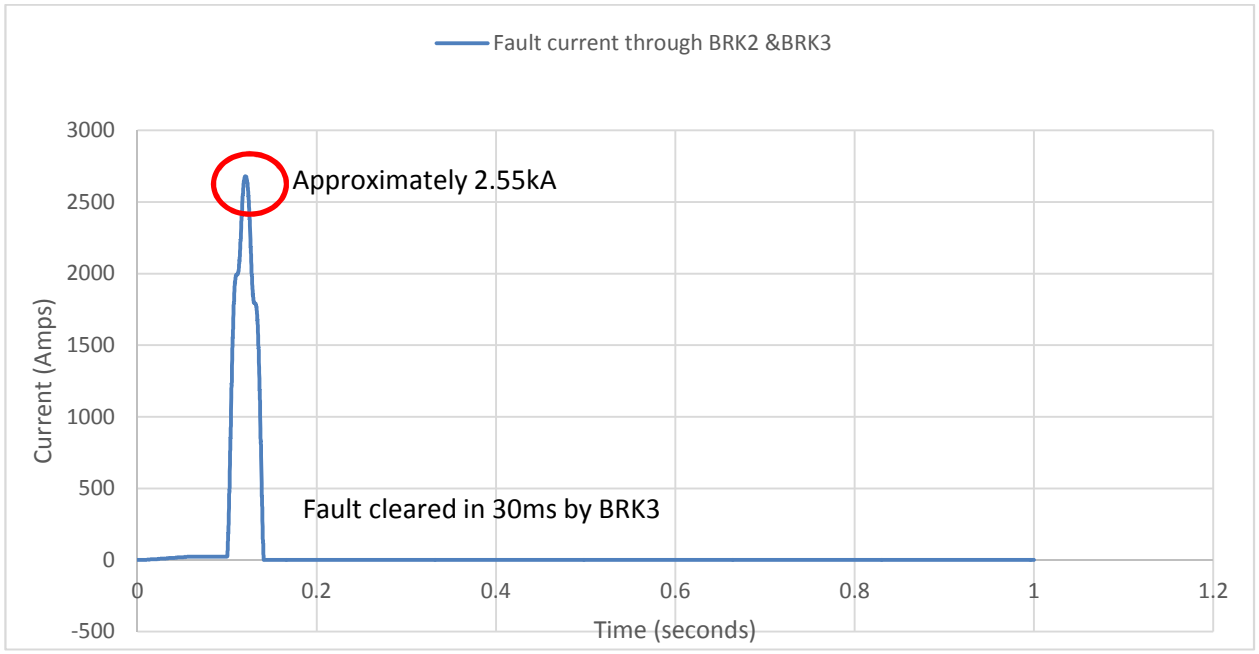

Figure 5.15 Fault cleared by BRK3 in case 3

However, in case the contribution from PVB is less than 115 amps (discussed further in section 5.7) and the value of current through BRK3 does not exceed 2500A (definite time threshold for BRK3), the tripping time for BRK3 shall be approximately 0.2 seconds (similar to case 2). As trip time for

of BRK3 equals the time required for PVB to trip on over current protection, even though the protection coordination is not disturbed, the PVB may trip. This is considered as a sympathetic tripping [27] (as no fault has occurred in the MBD2).and is undesirable. In order to rectify this situation, the over current tripping time for BRK3 should be reduced to a value (by adjusting the time setting) such that BRK3 always trips before the PVB. This will prevent tripping of PV systems connected to MDBs where no fault has occurred.

Case 4- Fault at the building main distribution box of building1 when both utility and PV system is connected to MDBs of all buildings.

Figure 5.16 represents the flow path for fault current during a three phase to earth fault in the MDB of building 1 when PV system is connected to the MDB of all four buildings in the housing complex.

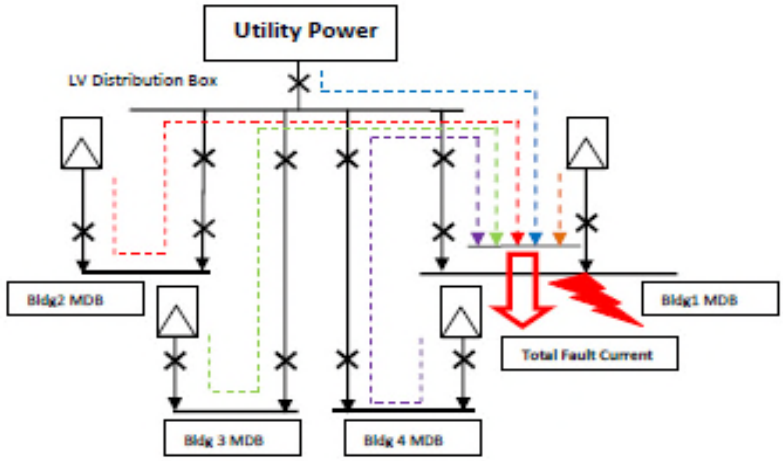

Figure 5.16 Fault current path – PV connected to all buildings

In this case there will be an additional fault current contribution of 144 amps (approximately) from PVA and 345 (3 times 115 amps) from PV systems connected to other three buildings .The value of total current at the point of fault from 2.9kA as compared to 2.7kA in case 3. The fault current flowing through circuit breaker BRK2 and BRK3 in this case will be 2.79 kA due to contribution from PV system installed in other buildings. At this value of current, as per the TCC shown in Figure 5.17, tripping time for both BRK2 and BRK3 will be instantaneous thus allowing no proper discrimination of tripping during fault at MDB 1 as there shall be no grading margin. This will reduce system reliability.

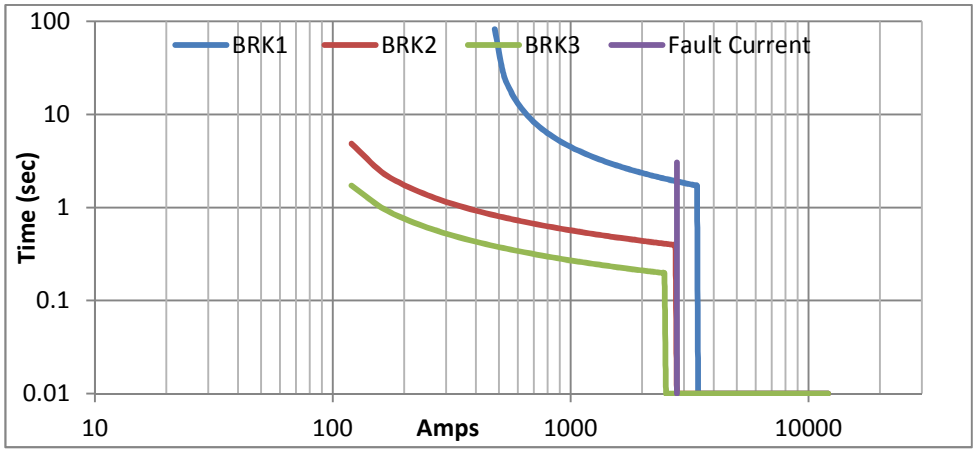

Figure 5.17 TCC –Loss of coordination (PV connected to all buildings)

5.7 Analysis of case studies

It is observed from the cases studied in section 5.6 that the contribution of fault current from the PV system connected to a MDB where fault occurs does not have any impact on the protection coordination of the distribution system and only the fault current from the PV systems connected to MDBs of other buildings (where no fault has occurred) has the potential to disturb the existing protection coordination. It is also important to note that, while the PV system connected to the MBD where fault has occurred will contribute the full (expected) magnitude (i.e.144 amps) of fault current to the point of fault, the fault current contribution from a PV connected to the a MDB of other buildings will be will be less than 144 amps. The available additional fault current flowing through BRK2 and BRK3 is not a direct multiple of the possible fault contribution from an individual PV but depends on a number of other factors. This includes, the bus voltage at the MDB of other buildings during the fault in the building 1 MDB, the loading of the buses and also the cable length between the MDB and the low voltage distribution board. Figure 5.18 shows simulation output bus voltages at MDBs of building 1 and building 2 during a fault in the MDB of building 1.

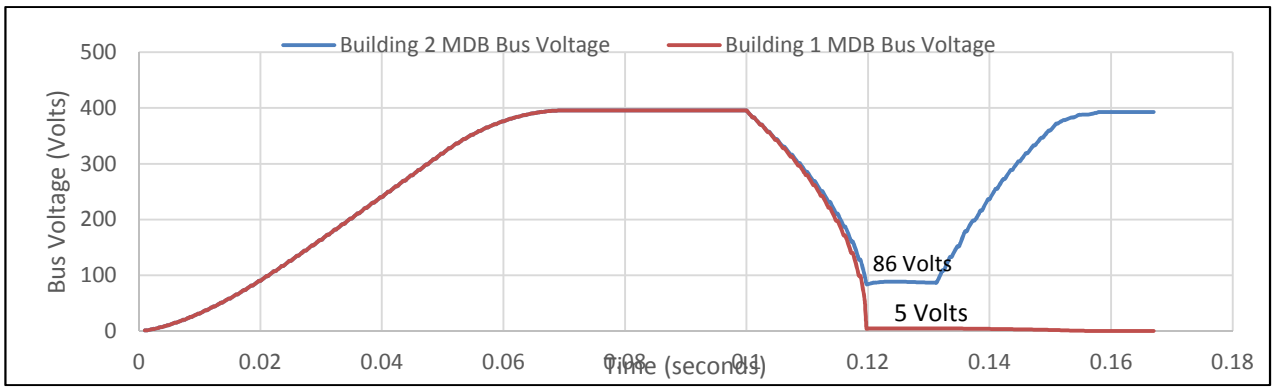

Figure 5.18 Bus voltage profile during building 1 MDB fault

The simulation output in the figure shows that the bus voltage at building 1 MDB is substantially lower than the bus voltage at building 2 MDB. When building 2 MDB is loaded to 50 kVA, the current contribution from PVB is 130 amps. However, only 115 amps flows to the point of fault back through BRK4 and BRK5 and rest of the current flows to the load. Figure 5.19 shows the simulation output of current contribution from PVB in this situation.

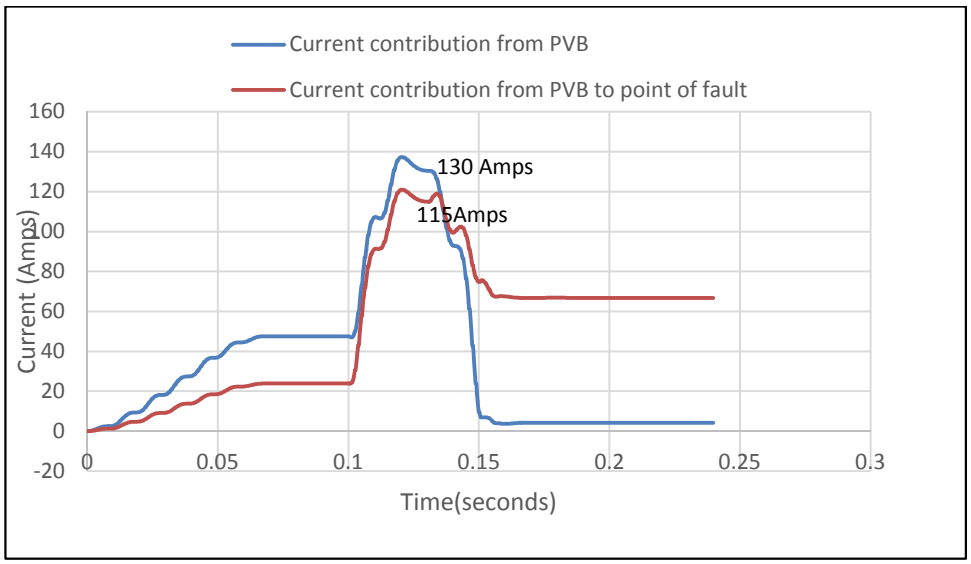

Figure 5.19 PVB fault current contribution to point of fault.

However, if the load on building 2 MDB is reduced from 50 kVA to 10 kVA, the current flowing from PVB to the point of fault will increase from 115 amps to 127 amps. Figure 5.20 shows the simulation output of current contribution from PVB in this situation.

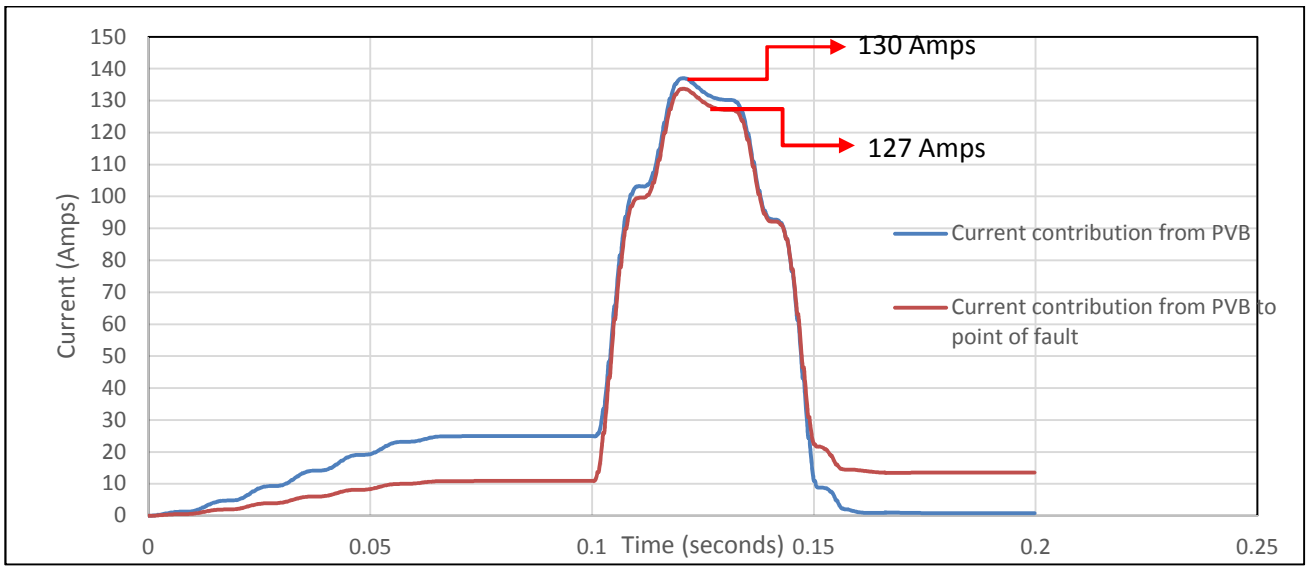

Figure 5.20 Increase in fault contribution from PVB to point of fault (building 2 MDB load -10 kVA)

This is due to there is increase in impedance offered to the PV voltage source when load is less as compared to the impedance offered to PV voltage source when load is higher.

Cable connection from MDB to the low voltage distribution board is the major impedance between the source of fault current (i.e. PVB) and the point of fault. In this study, it has been assumed that this cable length is 20 meters. The total impedance to the source PVB during fault is therefore 40 meters long, 25 mm^2, copper conductor cable. This offers insignificant impedance to cause reduction in fault current. However, in real case this factor will vary. The fault current contribution to point of fault from PVB will vary inversely to the length of cable and directly to the cable size (cross section area of conductor).

Considering the situation described in section 5.6, case-4, the instantaneous tripping time of BRK2 should be set for a time greater than the instantaneous tripping time of BRK3. As shown in Figure 5.17, no intentional time delay has been provided for definite time tripping of BRK2. A definite time delay of 0.1 second for definite time trip threshold of BRK2 is adequate to prevent loss coordination between BRK2 and BRK3. Figure 5.21 shows revised coordination setting for case 4. Theoretically the current threshold for definite time setting or the time setting can be increased to an absolute maximum value of short circuit withstand level of the bus and cable that the circuit breaker protects. However, the increase in setting may also be constrained due to the coordination grading margin that needs to be maintained with the upstream protection relay. Increase in threshold for instantaneous tripping of BRK2 (from 2750 amps to 2900 amps) will rectify the coordination problem, but effectiveness of this measure depends on the maximum fault current contribution from PV systems that will flow though BRK2 and BRK3. In the case studied, the 315 kVA transformer powering up the housing complex will be loaded to a maximum of 64% in absence of generation from the PV system. Therefore future addition of two new buildings with 50 kVA demand load is possible. If PV system of 50 kVA capacity is installed in each of the two new buildings then it is in case of fault in any building MDB, the fault current contribution will rise to 3.06kA (based on 115 amps contribution from each building) and the threshold limit for instantaneous trip of BRK2 has to be revised. Thus the trip setting for BRK2 will have to be revised every time a new PV unit is added .When delayed time setting is applied to maintain coordination gap with the BRK3, increase in fault current value will not effect the coordination of relays. Therefore adjusting the time setting of BRK2 is recommended as a better way of rectifying the coordination problem as compared to current threshold adjustment. Also it is observed that increase in fault current from the PV systems has no impact on the coordination between BRK1 and BRK2 except for increase in grading margin.

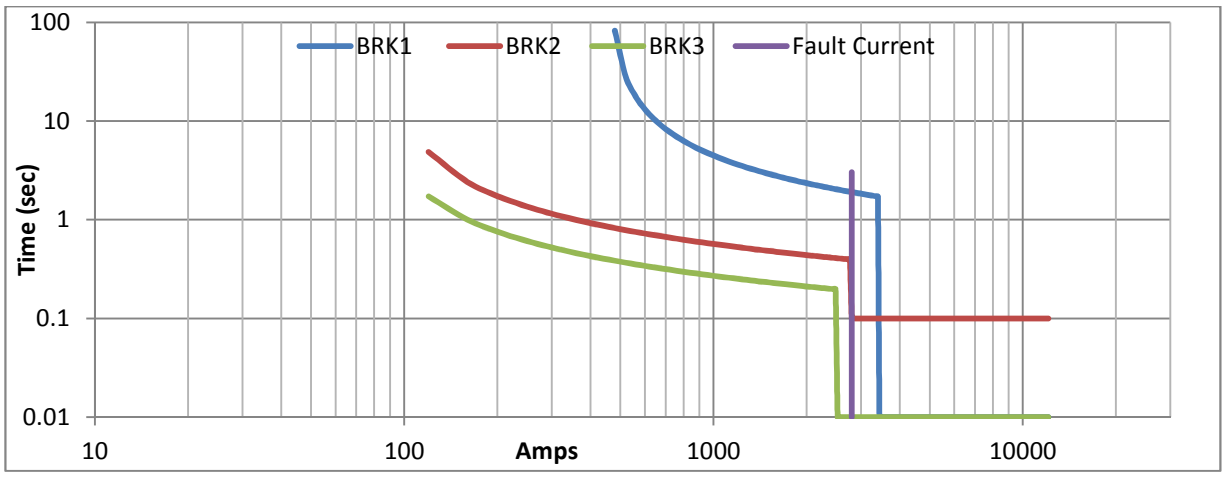

Figure 5.21 TCC – BRK2 definite time setting delayed by 0.1 s

5.8 Conclusion

From the analysis it can be concluded that, though the PV systems are inverter interfaced devices and contributes low fault current, high PV penetration level can disturb existing protection coordination. Analysis of various cases during this study shows that, during a fault at MDB, fault current from PV system connected to the MDB does not disturb the protection coordination for power supply to the MDB. The coordination is disturbed due to the fault current from PV systems installed in other buildings (i.e. remote MDBs). Also it is observed that, even though the industry rule of thumb is that the fault current contribution from a PV system is 2 times the full load amps of inverter, this is holds true only for PV connected to the MDB where the fault has occurred. The contribution of currents from PV systems connected to a remote MDB is dependent on factors like voltage at the remote bus, the impedance between the PV system and the point of fault and the load on the remote MDB buses. This implies that while analysing the impact of increment of fault current due to installation of PV on the protection system, it is important to consider the factors that determine the magnitude of fault current contribution from remote PV systems. While considering refinement of protection setting (due to PV penetration), increasing time grading margin with downstream protection device is more advantageous than increasing current threshold (in the instantaneous tripping zone of TCC). Also for a higher reliability of system, breaker closest to the point of fault should operate fast enough to prevent sympathetic tripping of other breakers. This study has considered arithmetic addition of utility contribution of fault current to PV contribution (i.e. in phase contribution from both the power sources) which represents a worst case scenario. Studies done in the past shows that fault current contribution from utility and PV are out of phase [28] and addition of current vectors will result in lower magnitude of fault current and thus increase the chances of sympathetic tripping of other breakers due to delayed tripping of breaker closest to the fault (i.e. BRK3 in this case).

Chapter 6 Conclusion and Future Work

6.1 Conclusion

The research work carried out has reaffirmed some of the findings of the works done in the past in the area of protection problems associated with grid tied PV generators and has added new observations and inferences to the current knowledge of the subject.

It is widely accepted that the addition of a distributed generator increases the fault levels at various points in distribution network and thus impacts the existing protection coordination. PV systems behave differently from conventional synchronous generators in terms of fault current contribution. This is due to the inherent property of PV inverters to limit fault current to about 2-2.5 times the inverter rated current. In chapter 2 the development of model of single phase PV system and investigations carried out to study the behaviour of PV inverter during fault has been described. The simulations of the grid tied PV model exhibits the current limiting characteristic of the inverter during a fault .This validates the accuracy of the model developed. The relatively lower value of the fault contribution from small PV systems may not be individually capable of making any impact on the capacity of switchgear or the protection coordination .However, this does not hold true for high PV penetration or for large sized PV generators.

Another aspect pointed out in the research which is relevant for both protection settings and interruption capacity of fault clearing device is the time for which PV inverter remains in circuit after initiation of fault. The duration of fault current contribution from PV systems is dependent on the control method of the PV inverter, the IGBT protection functions in the inverter and the islanding protection schemes. The duration and magnitude of fault current varies slightly from one PV manufacturer to other. Past works done in this field have been discussed in chapter 3 where experimental setups have been used to compare the response of inverters made by different inverter manufactures. A common phenomenon observed is that the fault current has a time varying magnitude with a peak for a few cycles and it then eventually reduces during the next few cycles. The simulation of the grid tied PV model described in chapter 2 shows a time varying profile of fault current. In addition to the impact on coordination and fault clearing capacity of devices, this also impacts the safety of system. If the fault contribution from PV system continues after grid supply is cut off till the islanding protection operates, the PV system can potentially feed power to a faulted system which is not safe.

Investigations and simulations results presented in chapter 4, considering contribution of single phase PV system in residential network strongly indicates the effect of cumulative build up of low magnitude fault current. In this particular case the PV penetration considered represented only 50% penetration with respect to load demand and the PV fault contribution has been considered to be lower than 200% of inverter rated current in order to observe the impact at a minimum. With higher level of penetration and with fault current contribution in the range of 200% of inverter capacity the fault current will increase appreciably at the customer distribution boards. This is caused due to contribution from PV systems installed in neighbouring residences powered by the network. This can make the utility side circuit breaker potentially inadequate in terms of fault interruption capacity. Failure of the circuit breaker to successfully clear the fault can lead to a fire and extensive damage to the distribution board and is a very unsafe situation. The distribution board busbars and internal wirings are rated for certain maximum fault –withstanding capacity and any increase of fault current shall lead beyond the withstanding capacity will lead to damage of switchboard. In most cases the customer end main distribution board at individual residences are designed to meet requirements of utility fault levels at the point of connection. With new PV systems being embedded extensively throughout the network, it is recommended that the utility companies ensure that the penetration of PV systems in a particular network circuit should not exceed the limit beyond which the existing customer distribution board fault ratings may be inadequate. Where necessary reviews should be conducted by the utility company to ensure that the distributions boards and the associated switchgear is capable of handling additional fault current caused by PV penetration. The customer connection agreement should specify any requirement of PV integration thus enabling power companies to control any undesired effect of increased fault level.

Investigations and simulations described in chapter 5 indicate the possible relay coordination issues with high penetration of three phase PV systems in a large building distribution network. It has been inferred that during a fault in a particular building distribution board, the effective flow of fault current from other PV systems installed in other buildings connected to the network will potentially upset the relay coordination of existing system. This calls for reviewing and fine tuning of the existing protection settings when a PV system is added. In reality this can be a difficult exercise to keep the protection settings updated with the addition of new PV systems in the network. The study therefore recommends a method of adjusting time setting to avoid repeated relay setting changes. The cases studied have highlighted the factors that should be considered during analytically estimating the contribution from a newly added PV system in the network to be considered for revised relay settings. While 200% of the inverter rating may be a reasonable magnitude of fault

current contributed from a PV system, it is unlikely that 200% fault current is contributed from PV systems connected to other buildings. The contribution is subject to a number of factors discussed in chapter 5. These factors needs to be considered in order to determine the maximum and minimum fault current levels in the network within which all protection relays should be well coordinated.

A summary of the major findings and recommendations of the study are as follows:

- The fault current contribution from PV system can cause issues for circuit breaker interruption capacity and fault withstanding capacity of the distribution board at the customer premises. Increase in magnitude of fault current beyond the design limit of the circuit breaker or the distribution board will lead to electrical and fire hazardous. Utility companies should therefore limit the maximum PV penetration in network based on proper review and recommend upgrade of distribution boards where necessary.
- The protection coordination of existing systems can potentially be disturbed by the addition of PV systems in the network. This should be reviewed when large PV systems are added to network. It is recommended that all factors that impact contribution of fault current from PV should be considered to estimate minimum and maximum fault current level of network Arithmetic addition of fault current from PV system (based up on 200% inverter rating and number of PV installed) is not sufficient for the purpose relay coordination.
- The magnitude of fault current contribution and the duration of fault current contribution from PV systems vary for different manufacturers of PV inverters. This poses potential problems both for developing PV models for power system studies and for properly analysing the impact of PV penetration on network protection. It is recommended that a standard should be established to regulate the response of PV systems during fault. With a common standard followed across industry, it would be easier to estimate the safe penetration level for PV systems in network.

6.2 Future Work

In this thesis various protection issues caused by connection of PV systems to power distribution networks have been investigated and results of the investigation have been presented. However, there are some areas that need to be further explored. The following recommendations are made for future research.

- This research has considered balanced loading of feeders and multiple PV panels of same size connected to network. A similar fault study carried out on test networks with unequally

loaded phases and unequal penetration level of PV in each phase may be performed to acquire better understanding of the problem.

- The fault current contribution from PV systems considered in this work is 150% to 200% of the inverter rated current. However, this represents the maximum possible contribution limited by the inverter electronics. As the power to the inverter is fed by the PV panels, the power generated by PV panel will affect the maximum fault current that is fed to the point of fault. The power generated by PV panels depends on the temperature and irradiance. Therefore the protection issues shall be impacted by variance in these factors. An investigation carried out using a PV model which allows variable fault contributions based on the weather conditions will add a valuable insight in the process of analysing the protection problems.
- In the investigations carried out in this research, the issue of disconnection of PV panels connected along a long low voltage distribution feeder at different instances of time during a network fault has not been considered. This occurs as the voltage at the output terminals of a PV inverter located near the point of fault is much lower than the voltage at output terminal of the PV inverter located away from the point of fault. A fault study carried out on a similar test network (as used in this research) including this aspect will help in understanding the impact of time varying fault current contribution from PV system on protection coordination.
- Voltage rise in feeders is a common effect when PV systems are connected to distribution feeders. This effect can be studied using data for grids connected to PV systems in Queensland. Based on the study, measures to mitigate this effect can be suggested. The results of the study can be used to review the guidelines provided in Australian standards for grid connected PV systems and suggestion for making changes in the standard can be made.
- Inverter performs additional control and protection functions which are critical for grid connection. Reliability of the current inverter technology to adapt to the intermittent nature of renewable power generation with respect to grid connection compliance is important. A study carried out to investigate this aspect will provide valuable insight into the grid interconnection problems caused by variation in power generated by PV panels due to changes in weather conditions.
- Dynamic PQ analysis in power network with high penetration of PV system under varying weather condition may be conducted to analyse the power quality problems like voltage rise, voltage flicker and power factor. The research work needs to consider solar panel data obtained different from PV manufacturers.

- Base load power generation systems have limited ability to response to increased power demand. The intermittent nature of PV power generation will cause sudden increases of power demand of the base load systems. The PV systems generally have high conversion efficiency and are capable of maintaining THD within acceptable limits. With reduction in cost of PV systems the PV penetration will increase with time. Therefore study needs to be carried out to identify the technical requirements of utility side power generation system and grid interconnection guidelines for PV systems. The study to identify technical issues needs to include different parameters like voltage regulation, harmonic distortion, power factor and islanded operations, whilst considering both the level of penetration and variability of power generation.
- PV systems functions as an effective energy source when connected to grid. There are a number of associated problems which requires further investigation and study. This includes dysfunction of phase fault relays at source substations, abnormal state of PV generation after islanding, switch-on sequencing and associated inverter problems.

References

[1] Department of Environment, "The Renewable Energy Target (RET) scheme," Australian Government, 2012. [Online]. Available: http//www.environment.gov.au/climatechange/renewable-energy-target-scheme. [Accessed 25 July 2014].

[2] "ETAP," Operation Technology Incoporated, [Online]. Available: http://etap.com/electrical-power system software/etap-products.htm. [Accessed 23 August 2104].

[3] "PSCAD," Manitoba HVDC Research Centre , [Online]. Available: https://hvdc.ca/pscad/. [Accessed 24 August 2014].

[4] Jenkins. N , Strbac.G and Ekanayake. J.B, in Distributed Generation, Institution of Engineering and Technology, 2009, pp. 40,41.

[5] "Sunpower E19/238 Solar Panel," [Online]. Available: http://www.cleanfuelconnection.com/solar-energy/brochures/e19-238.pdf. [Accessed 24 August 2014].

[6] S.A Kalogirou, "Photovoltaic Systems," in Solar Energy Engineering : processes and systems, Elsevier/Academic Press, 2009, pp. 481-514.

[7] M. E. Ropp and D. P Hohm, "Comparative study of maximum power point tracking algorithms using an experimental, programmable, maximum power point tracking test bed," IEEE Photovoltaic Specialists Conference, Anchorage, AK, USA, 2000.

[8] M. Rashid, "DC-DC Converters," in Power Electronics Handbook, Butterworth-Heinemann, 2011, p. 254.

[9] A. Girgis and S. Brahma,"Effect of Distributed Generation on Protective Device Coordination in Distributed Systems," IEEE Conference on Power Engineering LESCOPE, Halifax, Canada, 11th to 13th July, 2001, Pages 115-119.

[10] S. Chaitusaney and A. Yokoyama, "Impact of Protection Coordination on Sizes of several Distributed Generation Sources," IEEE Conference on Power Engineering,Singapore, 29th Nov to 2nd Dec, 2005, Vol-2, Pages 669-674.

[11] S. Chaitusaney and A. Yokoyama "An Appropriate Distributed Generation Sizing Considering Recloser- Fuse Coordination," IEEE Conference on Transmission and Distribution, Asia and Pacific, Dalian, China, 2005, Pages 1-6.

[12] S. Chaitusaney and A. Yokogama, "Prevention of Reliability Degradation from Recloser –Fuse miscoordination due to Distributed Generation," IEEE Transactions on Power Delivery, Vol 23, Issue 4, 2008, Pages 2545-2554.

[13] B. W. El-Khattam and T. S. Sidhu, "Restoration of Directional Overcurrent Relay Coordination in Distributed Generation System Utilizing Fault Current Limiter," IEEE Transactions on Power Delivery, Vol 23, Issue 2, 2008, Pages 576-585.

[14] D. Turcotte and F. Katiraei, "Fault Contribution of Grid Connected Inverters," IEEE conference on Electrical Power and Energy, Montreal, Canada, 22nd Oct to 23rd Oct, 2009, Pages 1-5

[15] C. W. So and K. K. Li, "Protection relay coordination on Ring Fed Distribution network with Distributed Generation," IEEE Conference on Computers Communications Control and Power Engineering, TELCON 02, 28th Oct to 31st Oct, 2002, Vol 3, Pages 1885-1888.

[16] S. M. Brahma and A. A. Girgis "Development of Adaptive protection scheme for Distribution System with High Penetration of Distributed Generation," IEEE transactions on Power Delivery, Vol 19, Issue 1, 2003, Pages 56-635.

[17] IEEE working group on Distributed Generation Integration,"Summary of Distributed Resources Impact on Power Delivery Systems," IEEE Transactions on Power Delivery, Vol 23, Issue 3, 2008, Pages 1636-1643.

[18] IEEE P1547 – Standard for Distributed Resources Interconnected with Electric Power Systems, IEEE 1547 Std, July 2003

[19] W. Rojewski, Z. A. Styczynski and J. Izykowski, "Selected Problems of Relaying for Distribution Network with Distributed Generation", IEEE Power and Energy Society General Meeting, Calgary, AB, 26th July to 30th July 2009, Pages 1-6.

[20] Mesut E Baran and Esmail El Markaby, "Fault Analysis on Distribution Feeders with Distributed Generators," IEEE Transactions on Power Systems, Vol 20, Issue 4 2005,Pages 1757-1764.

[21] S. Phuttapatimok, A. Sangswang, M. Seapan, D. Chenvidhya and K. Kirtikara, "Evaluation of Fault Contribution in the Presence of PV Grid Connected Systems," IEEE Photovoltaics Specialist Conference, San Diego, CA, USA, 11th to 16th May, 2008, Pages 1-5.

[22] S. Phuttapatimok, A. Sangswaang, "Effects on Short Circuit Level of PV Grid Connected Systems under Unintentional Islanding", IEEE International Conference on Sustainable Energy Technologies, ICSET 2008, Singapore, 24th to 27th Nov, Pages 928-932.

[23] R. Varma, J. Berge, I. Axente, V. Sharma and K. Walsh, "Determination of maximum PV Solar System Connectivity in a Utility Distribution Feeder", IEEE PES,Transmission and Distribution Conference and Exposition (T& D), Orlando, FL, 7th to 10th May, 2012, Page 1 – 8.

[24] J. Keller, B. Kroposki, R. Bravo, S. Robles, "Fault Current Contribution from Single Phase PV Inverters", 37th IEEE Photovoltaic Specialist Conference, Seattle, WA, 19th to 24th June, 2011, Pages 1822-1826.

[25] J E. Muljadi, M. Singh, R. Bravo and V. Gevorgian, "Dynamic Model Validation of PV inverters under short circuit condition," [Online], http://www.nrel.gov/docs/fy13osti/57341.pdf [Accessed 26.August 2014]

[26] C.A. Plet, M. Graovac,T. C. Green and R. Iravani, "Fault Response of Grid Connected Inverter Dominated Networks," IEEE Power and Energy Society General Meeting, Minneapolis, USA, 25th to 29th July, 2010, Pages 1-8.

[27] H. Yazdanahi, Y. W. Li and W. Xu, "A New Control Strategy to Mitigate the Impact of Inverter Based DG on Protection System," IEEE Transactions on Smart grid 2012, Vol 3, Issue 3, Pages 1427-1436

[28] F. Katiraei, "Investigation of Solar PV Inverter Current Contributions during Faults on Distribution and Transmission Systems Interruption Capacity," Western Protective Relay Conference, 2012, Pages5-6. [Online] http//quantatechnology.com/sites/default/files/docfiles/Solar%20PV%20Inverter%20formatted.pdf [Accessed 26.August 2014]

[29] H. Hooshyar, M. E. Baran, "Fault Analysis on Distribution Feeders with High Penetration of PV Systems," IEEE Transactions on Power Systems 2013, Vol 28, Pages 2890-2896.

[30] IEEE Recommended Practice for Utility Interface of Photovoltaic (PV) Systems, IEEE 929, 2000

[31] M E. Barun, H Hooshyar, Z. Shen and A. Huang, "Accomodating High Penetration on Distribution Feeder," IEEE Transactions on Smart Grid 2012, Vol 3, Pages 1039-1046.

[32] F. De Mango, M. Liserre, A. D. Aquila and A. Pigazo, "Overview of Anti –Islanding Algorithm for PV systems,Part I, Passive methods," IEEE Conference on Power Electronics and Motion Control, Portoroz, Slovenia, 30th Aug to 1st of Sep, 2006, Pages 1878-1883.

[33] B. Yu, Y. Jung, H. Hwang and G. Yu "A Robust Anti –Islanding Method for Grid Connected Photvoltaic Inverter," IEEEConference on Photovoltaic Energy Conversion, Waikoloa, HI, USA, May 2006, Pages 2242-2245.

[34] R. A. Walling and N.W. Miller, "Distributed Generation Islanding- Implications on Power System Dynamic Performance," IEEE Power Engineering Society Summer Meeting, Chicago, IL, USA, 25th July, 2002, Pages 92-96.

[35] S. Bhattacharya, T. Saha and M. J. Hossain, "Fault current contribution from photovoltaic systems in residential power networks," Australasian Universities Power Engineering Conference, Hobart, 29th Sep to 3rd Oct, 2013, Pages 1-6

[36] Australian Standard Grid connection of energy systems via inverter-Grid protection requirements, AS 4777.3, 2005.

[37] "Aerial," Nexans Olex, 2012. [Online] http//www.olex.com.au/2012/OLC12641_AerialCat.pdf. [Accessed 15 August 2014].

[38] Australian Standard, The calculation of short-circuit currents in three phase a.c. systems, AS 3851, 1991

[39] V. Mehta, "Electrical Design of Overhead Lines," in Principles of Power System , S Chand & Company Limited , 1992, pp. 271-272.

[40] "High Voltage -Olex," [Online]. Available: http://www.olex.com.au/Australia/2013/OLC12641_HighVoltageCat.pdf. [Accessed 15 August 2014]

[41] "Cables -Ergon Energy," 25 February 2003. [Online]. Available: https://www.ergon.com.au/__data/assets/pdf_file/0020/64235/Section-17-Cables.pdf. [Accessed 15 August 2014].
[42] Australian Standard-Electrical accessories –Circuit breaker for over current protection for household and similar installations. Part 1, AS/NZS 60898.1, 2004
[43] Fuji IGBT Module Application Manual, REH984, Fuji Electric Drive Technology Company Ltd, 2004, pp. 5/2-5/6.
[44] A Sattar, IXYS Corporation Insulated Gate Bipolar Transistors (IGBT),pp.13-14. [Online]. Available: http//www.ixys.com/Documents/AppNotes/IXYS_IGBT_Basic_I.pdf. [Accessed 15 August 2014].
[45] S.Bhattacharya, T. Saha and M. J. Hossain, "Fault current contribution from large photovoltaic systems in building power supply networks," (resubmitted on 15.8.2014 after first review for publication in Elsevier Journal of Energy and Buildings).
[46] Australian Standard-Electrical Installations – Selection of Cables- Cables for Alternating Voltages upto and including 0.6/1kV - Typical Australian Conditions, AS/NZS 3008.1.1, 2009

APPENDIX A PSCAD Model of PV systems

Temperature and irradiance based current and voltage output of PV

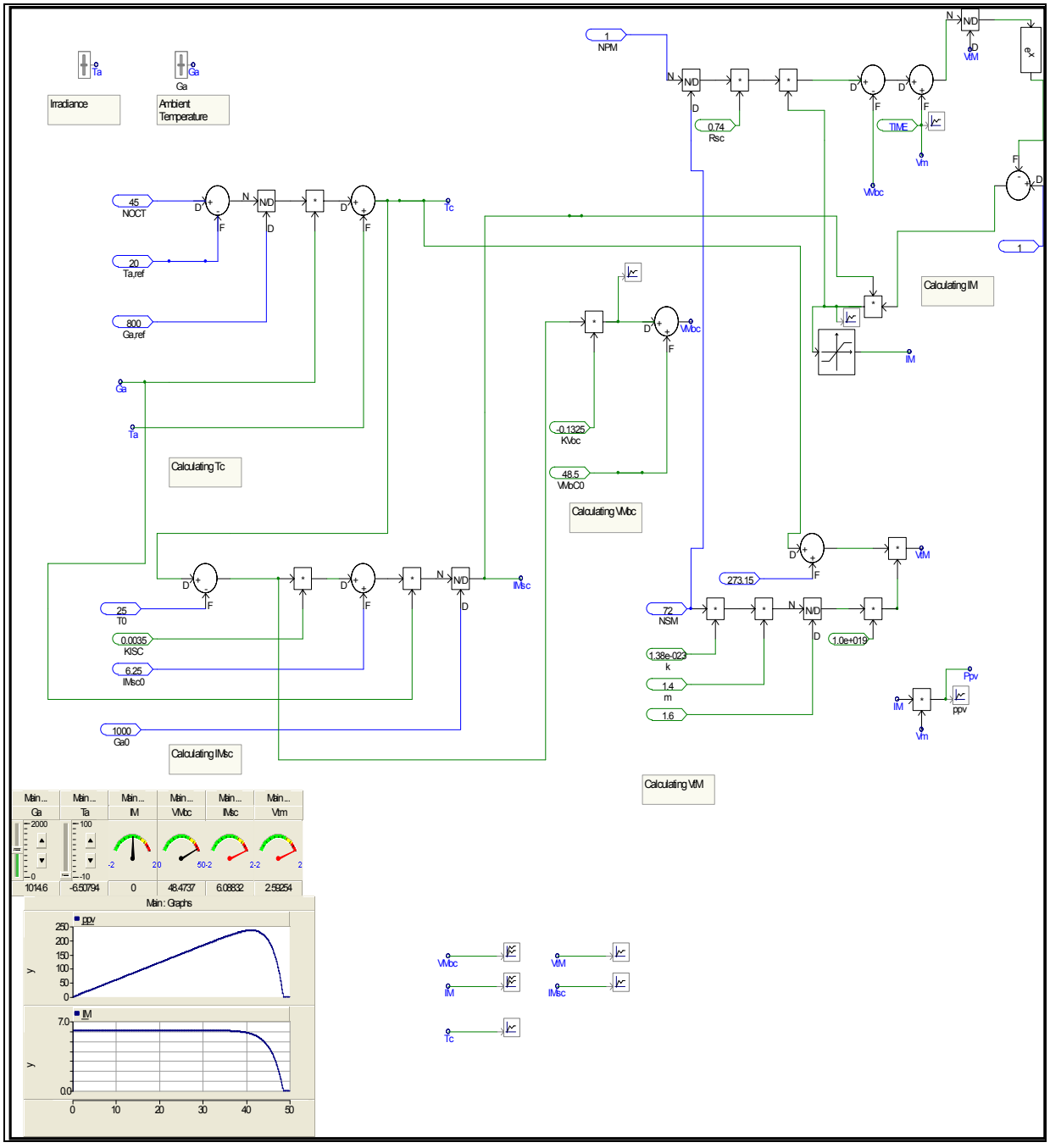

Figure A.1 Model - PV Panel

Implementation of P&O algorithm

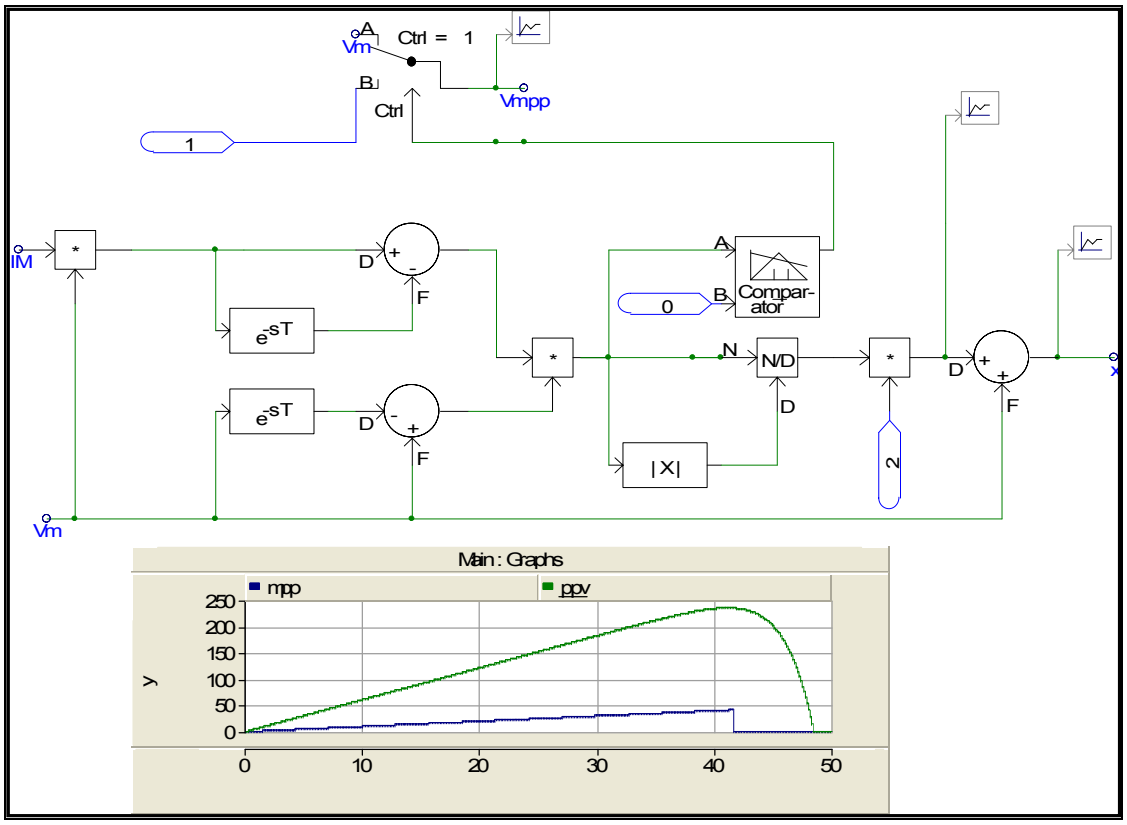

Figure A.2 Model- MPPT controller

Boost converter and control of duty cycle

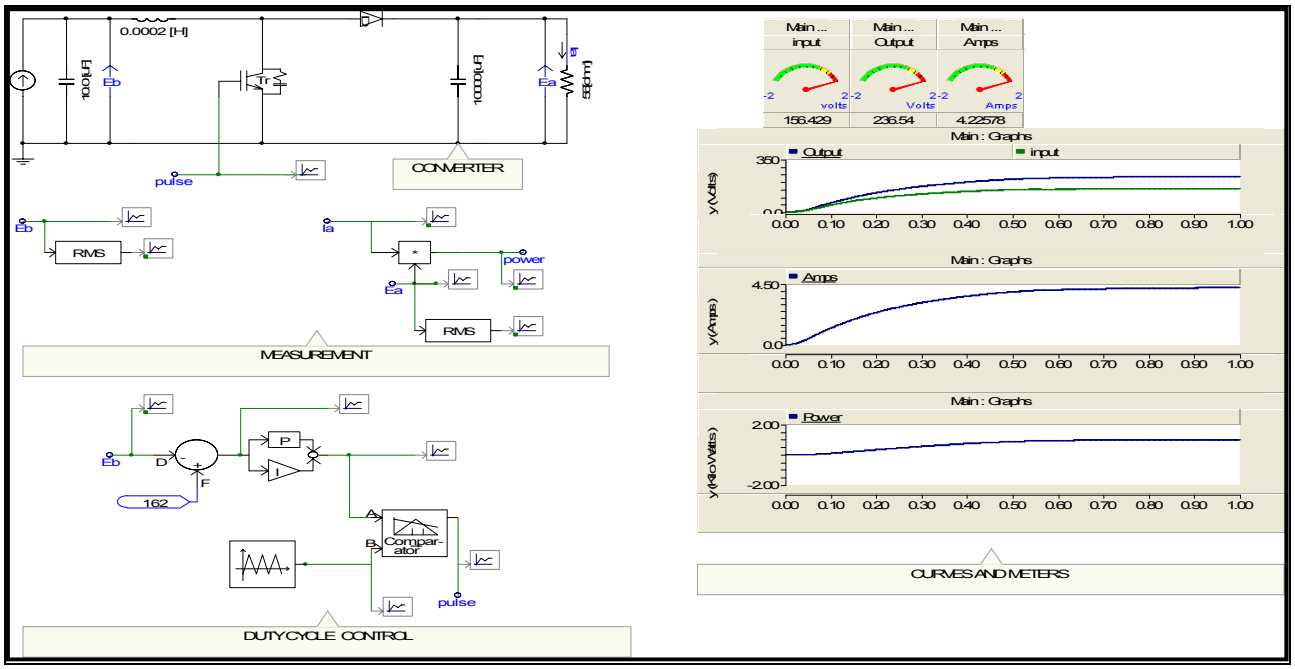

Figure A.3 Model -DC-DC controller

Single Phase inverter complete with firing control

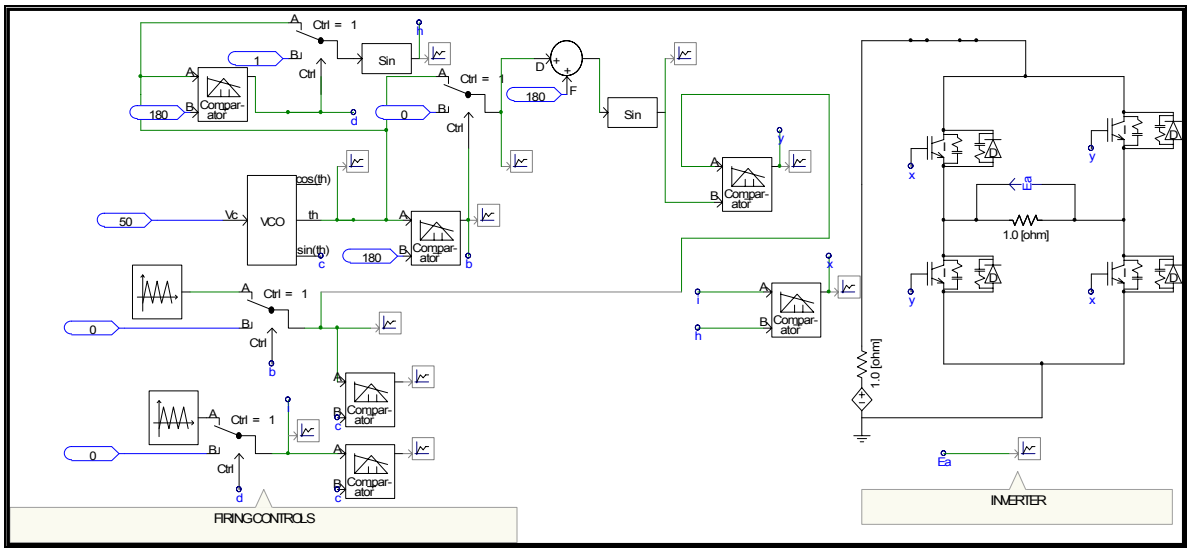

Figure A.4 Model –Single Phase inverter

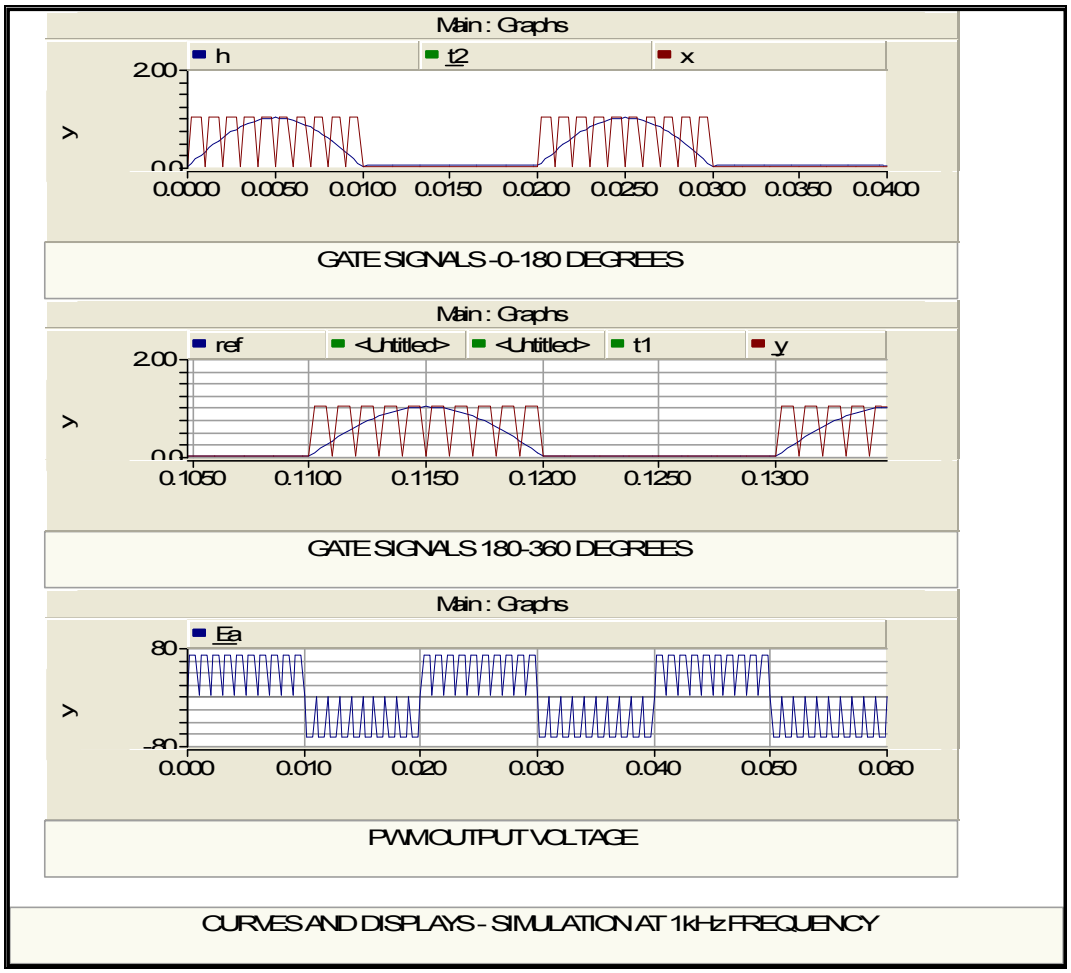

Figure A.5 Model –Output waveforms of inverter

Single Phase inverter grid tied system

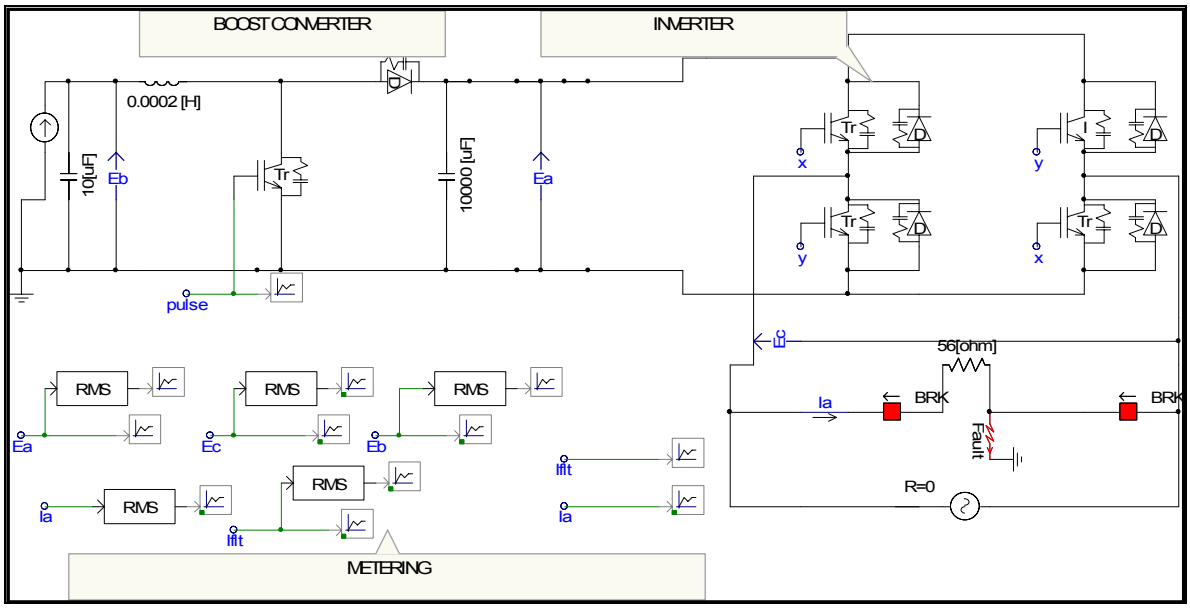

Figure A.6 Model – Grid Tied inverter

Firing control of grid tied inverter

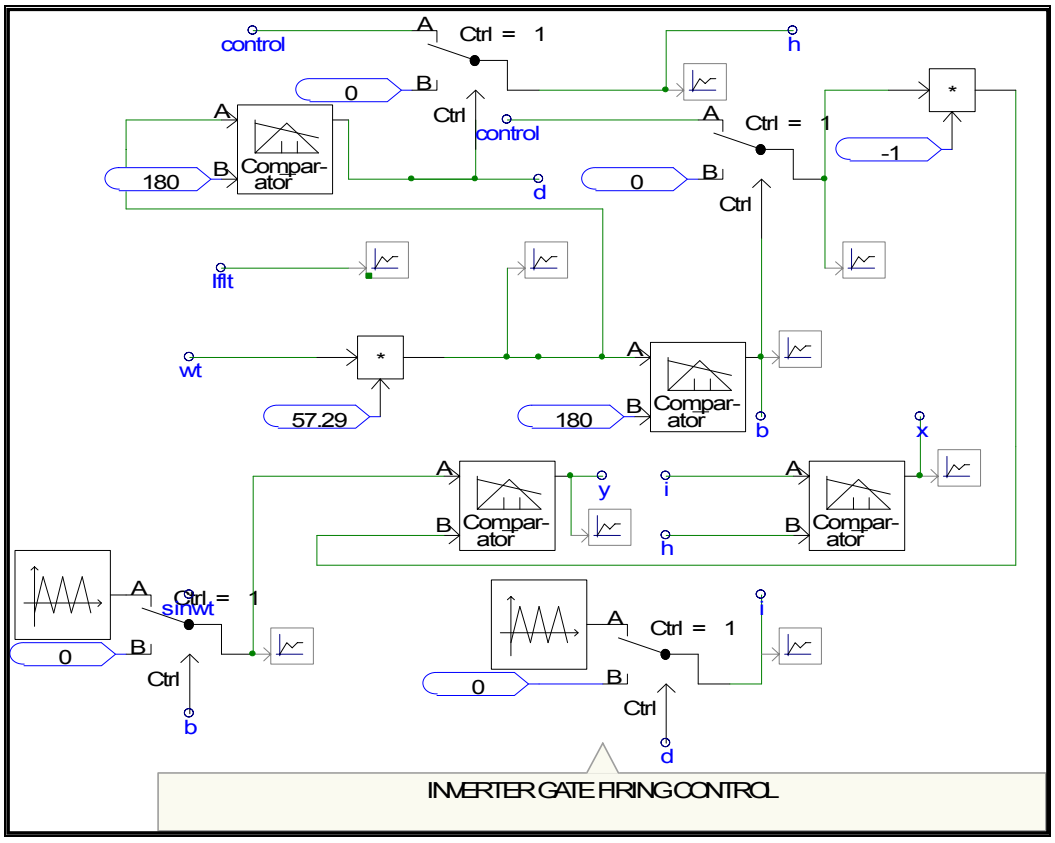

Figure A.7 Model – Grid Tied inverter –firing control

Phase locked loop

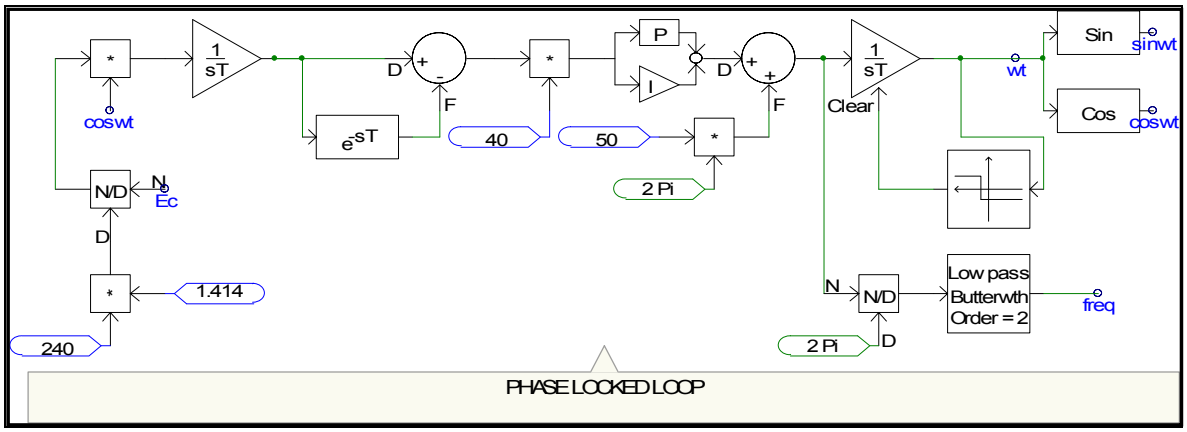

Figure A.8 Model – Phase Locked Loop

Control loops of grid tied inverter

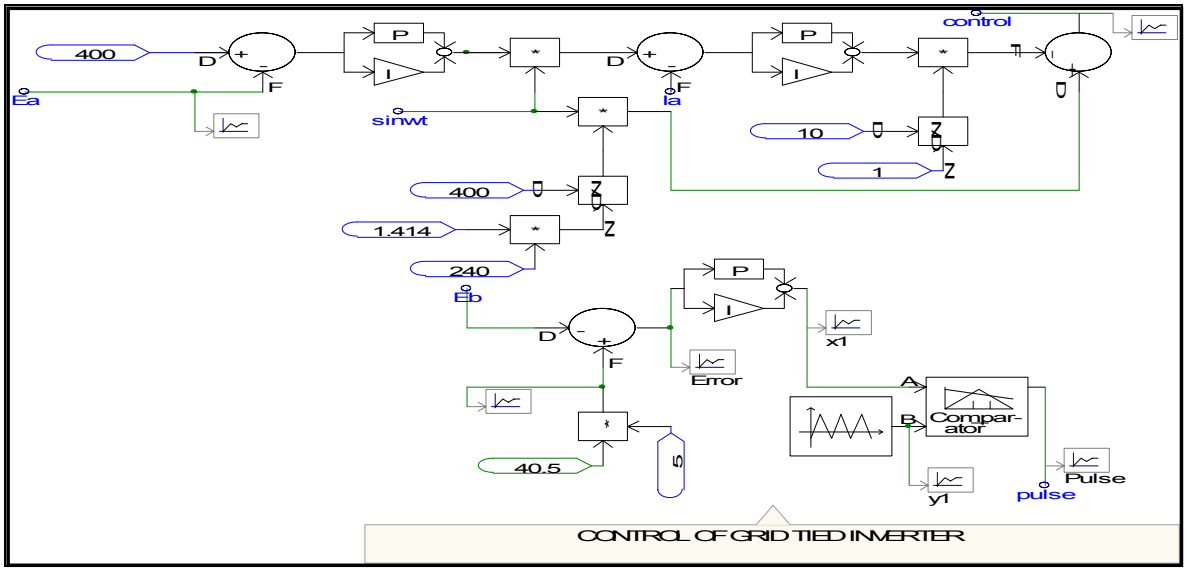

Figure A.9 Model – PV system control loop

Fault detection and tripping

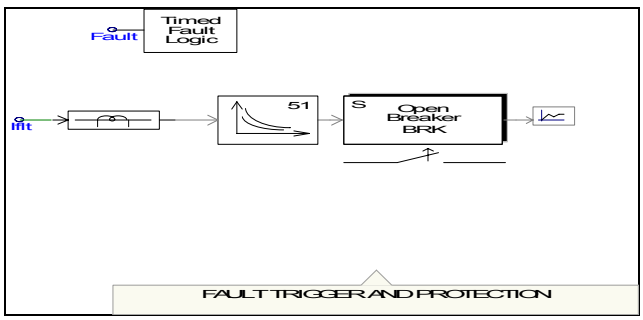

Figure A.10 Model – PV inverter over-current protection

APPENDIX B Simulation for evaluating fault current in network

Part 1 of network defined in Figure 4.5 in Chapter 4

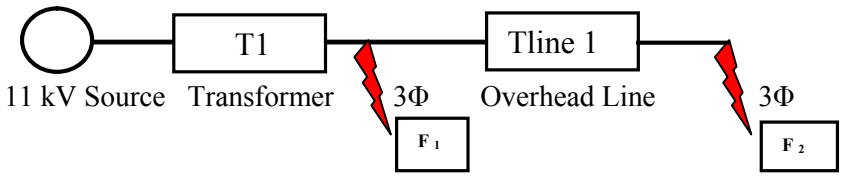

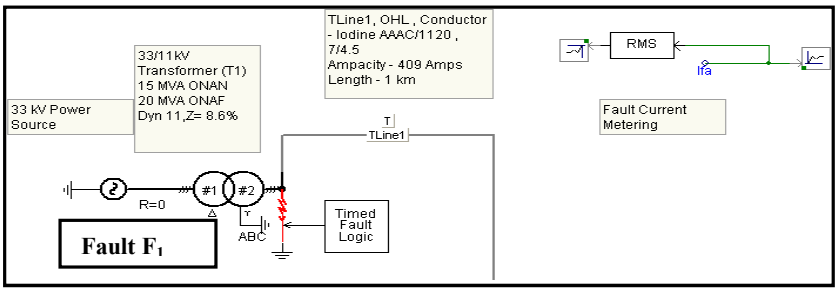

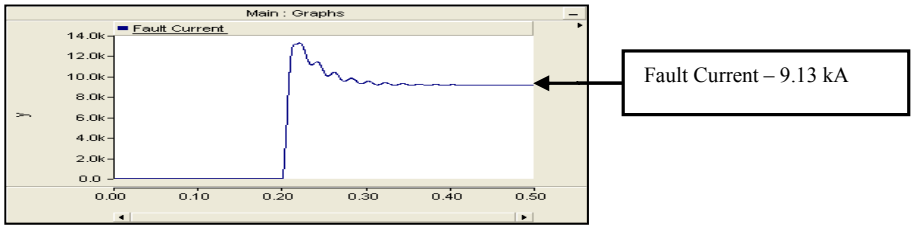

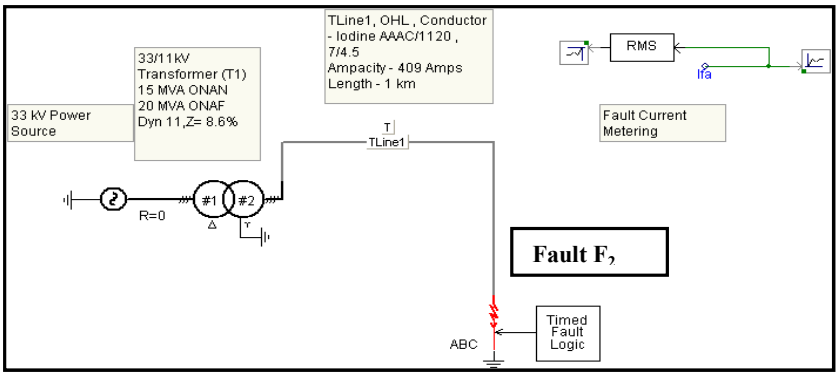

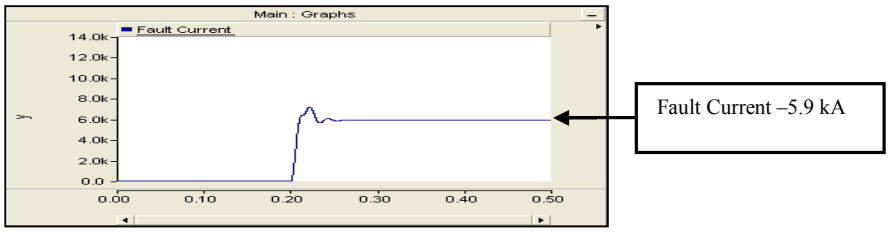

Figure B.1 PSCAD Simulation part-1

- Calculated value of 3Φ symmetrical fault current for fault at F_1-9.15 kA
- Simulation output record for value of 3 Φ symmetrical fault current for fault at F_1- 9.13 kA
- Calculated value of 3 Φ symmetrical fault current for fault at F_2 - 6.1 kA
- Simulation output record for value of 3 Φ symmetrical fault current for fault at F_2-5.9 kA

Part 2 of network defined in Figure 4.5 in Chapter 4

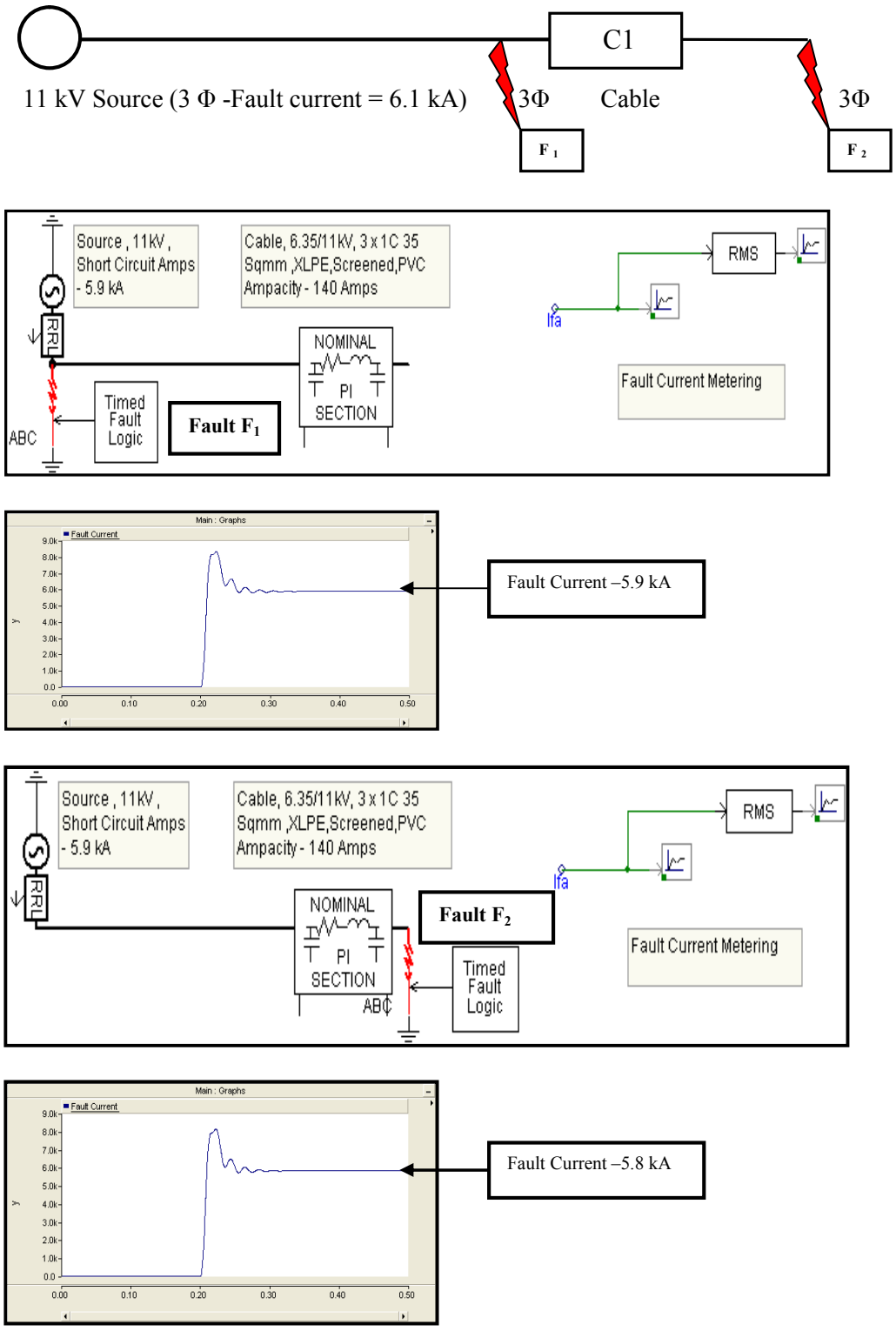

Figure B.2 PSCAD Simulation part-2

- Calculated value of 3Φ symmetrical fault current for fault at F_1-6.1 kA
- Simulation output record for value of 3Φ symmetrical fault current for fault at F_1- 5.9 kA
- Calculated value of 3Φ symmetrical fault current for fault at F_2 – 6.0 k A
- Simulation output record for value of 3Φ symmetrical fault current for fault at F_2-5.8 kA

Part 3 of network defined in Figure 4.5 in Chapter 4

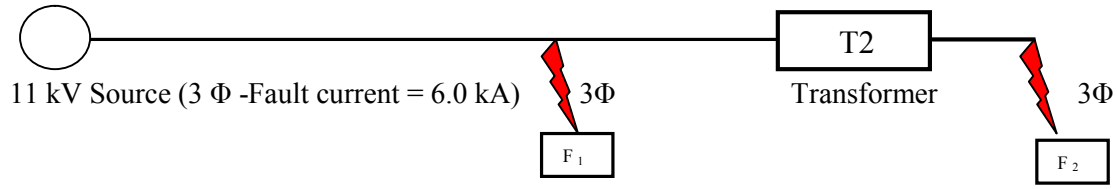

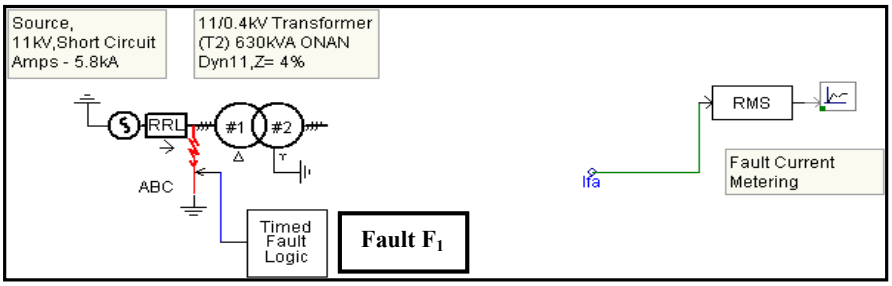

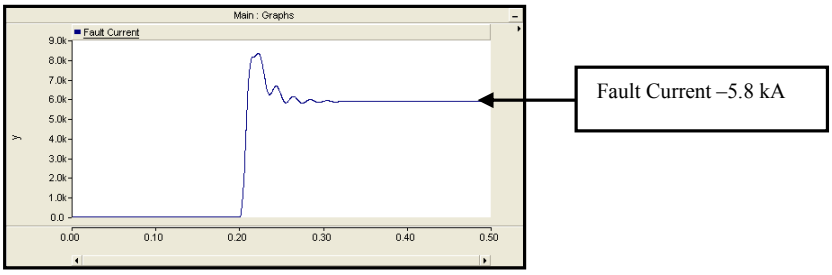

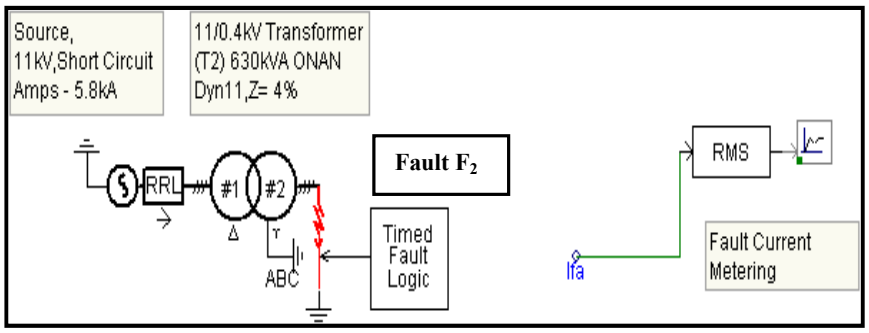

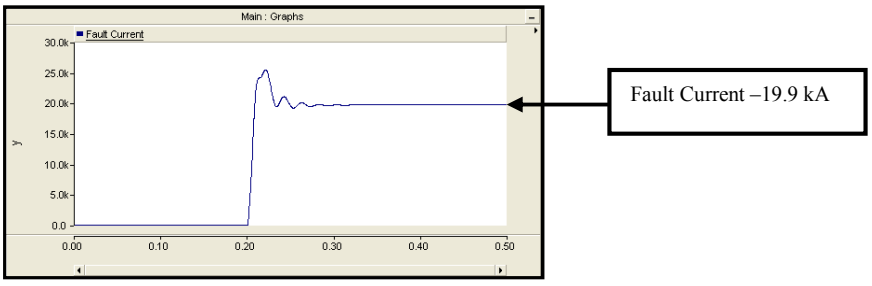

Figure B.3 PSCAD Simulation part-3

- Calculated value of 3Φ symmetrical fault current for fault at F_1-6.0 kA
- Simulation output record for value of t3Φ symmetrical fault current for fault at F_1- 5.8 kA
- Calculated value of 3Φ symmetrical fault current for fault at F_2 –20.0 kA
- Simulation output record for value of 3Φ symmetrical fault current for fault at F_2-19.9 kA

Part 4 of network defined in Figure 4.5 in Chapter 4

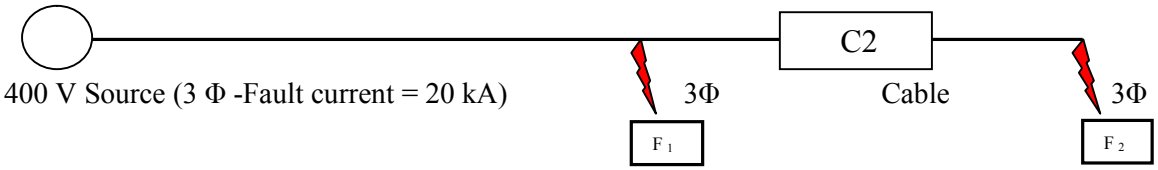

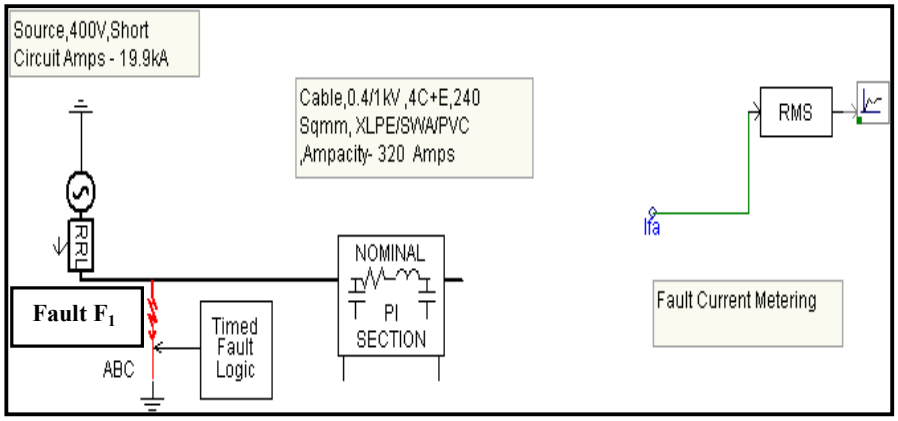

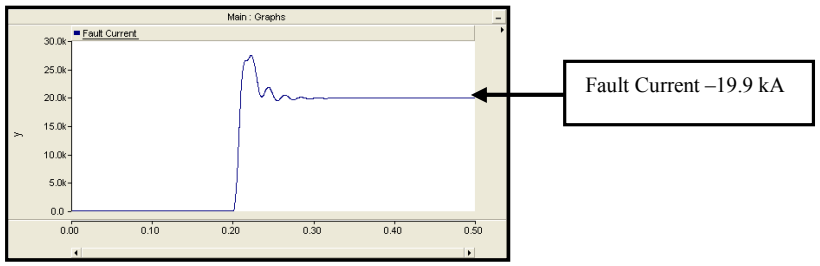

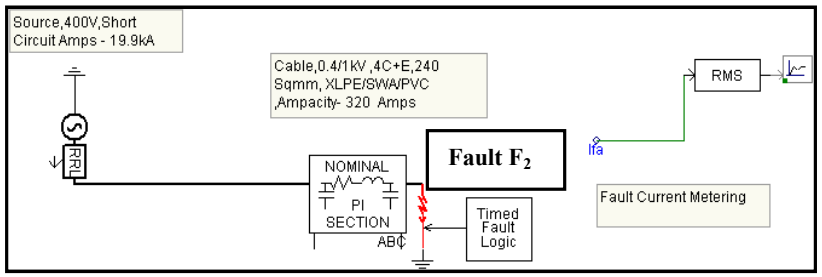

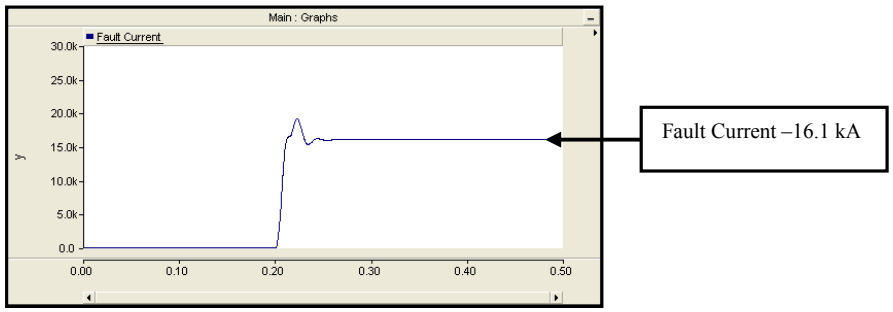

Figure B.4 PSCAD Simulation part-4

- Calculated value of 3 Φ symmetrical fault current for fault at F_1- 20 kA
- Simulation output record for value of 3 Φ symmetrical fault current for fault at F_1-19.9 kA
- Calculated value of 3 Φ symmetrical fault current for fault at F_2 -16.25 k A
- Simulation output record for value of 3 Φ symmetrical fault current for fault at F_2 -16.1 kA

Part 5 of network defined in Figure 4.5 in Chapter 4 (3 phase fault)

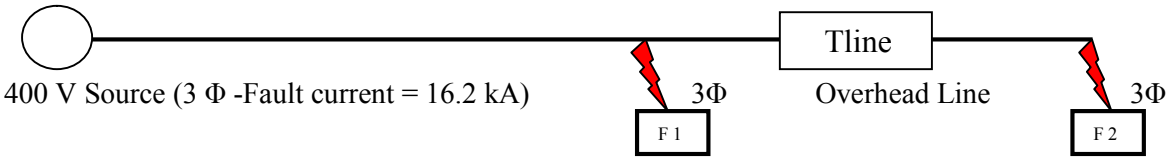

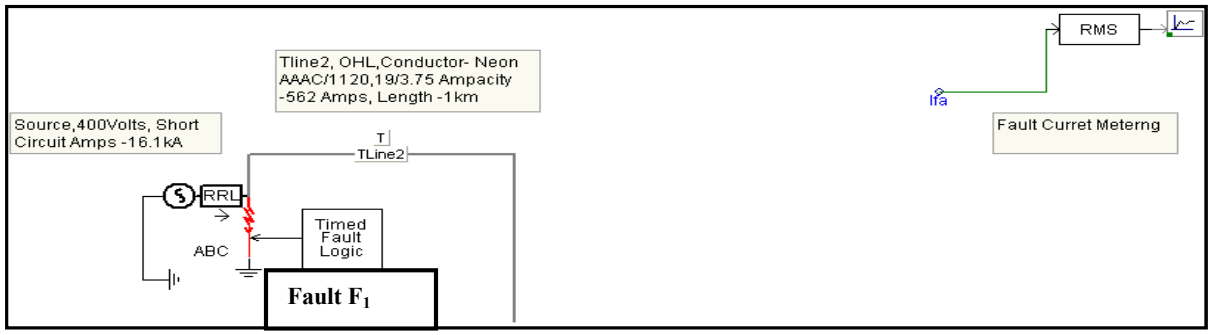

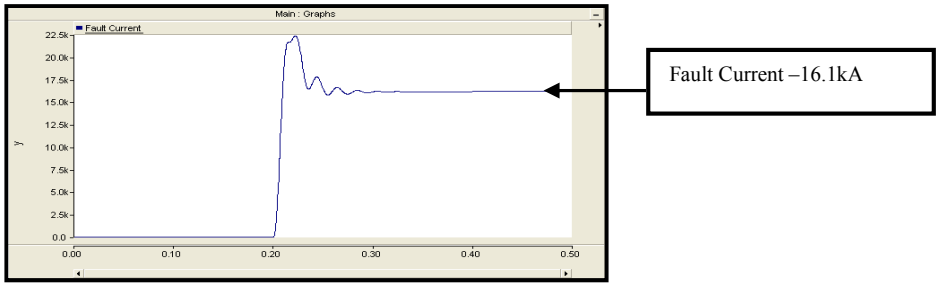

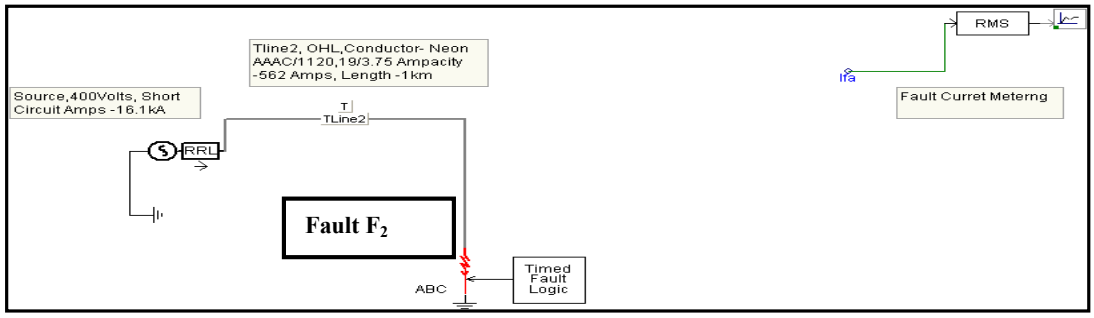

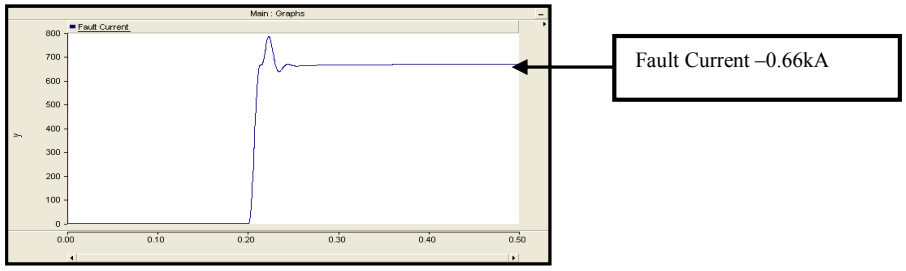

Figure B.5 PSCAD Simulation part-5 (3 Φ- fault)

- Calculated value of 3 Φ symmetrical fault current for fault at F_1- 16.2 kA
- Simulation output record for value of 3 Φ symmetrical fault current for fault at F_1-16.1 kA
- Calculated value of 3 Φ symmetrical fault current for fault at F_2 – 0.62k A
- Simulation output record for value of 3 Φ symmetrical fault current for fault at F_2 – 0.66 kA

Part 5 of network defined in Figure 4.5 in Chapter 4 (LG fault)

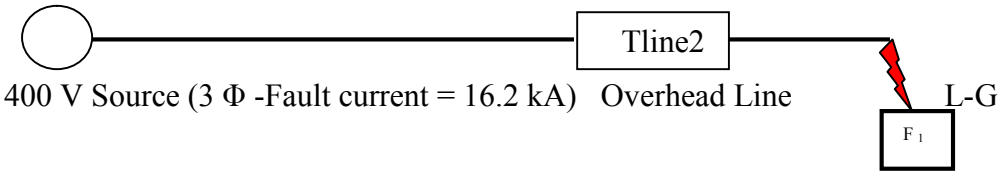

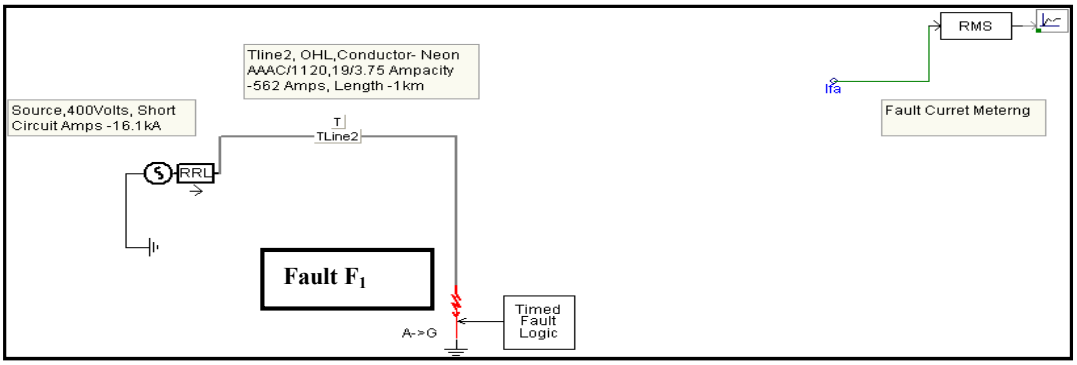

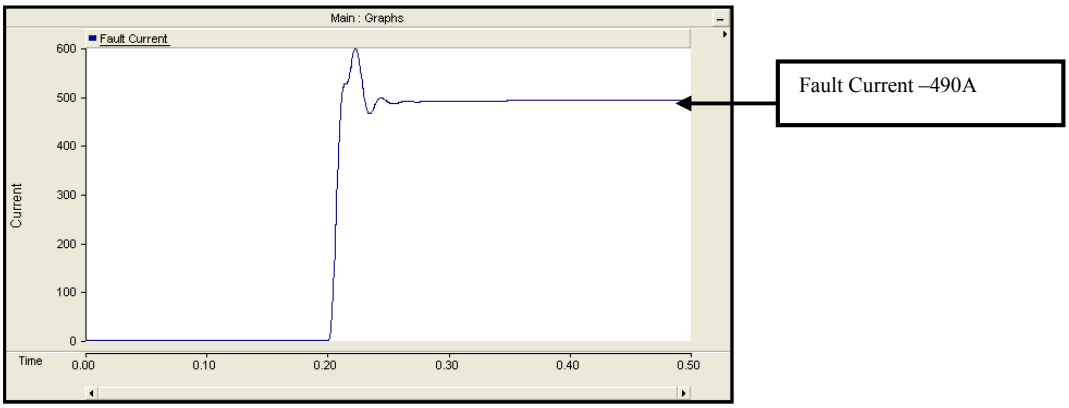

Figure B.6 PSCAD simulation part-5 (3 Φ- fault)

- Calculated value of single line to ground fault current for fault at F_1- 484A
- Simulation output record for value of single line to ground fault current for fault at F_1-490A

APPENDIX C – PSCAD Simulation –Single phase PV systems

Normal operation -PV disconnected -Single Residence

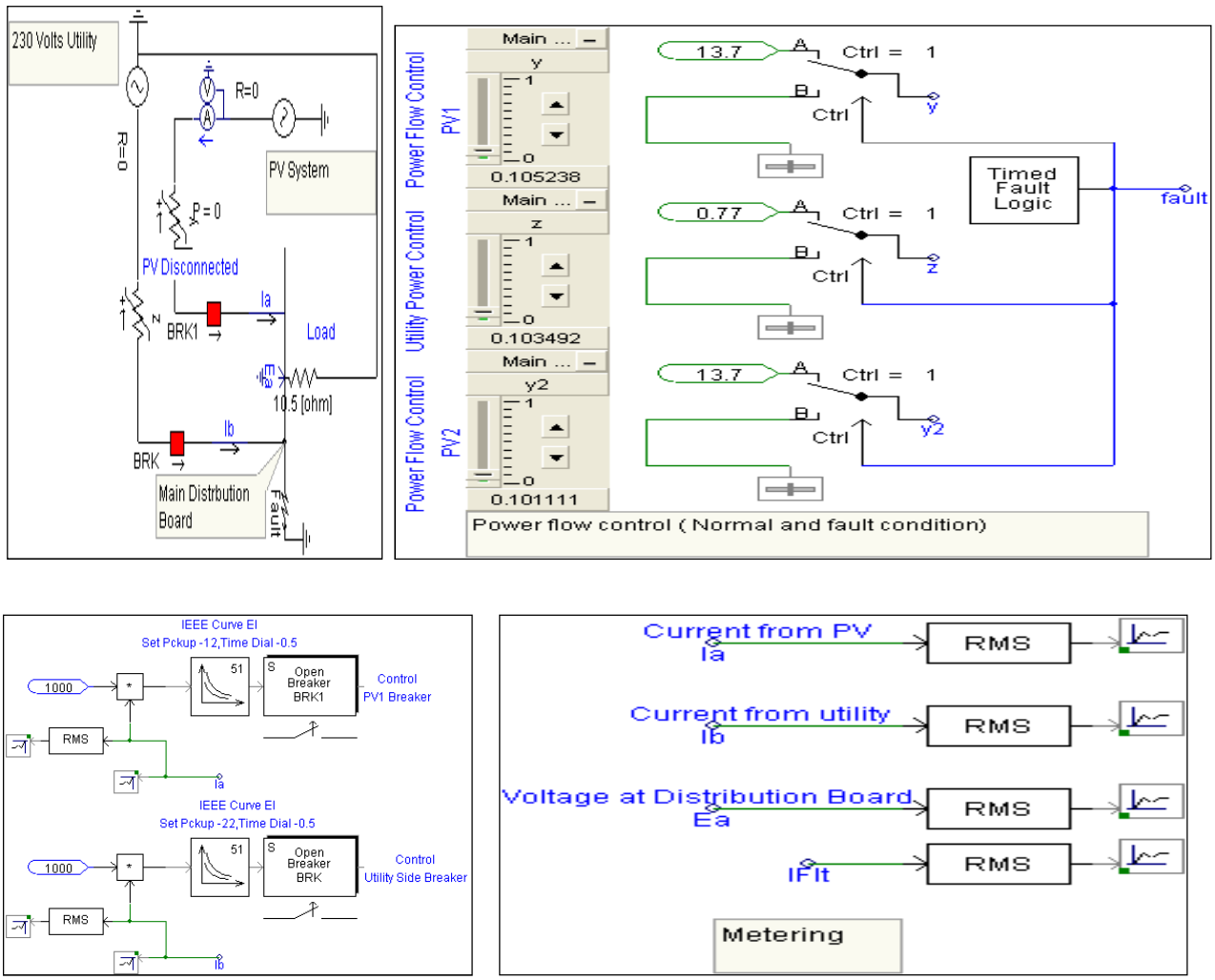

Figure C.1 Normal Operation PV Disconnected – Single Residence

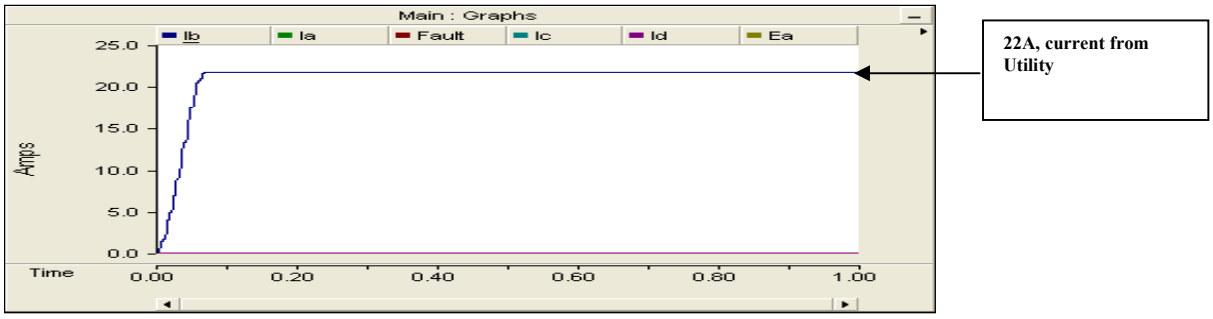

Figure C.2 RMS value of load current PV Disconnected (Single Residence)

Normal operation- PV connected -Single Residence

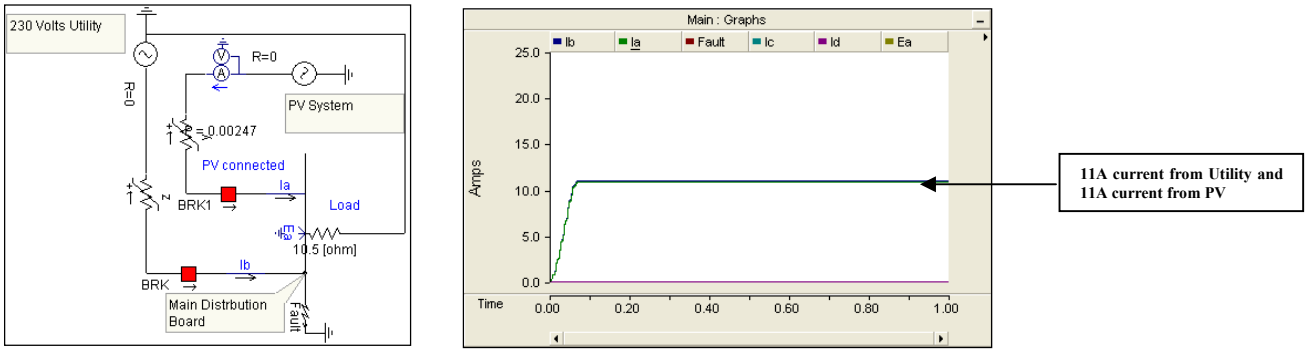

Figure C.3 Normal Operation PV Connected -Single Residence

Fault in main distribution board -PV disconnected -Single Residence

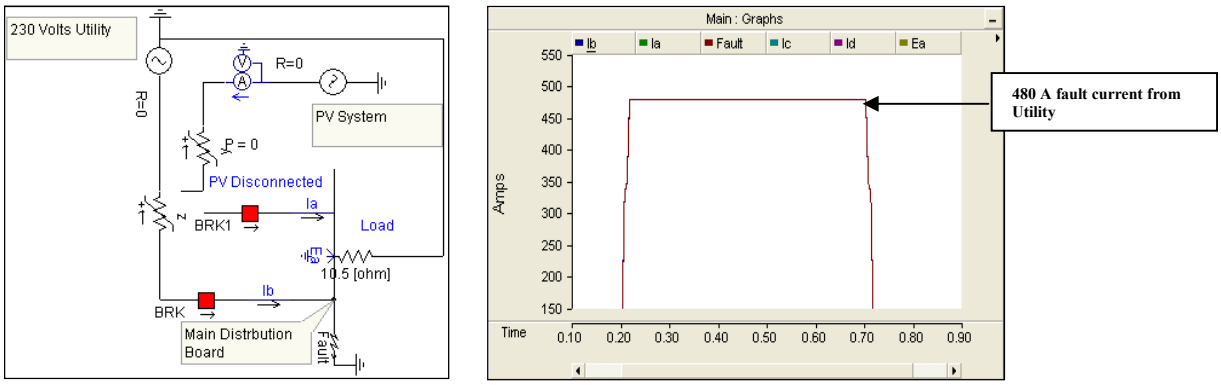

Figure C.4 Fault in MDB -PV Disconnected –Single Residence

Fault in main distribution board -PV connected, utility disconnected -Single Residence

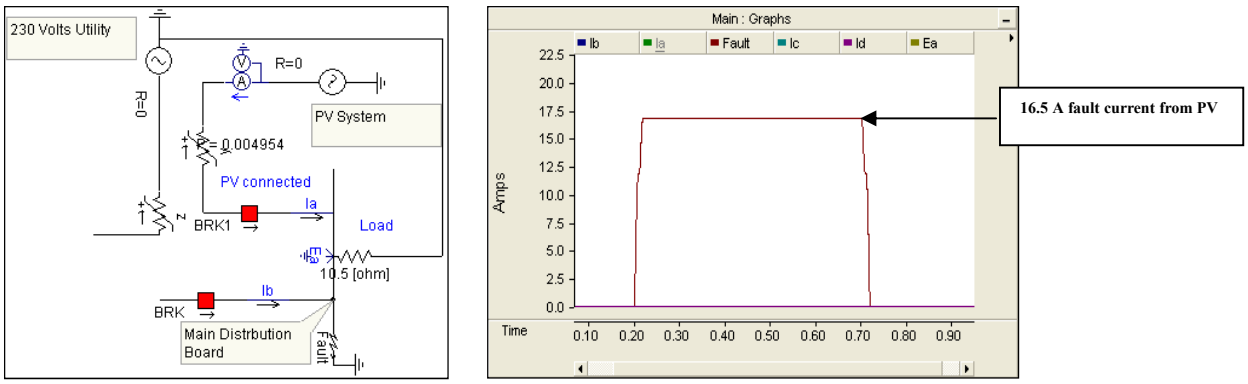

Figure C.5 Fault in MDB - PV Connected - Single Residence

Fault in main distribution board - PV connected - Single Residence

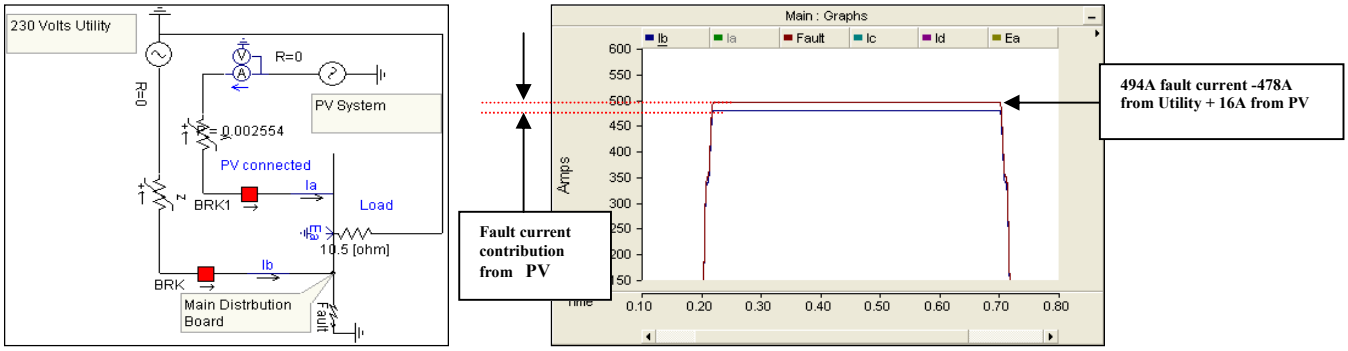

Figure C.6 Fault in MDB - PV1 Connected –Single Residence

Fault in main distribution board of residence 1 – PV1 & PV2 connected - Multiple Residences

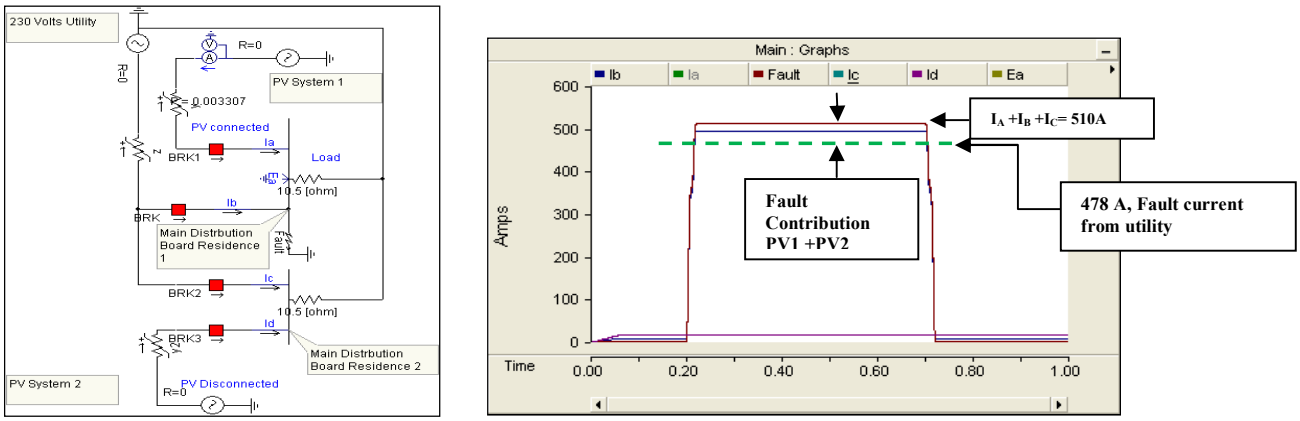

Figure C.7 Fault in MDB (Residence 1) - PV1 and PV2 Connected – Multiple Residences

APPENDIX D – PSCAD Model – Network Control and Protection

Network Protection – Protection functions for circuit breakers of Figure 5.1

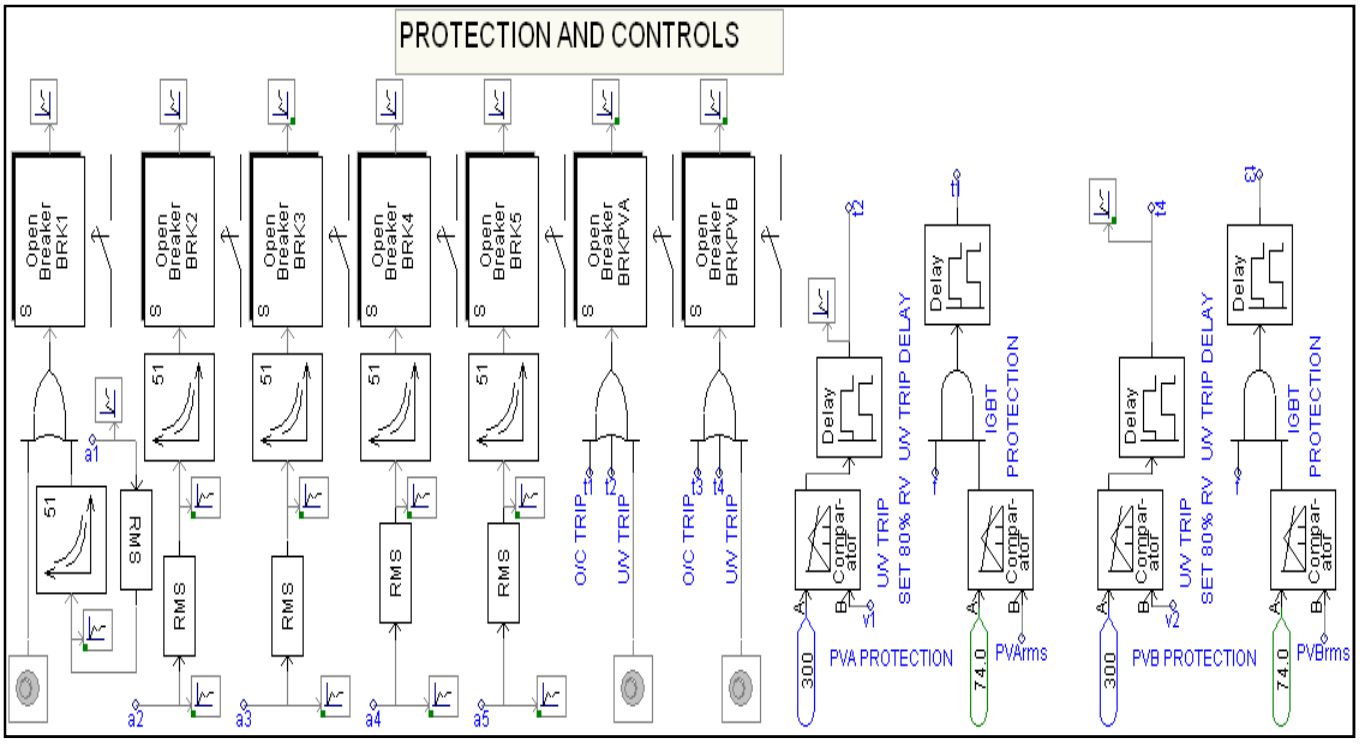

Figure D.1 Protection schematics for circuit breakers for networks studied in chapter 5

Fault feed control of PV systems shown in Figure 5.4

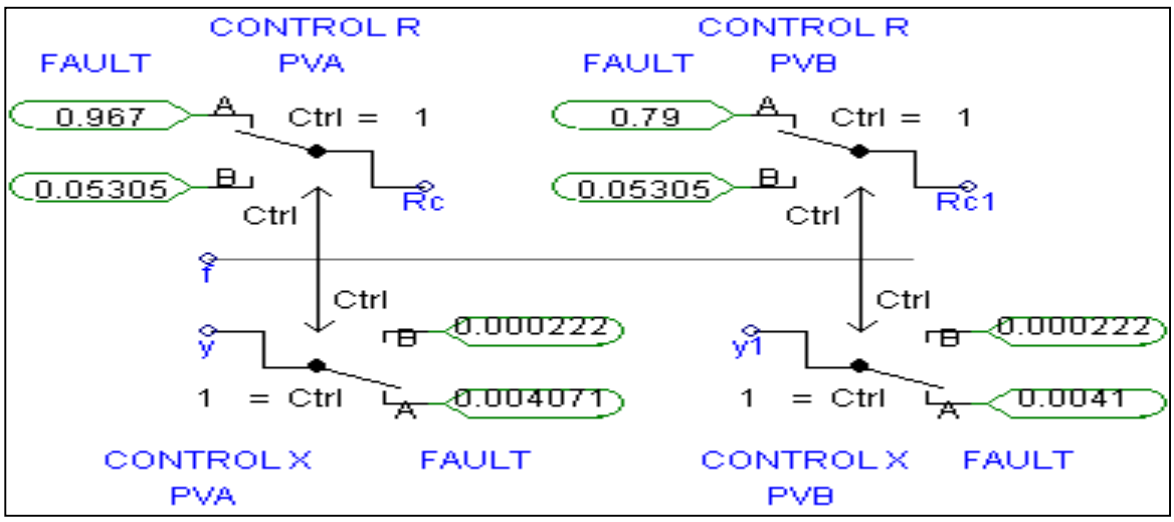

Figure D.2 PV source control during normal and faulted condition

Papers published and submitted during thesis research

Fault current contribution from photovoltaic systems in residential power networks

Subhashish Bhattacharya, *Member, IEEE*, Tapan Saha, *Senior Member, IEEE*, M. J. Hossain, *Senior Member, IEEE*

***Abstract*— This paper presents a detailed analysis for determining the impact of adding single phase photovoltaic (PV) systems in residential power distribution networks. This study highlights the issues arising due to the increase in fault levels in the network caused by the contribution from PV generators. A typical power distribution network for a suburban area has been modeled in PSCAD and the changes in fault current magnitude with the incremental addition of PV system has been studied. From this analysis it is found that PV generators can contribute fault current of considerable magnitude and thereby has an appreciable impact on the protection system if the PV penetration level is high.**

***Index Terms*—Fault current, Inverter, Insulated Gate Bipolar Transistor (IGBT), Miniature circuit breaker (MCB), main distribution board, Photovoltaic (PV) system**

I. INTRODUCTION

Generally solar PV systems are considered to make very minimum contribution to network in terms of fault current. It is therefore expected to make minimum impact on the fault rating of components in power network and protective device coordination. The industry rule of thumb for fault current contribution from PV systems considered for studies and modeling is twice the [1] the inverter rated current. This can however vary between 1.2 -2.5 times the inverter rated current depending on different types and manufacturers of inverters for PV systems. The low fault current contribution from PV system does not necessarily mean that proper evaluations of fault withstand capacity and relay coordination is not required when PV systems are added to network. Study carried out in the past indicate that there is an increase in the order of 7% in fault current magnitude [2] that can be caused due to PV systems introduced in network.

The magnitude of fault current contribution depends on the size and number of PV system installed in a particular network. Therefore the level of penetration of PV system in a particular size of network determines the importance of evaluation of impact of PV system on network fault and fault withstand capacity of the network devices. For a grid tied PV system inverter there is anti-islanding protection provided. As per IEEE standard 1547 [3], all grid connected inverter system shall successfully detect islanding and stop energizing within a given limit of time. In a grid tied system during a fault in the network, the grid side fault clearing device opens to clear the fault. The PV system then detects islanding and thereafter trips on detection of islanded condition within specified time (within 2 seconds) [3, 4].

However as the anti-islanding protection operates within 2 seconds from the instant of fault, the PV system can potentially contribute short circuit current to the point of fault for this duration. Therefore PV systems installed upstream of a fault clearing device may necessitate replacement of existing fault clearing device with a fault clearing device of higher breaking capacity as the contribution from PV system will increase the network fault level.

The objective of this paper is to investigate the effect of increase in fault current with increased penetration of PV systems in residential power supply networks.

The organization of the paper is as follows –

Section II describes the power network, Section III- provides the power system model which also includes studies for two cases, Section IV and V describes results and analysis which is followed by conclusions of the study.

II. DESCRIPTION OF NETWORK

A typical power distribution network for providing power to residential units in suburban area has been considered for the study as shown in Figure 1.

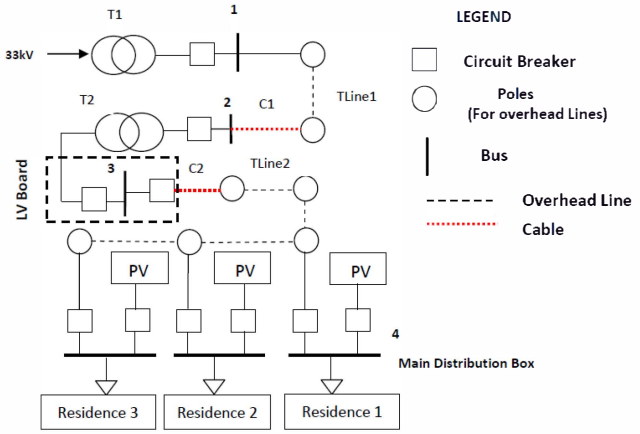

Figure 1 Suburban power distribution network

Three phase power at 33 kV is supplied via overhead line (OHL) from main substation to suburban area substation (SS1). SS1comprises a 33/11kV transformer and feeds 11kV power to the distribution network via three-phase OHL installed on poles. The OHL is terminated at the kiosk substation via high voltage cable. The kiosk comprises 11kV

S. Bhattacharya is a part time M Phil student at University of Queensland and is with SKM Brisbane, Australia Email: Subhashish.bhatta@gmail.com

*Prof Tapan Saha is with ITEE at the University of Queensland, Brisbane, Australia, Email: saha@itee.uq.edu.au

M. J. Hossain is with Griffith School of Engineering, Griffith University, Gold Coast, QLD 4222, Australia, Email:j.hossain@griffith.edu.au

ring main unit (with one transformer feeder), 11/0.4kV transformer (T2) and a 400 Volts distribution board. The 400 Volts distribution board receives power from the transformer secondary and feeds power to low voltage OHL using outgoing feeders and cables. Low voltage OHL installed on poles feed power to individual residential block. Power is tapped at pole tops of 400 volts OHL to feed three-phase or single-phase power to individual residential power distribution boxes at customer premises. To allow connection from grid and PV system, the customer main switch board has two incoming switches, each complete with over-current protection devices. Specifications of the components for the network in Figure 1 are provided in TABLE II in Appendix. For the purpose of this study single phase load distribution at customer premise is considered.

III. MODELING

A. *PSCAD Model- Power Distribution System*

The power system defined in section II has been modelled in PSCAD software environment and simulation output at end of each impedance component of the model has been compared with calculated value of fault level (calculated in accordance with AS 3851[5]) to validate the accuracy of model. The model has been split into five parts to check response of the model. Figure 2 shows five parts of the power system which has been analyzed for faulted conditions. Short circuit fault has been simulated at source and end of each part of the network.

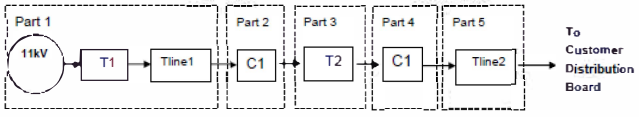

Figure 2 Network sections used for analysis

Single phase to earth fault has been applied on bus 4 of the distribution network shown in Figure 1(i.e. end of part 5 of Figure 2). The magnitude of fault current at the end of part 5 of network in Figure 2 has been used as the source short circuit level for models which are shown in section III B (Figure 7 & Figure 9). Output waveform for fault current is shown in Figure 3.

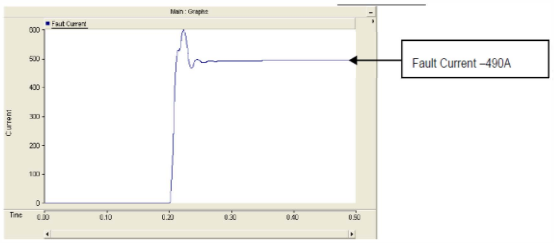

Figure 3 Fault Current–Line to earth fault

TABLE I lists the difference between analytical (calculated) and simulated value of fault current. Values listed in the table shows that simulated results are very close to the analytical results which prove the accuracy of the developed network model.

TABLE I ANALYTICAL AND SIMULATED VALUE OF FAULT CURRENT

Fault at end of part	Type of fault	Fault Current kA-simulation	Fault Current kA-analytical	Difference (%)
1	3 phase	9.15	9.13	0.2
2	3 phase	6.1	5.9	3.3
3	3 phase	19.9	20.0	0.5
4	3 phase	16.1	16.9	4.7
5	1phase-E	0.490	0.484	1.2

The PSCAD model of the power system described in section II is shown in Figure 4.

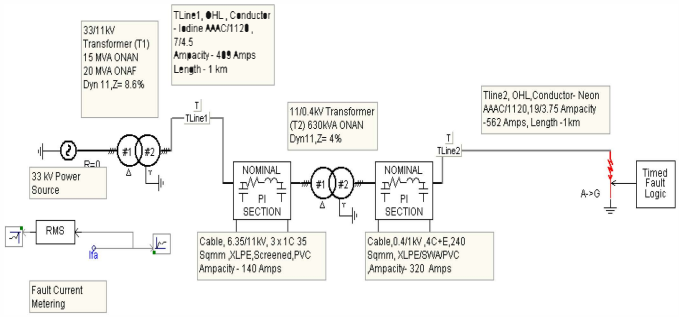

Figure 4 PSCAD Model of Network

B. *PSCAD Model - PV connection at residences*

As described in Section II, transformer T2 provides power to the 400 volts distribution board. The distribution board feeds two overhead line circuits using 400 amps outgoing feeders. The system (feeder with connected cable) is sized to cater for 221 kVA per circuit. A balanced three phase circuit can therefore feed 73 kVA per phase. Considering average domestic consumption of 5 kVA per residence, each phase can feed 14 residences which have been considered for this study.

To investigate the effect of adding a PV system as a power source for domestic power distribution board of residential units, a PV unit has been assumed to be installed in each of the 14 residences. PSCAD model for the distribution at customer main distribution board has been used to validate that connecting PV system will increase fault current at customer main distribution board. TABLE III in Appendix lists the values used for modeling the power distribution at individual residences.

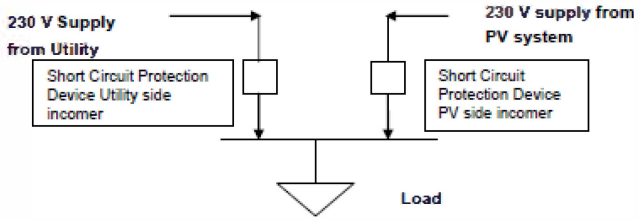

Figure 5 Power connections at main distribution board

Figure 5 shows a typical power distribution arrangement at customer's main distribution board. PV system has been modeled as constant voltage and constant current source in the studies done in the past [2].

In the model the PV system has been modeled as a voltage source that can contribute about 50% the power requirement for the 5kVA load. During a fault in the main distribution board the fault current contribution from the PV system is limited to a value of 1.5 times of inverter full load current.

Full load current for a 2.5 kW inverter (considering unity power factor) = 10.9 Amps. The maximum possible fault contribution from inverter during fault is 1.5 times 10.9 amps =16.5 amps (approximately).

The load of 5kVA is represented by a 10.5 ohms resistance which will absorb 5kVA at 230 V a.c and unity power factor.

Two cases have been simulated and analyzed during a fault in the main distribution board which is described below:

1) Fault current contribution from PV system connected to main distribution box of one residence.

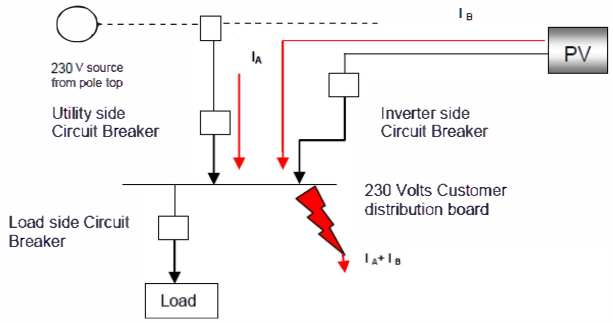

Figure 6 Fault Current Contribution – PV connected to one residence

Figure 6 represents the flow of fault current during a fault on main distribution board when a PV system is connected to the main distribution board of a single residence.

The PSCAD model of the scheme shown in Figure 6 is shown in Figure 7.

During a fault in the customer distribution board, fault current if:

- PV is not connected – I_A
- PV is connected – $I_A + I_B$

Where - I_A is the fault current contribution from utility and I_B is the fault current contribution from PV (refer Figure 13 in section IV). It can be observed that the utility side circuit breaker will have to successfully interrupt fault current contribution from the utility and the PV side circuit breaker has to interrupt the fault contribution from the PV unit. Circuit breakers are sized to interrupt the fault contribution from source. Addition of PV system will not cause any increase in fault current magnitude that the utility side circuit breaker will need to clear. Therefore no further upgrade or evaluation of breaking capacity of utility side breaker is required in this case. The other factor to consider is the effects of contribution of additional fault current from PV system on the fault withstand capacity of the busbar of the main distribution board. It is important that the busbar should be capable of withstanding the mechanical forces during the fault and the temperature rise caused by the raise in magnitude of current during the fault. With a 2.5kW PV system connected the addition in fault current is not significant and it is unlikely that the busbar fault withstand capacity will be exceeded.

Figure **7** shows that utility is disconnected, PV is connected and fault has been placed on main distribution box.

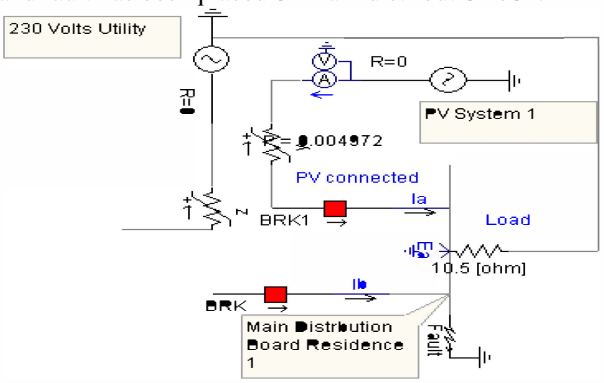

Figure 7 Model - PV connected to one residence

2) Fault current contribution from PV system connected to main distribution box of multiple residences

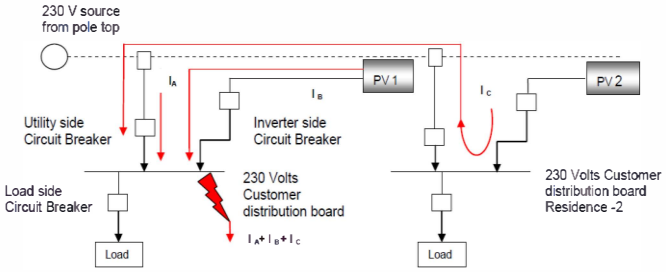

Figure 8 Fault Current Contribution – PV connected to multiple residences

Figure 8 represents the flow of fault current during a fault on main distribution board when PV systems are connected to the main distribution board in multiple residences. The PSCAD model of the scheme is shown in Figure 9.

During a fault in the customer distribution board, fault current if:

- PV is not connected – I_A
- PV is connected – $I_A + I_B + I_C$

Where I_A is the fault current contribution from utility, I_B and I_C is the fault current contribution from PV1 and PV2 respectively (refer Figure 14 in section IV).

Unlike the case where analysis is based on PV connection in single residence, with PV units installed in multiple residences, the utility side circuit breaker will now have to interrupt the summation of fault current contribution from utility side and fault current contribution from the PV units of other residences connected to the same phase of overhead line to successfully clear the fault. The fault current contribution from PV system connected to main distribution board of other residences will collectively contribute to the fault occurring in the distribution board of a particular residence. This fault will have to be cleared by the circuit breaker installed in the distribution board where the fault has occurred. While fault current contribution from a single PV unit may be not significant, with multiple PV units the magnitude of fault current will increase. It is therefore important to ensure that

the utility side circuit breaker and the busbar in distribution board are adequately sized for handling increased fault current.

Fault current contribution of 2.5 kW inverter is in the range of 16.5 to 22 amps. 14 such units together can collectively contribute 0.3 kA. Addition of more residences with PV or larger PV systems can significantly increase the fault current.

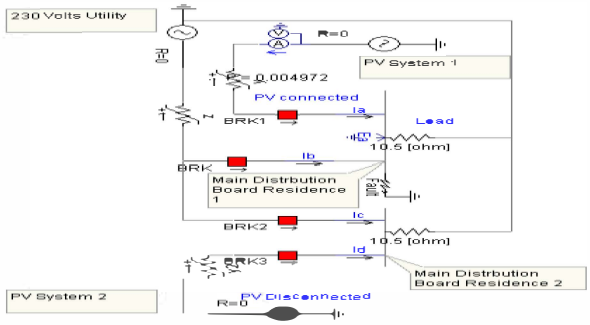

Figure 9 Model - PV connected to multiple residences

IV. OBSERVATIONS

Figure 10 shows simulation output for load current at main distribution box when there is no fault in system. It can be observed that the load is being equally shared between utility and the PV system.

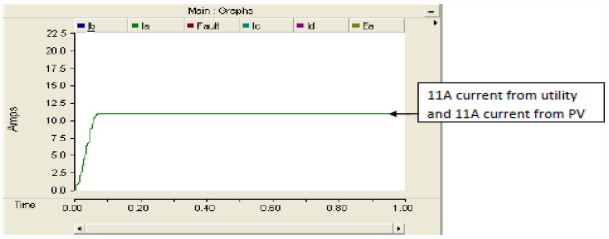

Figure 10 Load Current - PV and Utility connected –no fault

Figure 11shows the simulation output of fault current when only utility is connected to the main distribution box and a fault (single line to earth) is placed on the bus of main distribution box. The recorded fault current magnitude is 480 amps.

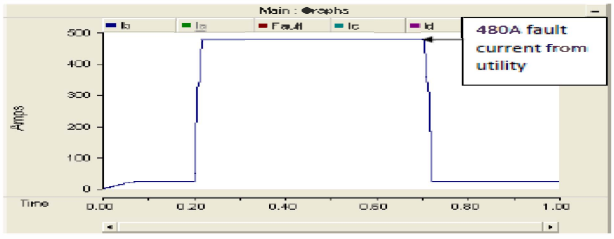

Figure 11 Fault Current - Utility connected –fault in main distribution box

Figure 12 shows the simulation output of fault current when only PV system is connected to the main distribution box (considering PV connected to only one residence) and a fault (single line to earth) is placed on the bus of main distribution box. The recorded fault current magnitude is 16.5 amps.

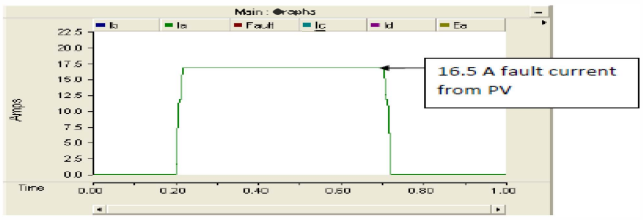

Figure 12 Fault current - PV connected –fault in main distribution box

Figure 13 shows the simulation output of fault current when both PV system and utility is connected to the main distribution box (considering PV connected to only one residence) and a fault (single line to earth) is placed on the bus of main distribution box. The recorded fault current magnitude is 494 amps. This fault current is made up of 478 amps contributed by the utility and 16amps contributed by the PV system. This represents case 1as described in section III.

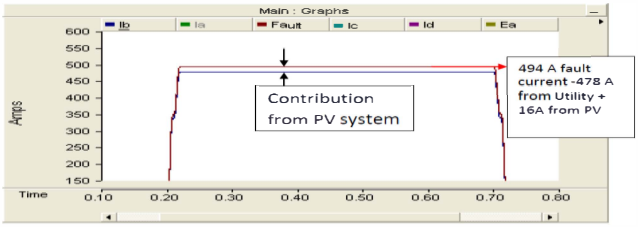

Figure 13 Fault Current - PV and Utility connected –fault in main distribution box (considering PV connected to only one residence)

Figure 14 shows the simulation output of fault current when both PV system and utility is connected to the main distribution box (considering PV connected to two residences, both the residences being connected to the same phase of the utility distribution system) and a fault (single line to earth) is placed on the bus of main distribution box of one residence. The recorded fault current magnitude is 510 amps. This fault current is made up of 478 amps contributed by the utility and 16 amps contributed by the PV system of the first residence and 16 amps by the PV system of the next residence. This represents case 2 as described in section III.

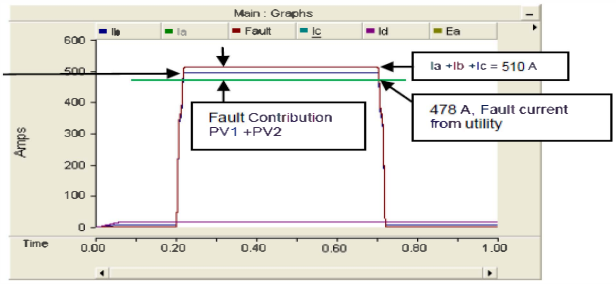

Figure 14 Fault Current -PV and Utility connected –fault in main distribution box (considering PV connected to only one residence)

V. ANALYSIS OF RESULT

In the simulation carried out effort has been made to illustrate the fact that even though individual PV system installed in residences might not contribute enough fault

current to be able to make an impact on the fault interruption capacity of switching device, multiple PV units connected to the network will make cumulative contribution to the point of fault and thus affect the ability of switching device to clear fault. An important factor to consider and analyze is the duration for which the PV system can contribute to the fault. This has a significant impact on the fault withstand capacity of the short circuit protection device as well as the downstream busbar system.

At the customer main distribution board, utility side switching device is 25 amps miniature circuit breaker (MCB) and the PV side switching device is 16 amps MCB (Curve C to AS/NZS 60898.1 [6], fault breaking capacity- 6 kA). The MCBs are sized on the basis of the load and inverter size.

A curve C, MCB has a trip characteristic which trips MCB at 5 to 10 times of rated current of the device almost instantaneously. At a current less than this but above 110% of rated current the device follows IDMT characteristics.

Therefore the magnitude of instantaneous tripping current for MCB on the utility side is 125 amps to 250 amps and PV side is 80 amps to 160 amps.

The fault current contributions from different sources during a single line to earth fault in main distribution box are-

- From Utility – 490 amps. (calculated value for fault current is 484 amps; simulation value is 490 amps)
- From single PV system - 16.5 Amps
- Form an network where 14 residences are connected to same phase of network and there is a 2.5kW, PV system connected to each residence 14 x 16.5= 231Amps

Total fault current seen at the point of fault in main distribution box is 490 + 231 = 721 amps. The fault seen by MCB on utility side is {490 + (n-1) x 16.5} amps, where 'n' is the number of residences. So the fault current seen by the utility side MCB is 704.5 amps (490 + 214.5) amps as shown in Figure 17 . This illustrates case 2 in section III. This value is 28 times the rated current of the circuit breaker and the breaker will trip in about 0.01 seconds as shown in Figure 15.

The magnitude of fault current fed by individual PV system is about 105% of the rated current rating of the MCB and it will not trip during short circuit as shown in Figure 16.

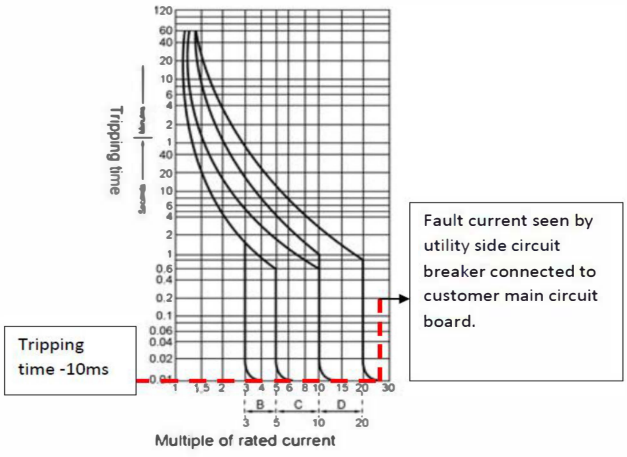

Figure 15 Utility side MCB tripping time

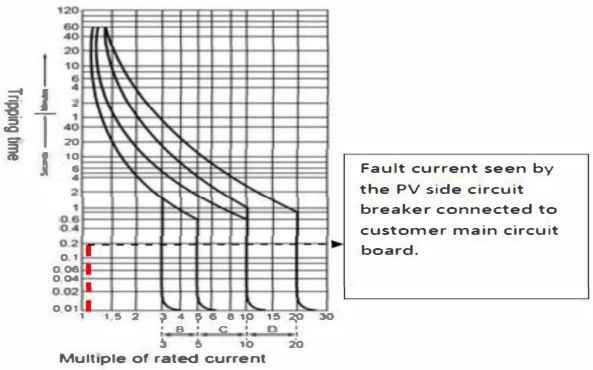

Figure 16 PV side MCB tripping time

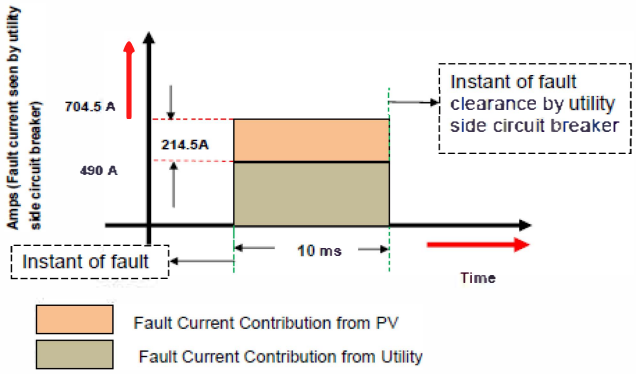

Figure 17 Fault Contribution from PV and Utility (seen by utility side CB) - Magnitude v/s Time

However for a PV system the MCB on the outgoing line is not the only device for isolating current feed to fault. The PV system produces alternating current power by inverting the dc power generated by photo-voltaic panel using inverters. At the inverter output ac power is available and this is connected to load and grid.

A single phase PV inverter converts DC power to AC by controlled firing of four IGBTs (Insulated Gate Bipolar Transistor). In event of a short circuit at the load side, IGBT collector current will increase. The time allowed between the start of short circuit until the current is cut off is limited by the short circuit withstand capacity of the IGBT [7]. Smaller the value of V_{GG+} (voltage across gate and emitter during conduction), higher is the short circuit endurance time. IGBT collector current is a function of the V_{GE} (gate emitter voltage) and temperature. The transfer characteristics of an IGBT indicate the maximum possible collector current at a particular V_{GE} is generally 1.5 to 1.8 times the nominal current which is much less than the short circuit current which is generally 6 to 7 times the nominal value [9]. The short circuit safe operating area (SC SOA) of IGBT, a curve with ratio of short circuit collector current to normal collector current on one axis and V_{CE} on the other, defines the limit of safe control of IGBT. The short circuit endurance time for a typical IGBT used in an inverter for similar application is in the order of 10 µS. At 1.5 to 2 times rated collector current (value of fault current fed by inverters), the inverter can keep feeding the fault for a time much longer than 10 µS, as it will be well within the safe short circuit operation zone of IGBT. The maximum time for which

the fault feed can happen at 1.5 times the full load current is limited by the temperature rise in the IGBT which will eventually lead to the destruction of the IGBT.

Studies undertaken in the past indicates that there had been post fault contribution from PV in the range of 4 to 10 cycles [8] which is longer than the fault clearance time of utility side MCB on a customer distribution board. Therefore due to the higher fault current contribution from PV systems the utility side MCB will clear a fault current of magnitude equal to the summation of fault current contribution from the utility and fault current contribution from PV systems. In order to limit possibilities of failure of fault breaking devices in customer main distribution boards due increase in fault level, limit needs to be established on maximum PV penetration in a particular network.

The other aspect to consider in terms of disconnection of PV inverter is disconnection by grid protection device of inverter.

The requirement as per Australian Standards [4] is that the grid protection device shall operate if supply from grid is disrupted or when grid goes outside set limits and to prevent islanding. The grid connection device shall incorporate passive anti-islanding protection in terms of under-over voltage and under-over frequency within 2 seconds. During fault the system will experience under- voltage and inverter anti-islanding protection will sense it, but the utility breaker will trip well before operation of anti- islanding protection and isolate fault. While this will lead to isolation of fault feed from PV units of neighboring units and utility, fault feed to main distribution board from the connected PV will continue for time until when the PV inverter over current protection isolates the system. If this fails to operate then subsequently grid anti islanding protection will isolate the PV system. Figure 18 illustrates the time sequence for isolation of power sources discussed in this paragraph.

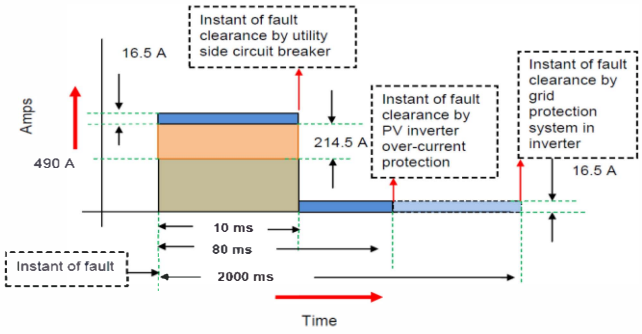

Figure 18 Fault Contribution from PV and Utility (seen by fault point at DB) - Magnitude v/s Time

VI. CONCLUSION

The investigation concludes that even though the fault current contribution from individual PV systems installed on residences is not high, collective contribution from multiple PV systems connected across the network can make significant increase in fault current. With increased level of PV penetration, networks needs to establish the level of penetration beyond which there can be significant problems in fault current interruption by existing fault clearing devices.

VII. APPENDIX

TABLE II SPECIFICATION FOR NETWORK COMPONENTS

Description	Specification
Network Parameters	
Supply Voltages	33kV,11kV ,400V
Fault Level (11 kV bus SS1)	I"kQ 3P- 9.15kA
Transformer	
T1 (in Substation SS1)	33/11kV, Dyn11,15/20 MVA,Z= 8.6%,
T2 (in Kiosk Unit)	11/0.433kV,Dyn11, 630 kVA, Z=4%
Overhead Lines	
TLine1 (From first pole near SS1 to pole near Kiosk)	Iodine, AAAC/1120, 7/4.75 (strand/ mm),124 mm^2, Length 1km,Current rating – 409A
TLine2 (From first pole near kiosk to residential cluster)	Neon, AAAC/1120, 19/3.75 (strand / mm), 210mm^2,Length 1km, Current rating– 562 A
Cable	
C1 (from 11kV pole top connection to ring main unit in kiosk)	6.35/11kV, 35 mm^2, Single Core, copper conductor XLPE/SCR/PVC sheathed, 30 m. Current carrying capacity (Trefoil & buried) -140A
C2 (from Low voltage board in kiosk unit to pole top connection for LV power supply)	0.6/1kV, 240mm^2, Four Core, Aluminum conductor XLPE/PVC, 30m.Current carrying capacity (buried)-320A

TABLE III SPECIFICATION FOR POWER DISTRIBUTION AT RESIDENCES

Description	Specification
Load per customer	5000 VA
Main distribution Board	230 Volts, 50 Hz ,Single Phase
PV Panel	Configuration- 72 cells per panel, 12 panels (3 parallel sets, each set made up of 4 panels connected in serial),total voltage -162 Volts, Power – 238 Watts /panel, total Power = 2.85 kW
PV Inverter	2.5 kW, 230 Volts Single Phase output

REFERENCES

[1] Jamie Keller, Benjamin Kroposki, Richard Bravo, Steven Robles, Fault Current Contribution from Single Phase PV Inverters, Photovoltaic Specialist Conference,2011, 37th IEEE, Pages 1822-1826

[2] S.Phuttapatimok, A.Sangswaang, M.Seapan, D.Chenvidhya and K.Kirtikara , Evaluation of Fault Contribution in presence of PV Grid connected systems, Photovoltaic Specialist Conference ,2008, 33rd IEEE, Pages 1-5

[3] IEEE Standard for Interconnecting Distributed Resources with Electric Power Systems, IEEE 1547, 2003

[4] Australian Standard Grid connection of energy systems via inverter-Grid protection requirements, AS 4777.3, 2005.

[5] Australian Standard The calculation of short-circuit currents in three phase a.c. systems, AS 3851,1991

[6] Australian Standard-Electrical accessories –Circuit breaker for over current protection for household and similar installations. Part 1, AS/NZS 60898.1, 2004

[7] *Fuji IGBT Module Application Manual*, *REH984*, Fuji Electric Drive Technology Company Ltd, 2004, pp. *5/2-5/6.*

[8] J E. Muljadi, M. Singh, R. Bravo, V. Gevorgian, Dynamic Model Validation of PV inverters under short circuit condition http://www.nrel.gov/docs/fy13osti/57341.pdf

[9] Abdus Sattar, IXYS Corporation Insulated Gate Bipolar Transistors(IGBT),pp.13-14.

ELSEVIER

Energy and Buildings

Fault contribution from large photovoltaic systems in building power supply networks

Subhashish Bhattacharya [a] ,Tapan Saha [a*] , M.J Hossain [b]

a ITEE , University of Queensland , Australia
b Griffith University, Australia

Abstract

This paper presents a detailed analysis for determining the impact of adding large three phase photovoltaic (PV) systems in building power distribution networks. The analysis highlights the protection relay coordination problems arising due to the increase in network fault levels caused due to the contribution from PV generators. A typical distribution network for power supply to large buildings with multiple apartments in a housing complex has been modeled and used as a test network. An analysis of observations of various cases studied shows that the magnitude of fault current contribution from PV system depends on a number of different factors and is not dependent only on the size of the PV system. The analysis emphasizes the requirement to review protection settings of similar installations prior to connection of PV generators to the network and suggests a method of protection coordination to minimize the requirement of reviewing the protection setting every time a new PV system is connected to the distribution network. It is found fault current contribution from PV systems, depending on the size, can cause significant relay coordination problems in terms of discrimination and thereby reduce system reliability.

Keywords —Fault current, Inverter; Insulated Gate Bipolar Transistor (IGBT), Air circuit breaker (ACB), Moulded case circuit breaker (MCCB), main distribution board (MDB), Photovoltaic (PV) system, Time current coordination (TCC).

1. Introduction

PV systems are considered to make very minimum contribution to network in terms of fault current. It is therefore expected to make minimum impact on protective device coordination. The industry rule of thumb for fault current contribution from PV systems considered for studies and modeling is twice [1] the inverter rated current. This can however vary between 1.2 -2.5 times the inverter rated current depending on different types and manufacturers of inverters for PV systems. The fault current contribution time generally varies from 4 cycles to 10 cycles [5]. The low fault current contribution from PV system does not necessarily mean that evaluations of existing relay coordination is not required when PV systems are added to network. Study carried out in the past indicates that an increase in the order of 7% in fault current magnitude [2] can be caused due to PV systems introduced in network. The magnitude of fault current contribution depends on the size and number of PV system installed in a particular network. Therefore the level of penetration of PV system in a particular size of network determines the impact of PV system on protection coordination.

* Corresponding author at ITEE, University of Queensland, Tel - +61 422001378
E-mail address: saha@itee.uq.edu.au

Most literature available, analyses protection problems in network caused by fault contribution from synchronous generators, which can feed substantial fault current and cause protection issues like fuse recloser coordination problems [10] and out of phase closing of recloser during fault. Such issues are more relevant for high voltage power distribution networks as recloser is generally used in high voltage networks. Some literature is available on fault current contribution from PV systems but studies described therein relates more to high voltage power networks [4]. A detailed investigation of protection and voltage regulation issues caused due to high penetration of PV systems in low voltage has been discussed in some literature [11][12]. However these papers focus on the protection issues in high voltage side of network caused by high PV penetration in the low voltage side of network. Not much literature is available on protection coordination issues in low voltage network due of high penetration of PV system in low voltage. Presently a number of large three phase PV systems are connected to low voltage networks, in particular **to large buildings with multiple apartments in a housing complex** or in commercial and industrial premises, which can cause protection problems in low voltage network. The objective of this paper is to present a detailed investigation of the effect of increase in fault current with high penetration of large PV systems in typical low voltage power supply networks on protection coordination of low voltage network and thereafter define the factors that should be considered for determining effective contribution of fault current from PV systems during fault. The paper also suggests preferred method of adjustment of time current coordination settings in order to avoid repeated adjustment of protective setting each time when a new PV system is added to the distribution network.
The organization of the paper is as follows – Section 2 describes the power network, Section 3- provides the power system model, Section 4 describes case studies and observation and 5 describes analysis of results which is followed by conclusions of the study.

2. Description of Network

A typical power distribution network for providing power to buildings with multiple apartments has been considered as a test network for the study. The network block diagram is shown in Fig 1. Three phase power at 11kV is supplied via overhead line (OHL) from main substation to pole mounted 11/0.4kV Transformer (T1). The transformer is protected by drop out fuse on the high voltage side and the secondary side is connected to a ground mounted low voltage distribution board using cable. The low voltage distribution board comprises one off 630 amps incoming air circuit breaker (ACB) and four off 160 amps outgoing feeder (moulded case circuit breakers -MCCBs). The outgoing MCCBs are connected to building main distribution board (MDB) using cable. To allow connection from grid and PV system, the MDB has two incoming switches. The utility side incomer is provided with over-current protection devices. The incoming power from PV source is protected and switched by PV system's integral switching and protection device. Specifications of the components for the network in Fig 1 are provided in Table III in Appendix. For the purpose of this study, four buildings, each made up of ten apartments has been considered. Assuming maximum demand of 5kVA per apartment, each building shall have a maximum load of 50kVA. A roof top photovoltaic system of 50kVA for each building has been considered.

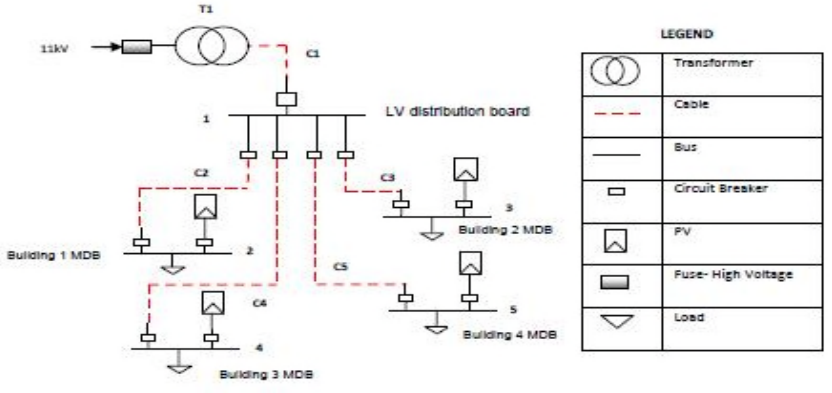

Fig. 1 Power distribution network – Power supply for buildings

2.1. Test Network Model

The power system defined in section above has been modeled in PSCAD software environment (simulation software produced developed by Manitoba HVDC centre). The power system model has been first developed and validated to check its accuracy without introducing the PV systems. Fault current magnitude calculated in accordance with Australian Standard AS 3851[8] has been compared with simulation output for faults at different points in the network. Fig 2 shows the points (A, B, C, D) in the power system at which fault has been placed and analytical values have been compared with simulation output. A fault level of 9.15kA at 11kV has been used as source fault level for the study. This is based on a zone substation transformer rating of 15MVA (33/11kV, Z=8.6%). The high voltage side protection has not been included in model as the high voltage protection device had no influence in the study done. For ease of modeling, without effecting overall accuracy, only two out of four buildings have been modeled and cumulative effect for fault contribution from PV systems installed in other two buildings has been considered in this study.

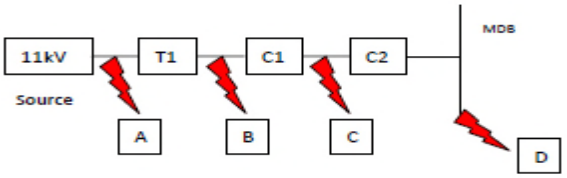

Fig. 2 Analytical and simulation output compared at points A, B, C, D.

Table I lists the difference between analytical (calculated) and simulated value of fault current. Simulated results are very close to the analytical results which prove the accuracy of the network model.

Table I Analytical and simulated value of fault current

Fault at Point	Type of fault	Fault Current kA-simulation	Fault Current kA-analytical	Difference (%)
A	3 phase	9.14	9.15	0.1
B	3 phase	10.7	10.8	0.9
C	3 phase	2.80	2.84	1.4
D	3 phase	2.44	2.47	1.2

Balanced load flow for the network without a PV system has also been validated. The PV system has then been introduced in the test network. Section 2.2 describes the PV system modeling in further details.
The test network model of the power system described in section 2 is shown in Fig 3 complete with PV systems connected.

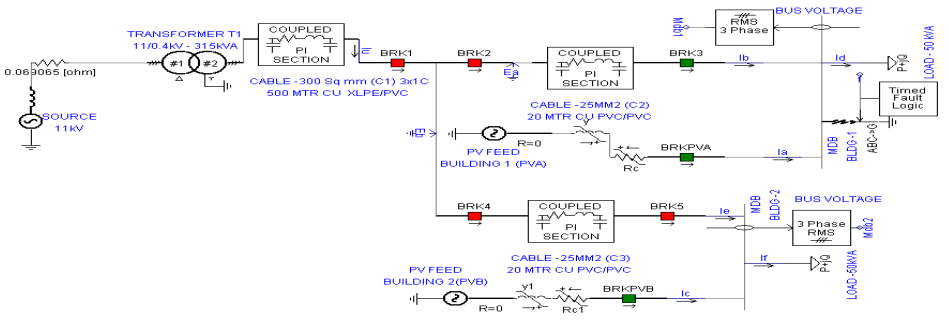

Fig. 3 PSCAD Model of Network

2.2. Model Modeling of PV System

As described in Section 2, transformer T1 provides power to the low voltage distribution board. The low voltage distribution board powers the MDB of each building using a 160 amps feeder. Each feeder (MCCB with connected cable) is sized to cater for 86 kVA per outgoing circuit. This study investigates the effect of adding a 50kVA roof top mounted PV system to each building. Table IV in Appendix lists the values used for modeling the PV system connected to MDB of individual buildings.

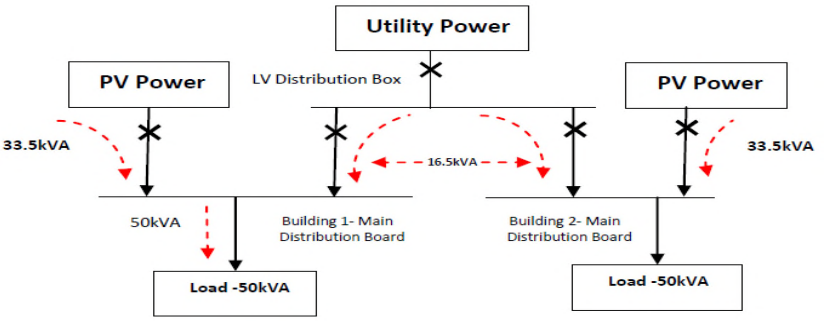

Fig. 4 Power flow at building main distribution board

Fig 4 shows the power distribution arrangement at the building MDB and the load sharing between PV and utility. PV system has been modeled as a constant voltage source which can contribute about 67% of the power requirement for the building (i.e. 33.5kVA) load and the rest 33% (i.e. 16.5kVA) is contributed by the utility power supply. Fig 5 shows the contribution from PV and utility to load during normal operation (i.e. when there is no fault).

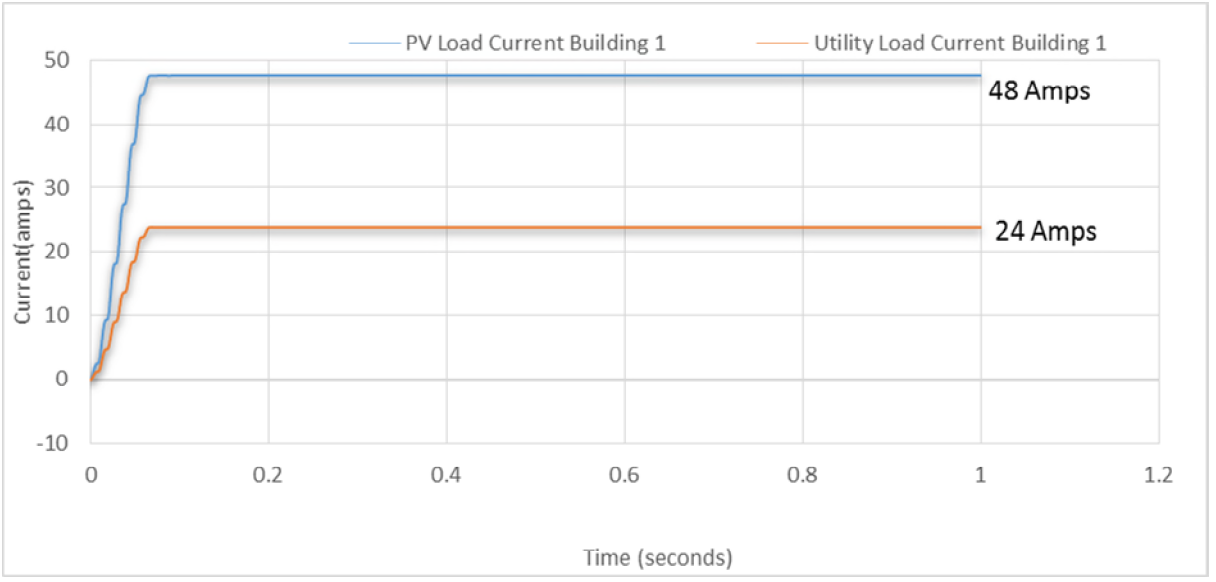

Fig. 5 Load sharing between PV and utility during normal operation

During a fault in the system, the PV system contribution is limited to a value of 2 times of inverter full load current. Full load current for a 50 kVA inverter interfaced system is 72 Amps. The maximum possible fault contribution from inverter during fault is 144 amps (2 times 72 amps approximately).
The control of contribution of current from the PV system during normal operation and fault is adjusted in the model by changing the source impedance of the constant voltage source used to represent the PV system [4].

2.3. Protective device setting and Over-current coordination

Over current protection devices controls the tripping of circuit breakers BRK1, BRK2, BRK3, BRK4 and BRK5 shown in Fig 3. When PV system is not connected, Time current coordination curve (TCC) ensures proper discrimination between upstream and downstream protection devices during fault and overload protection to devices during normal operation, thus ensuring reliability. The relay settings of the circuit breakers are shown the Table II below.

Table II Protection Settings

Circuit Breaker	IEC-225-3 Curve	Current Setting	TSM	Definite Time setting
BRK1	Normal Inverse	460	0.5	3400 (Delay 0s)
BRK2	Normal Inverse	125	0.2	2750 (Delay 0s)
BRK3	Normal Inverse	125	0.1	2500 (Delay 0s)
BRK4	Normal Inverse	125	0.2	2750 (Delay 0s)
BRK5	Normal Inverse	125	0.1	2500 (Delay 0s)

The integral output switching and protection unit of PV system is represented by circuit breaker BRKPVA for the system connected to main distribution board of building 1 and BRKPVB for the one connected to main distribution board of building 2. During a fault at the output of the inverter, the PV system shall trip using one of the two protective functions available –

- Inverter over-current –Trip on over current within 4 cycles to 10 cycles [5] .The over current trip function prevents damage caused by overheating of the IGBT in the inverter.
- Anti Islanding Protection –Trips on loss of mains within 2 seconds [6] of loss of utility power source.

Grid tied PV system inverters are provided with anti-islanding protection in addition to PV systems internal fault current limiting system.

As per IEEE standard 1547 [6], all grid connected inverter system shall successfully detect islanding and stop energizing within a given limit of time. In a grid tied system during a fault in the network, the grid side fault clearing device opens to clear the fault. The PV system then detects islanding and thereafter trips on detection of islanded condition within specified time (within 2 seconds) [6, 7].
Fig 6 shows the time current coordination requirement for the distribution system described in section 2.

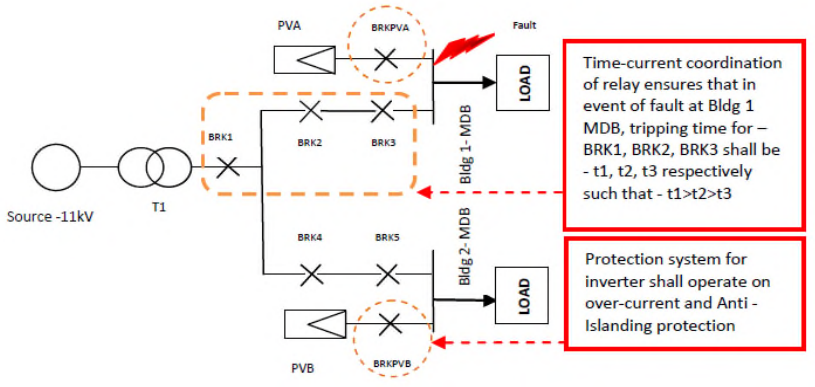

Fig. 6 Time current coordination requirement of the network

3. Case studies and observation

Four cases have been analyzed during a fault in the Building1 MDB. The cases have been described below:

3.1. Fault at the MDB of Building1 when only utility power source is connected to building MDB (PV system is not connected)-Case 1

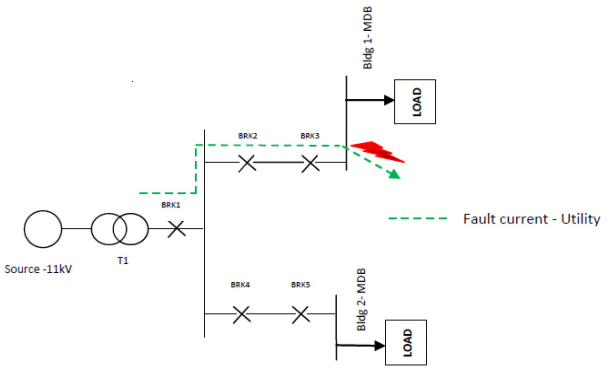

Fig. 7 Fault current path – PV not connected.

Fig 7 represents the flow path for fault current during a three phase fault in the MDB of building 1 when PV system is not connected to the building MDBs. The magnitude of fault current flowing through BRK2 and BRK3 is 2.44kA. The simulation output for the fault is shown in Fig 8.

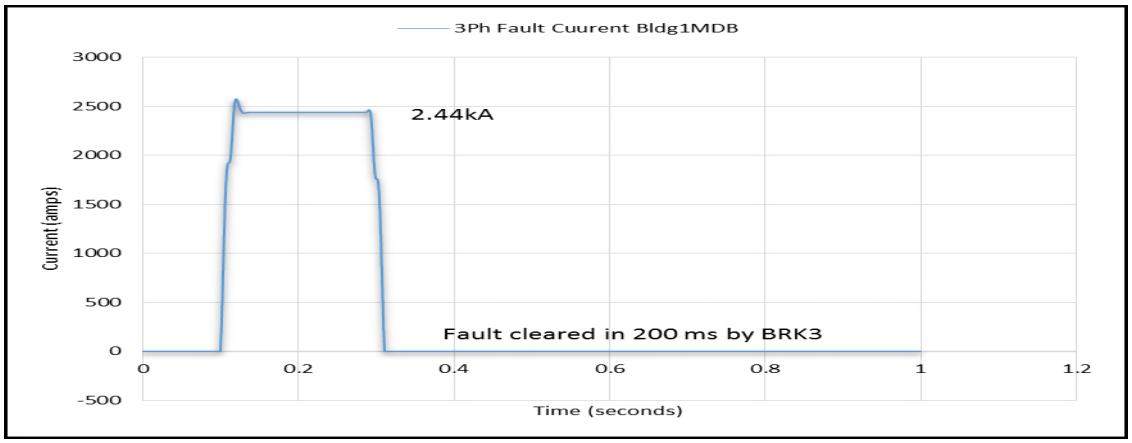

Fig. 8 RMS value of fault current for case 1

A three phase to earth fault was simulated at 0.1 seconds for duration of 0.3 seconds. The fault was cleared by BRK3 in approximately 0.2 seconds. This time equals the time indicted in TCC based on Table II shown in Fig 9. In this case the contribution to the fault current is made only by the utility power supply. In this situation the protection system is properly coordinated.

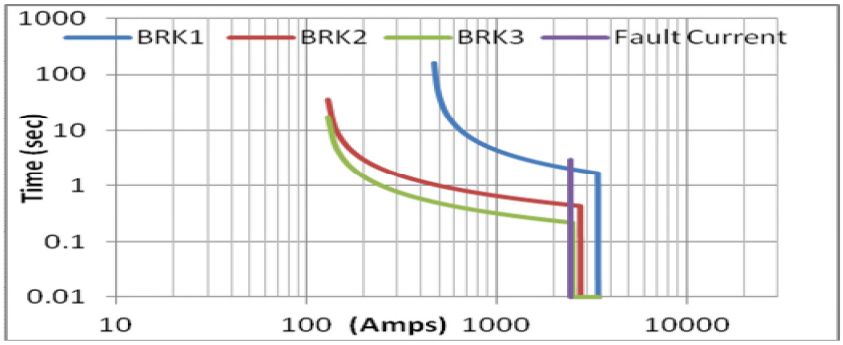

Fig. 9 TCC – Well coordinated system (PV is not connected)

3.2. Fault at the MDB of building1 when utility power source is available and PV system (PVA) is connected to MDB of Building1only.- Case 2

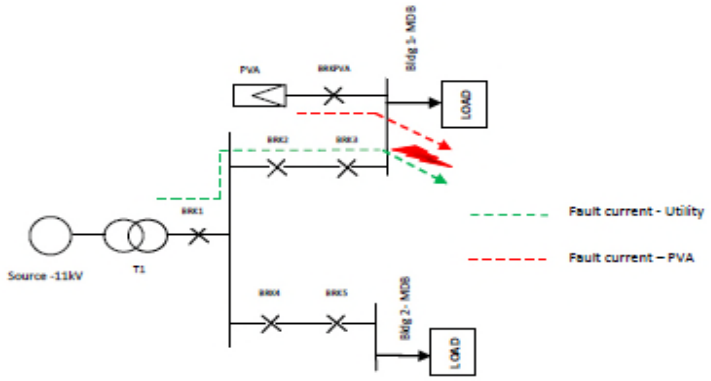

Fig. 10 Fault current path – PV connected to building1 MDB

Fig 10 represents the flow path for fault current during a three phase fault in the MDB of building 1 when PV system is connected to the MDB of building 1. The simulation output for the fault is shown in Fig 11.

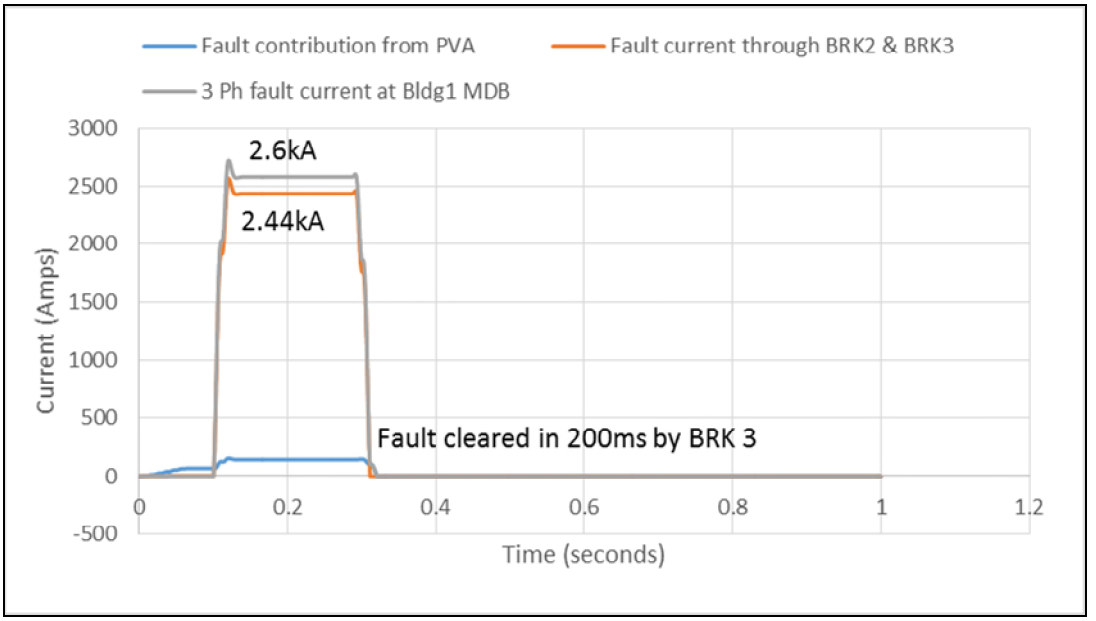

Fig. 11 RMS value of fault current for case 2

A three phase to earth fault at MDB of building 1 was simulated at 0.1 seconds for duration of 0.3 seconds. The fault was cleared by BRK3 in 0.25 seconds.
In this case additional fault current of 144 amps (approximately) is contributed by PVA. Though this additional fault current has increased the value of total current at the point of fault from 2.44kA to 2.6kA, the fault current flowing through circuit breaker BRK2 and BRK3 is still the same (i.e. 2.44kA) as case 1. The additional fault current contribution from PVA therefore does not disturb the protection coordination of the network as the additional 144amps of current does not flow through BRK2 and BRK 3.

3.3. Fault at the MDB of building1 when utility power source is available and PV systems PVA is connected to MDB of Building1and PVB is connected to MDB of Building2-Case 3

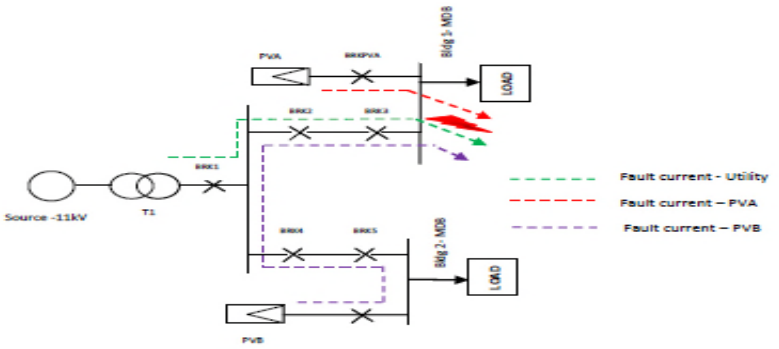

Fig. 12 Fault current path– PV connected to buildings1 & 2 MDBs

Fig 12 represents the flow path for fault current during a three phase fault in the MDB of building 1 when PV system is connected to the MDB of building 1and 2. The simulation output for the fault is shown in Fig 13
In this case, there will be an additional fault current contribution of 144 amps (approximately) from PVA and 115 amps from PVB. The value of total current at the point of fault will increase from 2.6kA (in case 2) to 2.7kA. The fault current flowing through circuit breaker BRK2 and BRK3 in this case will increase from 2.44kA to 2.55kA due to contribution of fault current from PVB.

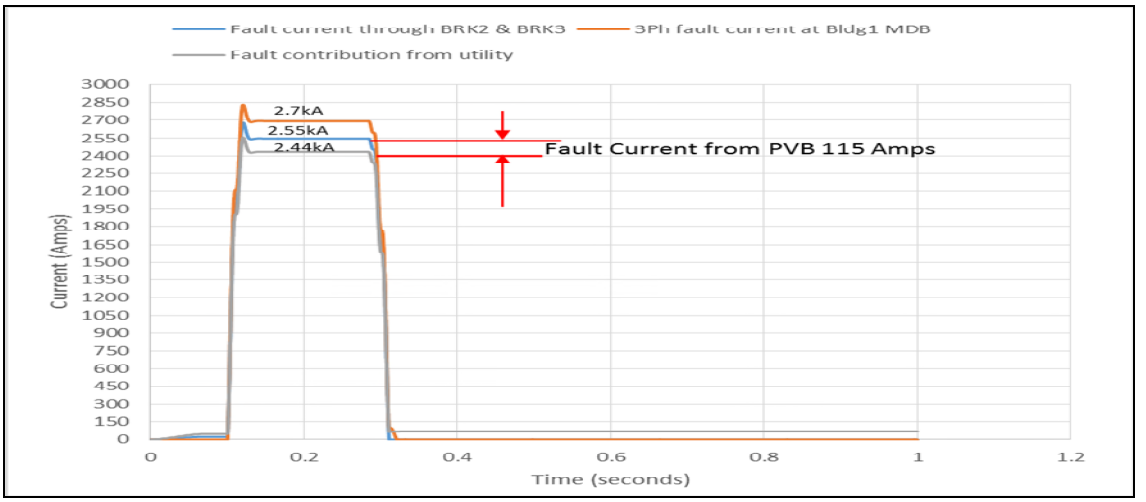

Fig. 13 RMS value of fault current for case 3

A three phase to earth fault simulated at 0.1 seconds for duration of 0.3 seconds at building 1 MDB was cleared by BRK3 in instantaneously as shown in Fig 14 (2550 amps > instantaneous trip threshold of BRK3). No impact on relay coordination is observed in this case.

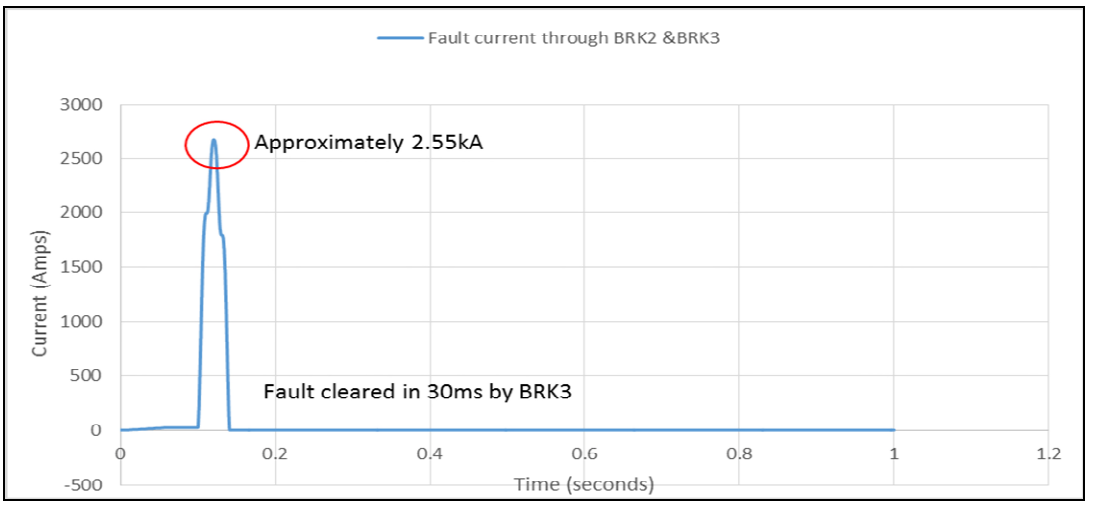

Fig. 14 Fault cleared by BRK3 in case 3

However, if fault current contribution from PVB is less than 115 amps (discussed further in Section 4) and therefore the magnitude of current flowing through BRK3 does not exceed 2500A (definite time threshold for BRK3), the tripping time for BRK3 shall be approximately 0.2 seconds (similar to case 2). In this situation the trip

time for of BRK3 will be equal to the time required for PVB to trip on over current protection (considering tripping time to be 10 cycles at 50 Hz). Even though the protection coordination is not disturbed in this case, the PVB may trip due to operation of over current protection. This is considered as a sympathetic tripping [3] (as no fault has occurred in the MBD2). Sympathetic tripping is undesirable and therefore in order to rectify this situation, the over current tripping time for BRK3 should be reduced to a value (by adjusting the time setting) such that BRK3 always trips before the PVB. This will prevent tripping of PV systems connected to MDBs where no fault has occurred.

3.4. Fault at the building main distribution box of building1 when both utility and PV system is connected to MDBs of all buildings-Case 4

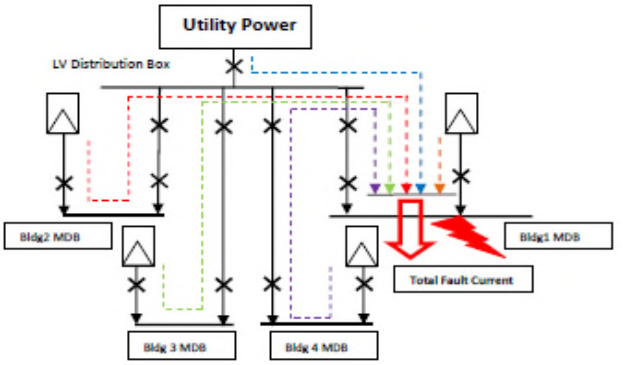

Fig. 15 Fault current path – PV connected to all buildings

Fig 15 represents the flow path for fault current during a three phase to earth fault in the MDB of building 1 when PV system is connected to the MDB of all four buildings in the housing complex.

In this case there will be an additional fault current contribution of 144 amps (approximately) from PVA and 345 (3 times 115 amps) from PV systems connected to other three buildings .The value of total current at the point of fault from 2.9kA as compared to 2.7kA in case 3. The fault current flowing through circuit breaker BRK2 and BRK3 in this case will be 2.79 kA due to contribution from PV system installed in other buildings. At this value of current, as per the TCC shown in Fig 16, tripping time for both BRK2 and BRK3 will be instantaneous thus allowing no proper discrimination of tripping during fault at MDB 1 as there shall be no grading margin. This will reduce system reliability.

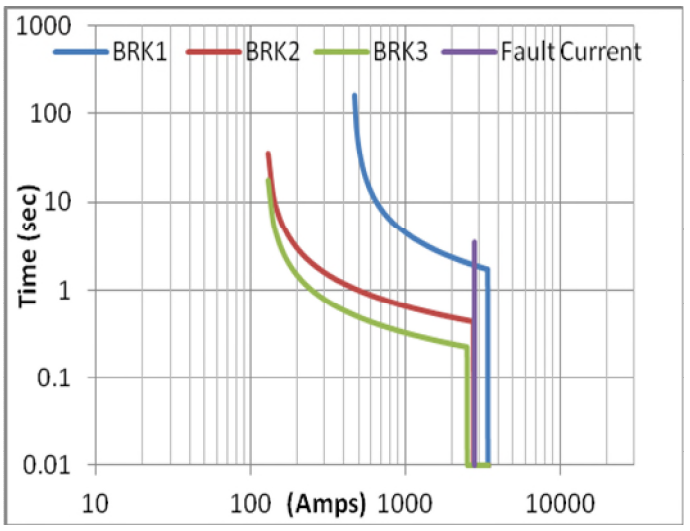

Fig. 16 TCC –Loss of coordination (PV connected to all buildings)

4. Analysis of results

Four cases have been considered in Section 3. The first case study does not consider any contribution from PV and case 2, 3 and 4 represents scenarios for studying effects of incremental contribution from PV systems on protection coordination. It is observed from the case 1 that the contribution of fault current from the PV system connected to a MDB where fault has occurred does not have any impact on the protection coordination of the system. It is only the fault current from the PV systems connected to MDBs of other buildings (where no fault has occurred) that has the potential to disturb the existing protection coordination of the protective devices supplying power to the MDB where the fault has occurred. As observed in case 3 and 4, it is also important to note that, while the PV system connected to the MBD where fault has occurred will contribute the full (expected) magnitude (i.e.144 amps) of fault current to the point of fault, the fault current contribution from a PV connected to the a MDB of other buildings will be will be less than 144 amps. The available additional fault current flowing through BRK2 and BRK3 is not a direct multiple of the possible fault contribution from an individual PV but depends on a number of other factors. This includes, the bus voltage at the MDB of other buildings during the fault in the building 1 MDB, the loading of the buses and also the cable length between the MDB and the low voltage distribution board. Fig 17 shows simulation output bus voltages at MDBs of building 1 and building 2 during a fault in the MDB of building 1.

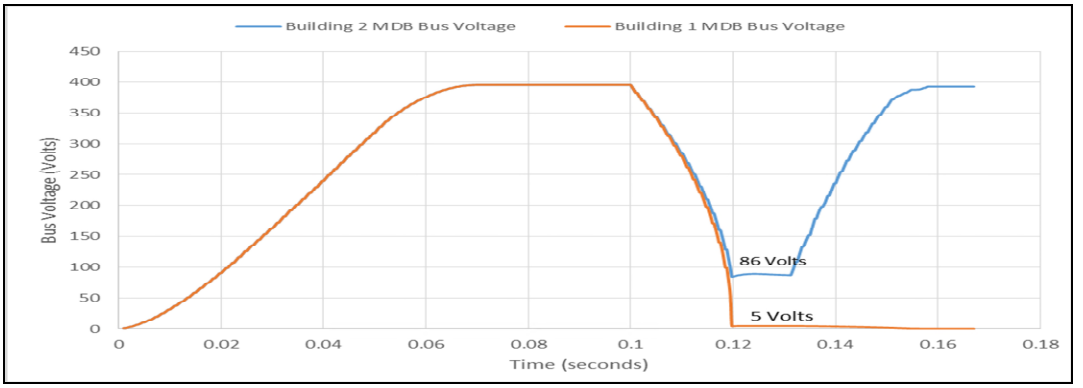

Fig. 17 Bus voltage profile during building 1 MDB fault

The simulation output in the Fig shows that the bus voltage at building 1 MDB is substantially lower than the bus voltage at building 2 MDB. When building 2 MDB is loaded to 50kVA, the current contribution from PVB is 130 amps. However, only 115 amps flows to the point of fault back through BRK4 and BRK5 and rest of the current flows to the load. Fig 18 shows the simulation output of current contribution from PVB in this situation.

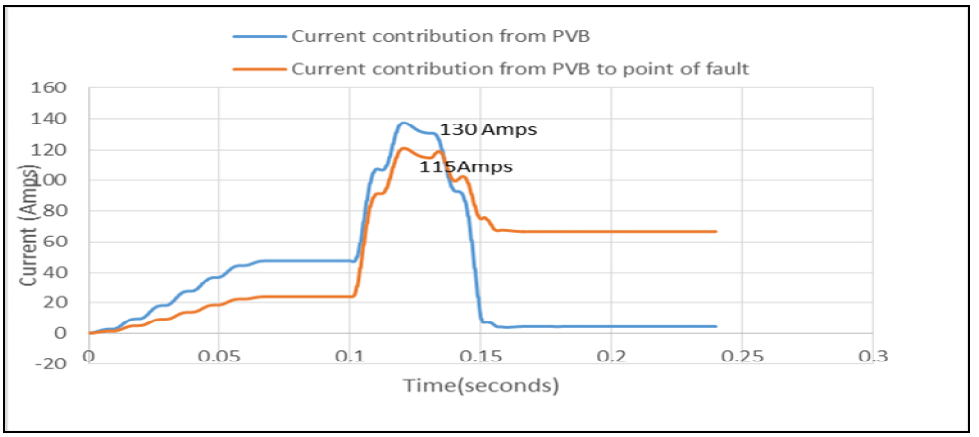

Fig. 18 PVB fault current contribution to point of fault

However, if the load on building 2 MDB is reduced from 50kVA to 10kVA, the current flowing from PVB to the point of fault will increase from 115 amps to 127 amps. This is due to there is increase in impedance offered to the PV voltage source when load is less as compared to the impedance offered to PV voltage source when load is higher. This illustrates the fact that magnitude of load on a particular power distribution board has an influence on the amount of fault current that the PV system connected to the distribution can contribute to the point of fault. Fig 19 shows the simulation output of current contribution from PVB in this situation.

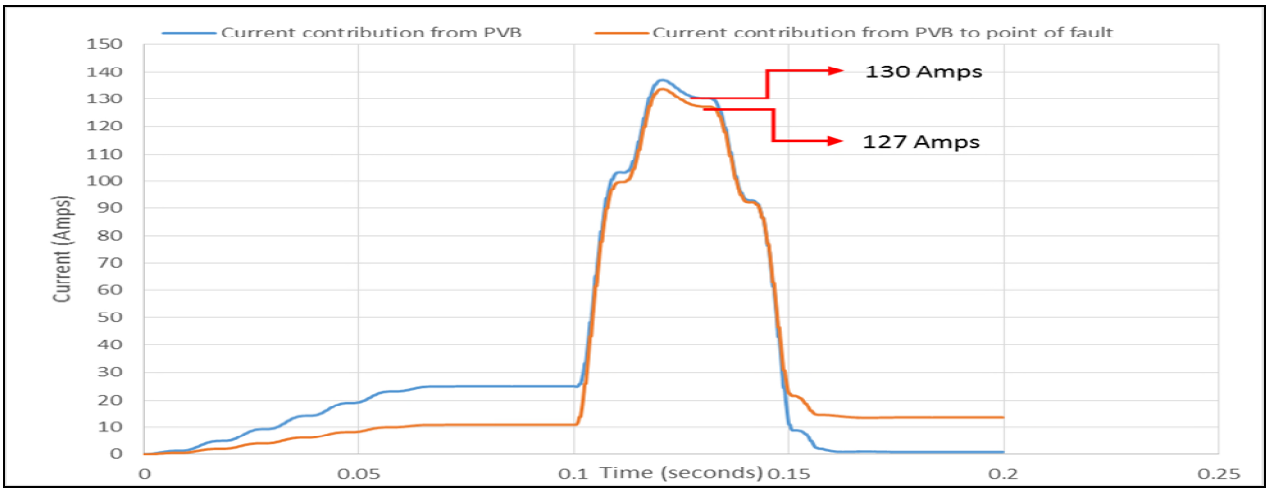

Fig. 19 Increase in fault current contribution from PVB to point of fault when building 2 MDB is lightly loaded (load -10kVA)

Cable connection from MDB to the low voltage distribution board is the major impedance between the source of fault current (i.e. PVB) and the point of fault. In this study, it has been assumed that this cable length is 20 meters. The total impedance to the source PVB during fault is therefore 40 meters long, 25 mm^2, copper conductor cable. This offers insignificant impedance to cause reduction in fault current. However in real case this factor will vary. The fault current contribution to point of fault from PVB will vary inversely to the length of cable and directly to the cable size (cross section area of conductor).

Considering the situation described in Section 3, case 4, instantaneous tripping time of BRK2 should be set for a time greater than the instantaneous tripping time of BRK3. As shown in Table 2, no intentional time delay has been provided for definite time tripping of BRK2. A definite time delay of 0.1 second for definite time trip threshold of BRK2 is adequate to prevent loss coordination between BRK2 and BRK3.

Fig 20 shows revised coordination setting for case 4. Theoretically the current threshold for definite time setting or the time setting can be increased to an absolute maximum value of short circuit withstand level of the bus and cable that the circuit breaker protects. However, the increase in setting may also be constrained due to the coordination grading margin that needs to be maintained with the upstream protection relay. Increase in threshold for instantaneous tripping of BRK2 (from 2750 amps to 2900 amps) will rectify the coordination problem, but effectiveness of this measure depends on the maximum fault current contribution from PV systems that will flow though BRK2 and BRK3. In the case studied, the 315kVA transformer powering up the housing complex will be loaded to a maximum of 64% in absence of generation from PV. Therefore future addition of two new buildings with 50 kVA demand load is possible. If PV system of 50kVA capacity is installed in each of the two new buildings then it is in case of fault in any building MDB, the fault current contribution will rise to 3.06kA (based on 115 amps contribution from each building) and the threshold limit for instantaneous trip of BRK2 has to be revised. Thus the trip setting for BRK2 will have to be revised every time a new PV unit is added .When delayed time setting is applied to maintain coordination gap with the BRK3, increase in fault current value will not effect the coordination of relays. Therefore adjusting the time setting of BRK2 is recommended as a better way of rectifying the coordination problem as compared to current threshold adjustment.

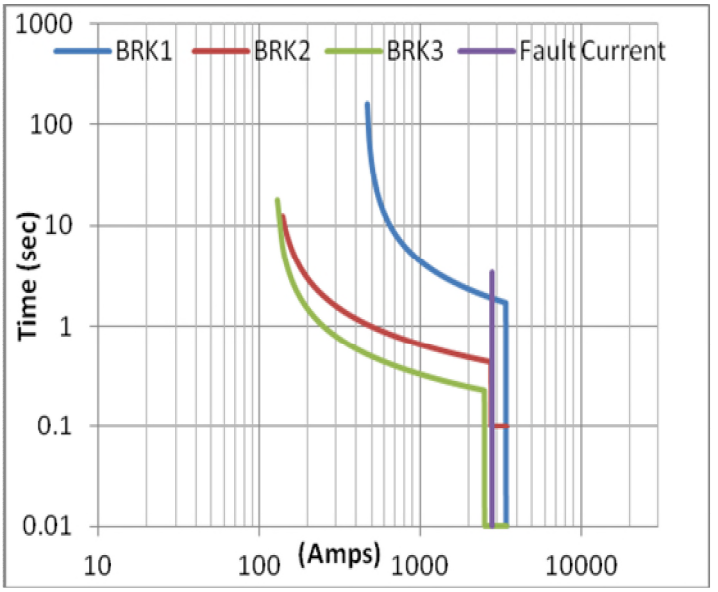

Fig. 20 TCC – BRK2 definite time setting delayed by 0.1 s

Also it is observed that increase in fault current from the PV systems has no impact on the coordination between BRK1 and BRK2 except for increase in grading .margin.

This investigation has been done considering only three phase faults at MDB. This is due to the fact that the three phase faults are more severe in nature and the higher magnitude of three phase current allows better illustrating the possible problems in coordination. A study for single phase to ground fault has been done in the past considering small single phase PV system connected to single phase distribution network connecting individual residences [13]

5. Conclusions

The investigation concludes that, though the PV systems are inverter interfaced devices and contributes low fault current, high PV penetration level can disturb existing protection coordination and suggests a preferred method for adjusting the TCC to meet the requirements of proper coordination of protective devices after adding a new PV system to the network. Analysis of various cases during this study shows that, during a fault at MDB, fault current from PV system connected to the MDB does not disturb the protection coordination for power supply to the MDB. The coordination is disturbed due to the fault current from PV systems installed in other buildings (i.e. remote MDBs). Also it is observed that, even though the industry rule of thumb is that the fault current contribution from a PV system is 2 times the full load amps of inverter, this is holds true only for PV connected to the MDB where the fault has occurred. The contribution of currents from PV systems connected to a remote MDB is dependent on factors like voltage at the remote bus, the impedance between the PV system and the point of fault and the load on the remote MDB buses. This implies that while analyzing the impact of increment of fault current due to installation of PV on the protection system, it is important to consider the factors that determine the magnitude of fault current contribution from remote PV systems. While considering adjustment of protection setting (due to PV penetration), increasing time grading margin with downstream protection device is more advantageous than increasing current threshold (in the instantaneous tripping zone of TCC).

To achieve higher reliability of system, circuit breaker closest to the point of fault should operate fast enough to prevent sympathetic tripping of other breakers. The study has considered arithmetic addition of utility side contribution of fault current and PV contribution (i.e. in-phase contribution from both the power sources) to determine the total magnitude of fault current flowing through the circuit breaker nearest to the point of fault. This represents a worst case scenario. Studies done in the past shows that fault current contribution from utility and PV are out of phase [9] and addition of current vectors will result in lower magnitude of fault current than the magnitude

obtained by arithmetic addition of fault currents. As discussed in Case 3 (Section 3), reduction in fault current will increase the chances of sympathetic tripping of PV systems connected to the MDBs installed in buildings where fault has not occurred due to delayed tripping of breaker closest to the fault (i.e. BRK3 in this case 3).

APPENDIX

Table III Specification of network components

Description	Specification
Utility	
Supply Voltage	11kV, 3Phase, 50 Hz
Fault Level at 11 kV	I''_{kQ} 3P- 9.15kA, X/R -10
Transformer –T1	
Located on pole top	11/0.433kV, Dyn11, 315kVA, Z=4%, Primary current – 17Amps, Secondary current – 455 Amps
Cable –C1,C2,C3,C4,C5	
C1 (connecting pole top transformer LV terminals to LV distribution board)	0.6/1kV, 300 mm^2, 3 x Single Core, copper conductor XLPE/PVC, 500m.Current carrying capacity - 469 amps
C2 (connecting circuit breaker outgoing terminals of LV distribution board to Building No1 -MDB)	0.6/1kV, 25mm^2, Four Core, Copper conductor, PVC /PVC, 20m.Current carrying capacity (directly buried) – 125 amps
C3(connecting circuit breaker outgoing terminals of LV distribution board to Building No2 -MDB)	0.6/1kV, 25mm^2, Four Core, Copper conductor, PVC /PVC, 20m.Current carrying capacity (directly buried) – 125 amps
C4(connecting circuit breaker outgoing terminals of LV distribution board to Building No3 -MDB)	0.6/1kV, 25mm^2, Four Core, Copper conductor, PVC /PVC, 20m.Current carrying capacity (directly buried) – 125 amps ground) - 125 amps
C5(connecting circuit breaker outgoing terminals of LV distribution board to Building No 4 -MDB)	0.6/1kV, 25mm^2, Four Core, Copper conductor, PVC / PVC, 20m.Current carrying capacity (directly buried) - 125 amps

Table IV Specification for power distribution at buildings

Description	Specification
Load per building MDB	50kVA (Each building has 10 apartment ,each with a load demand of 5kVA)
MDB	400Volts, 50 Hz , Three Phase
Individual PV panel rating	238 Watts /panel, V_{mpp} = 40.5V, I_{mpp}= 5.88A
PV Panel connection and installation	Configuration- 210 panel Number of panels connected in series - 11 panels Number of panels connected in parallel - 20 panels Total voltage - 445 Volts, Total current – 115 Amps Installation type – Building Roof Top Total Power – 50 kW
PV Inverter	50kVA ,400 Volts Three Phase output

References

[1] Jamie Keller, Benjamin Kroposki, Richard Bravo, Steven Robles, Fault Current Contribution from Single Phase PV Inverters, Photovoltaic Specialist Conference,2011, 37th IEEE, Pages 1822-1826

[2] S.Phuttapatimok, A.Sangswaang, M.Seapan, D.Chenvidhya and K.Kirtikara , Evaluation of Fault Contribution in presence of PV Grid connected systems, Photovoltaic Specialist Conference ,2008, 33rd IEEE, Pages 1-5

[3] H.Yazdanahi, Yun Wei Li, Wilsun Xu, A New Control Strategy to Mitigate the Impact of Inverter Based DG on Protection System ,Smart grid 2012 ,IEEE Transactions on, Pages 1427-1436
[4] Rajiv.K Verma, Jon Berge, I.Axente, Vinay Sharma, Ken Walsh, Determination of Maximum PV Solar System Connectivity in a Utility Distribution Feeder, Transmission and Distribution Conference and Exposition (T&D),2012, IEEE PES
[5] J E. Muljadi, M. Singh, R. Bravo, V. Gevorgian, Dynamic Model Validation of PV inverters under short circuit condition http://www.nrel.gov/docs/fy13osti/57341.pdf
[6] IEEE Standard for Interconnecting Distributed Resources with Electric Power Systems, IEEE 1547, 2003
[7] Australian Standard Grid connection of energy systems via inverter-Grid protection requirements, AS 4777.3, 2005
[8] Australian Standard The calculation of short-circuit currents in three phase a.c. systems, AS 3851,1991
[9] Farid Katiraei, Investigation of Solar PV Inverter Current Contributions during Faults on Distribution and Transmission Systems Interruption Capacity, Western Protective Relay Conference,2012,Pages 5-6.
http//quantatechnology.com/sites/default/files/docfiles/Solar%20PV%20Inverter%20formatted.pd
[10] S Chaitusaney, A Yokoyama An Appropriate Distributed Generation Sizing Considering Recloser- Fuse Coordination, Transmission and Distribution, IEEE Conference Asia and Pacific on ,2005, Pages 1-6
[11] Hossein Hooshyar,Mesut E.Baran, Fault Analysis on Distribution Feeders with High Penetration of PV Systems, Power Systems 2013, IEEE Transactions on, Vol 28, Pages 2890-2896
[12] Mesut E.Barun, Hossein Hooshyar, Zahn Shen, Alex Huang, Accomodating High Penetration on Distribution Feeder, Smart Grid 2012, IEEE Transactions on, Vol 3,Pages 1039-1046
[13] S.Bhattacharys, T.Saha, M.J Hossain, Fault current contribution from photovoltaic systems in residential power networks, Proceedings of the Australasian Universities Power Engineering Conference, Hobart, 2013, Australia, pp. 1-6.